



(43) International Publication Date  
24 August 2017 (24.08.2017)

- (51) International Patent Classification:  
C07K 16/28 (2006.01)
- (21) International Application Number:  
PCT/US2017/018255
- (22) International Filing Date:  
17 February 2017 (17.02.2017)
- (25) Filing Language: English
- (26) Publication Language: English
- (30) Priority Data:  
62/296,808 18 February 2016 (18.02.2016) US
- (71) Applicant: MAINE MEDICAL CENTER RESEARCH INSTITUTE [US/US]; MMCRI, 81 Research Drive, Scarborough, ME 04074 (US).
- (72) Inventors: BROOKS, Peter, C.; 85 Basin Cove Road, Harpswell, ME 04079 (US). CARON, Jennifer, M.; 18 Fowler Farm, Scarborough, ME 04074 (US).
- (74) Agents: CONLIN, David, G. et al.; Mintz Levin Cohn Ferris Glovsky and Popeo, P.C., One Financial Center, Boston, MA 02111 (US).
- (81) Designated States (unless otherwise indicated, for every kind of national protection available): AE, AG, AL, AM,

AO, AT, AU, AZ, BA, BB, BG, BH, BN, BR, BW, BY, BZ, CA, CH, CL, CN, CO, CR, CU, CZ, DE, DJ, DK, DM, DO, DZ, EC, EE, EG, ES, FI, GB, GD, GE, GH, GM, GT, HN, HR, HU, ID, IL, IN, IR, IS, JP, KE, KG, KH, KN, KP, KR, KW, KZ, LA, LC, LK, LR, LS, LU, LY, MA, MD, ME, MG, MK, MN, MW, MX, MY, MZ, NA, NG, NI, NO, NZ, OM, PA, PE, PG, PH, PL, PT, QA, RO, RS, RU, RW, SA, SC, SD, SE, SG, SK, SL, SM, ST, SV, SY, TH, TJ, TM, TN, TR, TT, TZ, UA, UG, US, UZ, VC, VN, ZA, ZM, ZW.

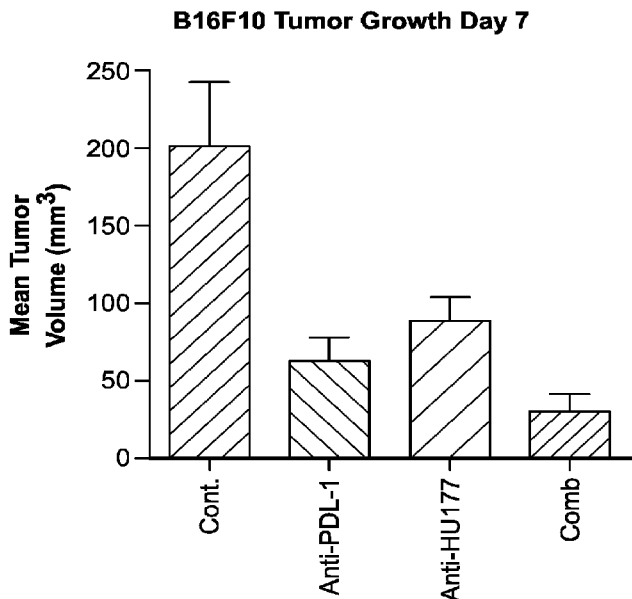
- (84) Designated States (unless otherwise indicated, for every kind of regional protection available): ARIPO (BW, GH, GM, KE, LR, LS, MW, MZ, NA, RW, SD, SL, ST, SZ, TZ, UG, ZM, ZW), Eurasian (AM, AZ, BY, KG, KZ, RU, TJ, TM), European (AL, AT, BE, BG, CH, CY, CZ, DE, DK, EE, ES, FI, FR, GB, GR, HR, HU, IE, IS, IT, LT, LU, LV, MC, MK, MT, NL, NO, PL, PT, RO, RS, SE, SI, SK, SM, TR), OAPI (BF, BJ, CF, CG, CI, CM, GA, GN, GQ, GW, KM, ML, MR, NE, SN, TD, TG).

**Published:**

- without international search report and to be republished upon receipt of that report (Rule 48.2(g))

(54) Title: ENHANCING THE THERAPEUTIC ACTIVITY OF AN IMMUNE CHECKPOINT INHIBITOR

**FIG. 27A**



(57) Abstract: The present invention provides antagonists and methods of use thereof in the treatment of cancer and abnormal immune suppression diseases.

WO 2017/143115 A2

## **ENHANCING THE THERAPEUTIC ACTIVITY OF AN IMMUNE CHECKPOINT INHIBITOR**

### **RELATED APPLICATIONS**

This application claims the benefit of priority under 35 U.S.C. § 119(e) to U.S. Provisional Application No: 62/296,808, filed February 18, 2016, which is incorporated herein by reference in its entirety.

### **GOVERNMENT SUPPORT**

This invention was made with government support under CA091645, HL065301, HL083151, P20 RR015555, P30 GM103392, and P20 RR181789, awarded by the National Institutes of Health, and W81XWH-13-OCRP-PA, awarded by the Department of Defense Ovarian Cancer Research Program. The government has certain rights in the invention.

### **BACKGROUND OF THE INVENTION**

Extracellular matrix (ECM) remodeling regulates angiogenesis. However, prior to the invention described herein, the precise mechanisms by which structural changes in ECM proteins contribute to angiogenesis were not fully understood. The role of integrin, e.g., integrin  $\alpha\beta3$  or integrin  $\alpha10\beta1$ , in angiogenesis is complex, as evidence exists for both positive and negative functions. As such, prior to the invention described herein, there was a pressing need to develop an understanding of the role of integrin in angiogenesis.

### **SUMMARY OF THE INVENTION**

The invention is based, in part, upon the surprising discovery that an antagonist (i.e., Mab XL313) specifically directed to a cryptic RGDKGE (SEQ ID NO: 1) - containing collagen epitope significantly enhanced the anti-tumor efficacy of an antibody that targets the immune checkpoint regulatory protein, PDL-1. Additionally, the invention is based, in part, on an antagonist of integrin  $\alpha\beta3$  that is used to enhance the therapeutic activity of an immune checkpoint inhibitor, e.g., cytotoxic T-lymphocyte-associated

protein 4 (CTLA-4), programmed death ligand-1 (PDL-1 or PD-L1), programmed cell death protein 1 (PD-1), lymphocyte-activation gene 3 (Lag3), leukocyte-associated immunoglobulin-like receptor 1 (LAIR1) and/or leukocyte-associated immunoglobulin-like receptor 2 (LAIR2) antibodies. The invention is also based, in part, upon the surprising discovery that an antagonist (i.e., Mab HU177) specifically directed to a cryptic CPGFPGFC (SEQ ID NO: 16)-containing collagen epitope enhanced the anti-tumor efficacy of an antibody that targets the immune checkpoint regulatory protein, PDL-1. The invention is also based, in part, upon the discovery that reducing the expression of an integrin receptor that can serve as a cell surface receptor for the HU177 epitope (i.e., integrin  $\alpha 10\beta 1$ ) can reduce expression of a potent immunosuppressive cytokine (i.e., IL-10) in melanoma cells in vitro. Conversely, as described in detail below, injecting a soluble version of the HU177 epitope itself induces expression of a second potent immunosuppressive molecule, TGF- $\beta$ , in mouse serum in vivo.

The present invention features compositions and methods for treating cancer and diseases characterized by abnormal immune suppression. For example, methods of treating cancer in a subject are carried out by identifying a subject, e.g., a human subject, that has been diagnosed with cancer; administering an immune checkpoint inhibitor; and administering an antagonist of collagen or a fragment thereof, thereby treating cancer in the subject. In some cases, the immune checkpoint inhibitor comprises an inhibitor of CTLA-4, PDL-1, PD-1, CTLA-4, Lag3, LAIR1 and/or LAIR2. For example, the inhibitor of PDL-1 comprises a PDL-1 antibody.

Suitable types of collagen include collagen type-I, collagen type-II, collagen type-III and collagen type-IV (e.g., the alpha 6 chain of collagen type-IV). In some cases, the antagonist of collagen or a fragment thereof comprises an antagonist of the XL313 cryptic collagen epitope or an antagonist of the HU177 cryptic collagen epitope. For example, the antagonist of the XL313 cryptic collagen epitope comprises an antibody that binds a cryptic RGDKGE (SEQ ID NO: 1) containing collagen epitope or wherein the antagonist of the HU177 cryptic collagen epitope comprises an antibody that binds a cryptic CPGFPGFC (SEQ ID NO: 16)-containing collagen epitope. Preferably, the antibody

comprises a monoclonal antibody, e.g., an XL313 monoclonal antibody or an HU177 monoclonal antibody.

Preferably, the antagonist of collagen or a fragment thereof enhances anti-tumor activity of the immune checkpoint inhibitor and inhibits an inflammatory condition. Exemplary inflammatory conditions include dermatitis, pneumonitis, or colitis.

The methods described herein can be used in conjunction with one or more chemotherapeutic or anti-neoplastic agents. In some cases, the additional chemotherapeutic agent is radiotherapy. In some cases, the chemotherapeutic agent is a cell death-inducing agent.

The term “antineoplastic agent” is used herein to refer to agents that have the functional property of inhibiting a development or progression of a neoplasm in a human, particularly a malignant (cancerous) lesion, such as a carcinoma, sarcoma, lymphoma, or leukemia. Inhibition of metastasis is frequently a property of antineoplastic agents.

Exemplary cancers are selected from the group comprising of melanoma, central nervous system (CNS) cancer, CNS germ cell tumor, lung cancer, leukemia, multiple myeloma, renal cancer, malignant glioma, medulloblastoma, breast cancer, ovarian cancer, prostate cancer, bladder cancer, fibrosarcoma, pancreatic cancer, gastric cancer, head and neck cancer, colorectal cancer. For example, a cancer cell is derived from a solid cancer or hematological cancer. The hematological cancer is, e.g., a leukemia or a lymphoma. A leukemia is acute lymphoblastic leukemia (ALL), acute myelogenous leukemia (AML), chronic lymphocytic leukemia (CLL), small lymphocytic lymphoma (SLL), chronic myelogenous leukemia (CML), or acute monocytic leukemia (AMoL). A lymphoma is follicular lymphoma, Hodgkin’s lymphoma (*e.g.*, Nodular sclerosing subtype, mixed-cellularity subtype, lymphocyte-rich subtype, or lymphocyte depleted subtype), or Non-Hodgkin’s lymphoma. Exemplary solid cancers include but are not limited to melanoma (*e.g.*, unresectable, metastatic melanoma), renal cancer (*e.g.*, renal cell carcinoma), prostate cancer (*e.g.*, metastatic castration resistant prostate cancer), ovarian cancer (*e.g.*, epithelial ovarian cancer, such as metastatic epithelial ovarian cancer), breast cancer (*e.g.*, triple negative breast cancer), and lung cancer (*e.g.*, non-small cell lung cancer).

Human dosage amounts can initially be determined by extrapolating from the amount of compound used in mice or nonhuman primates, as a skilled artisan recognizes it is routine in the art to modify the dosage for humans compared to animal models. In certain embodiments, it is envisioned that the dosage of the antagonist to collagen may vary from between about 0.1  $\mu\text{g}$  compound/kg body weight to about 25000  $\mu\text{g}$  compound/kg body weight; or from about 1  $\mu\text{g}$ /kg body weight to about 4000  $\mu\text{g}$ /kg body weight or from about 10  $\mu\text{g}$ /kg body weight to about 3000  $\mu\text{g}$ /kg body weight. In other embodiments this dose may be about 0.1, 0.3, 0.5, 1, 3, 5, 10, 25, 50, 75, 100, 150, 200, 250, 300, 350, 400, 450, 500, 550, 600, 650, 700, 750, 800, 850, 900, 950, 1000, 1050, 1100, 1150, 1200, 1250, 1300, 1350, 1400, 1450, 1500, 1600, 1700, 1800, 1900, 2000, 2500, 3000, 3500, 4000, 4500, 5000, 5500, 6000, 6500, 7000, 7500, 8000, 8500, 9000, 9500, 10000, 10500, 1100, 11500, 12000, 12500, 13000, 13500, 14000, 14500, 15000, 15500, 16000, 16500, 17000, 17500, 18000, 18500, 19000, 19500, 20000, 20500, 21000, 21500, 22000, 22500, 23000, 23500, 24000, 24500, or 25000  $\mu\text{g}$ /kg body weight. In other embodiments, it is envisaged that doses may be in the range of about 0.5  $\mu\text{g}$  compound/kg body weight to about 20  $\mu\text{g}$  compound/kg body weight. In other embodiments, the doses may be about 0.5, 1, 3, 6, 10, or 20 mg/kg body weight. Of course, this dosage amount may be adjusted upward or downward, as is routinely done in such treatment protocols, depending on the results of the initial clinical trials and the needs of a particular patient.

In some cases, the immune checkpoint inhibitor, e.g., the inhibitor of PDL-1, is administered at a dosage of 0.01-10 mg/kg (e.g., 0.01, 0.05, 0.1, 0.5, 1, 5, or 10 mg/kg) bodyweight. For example, the PDL-1 inhibitor is administered in an amount of 0.01-30 mg (e.g., 0.01, 0.05, 0.1, 0.5, 1, 5, 10, 20, or 30 mg) per dose. In another example, the immune checkpoint inhibitor, e.g., the anti-PD-L1 antibody, is administered in the dose range of 0.1 mg/kg to 10 mg/kg of body weight. In some cases, the XL313 antibody or the HU177 antibody is administered at a dosage of 0.01-10 mg/kg (e.g., 0.01, 0.05, 0.1, 0.5, 1, 5, or 10 mg/kg) bodyweight. For example, the XL313 antibody or the HU177 antibody is administered in an amount of 0.01-30 mg (e.g., 0.01, 0.05, 0.1, 0.5, 1, 5, 10, 20, or 30 mg) per dose. For example, the dose range of Mab X1313 or Mab HU177 is from 0.1 mg/kg to 25 mg/kg of body weight.

The compositions of the invention (e.g., inhibitor of PDL-1, XL313 antibody, and HU177 antibody) are administered once per month, twice per month (i.e., every two weeks), every week, once per day, twice per day, every 12 hours, every 8 hours, every 4 hours, every 2 hours or every hour. The compositions of the invention (e.g., inhibitor of PDL-1, XL313 antibody, and HU177 antibody) are administered for a duration of 1 day, 2 days, 3 days, 4 days, 5 days, 6 days, 7 days, 2 weeks, 3 weeks, 4 weeks, five weeks, six weeks, 2 months, 3 months, 4 months, 5 months, 6 months, 7 months, 8 months, 9 months, 10 months, 11 months, 12 months, 2 years, 3 years, 4 years, 5 years or more. For example, the composition of the invention (e.g., inhibitor of PD-L1, XL313 antibody, and HU177 antibody) are administered one dose every two weeks for 4 to 6 weeks or until the disease is treated.

Also provided is a method of treating a disease characterized by abnormal immune suppression in a subject by identifying a subject, e.g., a human, that has been diagnosed with a disease characterized by abnormal immune suppression, administering an immune checkpoint inhibitor, and administering an antagonist of an integrin, thereby treating in the subject.

Suitable immune checkpoint inhibitors comprise an inhibitor of CTLA-4, PD-1, PDL-1, Lag3, LAIR1, or LAIR 2. For example, the immune checkpoint inhibitor comprises a CTLA-4 antibody, a PD-1 antibody, a PDL-1 antibody, a Lag3 antibody, a LAIR1 antibody, or a LAIR 2 antibody.

Preferably, the integrin comprises integrin  $\alpha\beta3$ . For example, the antagonist of integrin  $\alpha\beta3$  comprises an antibody targeting  $\alpha\beta3$  binding RGDKGE (SEQ ID NO: 1) containing collagen epitope. Alternatively, the integrin comprises integrin  $\alpha10\beta1$ . For example, the antagonist of integrin  $\alpha10\beta1$  comprises an antibody targeting  $\alpha10\beta1$  binding CPGFPGFC (SEQ ID NO: 16)-containing collagen epitope.

The methods described herein can be used in conjunction with one or more chemotherapeutic or anti-neoplastic agents. In some cases, the additional chemotherapeutic agent is radiotherapy. In some cases, the chemotherapeutic agent is a cell death-inducing agent.

Suitable diseases characterized by abnormal immune suppression include Type I diabetes, lupus, psoriasis, scleroderma, hemolytic anemia, vasculitis, Graves' disease, rheumatoid arthritis, multiple sclerosis, Hashimoto's thyroiditis, Myasthenia gravis, and vasculitis

In some cases, the immune checkpoint inhibitor (e.g., CTLA-4 antibody, a PD-1 antibody, a PDL-1 antibody, Lag3, LAIR1, or LAIR 2) is administered at a dosage of 0.01-10 mg/kg (e.g., 0.01, 0.05, 0.1, 0.5, 1, 5, or 10 mg/kg) bodyweight. For example, the PDL-1 inhibitor is administered in an amount of 0.01-30 mg (e.g., 0.01, 0.05, 0.1, 0.5, 1, 5, 10, 20, or 30 mg) per dose. In another example, the antibody is administered in the dose range of 0.1mg/kg to 10mg/kg of body weight. In some cases, the antagonist of integrin  $\alpha\text{v}\beta\text{3}$  is administered at a dosage of 0.01-10 mg/kg (e.g., 0.01, 0.05, 0.1, 0.5, 1, 5, or 10 mg/kg) bodyweight. In some cases, the XL313 antibody or the HU177 antibody is administered in an amount of 0.01-30 mg (e.g., 0.01, 0.05, 0.1, 0.5, 1, 5, 10, 20, or 30 mg) per dose.

The compositions of the invention (e.g., immune checkpoint inhibitor and antagonist of integrin  $\alpha\text{v}\beta\text{3}$ ) are administered once per month, twice per month (once every two weeks), once a week, once per day, twice per day, every 12 hours, every 8 hours, every 4 hours, every 2 hours or every hour. The compositions of the invention (e.g., inhibitor of PDL-1, XL313 antibody, and HU177 antibody) are administered for a duration of 1 day, 2 days, 3 days, 4 days, 5 days, 6 days, 7 days, 2 weeks, 3 weeks, 4 weeks, 2 months, 3 months, 4 months, 5 months, 6 months, 7 months, 8 months, 9 months, 10 months, 11 months, 12 months, 2 years, 3 years, 4 years, 5 years or more. The composition of the invention (e.g., inhibitor of PDL-1, XL313 antibody, and HU177 antibody) are administered one dose every two weeks for 4 to 6 weeks or until the disease is treated

Also provided is a method of treating a disease characterized by an overactive immune response (e.g., an autoimmune disease) in a subject, e.g., a human subject, that has been diagnosed with an overactive immune response by administering a peptide comprising collagen or a fragment thereof, thereby treating overactive immune response in the subject. Suitable types of collagen include collagen type-I, collagen type II,

collagen type III, and collagen type-IV (e.g., the alpha 6 chain of collagen type-IV). For example, the peptide comprises RGDKGE (SEQ ID NO: 1) or CPGFPGFC (SEQ ID NO: 16).

In some cases, the autoimmune disease comprises Graves' disease, Hashimoto's thyroiditis, Systemic lupus erythematosus (lupus), Type 1 diabetes, multiple sclerosis or rheumatoid arthritis.

Methods for healing a wound in a subject, e.g., a human subject with a wound, are carried out by administering a peptide comprising collagen or a fragment thereof to the wound of the subject, thereby healing a wound in the subject. For example, the peptide is administered to a site that is about 0.1 mm, 0.5 mm, 1 mm, 2.5 mm, 5 mm, 10 mm, 15 mm, 20 mm, or 40 mm away from a perimeter or margin of the wound. Alternatively, the peptide is administered directly to the wound itself.

Suitable types of collagen include collagen type-I, collagen type II, collagen type III, and collagen type-IV (e.g., the alpha 6 chain of collagen type-IV). For example, the peptide comprises RGDKGE (SEQ ID NO: 1) or CPGFPGFC (SEQ ID NO: 16).

### ***Definitions***

Unless defined otherwise, all technical and scientific terms used herein have the meaning commonly understood by a person skilled in the art to which this invention belongs. The following references provide one of skill with a general definition of many of the terms used in this invention: Singleton et al., Dictionary of Microbiology and Molecular Biology (2nd ed. 1994); The Cambridge Dictionary of Science and Technology (Walker ed., 1988); The Glossary of Genetics, 5th Ed., R. Rieger et al. (eds.), Springer Verlag (1991); and Hale & Marham, The Harper Collins Dictionary of Biology (1991). As used herein, the following terms have the meanings ascribed to them below, unless specified otherwise.

By "agent" is meant any small molecule chemical compound, antibody, nucleic acid molecule, or polypeptide, or fragments thereof.

By "antibody" is meant any immunoglobulin polypeptide, or fragment thereof, having immunogen binding ability. As used herein, the term "antibodies" includes polyclonal antibodies, affinity-purified polyclonal antibodies, monoclonal antibodies, and

antigen-binding fragments, such as F(ab')<sub>2</sub> and Fab proteolytic fragments. Genetically engineered intact antibodies or fragments, such as chimeric antibodies, Fv fragments, single chain antibodies, and the like, as well as synthetic antigen-binding peptides and polypeptides, are also included. Non-human antibodies may be humanized by grafting non-human CDRs onto human framework and constant regions, or by incorporating the entire non-human variable domains. In certain preferred embodiments, humanized antibodies may retain non-human residues within the human variable region framework domains to enhance proper binding characteristics.

“Antigenic fragment” and the like are understood as at least that portion of a peptide capable of inducing an immune response in a subject, or being able to be specifically bound by an antibody raised against the antigenic fragment. Typically, antigenic fragments are at least 7 amino acids in length. Antigenic fragments can include deletions of the amino acid sequence from the N-terminus or the C-terminus, or both. For example, an antigenic fragment can have an N- and/or a C-terminal deletion of about 1, 2, 3, 4, 5, 6, 7, 8, 9, 10, 15, 20, 25, 30, 35, 40, 45, 50, 55, 60, 65, 70, 75, 80, 85, 90, 95, 100, 110, 120, 130, 140, 150, 160, 170, 180, 190, 200, or more amino acids. Antigenic fragments can also include one or more internal deletions of the same exemplary lengths. Antigenic fragments can also include one or more point mutations, particularly conservative point mutations. At least an antigenic fragment of protein can include the full length, wild-type sequence of the antigen. An antigenic fragment can include more than one potential antibody binding site. An antigenic fragment can be used to make antibodies for use in any of the methods provided herein.

By “autoimmune disease” is meant a disease characterized by a dysfunction in the immune system. The disease is characterized by the components of the immune system affected, whether the immune system is overactive or underactive, or whether the condition is congenital or acquired. In most cases, the disorder causes abnormally low activity or over activity of the immune system. In cases of immune system over activity, the body attacks and damages its own tissues (autoimmune). Immune deficiency diseases decrease the body’s ability to fight invaders, causing vulnerability to infections. In response to an unknown trigger, the immune system may begin producing antibodies that

instead of fighting infections, attack the body's own tissues. Treatment for autoimmune diseases generally focuses on reducing immune system activity.

By "blood vessel formation" is meant the dynamic process that includes one or more steps of blood vessel development and/or maturation, such as angiogenesis, arteriogenesis, vasculogenesis, formation of an immature blood vessel network, blood vessel remodeling, blood vessel stabilization, blood vessel maturation, blood vessel differentiation, or establishment of a functional blood vessel network.

By "blood vessel remodeling" or "vascular remodeling" is meant the dynamic process of blood vessel enlargement in shape and size to maintain the luminal orifice and blood flow. For example, vascular remodeling includes change in arterial size to adapt to plaque accumulation, effectively maintaining the lumen and blood flow to the myocardium.

As used herein, "binding" or "specific binding" is understood as having at least a  $10^3$  or more, preferably  $10^4$  or more, preferably  $10^5$  or more, preferably  $10^6$  or more preference for binding to a specific binding partner as compared to a non-specific binding partner (e.g., binding an antigen to a sample known to contain the cognate antibody).

By "cancer" is meant, comprising of but not limited to melanoma, central nervous system (CNS) cancer, CNS germ cell tumor, lung cancer, leukemia, multiple myeloma, renal cancer, malignant glioma, medulloblastoma, breast cancer, ovarian cancer, prostate cancer, bladder cancer, fibrosarcoma, pancreatic cancer, gastric cancer, head and neck cancer, colorectal cancer. For example, a cancer cell is derived from a solid cancer or hematological cancer. The hematological cancer is, e.g., a leukemia or a lymphoma. A leukemia is acute lymphoblastic leukemia (ALL), acute myelogenous leukemia (AML), chronic lymphocytic leukemia (CLL), small lymphocytic lymphoma (SLL), chronic myelogenous leukemia (CML), or acute monocytic leukemia (AMoL). A lymphoma is follicular lymphoma, Hodgkin's lymphoma (e.g., Nodular sclerosing subtype, mixed-cellularity subtype, lymphocyte-rich subtype, or lymphocyte depleted subtype), or Non-Hodgkin's lymphoma. Exemplary solid cancers include but are not limited to melanoma (e.g., unresectable, metastatic melanoma), renal cancer (e.g., renal cell carcinoma), prostate cancer (e.g., metastatic castration resistant prostate cancer), ovarian cancer (e.g.,

epithelial ovarian cancer, such as metastatic epithelial ovarian cancer), breast cancer (e.g., triple negative breast cancer), and lung cancer (e.g., non-small cell lung cancer).

By “control” or “reference” is meant a standard of comparison. As used herein, “changed as compared to a control” sample or subject is understood as having a level of the analyte or diagnostic or therapeutic indicator to be detected at a level that is statistically different than a sample from a normal, untreated, or control sample. Control samples include, for example, cells in culture, one or more laboratory test animals, or one or more human subjects. Methods to select and test control samples are within the ability of those in the art. An analyte can be a naturally occurring substance that is characteristically expressed or produced by the cell or organism (e.g., an antibody, a protein) or a substance produced by a reporter construct (e.g.  $\beta$ -galactosidase or luciferase). Depending on the method used for detection the amount and measurement of the change can vary. Determination of statistical significance is within the ability of those skilled in the art, e.g., the number of standard deviations from the mean that constitute a positive result.

By “cryptic” is meant that a motif may be inaccessible to cell surface receptors, and once the target protein is proteolyzed or denatured, a sequence becomes exposed or generates a fragment that is then recognized by the antibody. For example, the XL313 epitope, i.e., RGDKGE (SEQ ID NO: 1) core sequence within collagen type-I is cryptic in that the antibody does not react with normal collagen in its triple helical state, but once it is proteolyzed or denatured, the sequence becomes exposed or generates a fragment of collagen that is recognized by Mab XL313. Similarly, the HU177 epitope, i.e., CPGFPGFC (SEQ ID NO: 16) core sequence within collagen type-I is cryptic in that the antibody does not react with normal collagen in its triple helical state, but once it is proteolyzed or denatured, the sequence becomes exposed or generates a fragment of collagen that is recognized by Mab HU177.

As used herein, “detecting”, “detection” and the like are understood that an assay performed for identification of a specific analyte in a sample, e.g., an antigen in a sample or the level of an antigen in a sample. The amount of analyte or activity detected in the sample can be none or below the level of detection of the assay or method.

By “diagnosing” and the like as used herein refers to a clinical or other assessment of the condition of a subject based on observation, testing, or circumstances for identifying a subject having a disease, disorder, or condition based on the presence of at least one indicator, such as a sign or symptom of the disease, disorder, or condition. Typically, diagnosing using the method of the invention includes the observation of the subject for multiple indicators of the disease, disorder, or condition in conjunction with the methods provided herein. Diagnostic methods provide an indicator that a disease is or is not present. A single diagnostic test typically does not provide a definitive conclusion regarding the disease state of the subject being tested.

By the terms “effective amount” and “therapeutically effective amount” of a formulation or formulation component is meant a sufficient amount of the formulation or component, alone or in a combination, to provide the desired effect. For example, by "an effective amount" is meant an amount of a compound, alone or in a combination, required to ameliorate the symptoms of a disease relative to an untreated patient. The effective amount of active compound(s) used to practice the present invention for therapeutic treatment of a disease varies depending upon the manner of administration, the age, body weight, and general health of the subject. Ultimately, the attending physician or veterinarian will decide the appropriate amount and dosage regimen. Such amount is referred to as an "effective" amount.

The term "polynucleotide" or "nucleic acid" as used herein designates mRNA, RNA, cRNA, cDNA or DNA. As used herein, a “nucleic acid encoding a polypeptide” is understood as any possible nucleic acid that upon (transcription and) translation would result in a polypeptide of the desired sequence. The degeneracy of the nucleic acid code is well understood. Further, it is well known that various organisms have preferred codon usage, etc. Determination of a nucleic acid sequence to encode any polypeptide is well within the ability of those of skill in the art.

As used herein, “immunoassay” is understood as any antibody base detection method including, but not limited to enzyme linked immunosorbent assay (ELISA), radioimmune assay (RIA), Western blot, immunohistochemistry, immunoprecipitation assay such as Luciferase Immunoprecipitation System (LIPS see, e.g., US Patent

Publication 2007/0259336 which is incorporated herein by reference). In a preferred embodiment, the immunoassay is a quantitative. Antibodies for use in immunoassays include any monoclonal or polyclonal antibody appropriate for use in the specific immunoassay.

By “inhibitory nucleic acid molecule” is meant a polynucleotide that disrupts the expression of a target nucleic acid molecule or an encoded polypeptide. Exemplary inhibitory nucleic acid molecules include, but are not limited to, shRNAs, siRNAs, antisense nucleic acid molecules, and analogs thereof.

As used herein, “isolated” or “purified” when used in reference to a polypeptide means that a naturally polypeptide or protein has been removed from its normal physiological environment (e.g., protein isolated from plasma or tissue, optionally bound to another protein) or is synthesized in a non-natural environment (e.g., artificially synthesized in an in vitro translation system or using chemical synthesis). Thus, an “isolated” or “purified” polypeptide can be in a cell-free solution or placed in a different cellular environment (e.g., expressed in a heterologous cell type). The term “purified” does not imply that the polypeptide is the only polypeptide present, but that it is essentially free (about 90-95%, up to 99-100% pure) of cellular or organismal material naturally associated with it, and thus is distinguished from naturally occurring polypeptide. Similarly, an isolated nucleic acid is removed from its normal physiological environment. “Isolated” when used in reference to a cell means the cell is in culture (i.e., not in an animal), either cell culture or organ culture, of a primary cell or cell line. Cells can be isolated from a normal animal, a transgenic animal, an animal having spontaneously occurring genetic changes, and/or an animal having a genetic and/or induced disease or condition. An isolated virus or viral vector is a virus that is removed from the cells, typically in culture, in which the virus was produced.

As used herein, “kits” are understood to contain at least one non-standard laboratory reagent for use in the methods of the invention in appropriate packaging, optionally containing instructions for use. The kit can further include any other components required to practice the method of the invention, as dry powders, concentrated solutions, or ready to use solutions. In some embodiments, the kit comprises one or more

containers that contain reagents for use in the methods of the invention; such containers can be boxes, ampules, bottles, vials, tubes, bags, pouches, blister-packs, or other suitable container forms known in the art. Such containers can be made of plastic, glass, laminated paper, metal foil, or other materials suitable for holding reagents.

As used herein, “obtaining” is understood herein as manufacturing, purchasing, or otherwise coming into possession of.

The phrase “pharmaceutically acceptable carrier” is art recognized and includes a pharmaceutically acceptable material, composition or vehicle, suitable for administering compounds of the present invention to mammals. The carriers include liquid or solid filler, diluent, excipient, solvent or encapsulating material, involved in carrying or transporting the subject agent from one organ, or portion of the body, to another organ, or portion of the body. Each carrier must be “acceptable” in the sense of being compatible with the other ingredients of the formulation and not injurious to the patient. Some examples of materials which can serve as pharmaceutically acceptable carriers include: sugars, such as lactose, glucose and sucrose; starches, such as corn starch and potato starch; cellulose, and its derivatives, such as sodium carboxymethyl cellulose, ethyl cellulose and cellulose acetate; powdered tragacanth; malt; gelatin; talc; excipients, such as cocoa butter and suppository waxes; oils, such as peanut oil, cottonseed oil, safflower oil, sesame oil, olive oil, corn oil and soybean oil; glycols, such as propylene glycol; polyols, such as glycerin, sorbitol, mannitol and polyethylene glycol; esters, such as ethyl oleate and ethyl laurate; agar; buffering agents, such as magnesium hydroxide and aluminum hydroxide; alginic acid; pyrogen-free water; isotonic saline; Ringer’s solution; ethyl alcohol; phosphate buffer solutions; and other non-toxic compatible substances employed in pharmaceutical formulations.

Formulations of the present invention include those suitable for oral, nasal, topical, transdermal, buccal, sublingual, intramuscular, intracardiac, intraperitoneal, intrathecal, intracranial, rectal, vaginal and/or parenteral administration. The formulations may conveniently be presented in unit dosage form and may be prepared by any methods well known in the art of pharmacy. The amount of active ingredient that can be combined with

a carrier material to produce a single dosage form will generally be that amount of the compound that produces a therapeutic effect.

In some cases, a composition of the invention is administered orally or systemically. Other modes of administration include rectal, topical, intraocular, buccal, intravaginal, intracisternal, intracerebroventricular, intratracheal, nasal, transdermal, within/on implants, or parenteral routes. The term "parenteral" includes subcutaneous, intrathecal, intravenous, intramuscular, intraperitoneal, or infusion. Intravenous or intramuscular routes are not particularly suitable for long-term therapy and prophylaxis. They could, however, be preferred in emergency situations. Compositions comprising a composition of the invention can be added to a physiological fluid, such as blood. Oral administration can be preferred for prophylactic treatment because of the convenience to the patient as well as the dosing schedule. Parenteral modalities (subcutaneous or intravenous) may be preferable for more acute illness, or for therapy in patients that are unable to tolerate enteral administration due to gastrointestinal intolerance, ileus, or other concomitants of critical illness. Inhaled therapy may be most appropriate for pulmonary vascular diseases (e.g., pulmonary hypertension).

As used herein, the terms "prevent," "preventing," "prevention," "prophylactic treatment" and the like refer to reducing the probability of developing a disorder or condition in a subject, who does not have, but is at risk of or susceptible to developing a disorder or condition.

As used herein, "plurality" is understood to mean more than one. For example, a plurality refers to at least two, three, four, five, or more.

A "polypeptide" or "peptide" as used herein is understood as two or more independently selected natural or non-natural amino acids joined by a covalent bond (e.g., a peptide bond). A peptide can include 2, 3, 4, 5, 6, 7, 8, 9, 10, 11, 12, 13, 14, 15, 16, 17, 18, 19, 20, or more natural or non-natural amino acids joined by peptide bonds. Polypeptides as described herein include full length proteins (e.g., fully processed proteins) as well as shorter amino acids sequences (e.g., fragments of naturally occurring proteins or synthetic polypeptide fragments). Optionally the peptide further includes one or more modifications such as modified peptide bonds, i.e., peptide isosteres, and may

contain amino acids other than the 20 gene-encoded amino acids. The polypeptides may be modified by either natural processes, such as posttranslational processing, or by chemical modification techniques which are well known in the art. Such modifications are well described in basic texts and in more detailed monographs, as well as in a voluminous research literature. Modifications can occur anywhere in a polypeptide, including the peptide backbone, the amino acid side-chains and the amino or carboxyl termini. It will be appreciated that the same type of modification may be present in the same or varying degrees at several sites in a given polypeptide. Also, a given polypeptide may contain many types of modifications. Polypeptides may be branched, for example, as a result of ubiquitination, and they may be cyclic, with or without branching. Cyclic, branched, and branched cyclic polypeptides may result from posttranslation natural processes or may be made by synthetic methods. Modifications include acetylation, acylation, ADP-ribosylation, amidation, covalent attachment of flavin, covalent attachment of a heme moiety, covalent attachment of a nucleotide or nucleotide derivative, covalent attachment of a lipid or lipid derivative, covalent attachment of phosphatidylinositol, cross-linking, cyclization, disulfide bond formation, demethylation, formation of covalent cross-links, formation of cysteine, formation of pyroglutamate, formulation, gamma-carboxylation, glycosylation, GPI anchor formation, hydroxylation, iodination, methylation, myristoylation, oxidation, pegylation, proteolytic processing, phosphorylation, prenylation, racemization, selenoylation, sulfation, transfer-RNA mediated addition of amino acids to proteins such as arginylation, and ubiquitination. (See, for instance, *Proteins, Structure and Molecular Properties*, 2nd ed., T. E. Creighton, W.H. Freeman and Company, New York (1993); *Posttranslational Covalent Modification of Proteins*, B. C. Johnson, ed., Academic Press, New York, pgs. 1-12 (1983); Seifter et al., *Meth. Enzymol* 182:626-646 (1990); Rattan et al., *Ann. N.Y. Acad. Sci.* 663:48-62 (1992)).

The term “reduce” or “increase” is meant to alter negatively or positively, respectively, by at least 5%. An alteration may be by 5%, 10%, 25%, 30%, 50%, 75%, or even by 100%.

As used herein, a “reporter protein” or a “reporter polypeptide” is understood as a polypeptide that can be readily detected, preferably quantitatively detected, either directly

or indirectly. A reporter polypeptide typically has an enzymatic activity, luciferase activity, alkaline phosphatase activity, beta-galactosidase activity, acetyl transferase activity, etc. wherein catalysis of a reaction with the substrate by the enzyme results in the production of a product, e.g., light, a product that can be detected at a specific wavelength of light, radioactivity, such that the amount of the reporter peptide can be determined in the sample, either as a relative amount, or as an absolute amount by comparison to control samples.

A “sample” as used herein refers to a biological material that is isolated from its environment (e.g., blood or tissue from an animal, cells, or conditioned media from tissue culture) and is suspected of containing, or known to contain an analyte, such as a protein. A sample can also be a partially purified fraction of a tissue or bodily fluid. A reference sample can be a “normal” sample, from a donor not having the disease or condition fluid, or from a normal tissue in a subject having the disease or condition. A reference sample can also be from an untreated donor or cell culture not treated with an active agent (e.g., no treatment or administration of vehicle only). A reference sample can also be taken at a “zero time point” prior to contacting the cell or subject with the agent or therapeutic intervention to be tested or at the start of a prospective study.

“Sensitivity and specificity” are statistical measures of the performance of a binary classification test. The sensitivity (also called recall rate in some fields) measures the proportion of actual positives which are correctly identified as such (e.g. the percentage of sick people who are identified as having the condition); and the specificity measures the proportion of negatives which are correctly identified (e.g. the percentage of well people who are identified as not having the condition). They are closely related to the concepts of type I and type II errors. A theoretical, optimal prediction can achieve 100% sensitivity (i.e. predict all people from the sick group as sick) and 100% specificity (i.e. not predict anyone from the healthy group as sick).

The concepts are expressed mathematically as follows:

sensitivity = # true positives / # true positives + # false negatives

specificity = # true negatives / # true negatives + # false positives.

By "selectively" is meant the ability to affect the activity or expression of a target molecule without affecting the activity or expression of a non-target molecule.

By "substantially identical" is meant a polypeptide or nucleic acid molecule exhibiting at least 50% identity to a reference amino acid sequence (for example, any one of the amino acid sequences described herein) or nucleic acid sequence (for example, any one of the nucleic acid sequences described herein). Preferably, such a sequence is at least 60%, more preferably 80% or 85%, and more preferably 90%, 95% or even 99% identical at the amino acid level or nucleic acid to the sequence used for comparison.

Sequence identity is typically measured using sequence analysis software (for example, Sequence Analysis Software Package of the Genetics Computer Group, University of Wisconsin Biotechnology Center, 1710 University Avenue, Madison, Wis. 53705, BLAST, BESTFIT, GAP, or PILEUP/PRETTYBOX programs). Such software matches identical or similar sequences by assigning degrees of homology to various substitutions, deletions, and/or other modifications. Conservative substitutions typically include substitutions within the following groups: glycine, alanine; valine, isoleucine, leucine; aspartic acid, glutamic acid, asparagine, glutamine; serine, threonine; lysine, arginine; and phenylalanine, tyrosine. In an exemplary approach to determining the degree of identity, a BLAST program may be used, with a probability score between  $e^{-3}$  and  $e^{-100}$  indicating a closely related sequence.

A "subject" as used herein refers to an organism. In certain embodiments, the organism is an animal. In certain embodiments, the subject is a living organism. In certain embodiments, the subject is a cadaver organism. In certain preferred embodiments, the subject is a mammal, including, but not limited to, a human or non-human mammal. In certain embodiments, the subject is a domesticated mammal or a primate including a non-human primate. Examples of subjects include humans, monkeys, dogs, cats, mice, rats, cows, horses, goats, and sheep. A human subject may also be referred to as a patient.

A "subject sample" can be a sample obtained from any subject, typically a blood or serum sample, however the method contemplates the use of any body fluid or tissue from

a subject. The sample may be obtained, for example, for diagnosis of a specific individual for the presence or absence of a particular disease or condition.

A subject “suffering from or suspected of suffering from” a specific disease, condition, or syndrome has a sufficient number of risk factors or presents with a sufficient number or combination of signs or symptoms of the disease, condition, or syndrome such that a competent individual would diagnose or suspect that the subject was suffering from the disease, condition, or syndrome. Methods for identification of subjects suffering from or suspected of suffering from conditions associated with diminished cardiac function is within the ability of those in the art. Subjects suffering from, and suspected of suffering from, a specific disease, condition, or syndrome are not necessarily two distinct groups.

As used herein, “susceptible to” or “prone to” or “predisposed to” a specific disease or condition and the like refers to an individual who based on genetic, environmental, health, and/or other risk factors is more likely to develop a disease or condition than the general population. An increase in likelihood of developing a disease may be an increase of about 10%, 20%, 50%, 100%, 150%, 200%, or more.

As used herein, the terms “treat,” “treating,” “treatment,” and the like refer to reducing or ameliorating a disorder and/or symptoms associated therewith. It will be appreciated that, although not precluded, treating a disorder or condition does not require that the disorder, condition or symptoms associated therewith be completely eliminated.

Unless specifically stated or obvious from context, as used herein, the term “or” is understood to be inclusive.

Unless specifically stated or obvious from context, as used herein, the terms “a”, “an”, and “the” are understood to be singular or plural.

Unless specifically stated or obvious from context, as used herein, the term “about” is understood as within a range of normal tolerance in the art, for example within 2 standard deviations of the mean. About can be understood as within 10%, 9%, 8%, 7%, 6%, 5%, 4%, 3%, 2%, 1%, 0.5%, 0.1%, 0.05%, or 0.01% of the stated value. Unless otherwise clear from context, all numerical values provided herein can be modified by the term about.

The recitation of a listing of chemical groups in any definition of a variable herein includes definitions of that variable as any single group or combination of listed groups. The recitation of an embodiment for a variable or aspect herein includes that embodiment as any single embodiment or in combination with any other embodiments or portions thereof.

Any compositions or methods provided herein can be combined with one or more of any of the other compositions and methods provided herein.

Other features and advantages of the invention will be apparent from the following description of the preferred embodiments thereof, and from the claims. Unless otherwise defined, all technical and scientific terms used herein have the same meaning as commonly understood by one of ordinary skill in the art to which this invention belongs. Although methods and materials similar or equivalent to those described herein can be used in the practice or testing of the present invention, suitable methods and materials are described below. All published foreign patents and patent applications cited herein are incorporated herein by reference. Genbank and NCBI submissions indicated by accession number cited herein are incorporated herein by reference. All other published references, documents, manuscripts and scientific literature cited herein are incorporated herein by reference. In the case of conflict, the present specification, including definitions, will control. In addition, the materials, methods, and examples are illustrative only and not intended to be limiting.

### **BRIEF DESCRIPTION OF THE DRAWINGS**

Fig. 1A-Fig. 1F are bar graphs of cryptic RGD containing peptides from collagen type-I support cell adhesion. Peptides corresponding to the 5 different RGD-containing motifs of human collagen type-I were synthesized with flanking cysteines and immobilized non-tissue culture plates. The ability of stromal cells to attach (Fig. 1A- Fig. 1D) or monoclonal antibodies to bind the immobilized peptides (Fig. 1E- Fig. 1F) was assessed. Fig. 1A is a bar graph that depicts human umbilical vein endothelial cell (HUVEC) adhesion to immobilized peptides. Fig. 1B is a bar graph that depicts human retinal microvascular endothelial cell (HMVEC) adhesion to immobilized peptides. Fig.

1C is a bar graph that depicts HRMVEC adhesion to immobilized peptides. Fig. 1D is a bar graph that depicts human dermal fibroblast (HDF) adhesion to immobilized peptides. Fig. 1E is a bar graph that depicts reactivity of Mab XL313 to immobilized peptides. Fig. 1F is a bar graph that depicts reactivity of Mab XL166 to immobilized peptides. Data bars represent mean binding  $\pm$  SD from at least 3 experiments each using triplicate wells. \*  $P < 0.05$ .

Fig. 2A- Fig. 2D is a series of immunoblots and bar graphs depicting that Mab XL313 exhibits selective binding to proteolyzed collagen type-I. Purified collagen type-I and collagen type-IV were incubated with control buffer or activated MMP-2 over a time course and analyzed by Western blot (Fig. 2A, Fig. 2B and Fig. 2D) or ELISA (Fig. 2C). Fig. 2A is a Western blot depicting analysis of control not treatment (NT) and MMP-2 proteolyzed (Prot) collagen type-I (Left panel) and collagen type-IV (Right panel) probed with anti-collagen type-I specific antibody (Left panel) or anti-collagen type-IV specific antibody (Right panel). Fig. 2B is a Western blot depicting analysis of control non-proteolyzed and MMP-2 proteolyzed collagen type-I and type-IV following 16 hour incubation and probed with Mab XL313 directed to the RGDKGE (SEQ ID NO: 1) containing collagen motif. Fig. 2C is a bar graph depicting the detection of Mab XL313 reactive RGDKGE (SEQ ID NO: 1) motif in non-proteolyzed (Nat) or MMP-2 proteolyzed (Prot) collagen by ELISA. Data bars indicate mean reactivity from triple wells  $\pm$  SD. \*  $P < 0.05$ . Experiments were completed at least 3 times with similar results. Fig. 2D is a Western blot depicting the analysis of the time dependent generation of the Mab XL313 reactive epitope of collagen type-1.

Fig. 3A- Fig. 3E are data depicting the differential roles of cryptic RGD collagen motifs on angiogenesis and inflammation *in vivo*. Chick chorioallantoic membranes (CAMs) were either un-stimulated or stimulated with FGF-2 in the presence or absence of cortisone acetate. Fig. 3A shows images of representative examples of un-stimulated or FGF-2 stimulated CAM tissues stained with Mabs XL313 and XL166 (Green). Scale bars represent 50  $\mu$ m. Fig. 3B is a bar graph depicting the quantification of FGF-2 induced angiogenesis in the absence or presence of Mabs XL313, XL166 or non-specific control antibody. Data bars represent mean number of angiogenic branching vessels  $\pm$  S.E from 8-

10 animals per conditions. Experiments were completed at least 3 times with similar results. Fig. 3C shows images of un-stimulated or FGF-2 stimulated CAMs in the absence of cortisone acetate. Representative examples of inflammatory CAM thickening (Top panel), giemsa positive inflammatory infiltrates (Middle panel) and infiltration of macrophages (green) following staining with anti-avian specific macrophage marker KUL1 (Bottom Panel). Scale bars represent 50  $\mu$ m. Fig. 3D is a bar graph depicting the quantification of relative macrophage infiltration following FGF-2 stimulation in the absence of cortisone acetate. Data bars represent mean  $\pm$  S.E levels of KUL expressing avian macrophages per 100X microscopic field from 5 fields per CAM and 10 CAM per condition. \*P<0.05. Fig. 3E is a bar graph depicting the quantification of FGF-2 induced inflammation in the absence or presence of Mabs XL313, XL166 or non-specific control antibody. Data bars represent mean percentage inflammatory CAMs  $\pm$  S.E. Experiments were completed at least 3 times with similar results. \* P<0.05.

Fig. 4A- Fig. 4D are images depicting generation of XL313 cryptic RGDKGE (SEQ ID NO: 1) epitope. Fig. 4A is a Western blot of whole cell lysates (Right panel) or serum free conditioned medium (Left panel) from stromal cells probed with Mab XL313 or loading control antibodies for 13-Actin or MMP-9. Fig. 4B are images of representative examples of FGF-2 stimulated CAM tissues co-stained for expression of avian macrophages (Green) and the RGDKGE (SEQ ID NO: 1) containing epitope (Red). Scale bars indicate 50 $\mu$ m. Fig. 4C is a Western blot of whole cell lysates (Right panel) or serum free conditioned medium (Left panel) from macrophage cell lines probed with Mab XL313 or loading control antibodies for  $\beta$ -Actin or IGFBP-4. Fig. 4D is a Western blot of whole cell lysates or serum free conditioned medium from RAW 264.7 macrophage cell that were either not transfected (WT) or transfected with  $\alpha$ 2(I) specific shRNA (Col 1 Kd) or control non-specific shRNA (Cont Kd) with Mab XL313 (Left panel) or anti-collagen-1 antibody (right).

Fig. 5A- Fig. 5D are bar graphs depicting the induction of angiogenesis and inflammation *in vivo* by soluble RGDKGE (SEQ ID NO: 1) but not a related RGDAPG (SEQ ID NO: 11) containing collagen epitope. Fig. 5A is a bar graph depicting serum from chick embryos in which the CAMs had been either not stimulated (NT) or stimulated

with FGF-2 was collected. Relative levels of circulating Mab XL313 reactive epitope were quantified by solid-phase ELISA. Data represent mean Mab XL313 reactivity  $\pm$  S.E (N=12 to 13). Fig. 5B is a bar graph depicting quantification of dose dependent induction of angiogenesis by RGDKGE (SEQ ID NO: 1) containing collagen peptide P-2. Data bars indicate mean number of branch points  $\pm$  S.E from 8 to 12 animal per condition. Fig. 5C is a bar graph depicting quantification of CAM angiogenesis associated with RGD containing collagen peptides P-1 (KGDRGDAPG; SEQ ID NO: 2), P-2 (QGPRGDKGE; SEQ ID NO: 3) or control peptide P-C (QGPSGSPGE; SEQ ID NO: 4). Data bars indicate mean angiogenic index derived by subtracting the number of branch points from non-stimulated CAMs  $\pm$ S.E from 8 to 12 animals per condition. Fig. 5D is a bar graph depicting the quantification of CAM inflammation associated with RGD containing collagen peptides P-1 (KGDRGDAPG; SEQ ID NO: 2), P-2 (QGPRGDKGE; SEQ ID NO: 3) or control peptide P-C (QGPSGSPGE (SEQ ID NO: 4)). All experiments were conducted at least 3 times with similar results. \* P<0.05.

Fig. 6A- Fig. 6F are data depicting RGDKGE (SEQ ID NO: 1) containing collagen peptide P-2 induced angiogenesis depends on P38MAPK. Angiogenesis was induced within the chick CAMs and the relative level of P38MAPK was assessed. Fig. 6A is a Western blot of examples (N=3 per condition) of total lysate from un-stimulated (NT) or CAMs stimulation with P-1 (KGDRGDAPG (SEQ ID NO: 2)) or P-2 (QGPRGDKGE (SEQ ID NO: 3)) and probed for phosphorylated P38MAPK (P-p38), total P38MAPK (T-p38) or  $\beta$ -Actin. Fig. 6B is a bar graph depicting the quantification (Image-J) of the mean relative levels of phosphorylated P38MAPK from un-stimulated or following CAM stimulation with P-1 (KGDRGDAPG (SEQ ID NO: 2); SEQ ID NO: 2) or P-2 (QGPRGDKGE; SEQ ID NO: 3). Data bars represent mean levels of phosphorylated P38MAPK  $\pm$  S.D (N=8 to 10 CAMs per condition). Fig. 6C are images of representative examples of P-2 stimulated CAM tissues co-stained for expression of vWf and phosphorylated P38MAPK. Scale bar indicates 50.0  $\mu$ m. Fig. 6D is a Western blot analysis of endothelial cell (HUVEC) lysates from cells attached to collagen peptides P-1 (KGDRGDAPG; SEQ ID NO: 2), P-2 (QGPRGDKGE; SEQ ID NO: 3) and probed for phosphorylated P38MAPK (P-p38), total P38MAPK (T-p38) or  $\beta$ -Actin. Fig. 6E is a

Western blot analysis of endothelial cell (HRMVEC) lysates from cells attached to collagen peptides P-1 (KGDRGDAPG (SEQ ID NO: 2)), P-2 (QGPRGDKGE (SEQ ID NO: 3)) and probed for phosphorylated P38MAPK (P-p38), total P38MAPK (T-p38) or  $\beta$ -Actin. Fig. 6F is a bar graph depicting the quantification of collagen peptide P-2 (QGPRGDKGE (SEQ ID NO: 3)) induced angiogenesis in the chick CAM following treatment with P38MAPK inhibitor (P38IN) of DMSO control (Cont). Data bars represent angiogenic vessel branch points  $\pm$  S.E (N=8- 12 per condition). Experiments were conducted at least 3 times with similar results. \*  $P < 0.05$ .

Fig. 7A- Fig. 7G are images depicting collagen peptide P-2 binds and activates  $\alpha\beta 3$  and stimulates P38MAPK activation in a Src dependent manner. Fig. 7A and Fig. 7B are bar graphs depicting that endothelial cells (HUVECS) were allowed to bind to wells coated with either RGDKGE (SEQ ID NO: 1) containing collagen peptide P-2 (Fig. 7A) or RGDAPG (SEQ ID NO: 11) containing collagen peptide P-1 (Fig. 7B) in the presence or absence of function blocking anti-integrin antibodies. Data bars represent mean cell adhesion ( $\pm$  S.E. from 4 experiments). \* $p < 0.05$ . Fig. 7C is a Western blot of HUVEC lysates following binding to RGD containing collagen peptides P-1 or P-2 probed with anti-phosphorylated  $\beta 3$ -integrin (p-  $\beta 3$ ), total  $\beta 3$ -integrin (T-  $\beta 3$ ) or  $\beta$ -Actin. Fig. 7D is a Western blot of HUVEC lysates following binding to RGD containing collagen peptides P-1 or P-2 probed with anti-phosphorylated Src (P-Src), total Src (T-Src) or  $\beta$ -Actin. Fig. 7E is a Western blot of lysates prepared from HUVECs incubated in the presence or absence of a Src inhibitor PP2 (Src-IN) or control DMSO (cont) following binding to RGD containing collagen peptides P-1 or P-2 probed with anti-phosphorylated  $\beta 3$ -integrin (p-  $\beta 3$ ), total  $\beta 3$ -integrin (T-  $\beta 3$ ) or  $\beta$ -Actin. Fig. 7F is a Western blot of lysates prepared from HUVECs incubated in the presence or absence of a Src inhibitor PP2 (Src-IN) or control DMSO (cont) following binding to RGD containing collagen peptides P-1 or P-2 probed with anti-phosphorylated P38MAPK (p-P38), total P38MAPK- (T-P38) or  $\beta$ -Actin. Fig. 7G are images of representative examples of endothelial cells (HUVECs) attached to RGD containing collagen peptides P-1 and P-2 stained for F-actin. Scale bar indicates 50.0  $\mu\text{m}$ .

Fig. 8A- Fig. 8I are data depicting that cellular interactions with RGDKGE (SEQ ID NO: 1) collagen-containing peptide accelerates actin stress fiber formation and nuclear YAP

accumulation promoting endothelial growth. Fig. 8A are images of representative examples of endothelial cells (HUVECs) attached to RGD containing collagen peptides P-1 and P-2 stained for YAP (green). Scale bar indicates 50.0  $\mu\text{m}$ . Fig. 8B is a Western blot of cytoplasmic (left) and nuclear (right) fractions of HUVEC lysates following binding to RGD containing collagen peptides P-1 or P-2 probed with anti- YAP,  $\beta$ -tubulin and anti-total binding protein (TBP). Fig. 8C and Fig. 8D are bar graphs depicting the quantification of HUVEC (Fig. 8C) and HRMVEC (Fig. 8D) growth in the presence or absence of exogenously added RGD containing peptides P-1 or P-2. Data bars represent mean endothelial cell growth ( $\pm$  S.E) from 3 to 4 independent experiments expressed as percent of control. Fig. 8E is a Western blot of isolated nuclear fractions from cell lysates of endothelial cells (HRMVEC) following stimulation with soluble RGD containing collagen peptides P-1 or P2 and probed with YAP or total binding protein (TBP). Fig. 8F is a Western blot of isolated nuclear fractions from cell lysates of endothelial cells (HRMVEC) pre-incubated with Src or P38MAPK inhibitor and stimulation with soluble RGD containing collagen peptides P-1 or P-2 and probed with YAP or total binding protein (TBP). Fig. 8G and Fig. 8H are bar graphs depicting the quantification of endothelial cell growth in the presence or absence of exogenously added RGD containing peptides P-1 or P-2 from cells transduced with non-specific shRNA (Fig. 8G) or YAP specific shRNA (Fig. 8H). Data bars represent mean endothelial cell growth ( $\pm$  S.E) from 4 independent experiments. Fig. 8I is a bar graph depicting the quantification of endothelial cell growth in the presence or absence of exogenously added VEGF (50ng/ml) or 10% serum from cells transduced with YAP specific shRNA. Data bars represent mean endothelial cell growth ( $\pm$  S.E) from 4 independent experiments. \*  $P < 0.05$ .

Fig. 9 is a bar graph depicting that Mab XL313 enhances the anti-tumor activity of the immune checkpoint inhibitor for anti-PDL-1 antibody. Mice (C57BL/6) were injected with  $3.5 \times 10^5$  B16F10 melanoma cells. Mice were allowed to establish pre-existing tumors for 5 days prior to treatment. Mice were treated (100  $\mu\text{g}/\text{mouse}$ ) 3 times per week for 14 days. Data represents mean tumor volume at day 14  $\pm$  SE from 8 mice per condition.  $P < 0.05$  was considered significant.

Fig. 10 are images depicting that enhanced expression of PDL-1 in human M21 melanoma tumors as compared to M21L melanoma tumors lack  $\alpha\beta3$ . Mice (nude) were injected with either M21 ( $\alpha\beta3$  +) or M21L ( $\alpha\beta3$  -) melanoma cells. Mice were allowed to establish pre-existing tumors. Mice were sacrificed and tumors dissected and snap frozen. Tumor sections were analyzed for expression of the immune checkpoint regulatory protein PDL-1 by immunofluorescence staining. Red color indicates expression of PDL-1. Control indicates staining with secondary antibody only.

Fig. 11 are images depicting enhanced expression of PDL-1 in human M21 melanoma tumors as compared to M21 melanoma tumors in which  $\beta3$  integrin was knocked down. M21 melanoma cells that express integrin  $\alpha\beta3$  were transfected with non-specific control shRNA (M21 Cont) or  $\beta3$  specific shRNA (M21 $\beta3$ Kd). Mice (nude) were injected with either M21 Cont ( $\alpha\beta3+$ ) or M21 $\beta3$ Kd ( $\alpha\beta3-$ ) melanoma cells. Mice were allowed to establish pre-existing tumors. Mice were sacrificed and tumors dissected and snap frozen. Tumor sections were analyzed for expression of the immune checkpoint regulatory protein PDL-1 by immunofluorescence staining. Red color indicates expression of PDL-1. Control indicates staining secondary antibody only.

Fig. 12 are images depicting reduced expression of PDL-1 in Melanoma tumors in mice treated with an antibody targeting the  $\alpha\beta3$  ligand (RGDKGE (SEQ ID NO: 1) containing XL313 collagen epitope). Mice (C57BL/6) were injected with  $3.5 \times 10^5$  B16F10 melanoma cells. Mice were allowed to establish pre-existing tumors for 5 days prior to treatment. Mice were treated (100 $\mu$ g/mouse) 3 times a week for 14 days with an antibody targeting the  $\alpha\beta3$  binding RGDKGE (SEQ ID NO: 1) containing collagen epitope. Mice were sacrificed and tumors dissected and snap frozen. Tumor sections were analyzed for expression of the immune checkpoint regulatory protein PDL-1 by immunofluorescence staining. Red color indicates expression of PDL-1. Control indicates staining with secondary antibody only.

Fig. 13 are images depicting enhanced detection of lymphocytic infiltrates in melanoma tumors in mice treated with an antibody targeting the  $\alpha\beta3$  ligand (RGDKGE (SEQ ID NO: 1) containing XL313 collagen epitope). Mice (C57BL/6) were injected with  $3.5 \times 10^5$  B16F10 melanoma cells. Mice were allowed to establish pre-existing tumors

for 5 days prior to treatment. Mice were treated (100 $\mu$ g/mouse) 3 times a week for 14 days with an antibody targeting the  $\alpha$ v $\beta$ 3 binding RGDKGE (SEQ ID NO: 1) containing collagen epitope. Mice were sacrificed and tumors dissected. Tumor sections were analyzed for expression of the immune checkpoint regulatory protein PDL-1 by Giemsa staining. Black arrows indicate examples of areas with enhanced lymphocytic infiltrates.

Fig. 14A- Fig. 14C are blots depicting detection of enhanced levels of PDL-1 protein in melanoma and endothelial cells following binding to  $\alpha$ v $\beta$ 3 ECM ligand (denatured collagen-IV). Fig. 14A and Fig. 14B are blots of integrin  $\alpha$ v $\beta$ 3 expressing melanoma cells (M21 and CLL-49) and Fig. 14C is a blot depicting that endothelial cells (HUVEC) were allowed to attach to well coated with either a non- $\alpha$ v $\beta$ 3 binding ligand (native collagen-IV) or an  $\alpha$ v $\beta$ 3 binding ligand (denatured collagen-IV). Whole cell lysates were prepared and the relative levels of PDL-1 or loading control  $\beta$ -actin were assessed by Western blot.

Fig. 15 is a blot depicting enhanced levels of PDL-1 protein in melanoma cells following binding to  $\alpha$ v $\beta$ 3 ligand XL313 epitope (RGDKGE (SEQ ID NO: 1)). Integrin  $\alpha$ v $\beta$ 3 expressing melanoma cells (M21) were seeded on control uncoated wells or wells immobilized with the XL313 cryptic collagen epitope (RGDKGE (SEQ ID NO: 1)). Following a 15 minute incubation cell lysates were prepared. The relative levels of PDL-1 or loading control  $\beta$ -actin were assessed by Western blot.

Fig. 16 is a blot depicting a reduction in the levels of PDL-1 protein in melanoma cells following blocking binding to  $\alpha$ v $\beta$ 3 ECM ligand (denatured collagen-IV) with a  $\alpha$ v $\beta$ 3 specific antibody LM609. Integrin  $\alpha$ v $\beta$ 3 expressing melanoma cells (M21) were mixed with a control non-specific (normal mouse Ig) or  $\alpha$ v $\beta$ 3 specific antibody (Mab LM609) and added to wells coated with the  $\alpha$ v $\beta$ 3 binding ligand (denatured collagen-IV). Whole cell lysates were prepared following a 24 hour incubation period and the relative levels of PDL-1 or loading control  $\beta$ -actin were assessed by Western blot.

Fig. 17A- Fig. 17D show the generation of the HU177 epitope in ovarian tumors. Biopsies from frozen sections of malignant human ovarian tumors or benign granulomas were stained with Hematoxylin and Eosin (H&E) or with anti-HU177 antibody. Fig. 17A shows examples of H&E staining (left panel) or staining for the HU177 cryptic collagen

epitope (right panel) in malignant ovarian tumors. Fig. 17B shows examples of H&E staining (left panel) or staining for the HU177 cryptic collagen epitope (right panel) in benign granulomas. Fig. 17C shows the quantification of the relative levels of HU177 epitope within malignant ovarian tumors or benign granulomas. Data bars represent the mean relative levels of HU177 epitope + S.E from five 200X fields. \*  $P < 0.05$  as compared to controls. Fig. 17D shows examples of HU177 epitope (red) within SKOV-3 tumors, or normal ovaries, lungs and liver. Photos were at 200X. Scale bar 63 microns.

Fig. 18A- Fig. 18C show the inhibition of tumor growth by targeting the HU177 epitope. Fig. 18A and Fig. 18B shows graphs wherein SKOV-3 cells were seeded topically on the CAMs of chick embryos. Twenty-four hours later, the animals were untreated (NT) or treated once topically with anti-HU177 (100ug) or control antibody (100ug). Fig. 18A shows examples of tumors from each condition. Fig. 18B shows the quantification of mean tumor weights from each condition following a 7-day incubation period. Data bars represent mean tumor weights + S.E from 7 to 8 animals per condition. Fig. 18C is a graph wherein mice were injected subcutaneously in the flanks with SKOV-3 cells and 5 days later were untreated or treated i.p (100ug) with anti-HU177 antibody or control antibody 3 times per week for 28 days. Data points represent mean tumor volume + SE from 5 to 6 animals per condition. \*  $P < 0.05$  as compared to controls.

Fig. 19A- Fig. 19D show the analysis of SKOV-3 tumors growing in mice. Mice were injected subcutaneously in the flanks with SKOV-3 cells and following a 5-day incubation period were untreated or treated i.p with anti-HU177 (100ug) or control antibodies (100ug) 3 times per week for 28 days. Fig. 19A shows the analysis of the relative levels of Ki67 expression per 200X field + SE in SKOV-3 tumors. Fig. 19B (Top) shows an example of co-expression of CD-31 (green) and HU177 epitope (red) in untreated SKOV-3 tumors. Fig. 19B (Bottom) shows an example of co-expression of  $\alpha$ SMA (red) and HU177 epitope (green) in untreated SKOV-3 tumors. Fig. 19C is a photomicrograph wherein mice were injected subcutaneously in the flanks with SKOV-3 cells and following a 5 day incubation period were either untreated or treated i.p with 100ug of anti-HU177 or control antibody 3 times per week for 28 days. Fig. 19C (Top panels) show

examples of tumors from each condition stained for CD-31 (red). Fig. 19C (Bottom panel) show quantification of tumor angiogenesis with data bars representing mean vessels per 100X field + SE. Fig. 19D is a photomicrograph wherein mice were injected subcutaneously in the flanks with SKOV-3 cells and following a 5 day incubation period were either untreated or treated i.p with 100ug of anti-HU177 or control antibody 3 times per week for 28 days. Fig. 19D (Top panels) show examples of tumors from each condition stained for  $\alpha$ SMA (red). Fig. 19D (Bottom panel) shows quantification  $\alpha$ SMA expressing infiltrating stromal cells with data bars representing mean  $\alpha$ SMA expression per 100X field + SE. Scale bar 126 microns. \*P<0.05 as compared to controls.

Fig. 20A- Fig. 20D is a series of bar graphs showing that SKOV-3 tumor cells and fibroblast exhibit enhanced adhesion and migration on denatured collagen. Non-tissue culture wells and membranes from transwell migration chambers were coated with 5.0 ug/ml of native collagen (Nat-Coll) or denatured collagen (Den- Coll). SKOV-3 cells (Fig. 20A and Fig. 20C) or fibroblasts (Fig. 20B and Fig. 20D) were allowed to attach or migrate on either native or denatured collagen. Fig. 20A is a bar graph showing the quantification of mean SKOV-3 cell adhesion. Data bars represent mean cell adhesion + SE from 4 independent experiments expressed as percent of control with adhesion on native collagen set at 100%. Fig. 20B is a bar graph showing the quantification of mean fibroblast cell adhesion. Data bars represent mean cell adhesion + SE from 4 independent experiments expressed as percent of control with adhesion on native collagen set at 100%. Fig. 20C is a bar graph showing the quantification of mean SKOV-3 cell migration. Data bars represent mean cell migration + SE from 3 independent experiments expressed as percent of control with migration on native collagen set at 100%. Fig. 20D is a bar graph showing the quantification of mean fibroblast cell migration. Data bars represent mean cell migration + SE from 4 independent experiments expressed as percent of control with migration on native collagen set at 100%. \* P<0.05 as compared to controls.

Fig. 21A- Fig. 21H show that blocking the HU177 epitope inhibits basal adhesion and migration on denatured collagen. Non-tissue culture wells and membranes from transwell migration chambers were coated with 5.0ug/ml of native collagen or denatured collagen. SKOV-3 cells (Fig. 21A, Fig. 21B, Fig. 21E and Fig. 21F) or fibroblasts (Fig.

21C, Fig. 21D, Fig. 21G and Fig. 21H) were allowed to attach or migrate on either native or denatured collagen in the presence or absence of anti-HU177 antibody or control antibody (50ug/ml). Fig. 21A and Fig. 21B are bar graphs that show quantification of SKOV-3 cell adhesion to denatured or native collagen in the presence or absence of anti-HU177 or control antibody. Data bars represent mean cell adhesion indicated as percent of control + SE from 4 to 5 independent experiments with no treatment set at 100%. Fig. 21C and Fig. 21D are bar graphs that show quantification of fibroblast cell adhesion to denatured or native collagen in the presence or absence of anti-HU177 or control antibody. Data bars represent mean cell adhesion indicated as percent of control + SE from 3 to 7 independent experiments with no treatment set at 100%. Fig. 21E and Fig. 21F are bar graphs showing quantification of SKOV-3 cell migration on denatured or native collagen in the presence or absence of anti-HU177 or control antibody. Data bars represent mean cell migration indicated as percent of control + SE from 4 independent experiments with no treatment set at 100%. Fig. 21G and Fig. 21H are bar graphs showing the quantification of fibroblast cell migration on denatured or native collagen in the presence or absence of anti-HU177 or control antibody. Data bars represent mean cell migration indicated as percent of control + SE from 3 to 4 independent experiments with no treatment set at 100%. \*  $P < 0.05$  as compared to controls.

Fig. 22A- Fig. 22E are a series of bar charts and an immunoblot showing that targeting the HU177 epitope inhibits growth factor induced migration and Erk phosphorylation. Fibroblasts were resuspended in the presence or absence of SKOV-3 CM (Fig. 22A) or FGF-2 (Fig. 22B) in the presence or absence of anti-HU177 or control antibodies (50ug/ml). Fig. 22A and Fig. 22B are bar charts showing the quantification of fibroblasts cell migration on denatured collagen. Data bars represent mean migration indicated as percent of control + SE from 3 independent experiments. Fig. 22C is a photograph showing Western blot analysis of Erk in lysates from fibroblasts seeded on denatured collagen in the presence or absence of anti-HU177 or control antibody (50ug/ml). Fig. 22D is a bar chart showing the quantification of mean FGF2-induced Erk phosphorylation in the presence or absence of anti-HU177 antibody or control antibody from fibroblasts seeded on denatured collagen from 4 independent experiments. Fig. 22E

is a bar chart wherein fibroblasts were resuspended in the presence or absence of FGF2 and in the presence or absence of Mek inhibitor and allowed to migrate on denatured collagen. Data bars indicate mean cell migration indicated as percent of control + SE from 3 independent experiments. \*  $P < 0.05$  as compared to controls.

Fig. 23A- Fig. 23G show that integrin  $\alpha 10\beta 1$  binds the HU177 collagen epitope. Wells were coated with denatured collagen (Fig. 23A, and Fig. 23C- Fig. 23E), integrins  $\alpha 10\beta 1$  and  $\alpha 3\beta 1$  (Fig. 23B) or the synthetic HU177 epitope peptide or control peptide (Fig. 23F) and integrins (Fig. 23A, Fig. 23C- Fig. 23E) or denatured collagen (Fig. 23B) and allowed to bind. Fig. 23A is a line graph showing integrin binding to denatured collagen. Fig. 23B is a line graph showing binding of denatured collagen to immobilized integrins. Fig. 23C is a bar graph showing binding of  $\alpha 10\beta 1$  to denatured collagen in the presence or absence of anti-HU177 or control antibodies. Fig. 23D is a bar graph showing the binding of  $\alpha 2\beta 1$  to denatured collagen in the presence or absence of anti-HU177 or control antibodies. Fig. 23E is a bar graph showing the binding of  $\alpha V\beta 3$  to denatured collagen in the presence or absence of anti-HU177 or control antibodies. Fig. 23F is a bar graph showing integrin binding to synthetic HU177 epitope or control peptide. Fig. 23G is a bar graph showing integrin binding to denatured collagen in the presence of synthetic HU177 epitope or control peptide. Experiments were completed at least 3 times. \* $P < 0.05$  as compared to controls.

Fig. 24A- Fig. 24I is a series of photomicrographs, immunoblots, and bar charts showing the expression and migratory function of  $\alpha 10\beta 1$ . Fig. 24A is a photomicrograph showing an example of expression of  $\alpha 10\beta 1$  (green) in human ovarian tumor biopsy (left) and SKOV-3 tumors (right). Fig. 24B is a photomicrograph of an example of coexpression of  $\alpha 10\beta 1$  (green) and  $\alpha$ SMA (red) expressing stromal cells within SKOV-3 tumors. Photos were at 200X. Fig. 24C is an analysis of  $\alpha 10\beta 1$  expression in SKOV-3 cells or fibroblasts (HF) by western blot. Fig. 24D is a bar graph showing the quantification of FGF-2-induced fibroblasts migration in the presence or absence of anti- $\alpha 10\beta 1$  antibody or control. Data bars represent mean migration indicated as percent of control + SE from 3 independent experiments. Fig. 24E is a Western blot analysis of relative expression of  $\alpha 10$  integrin,  $\alpha 1$  integrin or  $\beta$ -actin in cell lysates from non-specific

control knock down fibroblasts (Con-Kd-HF) or  $\alpha 10$  integrin knock down fibroblasts ( $\alpha 10$ -Kd-HF). Fig. 24F is a bar chart showing the quantification of FGF-2-induced migration of wild type (WT-HF),  $\alpha 10$  integrin knock down fibroblasts ( $\alpha 10$ -Kd-HF) or non-specific control knock down fibroblasts (Con-Kd-HF) on denatured collagen. Data bars represent mean migration indicated as percent of control + SE from 3 independent experiments. Fig. 24G is a bar chart of SKOV-3 cell proliferation in the presence of control or fibroblast CM. Data bars represent mean O.D 490nm + SE. Fig. 24H is a Western blot analysis for Ki67 in lysates of SKOV-3 cells treated with fibroblast CM. Fig. 24I is a bar chart showing SKOV-3 proliferation in the presence or absence of fibroblast CM and in the presence of anti-IL-6 or control antibodies. Data bars represent mean O.D 490nm + SE. All experiments were completed at least 3 times with similar results. Scale bar 63 microns. \*  $P < 0.05$  as compared to controls.

Fig. 25A- Fig. 25D is a series of bar charts showing that the HU177 collagen epitope is recognized by integrin  $\alpha 10\beta 1$  which regulates expression of the immune suppressive cytokine IL-10. Fig. 25A is a bar chart wherein a peptide (cPG) containing the HU177 collagen epitope CPGFPGFC (SEQ ID NO: 16) was immobilized on microtiter wells and the ability of recombinant integrin receptors to bind was analyzed by ELISA. Data bars represent mean integrin binding to the HU177 collagen epitope. Fig. 25B- Fig. 25D is a series of bar charts showing that the expression of  $\alpha 10$  integrin chain in human C8161 melanoma cells was reduced by transfection of shRNA directed to the  $\alpha 10$  integrin chain. Twenty-four hour serum free conditioned medium from each melanoma variant was concentrated 10X and analyzed for the relative levels of cytokines. Fig. 25B is a bar graph wherein data bars represent relative levels of IL-10 as determined by ELISA. Fig. 25C is a bar graph wherein data bars represent relative levels of IL-2 as determined by ELISA. Fig. 25D is a bar graph wherein data bars represent relative levels of IL-4 as determined by ELISA.

Fig. 26A- Fig. 26C is a series of bar charts showing that the injection of a peptide (cPG) containing the HU177 collagen epitope induces expression of the immune suppressive growth factor TGF- $\beta$  in mouse circulation. C57BL/6 mice were injected subcutaneously with B16F10 melanoma cells ( $0.5 \times 10^6$ ) and tumors were allowed to form.

Mice were next injected 3X per week with 10ug per mouse of cPG peptide. Serum was collaged after 14 days. Serum was diluted in assay buffer and the relative levels of cytokines were examined by ELISA. Fig. 26A is a bar graph wherein data bars represent relative levels of TGF- $\beta$  as determined by ELISA from control (DMSO) treated mouse and two different cPG peptide treated mice. Fig. 26B is a bar graph wherein data bars represent relative levels of IL-4 as determined by ELISA from control (DMSO) treated mouse and two different cPG peptide treated mice. Fig. 26C is a bar graph wherein data bars represent relative levels of IL-1 $\beta$  as determined by ELISA from control (DMSO) treated mouse and two different cPG peptide treated mice.

Fig. 27A- Fig. 27B is a series of bar graphs showing that Mab HU177 enhances the anti-tumor activity of the immune checkpoint inhibitor anti-PDL-1 antibody. Mice (C57BL/6) were injected with  $3.5 \times 10^5$  B16F10 melanoma cells. Mice were allowed establish pre-existing tumors for 5 days prior to treatment. Mice were treated (100ug/mouse) with either anti-PD-L1 antibody alone, Anti-HU177 antibody alone or a combination of both antibodies 3 times a week for 15 days. Fig. 27A is a bar graph wherein data represents mean tumor volume at day 7 + SE from 7 mice per condition. Fig. 27B is a bar graph wherein data represents mean tumor volume at day 15 + SE from 7 mice per condition.

Fig. 28 is a bar graph showing that synthetic collagen peptides containing the amino acid sequence, RGD, support T-cell adhesion.

Fig. 29 is a bar graph showing that monoclonal antibody, Mab XL313, inhibits interactions between human T-cell and the cryptic collagen epitope peptide P-2 (CQGPRGDKGEC; SEQ ID NO: 6).

Fig. 30 is a line graph showing that the integrin receptor  $\alpha\beta3$  dose-dependently binds to the cryptic collagen epitope peptide P-2.

Fig. 31 is a bar graph showing that Mab XL313 inhibits recombinant integrin receptor  $\alpha\beta3$  binding to the cryptic collagen epitope peptide P-2.

Fig. 32 is a photograph of an immunoblot showing that reducing the expression of  $\beta3$  integrin leads to reduced expression of PD-L1 in human T cells.

Fig. 33 is a series of photographs of immunoblots showing that reducing the expression of B3 integrin prevents stimulation of PD-L1 by the XL313 cryptic collagen peptide P2 in human T cells.

Fig. 34 is a series of bar graphs showing that anti- XL313 antibody reverses the inhibitory effects of the cryptic collagen peptide P2 on T-cell migration.

Fig. 35 is a series of photographs of immunoblots showing that the cryptic collagen peptide P2 induces expression of the immunosuppressive molecule LAG3 in human T-cells.

Fig. 36 is a series of photomicrographs and a bar chart showing that anti-XL313 Mab reduces the levels of the immune suppressive molecule LAG-3 in melanoma tumors *in vivo*.

Fig. 37 is a bar chart showing that anti-XL313 Mab enhances the levels of CD8+ T cells in melanoma tumors *in vivo*.

Fig. 38 is a bar chart showing that anti-HU177 Mab reduces the levels of immune suppressive CD4+/CTLA-4 positive T-Reg cells in melanoma tumors *in vivo*.

### DETAILED DESCRIPTION OF THE INVENTION

Described herein is an RGD containing cryptic collagen epitope that is generated *in vivo*. As described in detail below, rather than inhibiting  $\alpha\beta3$  signaling, this collagen epitope promoted  $\alpha\beta3$  activation and stimulated angiogenesis and inflammation. Additionally, an antagonist of integrin  $\alpha\beta3$  that inhibits signaling from this receptor was used to enhance the therapeutic activity of PD-1/PDL-1 targeting drugs for the treatment of cancer and other diseases characterized by abnormal immune response. Also described herein is an antagonist specifically directed to the HU177 cryptic collagen epitope that is used to enhance the therapeutic activity of immune checkpoint targeting drugs for the treatment of cancer.

Also described herein is an endothelial cell mechano-signaling pathway in which a cryptic collagen epitope activates  $\alpha\beta3$  leading to a Src and P38MAPK-dependent cascade that leads to nuclear accumulation of YAP and stimulation of endothelial cell growth is defined. Collectively, the findings provide evidence for a mechano-signaling pathway,

but also define a potential therapeutic strategy to control  $\alpha\beta 3$  signaling by targeting a pro-angiogenic and inflammatory ligand of  $\alpha\beta 3$  rather than the receptor itself.

Angiogenesis, the process by which new blood vessels form from pre-existing vessels plays a critical role in normal and pathological events. Efforts are underway to more precisely define the interconnected mechanisms that control this crucial biological process in order to develop more effective strategies to control neovascular diseases (1, 2). Significant advances have been made in identifying molecular regulators of angiogenesis and their associated signaling pathways (3-5). A more precise understanding of angiogenic signaling pathways and the networks of regulatory feedback loops operating within distinct cellular compartments has provided important clues to help explain the modest clinical impact of many anti-angiogenic strategies (1-5). For example, while vascular endothelial growth factor (VEGF) induces pro-angiogenic signaling leading to enhanced endothelial cell migration, growth, and survival, VEGF-induced blood vessels are often characterized as immature, unstable, and leaky and can regress in the absence of additional signaling events (6). VEGF stimulation under specific circumstances may lead to inhibition of angiogenesis in the context of altered PDGF signaling do to disruption of pericyte recruitment (6). These unexpected findings provide evidence of a negative role for the VEGF/VEGFR signaling during new vessel development (6). Similarly, studies have provided evidence for both a positive and a negative role for integrin  $\alpha\beta 3$  in angiogenesis (7-9).

A wide array of alterations in the composition and biomechanical properties of extracellular matrix (ECM) proteins are known to occur during angiogenesis and studies are beginning to define how these changes contribute to new blood vessel development (18,21-23,51-53). Among the key cell surface molecules that play roles in mechano-transduction to facilitate information flow from outside the cell to the inside are integrin receptors. Integrins may act like information hubs by sensing diverse extracellular inputs and relaying this information into a complex network of intracellular circuits that ultimately modulate cellular behavior (4). The precise molecular mechanisms by which cells fine-tune their response to changes within the stromal microenvironment are not completely understood. Further complicating the understanding of new vessel

development is the expanding number of cell types that contribute to tissue specific control of angiogenesis such as distinct subsets of stromal fibroblasts, progenitor cells and a variety of inflammatory cells such as neutrophils, mast cells and macrophages. The roles played by these diverse cells during angiogenesis range from secretion of cytokines, chemokines and proteolytic enzymes to the differential expression of other pro and anti-angiogenic factors. Thus, tight control mechanisms must operate to allow coordination between these diverse compartments to govern tissue specific vascular responses.

Integrins are molecules with the ability to detect compositional and structural changes within the ECM and integrate this information into a network of signaling circuits that coordinate context dependent cell behavior. Among the most well studied integrins known to play a role in angiogenesis is  $\alpha\beta3$ . The complexity by which  $\alpha\beta3$  regulates angiogenesis is illustrated by the fact that this receptor may exhibit both pro and anti-angiogenic functions (7-15). It is indicated that the distinct biological responses stimulated by binding to  $\alpha\beta3$  may depend on many factors including the mechanical and biochemical features of the particular ligands, the cell types within which  $\alpha\beta3$  is expressed as well as the concentration and manner by which the ligands are presented to the receptor (7-9,24-27). For example, studies indicate that  $\alpha\beta3$  binding to specific NC1 domains of collagen or selected RGD peptides can induce apoptosis, induce arteriole contraction and inhibit angiogenesis (19,29,54) while other  $\alpha\beta3$  ligands may promote cell survival, induce vascular dilation and support angiogenesis (21-23,30,55). These observations are consistent with the notion that the final outcome of  $\alpha\beta3$ -mediated signaling may depend to a large extent on the particular characteristics of the ligand. While a wealth of data has shown that RGD peptides can inhibit angiogenesis when administered exogenously, the approach of using a cyclic RGD peptide to control tumor growth failed to significantly impact glioblastoma progression and patient survival in late stage clinical testing (31). Interestingly, studies have indicated that specific RGD peptides may activate  $\beta3$  integrins (56, 57) and under defined experimental conditions induce angiogenesis and tumor growth (30). These findings and other studies suggesting that amino acids C-terminal to the RGD motif play roles in governing integrin selective binding, prompted the

examination of the biological significance of naturally occurring RGD containing epitopes on angiogenesis.

For example, multiple pro-angiogenic roles have been proposed for  $\alpha\beta3$  as cyclic arginine-glycine-aspartic acid (RGD) containing peptides and antibodies targeting this integrin inhibit angiogenesis in animal models (10-12). In contrast, enhanced angiogenesis was detected in tumors growing in  $\alpha\beta3$  null mice (13). Interestingly, reduced pathological angiogenesis was detected in transgenic mice expressing signaling deficient  $\beta3$  integrin, which resulted in part from defective recruitment of bone marrow derived cells rather than specific endothelial cell defects (14). Moreover, evidence suggests that  $\beta3$  integrin may play a more prominent role in the early stages of angiogenesis when new vessels begin to form, as reduction in endothelial cell expression of  $\beta3$  integrin impaired early stage pathological angiogenesis, but had little effect on later maturation stages once vessels had formed (15). These studies, together with many others suggests  $\alpha\beta3$ -mediated regulation of angiogenesis is complex, temporally regulated and is not solely dependent on adhesive events, but also involves downstream signaling, the consequences of which may depend on the cell type and composition of the local extracellular microenvironment (4,9,12,16). Because of the opposing biological responses observed following modulation of some angiogenic regulatory molecules, it is not surprising that anti-angiogenic strategies based on targeting these factors have met with limited clinical success.

Given the importance of integrin-extracellular matrix (ECM) interactions in modulating the intensity and specificity of growth factor signaling (1-5, 17, 18), it is important to define how diverse components within the local vascular microenvironment function cooperatively to regulate angiogenesis. Interestingly, distinct  $\alpha\beta3$  ligands may stimulate opposing biological outcomes (7-15). For example, certain NC1 domains of collagen may bind  $\alpha\beta3$  and induce proapoptotic responses while binding of other  $\alpha\beta3$  ligands may promote cell growth and survival (19-22). Given these findings and the complex biological effects observed following direct targeting of  $\alpha\beta3$ , an alternative therapeutic approach to control signaling from  $\alpha\beta3$  might involve specific targeting of the pro-angiogenic ligands of  $\alpha\beta3$  rather than directly targeting the receptor itself.

Proteolytic remodeling of the ECM can generate integrin binding cryptic epitopes that play functional roles in angiogenesis including the LPGxPG containing HU177 cryptic epitope present in multiple types of collagen and the HUIV26 cryptic epitope, which is present in collagen type-IV (21-23). While the HUIV26 epitope is recognized by  $\alpha v\beta 3$ , it is not specifically composed of an RGD motif (21).

Sequence analysis of RGD sites within collagen type-I indicate that the KGE tripeptide motif that is C-terminal to the RGD site was highly conserved among diverse species, while considerable variation is observed in the other collagen RGD flanking sequences. While all five of the collagen RGD epitopes can support cell binding, the highly conserved RGDKGE (SEQ ID NO: 1) collagen peptide P-2 may play a functional role angiogenesis and inflammation given that Mab XL313 directed to this epitope but not an antibody that recognizes the other three RGD collagen sites inhibited angiogenesis and inflammation *in vivo*. While the precise difference between the three other naturally occurring non-RGDKGE (SEQ ID NO: 1) containing collagen epitopes, one or more of these epitopes were detected *in vivo* in addition to the RGDKGE (SEQ ID NO: 1) epitope. Given that these RGD containing epitopes are thought to be largely cryptic and not readily accessible to cell surface receptor, the findings are consistent with active collagen remodeling resulting in generation neoepitopes during new vessel formation.

Because of the importance of RGD sequences in mediating some integrin-dependent interactions and the roles of amino acids flanking the core RGD motif in establishing integrin-binding specificity and affinity (24-27), the ability of RGD motifs within collagen differentially regulate angiogenesis was determined. Sequence analysis of collagen type-I revealed that five different cryptic RGD motifs are present, each with unique flanking sequences. Surprisingly, the C-terminal KGE flanking sequence of one of these RGD motifs is highly conserved in species as diverse as xenopus and man. In contrast, significant sequence and positional variation exists within the other flanking sequences among different species.

ECM remodeling occurs as an early event during angiogenesis and multiple proteolytic enzymes including matrix metalloproteinase (MMPs) as well as serine and cysteine proteases the have the capacity to degrade intact or structurally altered forms of

collagen (18,58). While the *in vitro* studies indicate that MMP-2-mediated degradation of collagen can lead to the generation of low molecular weight fragments recognized by Mab XL313, the precise mechanism by which the RGDKGE (SEQ ID NO: 1) collagen epitope is generated *in vivo* is not completely understood. Analysis of angiogenic CAM tissues suggests that a subset of macrophages may be an important source of the RGDKGE (SEQ ID NO: 1) epitope. Activated macrophages with M2-like characteristics can express multiple enzymes capable of degrading collagen and in turn can internalize and further degrade collagen into small low molecular weight fragments (35,38). While little evidence exist that macrophages generate and deposit intact triple helical collagen type-I, studies have indicated that certain isoforms of collagen may be expressed (59). Consistent with previous reports, intact collagen was detected; however low molecular weight RGDKGE (SEQ ID NO: 1) containing collagen fragments in both whole cell lysates and serum free conditioned medium from macrophage like cell lines was detected. While the studies do not rule out macrophage mediated collagen internalization as a contributing factor to the *in vivo* generation the RGDKGE (SEQ ID NO: 1) collagen epitope, the *in vitro* studies were carried out in the absence of serum or exogenously added collagen, and thus are consistent the active generation of the RGDKGE (SEQ ID NO: 1) collagen fragment by macrophages.

Activated macrophages including M2-polarized macrophages have been implicated in supporting angiogenesis and inflammation as multiple factors secreted by these cells exhibit pro- angiogenic activities (35,60). While many studies indicate that synthetic RGD containing peptides inhibit angiogenesis and tumor growth, the findings provide the first evidence that macrophages may generate and release an RGDKGE (SEQ ID NO: 1) containing collagen epitope that may exhibit pro-angiogenic activity. Importantly, previous studies have suggested that certain RGD-peptides can activate  $\alpha v \beta 3$  (56,57) and may enhance vascular permeability (45,55), which might lead to release of inflammatory factors, which may in turn contribute to the formation of new blood vessels.

To examine possible mechanisms by which the RGDKGE (SEQ ID NO: 1) collagen peptide might regulate angiogenesis endothelial cell receptors for this motif were

identified. While the possibility that additional non-integrin receptors may bind this collagen epitope is not ruled out, the data suggest that  $\alpha\beta3$  can function as an endothelial cell receptor for the RGDKGE (SEQ ID NO: 1) motif. Interestingly,  $\alpha\beta3$  bound both the RGDKGE (SEQ ID NO: 1) and RGDAPG (SEQ ID NO: 11) collagen peptides, yet only RGDKGE (SEQ ID NO: 1) peptide significantly induced angiogenesis and inflammation *in vivo*. These findings are consistent with the notion that distinct RGD containing  $\alpha\beta3$  ligands may promote different biological responses. Signaling downstream from  $\alpha\beta3$  is complex and studies have indicated that simple binding of  $\beta3$  integrin does not necessarily lead to productive outside-in integrin signaling (61). In fact, the capacity of  $\beta3$  integrins to promote outside-in signaling depends on multiple factors including the extent of receptor clustering and subsequent generation of mechanical tension within the actin cytoskeleton, recruitment of adaptor and accessory proteins such as Ga13, and Kindlin-2 and the association of the integrin with protein tyrosine phosphatases and certain growth factor receptors (62-65). While the exact mechanisms leading to RGDKGE (SEQ ID NO: 1) - mediated  $\alpha\beta3$  signaling is not completely understood, endothelial cell interactions with the RGDKGE (SEQ ID NO: 1) peptide in the absence of serum led to enhanced phosphorylation of  $\beta3$  integrin on tyrosine 747 and of Src phosphorylation at tyrosine 416. These data and others are consistent with an early mechanical mediated activation of  $\beta3$  integrin that depends on Src given that blocking Src activity reduced  $\beta3$  phosphorylation following binding to the RGDKGE (SEQ ID NO: 1) motif.

Integrin signaling and Src activation are known to regulate the architecture of the actin cytoskeleton (66). Moreover, Src family kinases regulate P38MAPK, and activation of P38MAPK is thought to enhance actin stress fiber formation in endothelial cells and regulate angiogenesis *in vivo* (39-45). The findings provide insight into the coordinated roles of P38MAPK and Src in regulating RGD-dependent endothelial cell signaling through  $\alpha\beta3$  as interactions with the RGDKGE (SEQ ID NO: 1) cryptic collagen epitope leads to enhanced P38MAPK phosphorylation in a Src-dependent manner. Moreover, RGDKGE (SEQ ID NO: 1) -induced angiogenesis *in vivo* was associated with enhanced levels of phosphorylated P38MAPK, and this angiogenic response was reduced by an

inhibitor of P38MAPK. These findings are consistent with the notion that RGDKGE (SEQ ID NO: 1) stimulated angiogenesis depends on P38MAPK.

Recent studies have suggested a role for actin stress fibers and mechanical tension in promoting nuclear accumulation of YAP, where it is thought to function in conjunction TEAD transcription factors in regulating gene expression (46-50). Given data suggesting a role for YAP in regulating endothelial cell growth and angiogenesis, the subcellular distribution of YAP in endothelial cells following interaction with the RGDKGE (SEQ ID NO: 1) collagen peptide was examined. The data indicate that endothelial cell interaction with the RGDKGE (SEQ ID NO: 1) epitope was associated with enhanced nuclear accumulation of YAP. Integrin signaling may play a role in the regulation of YAP as studies have implicated a role for  $\beta 1$  integrins expressed in skeletal stem cells and  $\alpha \nu$  integrins expressed in osteoblasts in governing YAP subcellular localization (67,68). The findings are consistent with a mechanism by which  $\alpha \nu \beta 3$ -mediated binding to the RGDKGE (SEQ ID NO: 1) epitope, but not the related RGDAPG (SEQ ID NO: 11) epitope stimulates a signaling cascade leading to enhanced nuclear accumulation of YAP that depends on Src and/or P38MAPK. This possibility is supported by the findings that reduced levels of nuclear YAP was detected following  $\alpha \nu \beta 3$ -mediated interaction with RGDKGE (SEQ ID NO: 1) peptide in endothelial cells in which Src or P38MAPK was inhibited. Given the documented role of YAP in governing cell growth coupled with the ability of the RGDKGE (SEQ ID NO: 1) collagen peptide to stimulate nuclear accumulation of YAP and enhance endothelial cell growth, it is possible that the RGDKGE (SEQ ID NO: 1) collagen peptide-induced endothelial cell growth is YAP dependent. Consistent with this possibility, no enhancement of endothelial cell growth was detected following knockdown of YAP in endothelial cells stimulated with the RGDKGE (SEQ ID NO: 1) collagen peptide, even though these cells are capable of proliferating as stimulation with VEGF or high levels of serum enhanced their growth. Given the studies, it is possible that part of the FGF-2 induced angiogenic response observed in the chick CAM model might involve the recruitment of macrophages that generate a previously uncharacterized RGDKGE (SEQ ID NO: 1) containing cryptic collagen epitope that binds to  $\alpha \nu \beta 3$  leading to Src and P38MAPK activation and nuclear

accumulation of YAP. Given that YAP is known to regulate a wide array of genes that may impact angiogenesis and inflammation including CTGF and Cry61, it is likely that the RGDKGE (SEQ ID NO: 1) collagen epitope may initiate a complex pro-angiogenic program in vivo involving YAP-associated regulation of multiple pro-angiogenic molecules and not simply be restricted to only enhancing endothelial cell growth.

Collectively, the results presented herein provide evidence that a highly conserved RGDKGE (SEQ ID NO: 1) containing collagen epitope can be generated by a subset of macrophages and the RGDKGE (SEQ ID NO: 1) collagen epitope can stimulate pro-inflammatory and angiogenic activity. Binding of the RGDKGE (SEQ ID NO: 1) collagen epitope to  $\beta 3$  integrin can initiate a signaling pathway in endothelial cells leading to activation of Src and P38MAPK ultimately leading to nuclear accumulation of YAP and enhance cell growth. The results presented herein provide cellular and molecular insight into how an endogenously generated RGD containing cryptic collagen epitope may promote rather than inhibit angiogenesis. Given the complexity of  $\alpha v\beta 3$  functions and the growing body of evidence that the final outcome of  $\alpha v\beta 3$  binding may depend on the nature of the particular ligand, the findings provide support for an alternative strategy to help control the biological activity of  $\beta 3$  integrin by specific targeting of endogenous pro-angiogenic ligands of  $\alpha v\beta 3$  rather than direct targeting of the receptor itself.

Integrin  $\alpha v\beta 3$  plays a functional role in promoting immune suppression in part by upregulating the expression of the immune checkpoint regulatory protein PDL-1. Thus, targeting  $\alpha v\beta 3$  with function blocking (signal blocking) antagonists of  $\alpha v\beta 3$  or reducing expression of  $\alpha v\beta 3$  led to reduced expression of PDL-1. Thus antagonist of  $\alpha v\beta 3$  may enhance the anti-tumor efficacy of immune checkpoint therapy. Importantly, while immune check point inhibitors are known to provide some anti-tumor activity in humans, this partial anti-tumor activity is only observed in a fraction of treated subjects. Described herein is the identification of compounds and combination treatment strategies to enhance the efficacy of immune checkpoint inhibitors such as CTLA-4, PDL-1 and PD-1 antibodies.

Therapeutic blockade of immune checkpoint regulatory molecules such as CTLA-4 and PD-1/PDL-1 signaling is known to be associated with significant immune related

side effects including inflammation. Given these known side effects of immune checkpoint therapy and the ability of specific ligands of  $\alpha\text{v}\beta\text{3}$  integrin such as the RGDKGE (SEQ ID NO: 1) containing collagen epitope to potentially induce inflammation *in vivo* (and the anti-stromal cell migratory activity of Mab HU177), combining antagonist of  $\alpha\text{v}\beta\text{3}$  (or an antagonist of HU177 or an antagonist of  $\alpha\text{10}\beta\text{1}$ ) with anti-PD-1/PDL-1 antagonists may reduce the inflammatory side effects associated with immune checkpoint inhibitor therapy.

Herein, is *in vivo* animal data, which indicate that melanoma tumors that express integrin  $\alpha\text{v}\beta\text{3}$  express the immune checkpoint protein PDL-1, while the same tumor cell type that was selected for lack of functional  $\alpha\text{v}\beta\text{3}$  exhibited little detectable PDL-1. Second, cellular interactions of tumor cells as well as endothelial cells with ECM proteins (denatured collagen and the RGDKGE (SEQ ID NO: 1) collagen epitope) that documented ligands of integrin  $\alpha\text{v}\beta\text{3}$  lead to upregulated expression of PDL-1. Third, a function blocking antibody directed specifically to integrin  $\alpha\text{v}\beta\text{3}$  reduced expression of PDL-1 in tumor cells. Finally, an antibody (Mab XL313) that specifically blocks the binding of an RGDKGE (SEQ ID NO: 1) epitope to  $\alpha\text{v}\beta\text{3}$  and inhibits downstream signaling from  $\alpha\text{v}\beta\text{3}$  enhanced the anti-tumor efficacy of an immune checkpoint inhibitor (anti-PDL-1) *in vivo*.

Previous studies have indicated that blockade of immune checkpoint proteins such as PDL-1, PD-1, and LAG-3 can result in some anti-tumor activity. These anti-tumor effects, however were only partial and only occurred in a fraction of the treated subjects. Thus, described herein is the identification of compounds that enhance the effect of immune checkpoint inhibitors such as antibodies targeting CTLA-4, PD-1 and/or PDL-1. To this end, studies have suggested that combining immune checkpoint inhibitors with other chemotherapy drugs may enhance the anti-tumor activity. Importantly, a common side effect that can limit the use of immune checkpoint inhibitors is the active induction of inflammatory conditions such as dermatitis, pneumonitis and colitis. Part of the inflammatory process *in vivo* may involve alterations in expression of inflammatory cytokines and infiltration of activated stromal cells such as activated fibroblasts. In this regard, as described in detail herein, antagonists of the XL313 epitope (Mab XL313) not

only enhance the therapeutic activity of an anti-PDL-1 antibody therapy in a mouse model (Fig. 9), but Mab XL313 epitope potently inhibits inflammation *in vivo*. Antagonists of the HU177 epitope (Mab HU177) not only enhance the therapeutic activity of an anti-PDL-1 antibody therapy in a mouse model (Fig. 27), but as described in detail below, Mab HU177 inhibits activated fibroblast migration and accumulation within tumors *in vivo*. Additionally a  $\alpha\beta3$  binding RGDKGE (SEQ ID NO: 1) containing collagen epitope that stimulates  $\alpha\beta3$  integrin signaling was shown to significantly enhance inflammation *in vivo*. Given these findings, it is possible that blocking  $\alpha\beta3$  signaling with an antagonist of  $\alpha\beta3$  would not only enhance the therapeutic activity of an anti-PDL-1/PD-1 or CTLA-4 based therapy, but may also potently inhibit inflammation *in vivo*. These findings are consistent with the notion that combining an antagonist of XL313 epitope (or antagonist of  $\alpha\beta3$ ) or an antagonist of HU177 epitope (or antagonist of  $\alpha10\beta1$ ) with immune checkpoint inhibitor therapy not only enhances its efficacy, but also reduces the inflammatory side effects observed with the immune checkpoint inhibitor therapy.

Described herein is evidence that an RGDKGE (SEQ ID NO: 1) containing cryptic collagen epitope is generated by a subset of macrophages and this motif promoted rather than inhibited angiogenesis. These findings are surprising given the wealth of experimental data indicating the high concentration of RGD peptides inhibit rather than induce angiogenesis (11, 28, 29). Increasing evidence suggests that low concentrations of certain RGD peptides may actually enhance angiogenesis and tumor growth (30), which may explain at least in part the minimal impact of cyclic RGD peptide antagonists of  $\alpha\beta3$  and  $\alpha\beta5$  in human clinical trials (31). In addition to variations in concentrations that alter the biological response of certain RGD peptides, the specific composition of the amino acids C-terminal to RGD motif within naturally occurring epitopes may confer unique pro-angiogenic and inflammatory activity. Taken together, these results are consistent with a mechanism by which the RGDKGE (SEQ ID NO: 1) collagen epitopes induce angiogenesis and inflammation by stimulating mechanical activation of  $\alpha\beta3$  leading to Src-dependent phosphorylation of P38MAPKinase that promotes nuclear accumulation of the Yes- associated protein (YAP) and enhanced endothelial cell growth.

## EXAMPLES

### Example 1: Materials and methods

#### Reagents, Kits, Chemicals and Antibodies

Ethanol, methanol, acetone, bovine serum albumin (BSA), crystal violet, phosphate-buffered saline (PBS), purified human collagen type-IV and collagen type-I, AMPA, 3,3',5,5'-tetramethylbenzidine (TMB), phosphatase inhibitor cocktail, and cortisone acetate (CA) were from Sigma (St Louis, MO). MMP2 was from Chemicon/Millipore (Billerica, MA). FBS was from Science Cell (Carlsbad, CA). Fibroblast growth factor-2 (FGF-2) was obtained from R&D Systems (Minneapolis, MN). Nuclear/Cytoplasmic fractionation kit was from Thermo Scientific (Waltham, MA). P38MAPK inhibitor, SB202190 was obtained from CalBiochem (San Diego, CA). RIPA buffer, protease inhibitor, and Src inhibitor (PP2) were from Santa Cruz (Santa Cruz, CA). Anti-vWf antibody was from BD Pharmingen (San Diego, CA). Antibodies directed to P38MAPK, phospho-P38MAPK (Thr-180/Tyr-182), Src, and phospho-Src (Tyr 416), were from Cell Signaling Technology (Danvers, MA). Antibodies against tubulin, total binding protein (TBP), YAP,  $\beta$ 3, and phospho-133 (Tyr747) were from Santa Cruz (Santa Cruz, CA). Anti-Igfbp4 and anti-MMP9 antibodies were obtained from Abcam (Cambridge, MA). Function blocking antibodies P4C10 (anti- $\beta$ 1), LM609 (anti- $\alpha$ v  $\beta$ 3) and P1F6 (anti- $\alpha$ v  $\beta$ 5) were from R&D Systems (Minneapolis, MN). HRP-conjugated secondary antibodies were from Promega (Madison, WI). Anti-collagen type-I antibody was from Rockland (Limerick, PA) and anti-collagen type-IV was from Millipore (Billerica, MA). Mouse monoclonal antibodies XL313, and XL166 were developed. Alexa-488, Alexa-594, streptavidin Alexa-594, and phalloidin Alexa-594 labeled antibodies were from Invitrogen (Carlsbad, CA). Synthetic collagen RGD containing peptides (P-1; CKGDRGDAPGC (SEQ ID NO: 5), P-2; CQGPRGDKGEC (SEQ ID NO: 6), P-3; CAGSRGDGGPC (SEQ ID NO: 7), P-4; CQGIRGDKGE (SEQ ID NO: 8), P-5; CRGPRGDQGPC (SEQ ID NO: 9) and peptide control (P-C; CQGPSGAPGEC; SEQ ID NO: 10) were obtained from QED Biosciences (San Diego, CA).

### Cells and cell culture

RAW 264.7 and THP-1 cells were from ATCC (Manassas, VA) and cultured in DMEM and RPMI respectively in the presence of 10% FBS, 1.0% pen-strep and 1.0% sodium pyruvate. Immortalized BV-2 cells, and were cultured in DMEM with 10% FBS, 1.0% pen-strep and 1.0% sodium pyruvate. Human dermal fibroblasts (HDF) were obtained from Science Cell (Carlsbad, CA) and cultured in fibroblast growth medium with 2.0% FBS and used between passages 4 to 9. Human retinal microvascular endothelial cells (HRMVECs) were obtained from Applied Cell Biology Institute (Kirkland, WA) and cultured in EBM2 supplemented with EGM-2 growth factors. Human umbilical vein endothelial cells (HUVECS), human microvascular endothelial cells (HMVECS) were obtained from ATCC (Manassas, VA) and cultured in EBM2 with supplemental growth factors EGM-2 or EGM-2MV respectively. All endothelial cell growth media contained 2% FBS, 1.0% pen-strep and 1.0% sodium pyruvate and used experimentally between passages 3 to 9. For collection of conditioned media, cells were cultured in basal media under serum free conditions for 24 hours. Conditioned media was collected and concentrated 10x using an Amicon Ultracell, 3kDa centrifugal ultrafiltration cartridge.

### Cell adhesion assays

RGD peptides (P-1, P-2, P-3, P-4, P-5, and P-C) were immobilized (100µg/ml) to wells. HUVEC, HMVEC, HRMVEC, and HDF cells were suspended in adhesion buffer (RPMI containing 1mM MgCl<sub>2</sub>, 0.2mM MnCl<sub>2</sub> and 0.5% BSA) and 1x10<sup>5</sup> cells were seeded into the wells in the presence or absence of P4C10, LM609, P1F6 or control antibodies (100µg/ml). Cells were allowed to attach for 25 min at 37°C. Media containing non-attached cells was aspirated and attached cells were washed with PBS and stained with crystal violet. Cell adhesion was quantified by measuring the optical density of eluted dye. Adhesion assays were completed at least three times with triplicate wells.

### Collagen Proteolysis and Solid Phase Binding Assays

Collagen type-I and collagen type-IV were heat denatured for 15 min and then incubated with APMA-activated MMP2 for 0.5h, 1h, 4h, 8h, and 20h, at 37°C, followed by a five minute boil to deactivate remaining MMP. For solid phase ELISAs, synthetic RGD-containing collagen peptides (P-1, P-2, P-3, P-4, P-5, and P-C) were immobilized

(100µg/ml) to wells or wells were, coated with 10µg/ml of native or MMP2-proteolyzed collagen type-I or type-IV. Wells were blocked with 1% BSA in PBS for 1 hour and then incubated with 1µg/ml of Mabs XL313 or XL166 for 1h, washed, and incubated with antimouse HRP-conjugated antibodies (1:5000). Bound Mabs were detected with a TMB substrate as per manufactures instructions and quantified via spectrometer measurements. All assays were carried out at least four times in triplicate wells.

#### Chick Cam Inflammation and Angiogenesis Assays

The chick chorioallantoic membrane (CAM) assays were carried out with some modifications (19). For all experiments CAMs of 10-day-old chick embryos obtained from Charles River (North Franklin, CT) were separated from the shell membrane. Filter discs either non-treated (inflammation assays) pretreated (angiogenesis assays) with cortisone acetate (3.0mg/ml) containing RPMI only or FGF-2 (40ng). CAMs were either non-treated or treated topically with Mab XL313, XL166 or a non-specific control antibody (10µg/embryo every 24h for three consecutive treatments). For peptide induction experiments, CAMs were stimulated with 100ng/ml of the RGD peptides (P-1, P-2, P-C) in the presence or absence of the P38MAPK inhibitor, SB202190 (10µM). At the end of the incubation period the embryos were sacrificed and the CAM tissues were analyzed. Angiogenesis was quantified by counting the number of angiogenic branching blood vessels within the area of the filter disc. The angiogenic index was determined by subtracting the mean number of blood vessel branch points from untreated CAMs from each experimental condition. Eight to twelve embryos were used per condition and experiments were repeated at least three times.

#### Immunohistochemistry and Immunofluorescence Analysis

CAMs examined for accumulation of granulation tissue were harvested, fixed in 4% PFA and paraffin embedded and sectioned (4µm) and stained with Giemsa. CAM tissues analyzed via immunofluorescence were harvested, embedded with OCT, snap frozen and sectioned (4µM). Frozen sections were fixed in 50% methanol/50% acetone, air dried and blocked with 2.5% BSA for 1h at 37°C. For expression of the XL313 and XL166 epitopes as well as monocyte/macrophages, FGF-2 stimulated CAM tissues were stained with Mabs XL313, XL166 (50µg/ml) or KUL1 (1:250) and then incubated with

Alexa-488 labeled secondary antibodies (1:2000 dilution). Co-staining of monocytes/macrophages and the Mab XL313 reactive epitope in FGF-2 stimulated CAMs was performed by sequential staining by first probing with KUL1 (1:250) and then with a biotinconjugated Mab XL313 (50 $\mu$ g/ml), and with secondary antibodies Alexa-488 and streptavidin Alexa-594 (1:2000) respectively. Using a similar strategy, sections of RGD peptide-treated CAM tissues were analyzed for phosphorylated-P38MAPK in angiogenic vessels by co-incubation of anti-phospho-P38MAPK (1:50) and anti-vWf (1:500) antibodies. Subcellular localization of YAP was observed in HUVECS attached to P-2 and P-1 coated glass coverslips. Cells were allowed to attach for 15, 30, or 60 min in the absence of serum and were fixed with 4% PFA. Fixed cells were washed and blocked with 2.5% BSA and stained with anti-YAP (1:200) and phalloidin (1:500). All sections and slides were counter stained with DAPI.

#### Cell Proliferation Assays

HUVECs (WT, shYAP1 or control transfected) or HRMVECs were plated at 2,000 cells per well with complete EGM-2 media containing 2.0% FBS in the absence or presence of P-1, P-2 or P-C (100ng/ml) and allowed to grow for 24 hours. Cell growth was monitored using a BrdU or MMT assay kits according to manufacturer's instructions. All assays were completed at least three times in triplicate wells.

#### Inhibitor Experiments

Endothelial cells (HUVECs or HRMVECs) were incubated in serum free media with 1mM MgCl<sub>2</sub>, 0.2mM MnCl<sub>2</sub> in the presence of a Src inhibitor, PP2, (10 $\mu$ M) a P38MAPK inhibitor, SB202190 (10 $\mu$ M) or vehicle only (DMSO) for 10 min at 37°C. Treated cells were then seeded on to immobilized P-1 and P-2 and lysates were collected at 15 min.

#### Western Blots

Whole cell and CAM tissue lysates were collected in RIPA buffer supplemented with 1x protease inhibitor and 1x phosphatase inhibitor and were run on polyacrylamide gels using denaturing conditions. Prior to loading the gels, 6x sample buffer was added to each of the lysates (final concentration 1x) and boiled for five minutes. Twenty to 50  $\mu$ g of total protein were loaded into each lane. For detection of proteins larger than 50kD,

10% gels were used; for proteins smaller than 50kD 15% gels were used. Gels were run at 60 volts (v) until the dye front passed through the stacking gel, and then the voltage was increased to 100V for the remainder of the separation. Precision Plus protein standards (Bio-Rad) were used to visualize migration. Protein was transferred to nitrocellulose membranes using a wet tank system and blocked for 1h using 10% non-fat dried milk in tris-buffered saline with 0.01% Tween-20 (TBS-T). Membranes were incubated with primary antibodies (anti-coll-I (1:250), anti-coll-IV (1:250), Mab XL313 (2 $\mu$ g/ml), Mab XL166 (2 $\mu$ g/ml) anti- $\beta$ -actin (1:5000), anti-phospho- $\beta$ 3 (1:7000), anti- $\beta$ 3 (1:1000), anti-phospho-Src (1:500), anti-Src (1:500), anti-phospho-P38MAPK (1:500), anti P38MAPK (1:2000), anti-YAP (1:500), anti-Tubulin (1:2000), anti-TBP (1:1000)) in 5% BSA in TBS-T overnight at 4°C with gentle agitation. Membranes were washed 3 times in TBS-T for five minutes. Blots were then incubated with HRP conjugated secondary antibodies (1:15000) in 1% non-fat milk in TBS-T for 1h. Membranes were washed a second time as indicated above and exposed to chemiluminescent substrate for three minutes prior to exposure to autoradiography film in a dark room. Western blot bands were quantified using Image J software based on pixel intensity.

#### Transfections and Lentiviral Transductions

Raw cells were transfected with 1  $\mu$ g of HuSH shRNA plasmids for collagen type I, alpha 2 using Amaxa cell line nucleofector kit V (program #T024). Constructs expressing 21-nucleotide short hairpin RNAs (shRNA) targeting human YAP (shYAP) or non-targeting control (shNT, Sigma-Aldrich, SHC002) were used. Humantargeting shYAP1 lentiviral shRNA was obtained from the Thermo Scientific RNAi consortium (TRCN0000107625). Constructs were packaged into lentivirus, pseudotyped with the vesicular stomatitis virus glycoprotein. Transduction was performed by incubating cells with lentivirus, and stably transduced cells were subsequently used for studies. All cell lines were verified by morphology and mouse and human YAP-specific PCR. The efficacy of YAP knock down was determined to be between 70%-80%. Endothelial cells were certified mycoplasma-negative by PCR (Lonza), and primary cell cultures were used within the indicated passage numbers. Cells were transduced and selected using puromycin.

### Statistical Analysis

Statistical analysis was performed using the InStat statistical program for Macintosh computers. Data were analyzed for statistical significance using Student T test. P values < 0.05 were considered significant.

### Example 2: Cryptic RGD containing peptides from collagen type-1 support cell adhesion

Studies have documented the capacity of extracellular matrix (ECM) proteins containing the short amino acid sequence RGD to support interactions mediated by integrin receptors (33). The ability of cells to interact with RGD sites within the context of larger glycoproteins depends on many factors, some of which include the adjacent flanking sequences surrounding the core RGD tri-peptide as well as the geometrical configuration of the intact molecule and how these molecules are oriented within the context of the interconnected network of other ECM proteins (24,25,33). Flanking sequences immediately C-terminal to the RGD site can govern integrin selective binding (24,25,33). RGD motifs can be cryptic and inaccessible to cell surface receptors as is illustrated in the case of triple helical collagen (34). In this regard, five different cryptic RGD containing sites exist within human collagen type-I, each with distinct flanking sequences (Table 1).

Table 1. RGD containing epitopes of collagen type-I.

<b>Peptide</b>	<b>AA Sequence</b>	<b>Location</b>
P-1	KGDRGDAPG	Colla1 742-750
P-2	QGPRGDKGE	Colla1 1090-1098
P-3	AGSRGDGGP	Colla2 774-782
P-4	QGIRGDKGE	Colla2 1002-1010
P-5	RGPRGDQGP	Colla2 819-827
P-C	QGPSGAPGE	NA

Five different cryptic RGD containing sites exist within human collagen type-I, each with distinct flanking sequences. Synthetic peptides of these five sequences were generated and designated P-1 through P-5 as shown above. Additionally, a control peptide (P-C) was generated lacking the RGD tri-peptide motif. The sequences in Table 1 correspond to the following SEQ ID NOs.: KGDRGDAPG (SEQ ID NO: 2),

QGPRGDKGE (SEQ ID NO: 3), AGSRGDGGP (SEQ ID NO: 12), QGIRGDKGE (SEQ ID NO 13); RGPRGDQGP (SEQ ID NO: 14); and QGPSGAPGE (SEQ ID NO: 15).

#### RGD peptides are capable supporting cell adhesion

Due to the importance of the RGD tri-peptide motif, the flanking sequences within collagen type-I that surround the core RGD site may alter its cellular recognition were determined. To assess whether these cryptic collagen RGD motifs were redundant or whether the flanking sequences help convey distinct properties, each of the collagen type-I RGD epitopes were synthesized, along with their associated flanking sequences. The five different RGD peptides were immobilized and their ability to facilitate cell adhesion was examined. As shown in Fig. 1A, all five collagen RGD peptides (P1-P5) support human umbilical vein endothelial cell (HUVEC) adhesion, with peptide 5 (P-5) promoting the highest levels of adhesion. In contrast, a peptide control (P-C) in which the RGD motif of P-2 was replaced with SGA failed to support adhesion. To confirm that the adhesion promoting ability was not specific to only HUVECs similar assays were carried out with human microvascular endothelial cells (HMVEC), human retinal microvascular endothelial cells (HRMVEC) and human dermal fibroblasts. All endothelial cells and fibroblast bound the five RGD containing collagen peptides while the control peptide failed to support interactions (Fig. 1B-Fig.1D). These data indicate that while some differences were observed, all five RGD peptides were capable supporting cell adhesion.

#### Cryptic collagen RGD epitopes using monoclonal antibodies

To study these cryptic collagen RGD epitopes, monoclonal antibodies were generated. Two distinct antibodies were isolated with the ability to specifically discriminate between different RGD containing epitopes. As shown in Fig. 1E, Mab XL313 specifically bound to collagen peptides P-2 and P-4 containing the conserved RGDKGE (SEQ ID NO: 1) motif (Table 1), but showed no significant reactivity with other RGD peptides including P-1, P-3 or P-5. A second antibody termed XL166 recognized RGD containing collagen peptides P-1, P-3 and P-5, but failed to bind to the RGDKGE (SEQ ID NO: 1) containing peptides P-2 and P-4 (Fig. 1F). Neither Mab XL313 nor XL166 showed interaction with the control peptide (P-C).

Example 3: XL313 exhibits selective binding for proteolyzed collagen type –I

The capacity of Mab XL313 to bind its RGD motif within the context of the full-length collagen molecule was determined. To facilitate these studies, denatured collagen type-1 or IV was incubated with MMP-2 for 12hrs to generate proteolyzed collagen. MMP-2 mediated proteolysis of collagen type-I and IV resulted in the generation of multiple fragments as indicated by Western blot analysis using antibodies specifically directed to either collagen type-I (Fig. 2A left) or collagen type-IV (Fig. 2A right). Mab XL313 specifically directed to the RGDKGE (SEQ ID NO: 1) collagen sequence exhibited minimal reactivity with intact collagen type I or type IV under denaturing and reducing conditions (Fig. 2B) or under non-denaturing and non-reducing conditions of the ELISA (Fig. 2C). In contrast, Mab XL313 readily detected low molecular weight fragments of collagen type-I, but not collagen type-IV following proteolysis (Fig. 2B). Mab XL313 failed to recognize other RGD containing ECM proteins including vitronectin or fibronectin.

To further examine the generation of the low molecular weight RGDKGE (SEQ ID NO: 1) containing collagen fragments, a time course of MMP-2 mediated collagen proteolysis was examined. MMP-2 mediated degradation of collagen type-I resulted in a time dependent generation of Mab XL313 reactive collagen fragments (Fig. 2D). The majority of the collagen was proteolyzed into Mab XL313 reactive fragments of approximately 14Kd to 16Kd by 8 hours. These findings indicated that XL313 collagen epitopes were cryptic within the intact non-denatured collagen type-1 molecule and that proteolytic degradation was required to efficiently expose the hidden RGDKGE (SEQ ID NO: 1) containing motif.

Example 4: Differential roles of cryptic RGD collagen motifs on angiogenesis and inflammation *in vivo*

Studies have shown that collagen remodeling within the vascular basement membrane can result in exposure of multiple non-RGD cryptic collagen sites including the HUIV26 and HU177 epitopes that can play active roles in angiogenesis (21,23). Given these findings, it was determined whether distinct RGD containing epitopes were exposed

*in vivo*. First, to examine whether these RGD epitopes could be generated during angiogenesis the chick chorioallantoic membrane (CAM) model (19) was used. The CAMs of chick embryos were stimulated with FGF-2, and the generation of RGD containing collagen epitopes was examined using Mabs XL313 and XL166. As shown in Fig. 3A, little Mab XL313 or XL166 reactive epitope was detected in non-stimulated CAMs. In contrast, RGD containing collagen epitopes (Green) were readily detected in FGF-2 stimulated CAM tissues confirming the differential generation of RGD containing epitopes recognized by these antibodies. Mab XL313 and XL166 reactive RGD epitopes did not exhibit a typical extracellular fibril collagen pattern, but rather exhibited punctate distribution with both intracellular and scattered extracellular localization. The intracellular distribution is similar to the staining pattern of collagen degradation products previously documented within intracellular vesicles of macrophages (35).

Given the generation of these distinct sets of RGD containing epitopes, their active roles in regulating angiogenesis and inflammation were examined. Angiogenesis was induced within the CAMs of 10-day old chick embryos with FGF-2 using filter discs coated with cortisone acetate (CA) to reduce growth factor associated inflammation. As shown in Fig. 3B, treatment with Mab XL313 directed to the cryptic RGDKGE (SEQ ID NO: 1) containing epitope ( $P < 0.05$ ) inhibited FGF-2 induced angiogenesis by greater than 75% as compared to non-treated or control antibody. Mab XL166 that specifically binds the remaining three cryptic RGD collagen peptides (P-1, P-3, and P-5) had no effect. These findings were consistent with the notion that while distinct RGD containing collagen epitopes were readily generated *in vivo*, were not functionally redundant. FGF-2 induced inflammation is associated with recruitment and accumulation of granulation-tissue associated macrophages.

The chick CAM has been routinely used to assess inflammation and granulation tissue formation, which are largely dependent on infiltration of chick heterophils (the avian equivalent of neutrophils), macrophages and activated fibroblasts (36,37). To study the potential differential biological impact of RGD epitopes, FGF-2 induced inflammation was examined by carrying out similar experiments in the absence of cortisone acetate and quantifying CAM thickening. As shown in Fig. 3C, treatment with

FGF-2 induced CAM inflammation as indicated by robust tissue thickening (top panels), extensive infiltration of inflammatory infiltrates as indicated by Giemsa stain (middle panel) and increased accumulation of monocytes and macrophages (bottom panel) following staining with an antibody directed to avian specific monocytes and macrophages. Macrophage infiltration of the CAMs stimulated with FGF-2 was ( $P < 0.05$ ) enhanced over 2-fold as compared to control (Fig. 3D) indicating that FGF-2 induced inflammation in this model is associated with the recruitment and accumulation of granulation-tissue associated macrophages.

FGF-2 induced inflammatory response in the presence or absence of anti-RGD specific antibodies of XL313 and XL166

To examine whether the RGD containing collagen epitopes play a role in the FGF-2 stimulated inflammatory response, this FGF-2 induced inflammatory response was examined in the presence or absence of anti-RGD specific antibodies XL313 and XL166. Quantification indicated that FGF-2 stimulation in the absence of cortisone acetate resulted in approximately 50% of the CAMs showing robust formation of thick granulation tissue (Fig. 3E). Treatment of CAMs with cortisone acetate, a well document anti-inflammatory agent significantly ( $P < 0.05$ ) reduced the percentage of CAMs exhibiting thickening by greater than 80% as compared to either no treatment or control antibody. Interestingly, treatment of CAMs with Mab XL313 also ( $P < 0.05$ ) inhibited the number of CAMs exhibiting inflammation by approximately 75% as compared to controls. In contrast, treatment of CAMs with Mab XL166 showed no significant ( $P > 0.05$ ) impact. These data are consistent findings while examining angiogenesis indicating a differential role for specific cryptic RGD epitopes *in vivo*.

Example 5: Generation of XL313 cryptic RGDKGE (SEQ ID NO: 1) epitope

During angiogenesis and inflammation, multiple cell types including endothelial cells, fibroblasts and macrophages proteolytically remodel extracellular collagen creating a permissive microenvironment that facilitates stromal cell infiltration and new blood vessel growth. A variety of cells including fibroblasts and endothelial cells express collagen and, partially degraded collagen can be internalized and further processed by

activated M2-like macrophages leading to the generation of low molecular weight fragments (35,38). Because of the unique pattern of Mab XL313 immunoreactivity observed *in vivo*, it was determined whether stromal cells associated with angiogenesis and inflammation could generate the RGDKGE (SEQ ID NO: 1) containing epitope. Whole cell lysates were prepared from fibroblasts and endothelial cells and Western blots were performed. While some Mab XL313 reactive species was detected in lysates of endothelial cells and fibroblasts, the major immunoreactive species migrated between approximately 75Kd to 28Kd indicating that these species were unlikely to represent intact collagen. In addition, minimal amounts of low molecular weight species were detected that corresponds to the major 14Kd to 16Kd collagen fragments detected following MMP-2 mediated proteolysis. While a small amount of an approximately 20 Kd XL313 reactive species was detected in serum free conditioned medium (CM) collected from HUVECS, no significant levels of immunoreactive fragments in fibroblast CM was detected.

Given the minimal reactivity observed in these cell types known to express collagen, and that FGF-2 induced a strong angiogenic and inflammatory response in CAMs that was associated with an extensive infiltration of macrophages, FGF-2 treated CAM tissues for the co-distribution of the XL313 epitope and macrophages was examined. As shown in Fig. 4B, the XL313 reactive epitope (Red) co-localized with a subset of macrophages (Green) in FGF-2 stimulated CAMs, indicating that macrophages may be one source of the XL313 collagen epitope. To study this possibility, both whole cell lysates (Fig. 4C left) and serum free CM (Fig. 4C right) from three different macrophage-like cell lines were examined. In contrast, to endothelial cells and fibroblasts, strong immunoreactive species were readily detected in cell lysates and CM from multiple macrophage cell lines including Raw 264.7, THP1 and BV2. Importantly, low molecular weight immunoreactive species migrating between 14Kd to 16Kd were readily detected in serum free CM (Fig. 4C right). These 14Kd to 16Kd immunoreactive species corresponded to the size of low molecular weight Mab XL313 reactive collagen fragments detected following MMP-mediated proteolytic digestion of purified collagen. To further study the XL313 immunoreactive species detected in macrophages, the generation of the 14Kd to 16Kd RGDKGE (SEQ ID NO: 1) containing XL313 fragments in Raw 264.7

macrophages was examined. First, to examine the expression of collagen in these macrophages, the expression of mRNA for the alpha 1 and alpha 2 chains of collagen type-I in RAW macrophages by PCR was confirmed. Secondly, while no full length collagen type-I was detected in either cell lysates or CM from macrophages using anti-collagen type-I specific antibodies, low molecular weight fragments migrating at the same molecular weight as the RGDKGE (SEQ ID NO: 1) containing epitope in both cell lysates and CM using either Mab XL313 or an anti-collagen-I specific antibody (Fig. 4D) was detected. Importantly, shRNA-mediated knockdown of the alpha 2 chain of collagen type-I reduced immune-detection of the low molecular species (14Kd to 16Kd) in both lysates and CM when using either anti-collagen specific antibodies or Mab XL313 (Fig. 4D). Together, these findings were consistent with the possibility that macrophages were one cellular source of the RGDKGE (SEQ ID NO: 1) collagen epitope.

Example 6: Induction of angiogenesis and inflammation *in vivo* by soluble RGDKGE (SEQ ID NO: 1) but not a related RGDAPG (SEQ ID NO: 11) containing collagen epitope.

Due to the differential expression and bio-distribution of the RGDKGE (SEQ ID NO: 1) epitope in angiogenic CAM tissues and its expression in macrophage-conditioned medium, it was determined whether a soluble circulating form of this RGDKGE (SEQ ID NO: 1) epitope could be generated. To examine this possibility, chick embryos were either un-treated or stimulated with FGF-2 and serum, and collected three days later. As shown in Fig. 5A, low levels of circulating Mab XL313 immunoreactive epitope was detected in the serum from non-stimulated control chick embryos. In contrast, a ( $P < 0.05$ ) 2-fold increase was detected in the levels of circulating XL313 epitope following FGF-2 stimulation. These findings indicated the differential release of a soluble form of this RGDKGE (SEQ ID NO: 1) containing collagen epitope.

Soluble peptide containing the XL313 epitope actively regulates angiogenesis and inflammation

Because a soluble form of the RGDKGE (SEQ ID NO: 1) epitope was detected *in vivo*, it was next determined whether a soluble peptide containing the XL313 epitope

actively regulated angiogenesis and inflammation. To examine this possibility, the effects of the RGDKGE (SEQ ID NO: 1) containing collagen peptide on angiogenesis and inflammation in the chick CAM were assessed. As shown in Fig. 5B, the XL313 RGDKGE (SEQ ID NO: 1) containing collagen peptide (P-2) dose dependently enhanced angiogenesis with maximum induction observed at a dose of 100ng/CAM. Stimulation of CAMs with the RGDKGE (SEQ ID NO: 1) containing collagen peptide P-2, but not the related RGDAPG (SEQ ID NO: 11) containing collagen peptide P-1, or peptide control (P-C) significantly ( $P>0.05$ ) induced angiogenesis as compared to no treatment (Fig. 5C).

The effects of the soluble RGD containing collagen peptides on inflammation were examined. As shown in Fig. 5D, FGF-2 induced a strong inflammatory response in the chick CAM in the absence of cortisone acetate as indicated by approximately 55%-60% of the CAMs exhibiting extensive tissue thickening. Minimal evidence of tissue inflammation was observed following stimulation with either control peptide (P-C) or the RGDAPG (SEQ ID NO: 11) containing collagen peptide P-1, while the RGDKGE (SEQ ID NO: 1) collagen peptide P-2 significantly ( $P<0.05$ ) induced inflammation to nearly that of FGF-2 stimulation (Fig. 5D). These studies indicated that the biological impact of RGD containing collagen peptides on angiogenesis and inflammation in the chick CAM depended on their associated flanking sequences.

#### Example 7: RGDKGE (SEQ ID NO: 1) containing peptide P-2 induced angiogenesis depends on P38MAPK

Studies have indicated that angiogenesis and inflammation in the chick CAM is associated with alterations in MAP kinase signaling including P38MAPK (40,41). To examine mechanisms that regulate angiogenesis following stimulation with the RGDKGE (SEQ ID NO: 1) containing collagen peptide P-2, CAM tissues from untreated or RGD peptide treated animals was examined. As shown in Fig. 6A, elevated levels of phosphorylated P38MAPK were detected in lysates from CAMs treated with RGDKGE (SEQ ID NO: 1) containing peptide P-2 as compared to either untreated or RGDAPG (SEQ ID NO: 11) containing peptide P-1 treated animals. Quantification of CAM tissues (N=12) indicated a  $P<0.05$ ) 4-fold increase in phosphorylation of P38MAPK as compared to

controls (Fig. 6B). Consistent with studies, while activated P38MAPK was detected in multiple cell types in chick CAMs, co-staining analysis indicated expression of phosphorylated P38MAPK in vWf positive blood vessels (Fig. 6C).

The effects of the RGD containing collagen peptides on the levels of phosphorylated P38MAPK in endothelial cells were examined. As shown in Fig. 6D and Fig. 6E, while both RGD containing collagen peptides P-1 and P-2 support cell binding, interactions with RGDKGE (SEQ ID NO: 1) collagen peptide P-2 resulted in enhanced phosphorylation of P38MAPK as compared to RGDAPG (SEQ ID NO: 11) collagen peptide P-1 in HUVECs (Fig. 6D) or HRMVEC (Fig. 6E). A functional role for P38MAPK in mediating RGDKGE (SEQ ID NO: 1) peptide P-2 induced angiogenesis *in vivo* was demonstrated as P-2 induced angiogenesis was ( $P<0.05$ ) reduced by P38MAPK inhibitor (Fig. 6F). Together, these data indicate a role for P38MAPK in the peptide P-2 stimulated pro-angiogenic response observed *in vivo*.

Example 8: Collagen peptide P-2 binds and activates  $\alpha v\beta 3$  and stimulates P38MAPK activation in a Src dependent manner.

It is well established that multiple integrins recognize RGD amino acid motifs within ECM proteins. However, the ability of an integrin to bind distinct RGD epitopes depends in part on its orientation within the parent molecule and the C-terminal amino acid sequences flanking the RGD motif (25-27). Potential cell surface receptors that mediate interactions with the RGDKGE (SEQ ID NO: 1) containing collagen P-2 peptide were identified. The ability of endothelial cells to bind the RGD collagen peptides P-1 and P-2 in the presence or absence of function blocking anti-integrin antibodies was examined. As shown in Fig. 7A, anti- $\beta 1$  specific antibody had minimal effect on HUVEC adhesion to peptide P-2 while anti- $\alpha v\beta 3$  antibody ( $P<0.05$ ) inhibited interactions by approximately 90% as compared to control. Anti- $\alpha v\beta 5$  antibody showed little inhibition. Similar results were observed with P-1, which contains the RGDAPG (SEQ ID NO: 11) sequence (Fig. 7B). These data indicate that  $\alpha v\beta 3$  functions as a receptor for both RGD containing peptides in endothelial cells.

### RGD peptides differentially altered $\alpha\beta3$ -mediated signaling

Because both RGD containing peptides bind  $\alpha\beta3$  coupled with the differential effect of these peptides on angiogenesis and inflammation, it was determined whether the RGD peptides differentially altered  $\alpha\beta3$ -mediated signaling. Endothelial cells were allowed to attach to P-1 and P-2 and the relative level of  $\beta3$ -integrin phosphorylation was examined. As shown in Fig. 7C, in the absence of any growth factors,  $\beta3$  phosphorylation ( $P < 0.05$ ) increased over 3-fold following ligation of RGDKGE (SEQ ID NO: 1) peptide P-2, as compared to RGDAPG (SEQ ID NO: 11) peptide P-1. Ligand binding of  $\beta3$  integrin induced receptor clustering and initiated down-stream signaling events including activation of protein kinases including Fak and Src. Therefore, the differential phosphorylation of these protein kinases following the early mechanical-mediated interactions with the RGD containing collagen peptides was assessed. Minimal Fak phosphorylation was detected following ligation of either P-1 or P-2 under these serum free conditions. In contrast, Src phosphorylation was enhanced by nearly 2-fold following interactions with P-2 as compared to P-1 (Fig. 7D). Moreover, activation of  $\beta3$  integrin and P38MAPK in endothelial cells following binding to P-2 was dependent on Src as incubation of endothelial cells with a Src inhibitor reduced  $\beta3$  and P38MAPK phosphorylation following binding to collagen peptide P-2 (Fig. 7E and Fig. 7F). Activation of Src and P38MAPK leads to enhanced actin polymerization and stress fiber formation (43-45), therefore the actin cytoskeleton in endothelial cells following binding to the RGD collagen peptides was examined. Endothelial cell interactions with the RGDKGE (SEQ ID NO: 1) collagen peptide P-2 resulted in accelerated actin stress fiber formation as compared to interactions with RGDAPG (SEQ ID NO: 11) collagen peptide P-1 (Fig. 7G). Cumulatively, these findings indicate the ability of the conserved RGDKGE (SEQ ID NO: 1) collagen epitope to stimulate initiation of a  $\beta3$ - integrin dependent mechano-transduction pathway.

Example 9: Cellular interactions RGDKGE (SEQ ID NO: 1) containing peptide enhances nuclear YAP accumulation and endothelial cell growth.

The data indicate that while both RGD containing collagen peptides P-1 and P-2 support an initial  $\beta$ 3-integrin-mediated endothelial cell adhesive interaction, collagen peptide P-2 selectively enhanced  $\beta$ 3-integrin phosphorylation leading to increased activation of P38MAPK and accelerated actin stress fiber formation. Actin stress fiber formation and enhanced mechanical tension contribute to re-localization of the transcriptional co-activator Yes-associated protein (YAP) to the nucleus (46). Moreover, YAP is implicated in regulating angiogenesis and endothelial cell growth (47,48). YAP localization following endothelial cell binding to the distinct collagen RGD containing peptides in the absence of growth factor stimulation was examined. As shown in Fig. 8A, enhanced level of nuclear localized YAP was detected by 15 minutes following endothelial cell binding to collagen peptide P-2 as compared to P-1. The differential nuclear localization of YAP was not consistently detected at later time points. To confirm this enhanced nuclear accumulation of YAP, Western blot analysis was carried out. As shown in Fig. 8B, the levels of nuclear YAP increased by approximately 2-fold in endothelial cells attached to the peptide P-2 as compared to peptide P-1.

Effects of RGD containing collagen peptides on HUVEC and HRMVEC growth

Nuclear localization of YAP contributes to the regulation of endothelial cell growth. Therefore, the effects of RGD containing collagen peptides on HUVEC and HRMVEC growth were examined. Addition of soluble P-2 significantly ( $P < 0.05$ ) enhanced endothelial cell growth while stimulation with RGDAPG (SEQ ID NO: 11) peptide P-1 had a minimal effect (Fig. 8C and Fig. 8D). The selective ability of P-2 to enhance Src-dependent activation of P-38MAPK, the ability of the enhanced nuclear accumulation of YAP following RGDKGE (SEQ ID NO: 1) peptide P-2 stimulation was Src-dependent and /or P38MAPK dependent was assessed. As shown in Fig. 8E and Fig. 8F, nuclear YAP accumulation following P-2 stimulated endothelial cells was reduced by approximately 50% by treatment with either Src or P38MAPK inhibitors as compared to control. These data are consistent with a role for Src and P38MAPK in mediating the RGDKGE (SEQ ID NO: 1) P-2 stimulated nuclear accumulation of YAP.

P-2 stimulated endothelial cell growth depends on YAP

YAP plays roles in regulating the expression of multiple angiogenesis and inflammatory factors; therefore it was examined whether P-2 stimulated endothelial cell growth depends on YAP. Endothelial cells with YAP specific or non-specific shRNAs were transduced. Addition of soluble RGDKGE (SEQ ID NO: 1) containing collagen peptide P-2 to endothelial cells, but not the related RGDAPG (SEQ ID NO: 11) containing peptide P1, ( $P < 0.05$ ) enhanced growth in control transduced cells (Fig. 8G), while the RGDKGE (SEQ ID NO: 1) peptide P-2 failed to induce growth in endothelial cells in which YAP was knocked down (Fig. 8H). YAP knock down cells were capable of proliferating as enhanced growth was observed following VEGF or high serum stimulation (Fig. 8I). Together, the findings are consistent with a mechanism by which RGDKGE (SEQ ID NO: 1) containing collagen peptide P-2 initiated a unique mechano-signaling cascade leading to the activation of P38MAPK in a Src-dependent pathway that ultimately led to nuclear YAP accumulation and enhanced endothelial cell growth.

Example 10: Enhanced expression of PDL-1 in human M21 melanoma tumors as compared to M21L melanoma tumors lacking  $\alpha\beta3$ .

Nude mice were injected with either M21 ( $\alpha\beta3+$ ) or ML21 ( $\alpha\beta3-$ ) melanoma cells and were allowed to establish pre-existing tumors. Tumor sections were analyzed for expression of the immune checkpoint regulatory protein PDL-1 by immunofluorescence staining (Fig. 10).

Example 11: Enhanced expression of PDL-1 in human M21 melanoma tumors as compared to M21 melanoma tumors in which  $\beta3$  integrin was knocked down.

M21 melanoma cells that express integrin  $\alpha\beta3$  were transfected with non-specific control shRNA (M21 Cont) or  $\beta3$  specific shRNA (M21 $\beta3$ Kd) (Fig. 11). Nude mice were injected with either M21 Cont ( $\alpha\beta3+$ ) or M21 $\beta3$ Kd ( $\alpha\beta3-$ ) melanoma cells and were allowed to establish pre-existing tumors. Tumor sections were analyzed for expression of the immune checkpoint regulatory protein PDL-1 by immunofluorescence staining.

Example 12: MabXL313 enhanced the anti-tumor activity of the immune checkpoint inhibitor anti-PDL-1 antibody

Mice were injected with B16F10 melanoma cells and were allowed to establish pre-existing tumors for 5 days prior to treatment (Fig. 9). Data in Fig. 9 represent mean tumor volume at day 14  $\pm$  SE from 8 mice per condition.

Example 13: Reduced expression of PDL-1 in melanoma tumors in mice treated with an antibody targeting the  $\alpha\beta3$  ligand (RGDKGE (SEQ ID NO: 1) containing XL313 collagen epitope).

Mice were injected with melanoma cells and were allowed to establish pre-existing tumors for 5 days prior to treatment. Mice were treated 3 times a week for 14 days with an antibody targeting the  $\alpha\beta3$  binding RGDKGE (SEQ ID NO: 1) containing collagen epitope. Tumor sections were analyzed for expression of the immune checkpoint regulatory protein PDL-1 by immunofluorescence staining (Fig. 12).

Example 14: Enhanced detection of lymphocytic infiltrates in melanoma tumors in mice treated with an antibody targeting the  $\alpha\beta3$  ligand (RGDKGE (SEQ ID NO: 1) containing XL313 collagen epitope).

Mice were injected with melanoma cells and were allowed to establish pre-existing tumors for 5 days prior to treatment. Mice were treated 3 times a week for 14 days with an antibody targeting the  $\alpha\beta3$  binding RGDKGE (SEQ ID NO: 1) containing collagen epitope (Fig. 13). Tumor sections were analyzed for expression of the immune checkpoint regulatory protein PDL-1.

Example 15: Detection of enhanced levels of PDL-1 protein in melanoma and endothelial cells following binding to 3 ECM ligand (denatured collagen-IV)

Integrin  $\alpha\beta3$  expressing melanoma cells M21 (Fig. 14A) and CCL-49 (Fig. 14B) and endothelial cells (HUVEC) (Fig. 14C) were attached to wells coated with either a non- $\alpha\beta3$  binding ligand (native collagen-IV) or an  $\alpha\beta3$  binding ligand (denatured collagen -

IV). Whole cell lysates were prepared and the relative levels of PDL-1 or  $\beta$ -actin loading control were assessed.

Example 16: Enhanced levels of PDL-1 protein in melanoma cells following binding to  $\alpha$ v $\beta$ 3 ligand XL313 epitope (RGDKGE (SEQ ID NO: 1)).

Integrin  $\alpha$ v $\beta$ 3 expressing melanoma cells (M21) were seeded onto control uncoated wells or wells immobilized with the XL313 cryptic collagen epitope (RGDKGE (SEQ ID NO: 1)) (Fig. 15). Following an incubation period, cell lysates were prepared and relative levels of PDL-1 were assessed.

Example 17: Reduction in the levels of PDL-1 protein in melanoma cells following blocking binding to  $\alpha$ v $\beta$ 3 ECM ligand (denatured collagen-IV) with a  $\alpha$ v $\beta$ 3 specific antibody LM609.

Integrin  $\alpha$ v $\beta$ 3 expressing melanoma cells (M21) were mixed with a control non-specific (normal mouse Ig) or  $\alpha$ v $\beta$ 3 specific antibody (Mab LM609) and was added to wells coated with  $\alpha$ v $\beta$ 3 binding ligand (denatured collagen-IV) (Fig. 16). Whole cell lysates were prepared following a 24 hour incubation period and the relative levels of PDL-1 or loading control were assessed.

The following references were cited in Examples 1-17.

#### **REFERENCES CITED**

1. Bergers, G., and Hanahan, D. (2008) Modes of resistance to anti-angiogenic therapy. *Nat. Rev. Cancer.* 8, 593-604
2. Chung, A. S., Lee, J., and Ferrara, N. (2010) Targeting the tumor vasculature: insight from physiological angiogenesis. *Nat. Rev. Cancer.* 10, 505-514
3. Cao, Y., Arbiser, J., D'Amato, R. J., D'Amore, P. A., Ingber, D. E., Kerbel, R., Klagsburn, M., Lim, S., Moses, M. A., Zetter, B., Dvorak, H., and Langer, R. (2011) Forty-year journey of angiogenesis translational research. *Sci. Transl. Med.* 3, 114rv3
4. Contois, L., Akalu, A., and Brooks, P. C. (2009) Integrins as functional hubs in the regulation of pathological angiogenesis. *Sem. Can. Biol.* 19, 318-328

5. Moserle, L., Jimenez-Valerio, G., and Casanovas, O. (2014) Antiangiogenic therapies: going beyond their limits. *Can. Discov.* 4, 31-41
6. Greenberg, J. I., Shields, D. J., Barillas, S. G., Acevedo, L. M., Murphy, E., Huang, J., Scheppke, L., Stockmann, C., Johnson, R. S., Angle, N., and Chersesh, D. A. (2008) A role for VEGF as a negative regulator of pericyte function and vessel maturation. *Nature.* 456, 809-813
7. Hodivala-Dilke, K. (2008)  $\alpha\beta3$  integrin and angiogenesis: a moody integrin in a changing environment. *Curr. Opin. Cell. Biol.* 20, 514-519
8. Atkinson, S. J., Ellison, T. S., Steri, V., Gould, E., and Robinson, S. D. (2014) Redefining the role(s) of endothelial  $\alpha\beta3$ -integrin in angiogenesis. *Biochem. Soc. Trans.* 42, 1590-1595
9. Robinson, S. D., and Hodivala-Dilke, K. H. (2011) The role of  $\beta3$ -integrins in tumor angiogenesis: context is everything. *Curr. Opin. Cell. Biol.* 23, 630-637
10. Brooks, P. C., Clark, R. A., and Chersesh, D. A. (1994) Requirement of vascular integrin alpha v beta 3 for angiogenesis. *Science.* 264, 569-571
11. Brooks, P. C., Montgomery, A. M., Rosenfeld, M., Reisfeld, R. A., Hu, T., Klier, G., and Chersesh, D. A. (1994) Integrin  $\alpha\beta3$  antagonists promote tumor regression by inducing apoptosis of angiogenic blood vessels. *Cell.* 79, 1157-1164
12. Contois, L. W., Akalu, A., Caron, J. M., Tweedie, E., Cretu, A., Henderson, T., Liaw, L., Friesel, R., Vary, C., and Brooks, P. C. (2014) Inhibition of tumor-associated  $\alpha\beta3$  integrin regulates the angiogenic switch by enhancing expression of IGFBP-4 leading to reduced melanoma growth and angiogenesis in vivo. *Angiogenesis.*
13. Reynolds, L. E., Wyder, L., Lively, J. C., Robinson, S. D., Huang, X., Sheppard, D., Hynes, R. O., and Hodivala-Dilke, K. M. (2002) Enhanced pathological angiogenesis in mice lacking beta 3 integrin or beta 3 and beta 5 integrins. *Nat. Med.* 8, 27-34
14. Feng, W., McCabe, N. P., Mahabeleshwar, G. H., Somanah, P. R., Phillips, D. R., and Byzova, T. (2008) The angiogenic response is dictated by  $\beta3$  integrin on bone marrow-derived cells. *J. Cell. Biol.* 183, 1145-1157
15. Steri, V., Ellison, T. S., Gontarczyk, A. M., Weilbaecher, K., Schneider, J. G., Edwards, D., Fruttiger, M., Hodivala-Dilke, K. M., and Robinson, S. D. (2014) Acute

depletion of endothelial  $\beta$ 3-integrin transiently inhibits tumor growth and angiogenesis in mice. *Cir. Res.* 114, 79-91

16. Gong, Y., Yang, X., He, Q., Gower, L., Prudovsky, I., Vary, C. P. H., Brooks, P. C., and Friesel, R. E. (2013) Sprouty4 regulates endothelial cell migration via modulating integrin  $\beta$ 3 stability through c-Src. *Angiogenesis.* 16, 861-875
17. Adair-Kirk, T. L., and Senior, R. M. (2008) Fragments of extracellular matrix as mediators of inflammation. *Int. J. Biochem. Cell. Biol.* 40, 1101-1110
18. Davis, G. E. (2011) Angiogenesis and proteinases: influence on vascular morphogenesis, stabilization and regression. *Drug. Discov. Today. Dis. Models.* 8, 13-20
19. Petitclerc, E., Boutaud, A., Prestayko, A., Xu, J., Sado, Y., Ninomiya, Y., Sarras, M. P., Hudson, B. G., and Brooks, P. C. (2000) New functions for non-collagenous domains of human collagen type-IV: novel integrin ligands inhibiting angiogenesis and tumor growth in vivo. *J. Biol. Chem.* 275, 8051-8061
20. Sudhakar, A., Sugimoto, H., Yang, C., Lively, J., Zeisberg, M., and Kalluri, R. (2003) Human tumstatin and endostatin exhibit distinct antiangiogenic activities mediated by  $\alpha$ v $\beta$ 3 and  $\alpha$ 5 $\beta$ 1 integrins. *Proc. Natl. Acad. Sci. USA.* 100, 4766-4771
21. Xu, J., Petitclerc, E., Kim, J. J., Hangai, M., Moon, Y. S., Davis, G. E., and Brooks, P. C. (2001) Proteolytic exposure of a cryptic site within collagen type-IV is required for angiogenesis and tumor growth in vivo. *J. Cell Biol.* 154, 1069-1079
22. Hangai, M., Kitaya, N., Xu, J., Chan, C. K., Kim, J. J., Werb, Z., Ryan, S. J., and Brooks, P. C. (2002) Matrix metalloproteinase-9-dependent exposure of a cryptic migratory control site in collagen is required before retinal angiogenesis. *Am. J. Pathol.* 161, 1429-1437
23. Cretu, A., Roth, J. M., Caunt, M., Akalu, A., Policarpio, D., Formenti, S., Gagne, P., Liebes, L., and Brooks, P. C. (2007) Disruption of endothelial cell interactions with the novel HU177 cryptic collagen epitope inhibits angiogenesis. *Clin. Cancer. Res.* 15, 3068-3078
24. Pierschbacher, M. D., and Ruoslahti, E. (1987) Influence of stereochemistry of the sequence Arg-Gly-Asp-Xaa on binding specificity in cell adhesion. *J. Biol. Chem.* 262, 1729-1798

25. Kunicki, T. J., Annis, D. S., and Felding-Haberman. (1997) Molecular determinants of Arg-Gly-Asp ligand specificity for  $\beta 3$  integrins. *J. Biol. Chem.* 272, 4103-4107
26. Gurrath, M., Muller, G., Kessler, H., Aumilley, M., and Timpl. (1992) Conformational/activity studies of rationally designed potent anti-adhesive RGD peptides. *Eur. J. Biochem.* 210, 911-921
27. Kostidis, S., Stavrakoudis, A., Biris, N., Tsoukatos, D., Sakarellos, C., and Tsikaris, V. (2004) The relative orientation of the Arg and Asp side chains defined by a pseudodihedral angle as a key criterion for evaluating the structure-activity relationship of RGD peptides. *J. Peptide. Sci.* 10, 494-509
28. Miyoshi, T., Hirohata, S., Ogawa, H., Doi, M., Obika, M., Yonezawa, T., Sado, Y., Kusachi, S., Kyo, S., Kondo, S., Shiratori, Y., Hudson, B. G., and Ninomiya, Y. (2006) Tumor-specific expression of the RGD- $\alpha 3$ (IV)NC1 domain suppresses endothelial tube formation and tumor growth in mice. *FASEB. J.* 20, 1264-1275
29. Danhier, F., Breton, A. L., and Preat, V. (2012) RGD-based strategies to target alpha (v) beta (3) integrin in cancer therapy and diagnosis. *Mol. Pharmaceutics.* 9, 2961-2973
30. Reynolds, A. R., Hart, I. R., Watson, A. R., Welti, J. C., Silva, R., Robinson, S. D., Violante, G. D., Gouraouen, M., Salih, M., Jones, M. C., Jones, D. T., Sunders, G., Kostourou, V., Perron-Sierra, F., Norman, J. C., Tucker, G. C., and Hodivala-Dilke, K. M. (2009) Stimulation of tumor growth and angiogenesis by low concentrations of RGD-mimetic integrin inhibitors. *Nat. Med.* 15, 392-400
31. Stupp, R., Hegi, M. E., Gorlia, T., Erridge, S. C., Perry, J., Hong, Y-K., Aldape, K. D., Lhermitte, B., Pietsch, T., Grujicic, D., Steinbach, J. P., Wick, W., Tarnawski, R., Nam, D-H., Hau, P., Weyerbrock, A., Taphoon, M. J. B., Shen, C-C., Rao, N., Thurzo, L., Herrlinger, U., Gupta, T., Kortmann, R. D., Adamska, K., McBain, C., Brandes, A. A., Tonn, J. C., Schnell, O., Wiegel, T., Kim, C-Y., Nabors, L. B., Readon, D. A., van den Bent, M. J., Hicking, C., Markivsky, A., Picard, M., and Weller, T. (2014) Cilengitide combined with standard treatment for patients with newly diagnosed glioblastoma with methylated MGMT promoter (CENTRIC EORTC 26071-22072 study): a multicenter, randomized, open-label, phase 3 trial. *Lancet.* 15, 1100-11008

32. Blasi, E., Barluzzi, R., Bocchini, V., Mazzolla, R., and Bistoni, F. (1990) Immortalization of murine microglial cells by a v-raf/v-myc carrying retrovirus. *J. Neuroimmun.* 27, 229-237
33. Rouslahti, E. (1996) RGD and other recognition sequences for integrins. *Annu. Rev. Cell Biol.* 12, 697-715
34. Montgomery, A. M., Reisfeld, R. A., and Cheresch, D. A. (1994) Integrin alpha v beta 3 rescues melanoma cells from apoptosis in three-dimensional dermal collagen. *Proc. Natl. Acad. Sci. USA.* 91, 8856-8860
35. Madsen, D. H., Leonard, D., Masedunskas, A., Mayer, A., Jurgensen, H. J., Peters, D. E., Amornphimoltham, P., Selvaraj, A., Yamada, S. S., Brenner, D. A., Burgdorf, S., Engelholm, L. H., Behrendt, N., Holmbeck, K., Weigert, R., and Bugge, T. H. (2013) M2-like macrophages are responsible for collagen degradation through a mannose receptor-mediated pathway. *J. Cell. Biol.* 202, 951-966
36. Zwadlo-Klarwasser, G., Gorlitz, K., Hafemann, B., Klee, D., and Klosterhahle, B. (2001) The chorioallantoic membrane of the chick embryo as a simple model for the study of the angiogenic and inflammatory response to biomaterials. *J. Mater. Sci. Mater. Med.* 12, 195-199
37. Deryugina, E. I., and Quigley, J. P. (2008) Chick embryo chorioallantoic membrane models to quantify angiogenesis induced by inflammatory and tumor cells or purified effector molecules. *Meth. Enzymol.* 444, 21-41
38. Skjot-Arkil, H., Barascuk, N., Register, T., and Karsdal, M. (2010) Macrophage-mediated proteolytic remodeling of the extracellular matrix in atherosclerosis results in neoepitopes: a potential new class of biochemical markers. *Drug. Dev. Technol.* DOI: 10.1089/adt.2009.0258
39. Rajashekhar, G., Kamocka, M., Marin, A., Suckow, M. A., Wolter, W. R., Badve, S., Sanjeevaiah, A. R., Pumiglia, K., Rosen, E., and Clauss, M. (2010) Pro-inflammatory angiogenesis is mediated by p38 MAP Kinase. *J. Cell Physiol.* DOI: 10.1002/jcp22404
40. Matsumoto, T., Turesson, I., Book, M., Gerwins, P., and Claesson-Welsh, L. (2002) p38 MAP Kinase negatively regulates endothelial cell survival, proliferation, and differentiation in FGF-2 stimulated angiogenesis. *J. Cell. Biol.* 156, 149-160

41. Contois, L. W., Nugent, D. P., Caron, J. M., Cretu, A., Tweedie, E., Akalu, A., Liebes, L., Friesel, R., Rosen, C., Vary, C., and Brooks, P. C. (2012) Insulin-like growth factor binding protein-4 differentially inhibits growth factor-induced angiogenesis. *J. Biol. Chem.* 287, 1779-1789
42. Mitra, S. K., and Schlaepfer, D. D. (2006) Integrin-regulated FAK-Src signaling in normal and cancer cells. *Curr. Opin. Cell Biol.* 18, 516-523
43. McMullen, M., Keller, R., Sussman, M., and Pumiglia, K. (2004) Vascular endothelial growth factor-mediated activation of p38 is dependent upon Src and RAFTK/Pyk2. *Oncogene.* 23, 1275-1282
44. Rousseau, S., Houle, F., Landry, J., and Huot, J. (1997) p38 MAP kinase activation by vascular endothelial growth factor mediates actin reorganization and cell migration in human endothelial cells. *Oncogene.* 15, 2169-2177
45. Alghisi, G. C., Ponsonnet, L., and Ruegg, C. (2009) The integrin antagonist cilengitide activates  $\alpha\beta3$ , disrupts VE-cadherin localization at cell junctions and enhances permeability in endothelial cells. *PloS. One.* 4, e449
46. Dupont, S., Morsut, L., Aragona, M., Enzo, E., Giulitti, S., Cordenonsi, M., Zanconato, F., Le Digabel, J. Forcato, M., Bicciato, S., Elvassore, N., and Piccolo, S. (2011) Role of YAP/TAZ in mechanotransduction *Nature.* 474, 179-183
47. Shen, Z., and Stanger, B. Z. (2015) YAP regulates S-phase entry in endothelial cells. *PloS One.* DOI: 10.1371/journal.pone.0117522
48. Dai, X., She, P., Chi, F., Feng, Y., Liu, H., Jin, D., Zhao, Y., Guo, X., Jiang, D., Guan, K-L., Zhong, T. P., and Zhao, B. (2013) Phosphorylation of angiotenin by Lats1/2 kinase inhibits F-actin binding, cell migration and angiogenesis. *J. Biol. Chem.* 288, 34041-34051
49. Adler, J. J., Johnson, D. E., Heller, B. L., Bringman, L. R., Ranahan, W. P., Conwell, M. D., Sun, Y., Hudman, A., and Wells, C. D. (2013) Serum deprivation inhibits the transcriptional co-activators YAP and cell growth via phosphorylation of the 130-Kda isoform of angiotenin by the LATS1/2 protein kinase. *Proc. Natl. Acad. Sci. USA.* 110, 17368-17373

50. Johnson, R., and Halder, G. (2014) The two faces of hippo: targeting the hippo pathway for regenerative medicine and cancer treatment. *Nat. Rev. Drug. Discov.* 13, 63-79
51. Brooke, B. S., Karnik, S. K., and Li, D. Y. (2003) Extracellular matrix in vascular morphogenesis and disease: structure versus signal. *Trend. Cell. Biol.* 13, 51-56
52. Bonnans, C., Chou, J., and Werb, Z. (2014) Remodeling the extracellular matrix in development and disease. *Nat. Rev. Mol. Cell Biol.* 15, 786-801
53. Pickup, M. W., Mouw, J. K., and Weaver, V. M. (2014) The extracellular matrix modulates the hallmarks of cancer. *EMBO Reports*. DOI: 10.15252/embr.201439246
54. Yip, K-P., and Marsh, D. J. (1997) An Arg-Gly-ASP peptide stimulates constriction in rat afferent arteriole. *Am. J. Physiol.* 273, 768-776
55. Mogford, J. E., Davis, G. E., Platts, S. H., and Meininger, G. A. (1996) Vascular smooth muscle alpha v beta 3 integrin mediates arteriolar vasodilation in response to RGD peptides. *Cir. Res.* 79, 821-826
56. Du, X., Plow, E. F., Frelinger, A. L., O'Toole, T. E., Loftus, J. C., and Ginsberg, M. H. (1991) Ligands activate integrin  $\alpha\text{IIb}\beta\text{3}$  (Platelet GPIIb-IIIa). *Cell.* 65, 409-416
57. Legler, D. FD., Wiedle, G., Ross, P. F., and Imhof, B. A. (2001) Superactivation of integrin  $\alpha\text{v}\beta\text{3}$  by low antagonists concentrations. *J. Cell. Sci.* 114,1545-1553
58. Deryugina, E. I., Zajac, E., Juncker-Jensen, A., Kupriyanova, T. A., Welter, L., and Quigley, J. P. (2014) Tissue-infiltrating neutrophils constitute the major in vivo source of angiogenesis-inducing MMP-9 in the tumor microenvironment. *Neoplasia.* 16, 771-788
59. Schnoor, M., Cullen, P., Lorkowski, J., Stolle, K., Robenek, H., Troyer, D., Rauterberg, J., and Lorkowski, S. (2008) Production of type VI collagen by human macrophages: a new dimension in macrophage functional heterogeneity. *J. Immunol.* 180, 5707-5719
60. Jetten, N., Verbruggen, S., Gijbels, M. J., Post, M. J., De Winther, M. P. J., Donners, M. M. P. (2014) Anti-inflammatory M2, but not pro-inflammatory M1 macrophage promote angiogenesis in vivo. *Angiogenesis.* 17, 109-118
61. Shen, B., Delaney, M. K., and Du, X. (2012) Inside-out, outside-in, and inside-outside-in: G protein signaling in integrin-mediated cell adhesion, spreading, and retraction. *Curr.*

Opin. Cell. Biol. 24, 600-606

62. Gong, H., Shen, B., Flevaris, P., Chow, C., Lam, S., C-T., Voyno-Yasenetskaya, T. A., Kozasa, T., and Du, X. (2010) G-protein subunit  $G\alpha_{13}$  binds to integrin  $\alpha IIb\beta 3$  and mediates integrin outside-in signaling. *Science*. 327, 340-343

63. Liao, Z., Kato, H., Pandey, M., Cantor, J. M., Ablooglu, A. J., Ginsberg, M. H., and Shattil, S. J. (2015) Interaction of kindlin-2 with integrin  $\beta 3$  promotes outside-in signaling responses by the  $\alpha v\beta 3$  vitronectin receptor. *Blood*. Doi:10.1182/blood-2014-09-603035

64. Von Wichert, G., Jiang, G., Kostie, A., De Vos, K., Sap, J., and Sheetz, M. (2003) RPTP- $\alpha$  acts as a transducer of mechanical force on  $\alpha v\beta 3$ -integrin-cytoskeleton linkage. *J. Cell. Biol.* 161, 143-153

65. Somanath, P. R., Malinin, N. L., and Byzova, T. V. (2009) Cooperation between integrin  $\alpha v\beta 3$  and VEGFR2 in angiogenesis. *Angiogenesis*. 12, 177-185

66. Yu, C-H., Law, J. B. K., Suryana, M., Low, H. Y., and Sheetz, M. P. (2011) Early integrin binding to Arg-Gly-Asp peptide activates actin polymerization and contractile movement that stimulates outward translocation. *Proc. Natl. Acad. Sci. USA*. 108, 20585-20590

67. Tang, Y., Rowe, G., Botvinick, E. L., Kurup, A., Putman, A. J., Seiki, M., Weaver, V. M., Keller, E. T., Goldstein, S., Dai, J., Begun, D., Saunders, T., and Weiss, S. J. (2013) MT1-MMP-dependent control of skeletal stem cell commitment via a  $\beta 1$ -integrin/YAP/TAZ signaling axis. *Dev. Cell*. 25, 402-416

68. Kaneko, K., Ito, M., Naoe, Y., Lacy-Hulbert, A., and Ikeda, K. (2014) Integrin  $\alpha v$  in the mechanical response of osteoblast lineage cells. *Biochem. Biophys. Res. Commun.* 447, 352-357

Example 18: Inhibition of ovarian tumor growth by targeting the HU177 cryptic collagen epitope.

Described herein are results demonstrating the anti-angiogenic and anti-tumor activity of antibody antagonists directed to the HU177 cryptic collagen epitope. As

described in detail below, antagonists of the HU177 epitope reduce stromal cell infiltration of tumors and inhibit angiogenesis and tumor growth.

As described in detail below, the HU177 epitope regulates ovarian tumor growth. Evidence suggests that stromal cells play critical roles in tumor growth. As described herein, uncovering new mechanisms that control stromal cell behavior and their accumulation within tumors leads to development of more effective treatments for malignant cancers. Described herein is evidence that the HU177 cryptic collagen epitope is selectively generated within human ovarian carcinomas and that this collagen epitope plays a functional role in SKOV-3 ovarian tumor growth in vivo. The ability of the HU177 epitope to regulate SKOV-3 tumor growth depends in part on its ability to modulate stromal cell behavior as targeting this epitope inhibited angiogenesis and surprisingly, the accumulation of  $\alpha$ SMA expressing stromal cells. As described in detail below, integrin  $\alpha$ 10 $\beta$ 1 can serve as a receptor for the HU177 epitope in  $\alpha$ SMA expressing stromal cells and subsequently regulates Erk-dependent migration. The findings presented herein are consistent with a mechanism by which the generation of the HU177 collagen epitope provides a previously unrecognized  $\alpha$ 10 $\beta$ 1-ligand that selectively governs angiogenesis and the accumulation of stromal cells, which in turn secrete pro-tumorigenic factors that contribute to ovarian tumor growth. Taken together, the findings presented herein provide new mechanistic understanding into the roles by which the HU177 epitope regulates ovarian tumor growth and provide new insight into the clinical results from a phase-I human clinical study of Mab D93/TRC093 in subjects with advanced malignant tumors.

The importance of stromal cells such as endothelial cells, fibroblasts, pericytes and inflammatory infiltrates in tumor growth has been appreciated for years (1-4). This insight has led investigators to begin developing novel approaches to regulate stromal cell behavior (5-8). However, given the functions of stromal cells in normal physiological processes, it is important to create strategies that might restrict the impact on stromal cells to that within the tumor microenvironment. In this regard, the structures of extracellular matrix (ECM) proteins that compose the architectural framework of most normal tissues are largely intact. In contrast, tumors often exhibit an altered ECM structure with

proteolytically degraded matrix proteins (9,10). As described herein, this differential ECM configuration provides a unique means for selectively regulating stromal cell behavior within tumors since cellular interactions with remodeled or denatured matrix proteins such as collagen alters adhesion, migration, proliferation and survival (11-14).

Previous studies uncovered functional cryptic sites within ECM molecules (14-16). As described herein, the process of generating cryptic elements is likened to that of a biomechanical ECM switch, in which structural alterations in these molecules initiated by either proteolytic cleavage or other physical mechanisms leads to the generation of cryptic regulatory epitopes which contribute to the initiation of unique signaling cascades that facilitate angiogenesis, tumor growth and metastasis (11-17). Recently, a new cryptic ECM epitope was identified within multiple forms of collagen (15). The HU177 epitope was generated within the ECM of angiogenic vessels and regulates endothelial cell behavior, as a monoclonal antibody directed to this epitope selectively inhibited endothelial cell adhesion and migration on denatured collagen and blocked angiogenesis in vivo (15). This antibody was humanized (Mab D93/TRC093) and a phase-I human clinical trial was completed (18-20). Clinical findings suggested that the HU177 epitope plays a role in tumor growth as 26% of the treated subjects exhibited stable disease and a reduction in liver lesions was observed in a subject with ovarian cancer (20).

Ovarian cancer is a heterogeneous disease classified by distinct histological subtypes (21-25). The molecular complexity of these tumors is demonstrated by the fact that low-grade type-I tumors often exhibit alterations in KRAS, BRAF and PTEN, while high-grade type-II tumors often have alterations in TP53 and BRCA1/2 (21-25). Importantly, stromal cells such as endothelial cells and activated fibroblasts may contribute to the development of ovarian carcinoma (26-28). Prior to the invention described herein, while collagen remodeling occurs during ovarian tumor growth, it was not known whether these changes are sufficient to generate the HU177 epitope or what role it plays in ovarian tumor growth.

Described herein is evidence that the HU177 cryptic collagen epitope is abundantly generated within human ovarian tumors, while little is expressed in benign granulomas. As described in detail below, antibodies directed to this epitope inhibited

SKOV-3 tumor growth in vivo, which was accompanied by reductions in proliferation, angiogenesis and the accumulation of  $\alpha$ SMA expressing stromal cells. While these studies indicate that  $\alpha$ 2 $\beta$ 1 integrin can bind the HU177 site, the little understood integrin  $\alpha$ 10 $\beta$ 1 plays an important role as a functional receptor in  $\alpha$ SMA-expressing stromal cells. Blocking interactions of the HU177 collagen epitope with  $\alpha$ 10 $\beta$ 1 integrin expressing fibroblasts reduced FGF2-stimulated Erk phosphorylation and migration on denatured collagen. Given the emerging roles of fibroblast-like cells in promoting tumor growth, these findings are consistent with a mechanism by which blocking the HU177 epitope reduces  $\alpha$ 10 $\beta$ 1-dependent accumulation of  $\alpha$ SMA expressing stromal cells in ovarian tumors, leading to the reduction of an important source of pro-tumorigenic cytokines that contribute to tumor progression.

The following Materials and Methods were utilized for Example 18.

Reagents, Chemicals and Antibodies.

Collagen type-I was from Sigma (St Louis, MO). Denatured collagen was prepared by boiling the solution of commercially obtained collagen for 15 minutes. The denatured collagen was allowed to cool for 5 minutes prior to use. Fibroblast growth factor-2 (FGF-2), integrins  $\alpha$ 1 $\beta$ 1,  $\alpha$ 2 $\beta$ 1,  $\alpha$ 3 $\beta$ 1,  $\alpha$ 10 $\beta$ 1,  $\alpha$ v $\beta$ 3 and antibodies directed to  $\alpha$ 1,  $\alpha$ 2,  $\alpha$ v integrins and IL-6 were from R&D Systems (Minneapolis, MN). Anti-CD-31 antibody was from BD Pharmingen (San Diego, CA). Anti- $\alpha$ SMA and anti-Ki67 antibodies were from Abcam (Cambridge MA). Anti-Erk antibodies were from Cell Signaling Technology (Danvers, MA). Anti-collagen-I antibody was from Rockland (Gilbertsville, PA). Antibody to  $\alpha$ 10 $\beta$ 1 was from Novus Biologicals (Littleton CO). BrdU kit was from Millipore (Bedford, MA).

Secondary antibodies were from Promega (Madison, WI). Mab HU177 was developed in a laboratory and shown to bind a PGxPG containing epitopes exposed within denatured, but not intact collagen from multiple species (11-16). Mab D93/TRC093 is a humanized version of Mab HU177 that also binds the PGxPG containing epitopes within denatured collagen from multiple species and was obtained from TRACON (San Diego, CA). The control antibody (Mab XL166) was generated in a laboratory and is directed to

an RGD collagen epitope. Collagen PGF- peptide (CPGFPGFC; SEQ ID NO: 16) and Cont-peptides (CQGPSGAPGEC; SEQ ID NO: 10), (CTWPRHHTTDALL; SEQ ID NO: 17) and (CNSYSYPSLRSP; SEQ ID NO: 18) were from QED Biosciences (San Diego CA). MEK inhibitor (PD98059) was from CalBiochem (San Diego, CA).

#### Analysis of tissue antigens.

Human ovarian tissues were from MMC under IRB exempt protocol (No. 3175x). For quantification of the HU177 epitope, biopsies (N=9) from high-grade ovarian tumors (serous and endometrial) or benign ovarian granulomas (N=9) were stained with Mab HU177. OCT compound embedded frozen sections (4.0 um) of biopsies of human ovarian tumor tissues were either stained by routine hematoxylin and eosin (H&E) procedure or by immunofluorescence. Immunofluorescence staining was performed on frozen sections by first blocking the tissue sections with 1.0% BSA in PBS for 1 hr followed by washing 3x with PBS. Tissue sections were next incubated with anti-HU177 antibody (100ug/ml) for 1 hour at room temperature. Tissues sections were next washed 3X with PBS followed by incubation with FITC-labeled secondary antibody for 1 hr. For quantification, stained tissue sections were scanned using Kodak ID system and pixel density quantified from five 200x fields from each of 5 specimens from each condition using Molecular Analyst Software ver 2.1 (29). Tumors were analyzed for apoptosis using TUNEL staining, for proliferation using anti-Ki67 antibody staining (1:1000), for angiogenesis using anti-CD31 antibody staining (1:300) and for CAF-like stromal cells using a combination of anti- aSMA (1:1000), anti-PDGF-R $\alpha$  (1:500) and anti-FAP (1:300) antibody staining. Quantification was performed within 5, 200X fields from each of 3 to 5 tumors.

#### Cells and Cell Culture.

SKOV-3 cells, were from ATCC (Manassas, VA) and cultured in RPMI in the presence of 5% FBS. Human umbilical vein endothelial cells (HUVECs) were obtained from Lonza (Walkersville, MD) and cultured in EBM-2 medium in 2% FBS and supplements (Lonza). Human dermal fibroblasts were obtained from Science Cell (Carlsbad, CA) and cultured in medium with 2.0% FBS.

#### Solid-Phase Binding Assays.

Plates were coated with 25µg/ml of native or denatured (boiled 15 minutes) collagen. Collagen epitope peptide PGF and Cont-peptides were immobilized at 100µg/ml. Integrins (0-2.0µg/ml) were diluted in binding buffer containing 20mM Tris, 15mM NaCl, 1mM MgCl<sub>2</sub>, 0.2 mM MnCl<sub>2</sub>, 0.5% BSA pH 7.4 as described (13). Integrins were allowed to bind for 1hr and plates washed and incubated with anti-integrin antibodies (1:100 dilution) for 1hr. Plates were washed and incubated with HRP-labeled secondary antibodies (1:5000 dilution). In a second assay, integrins (0.5µg/ml) were coated in binding buffer and plates were washed, blocked as before and denatured (boiled 15minutes) collagen was added (0-10.0µg/ml). Denatured collagen was detected with anti-collagen antibody (1:1000). For integrin blocking ELISAs, wells were coated with denatured collagen and pre-treated (0.1µg/ml) with anti-HU177 or control antibody. Following washing, wells were incubated with integrins (2.0µg/ml) and binding was detected as described. Assays were carried out at least 3 times.

#### Cell Adhesion Assays.

The wells of non-tissue culture forty-eight well cluster plates were coated for 12hrs at 4°C with 5µg/ml of native or denatured (boiled 15 minutes) collagen prepared as described above. SKOV-3 and fibroblasts were suspended in adhesion buffer containing RPMI 1640, 1mM MgCl<sub>2</sub>, 0.2mM MnCl<sub>2</sub> and 0.5% BSA (13) and 1x10<sup>5</sup> cells were added in the presence or absence of anti-HU177 or control antibodies (100µg/ml). Cells were allowed to attach for 25 minutes. Non-attached cells were removed by washing and attached cells stained with crystal violet as described (13). Wells were washed and the cell-associated crystal violet was eluted with 100ul per well of 10% acetic acid. Cell adhesion was quantified by measuring the optical density of the eluted crystal violet as described (15). Assays were completed at least 3x.

#### Cell Migration Assays.

Transwell membranes (8.0µm pore size) were coated with 5µg/ml of native or denatured collagen for 12 hrs at 40 C as described previously (13). Migration buffer containing RPMI 1640, 1mM MgCl<sub>2</sub>, 0.2mM MnCl<sub>2</sub> and 0.5% BSA in the presence or absence of 5X concentrated serum free SKOV-3 CM or 20ng/ml FGF-2 was placed in the

lower chambers. SKOV-3 or fibroblasts ( $1 \times 10^5$ ) were resuspended in migration buffer containing RPMI 1640, 1mM MgCl<sub>2</sub>, 0.2mM MnCl<sub>2</sub> and 0.5% BSA in the presence or absence of antibodies directed to the HU177 epitope, or  $\alpha 10\beta 1$ , (10 $\mu$ g/ml) or 100uM of the MEK inhibitor (PD98054). Cells were added to the top chamber and allowed to migrate from 2 to 4 hrs. Cells remaining on the top of the membranes were removed and cells that had migrated to the underside of the membrane were quantified by direct cell counts of crystal violet stained cells or by measuring the optical density of eluted cell-associated crystal violet dye as previously described (15). Assays were completed at least 3x.

#### Cell Proliferation Assays.

To prepare serum free fibroblast CM,  $2.0 \times 10^6$  cells were seeded in the presence of serum for 2hrs. Serum containing medium was removed and cells were washed and serum free RPMI was added. Serum free medium was collected at 24hrs and concentrated 10-fold. SKOV-3 cells were resuspended in the presence (150 $\mu$ l) of control (10X) RPMI or (10X) fibroblast CM. Cells were added to wells and allowed to growth for 24 or 72 hrs. Cell proliferation was quantified at 24 or 72hrs using BrdU kit according to manufactures instructions. Assays were completed 3 times.

#### Tumor Growth Assays.

Briefly, CAMs of 10-day chicks (N=6-8) were prepared as described (13) by separating the CAM from the shell membrane. Single cell suspensions of SKOV-3 cells ( $3 \times 10^6$ ) were applied topically to the CAMs in a total volume of 40 $\mu$ l (30). Twenty-four hours later embryos were either untreated or treated with a single topical application of 100 $\mu$ g of anti-HU177 antibody or control non-specific antibody (100 $\mu$ g/embryo) in a total volume of 40 $\mu$ l. Tumors were allowed to grow for a total of 7 days. At the end of the 7-day growth period the embryos were sacrificed and the tumors dissected and wet weights determined as described previously (13). For murine experiments, nude (NCRNU-F) mice (N=6-8) were injected subcutaneously into the flanks with SKOV-3 cells ( $3.0 \times 10^6$ /mouse). Mice were allowed to form tumors for 5 days and then untreated or injected (i.p) with Mab D93 or control antibody (0-100 $\mu$ g/ml) 3x per week for 28 days. Tumors were measured

with calipers and volumes calculated using the formula  $V = L^2 \times W/2$  where  $V$ = volume,  $L$ = length,  $W$ =width. Experiments were completed 3x.

#### Western Blot Analysis.

Cells from culture or cells seeded on native or denatured (boiled for 15 minutes) collagen type-I coated plates were allowed to attach for 15 minutes then were lysed in RIPA buffer (Santa Cruz, CA) with 1X protease inhibitor cocktail. Lysates were separated by SDS PAGE and probed with antibodies directed to  $\alpha 10$ , or  $\alpha 1$  integrins, total and phosphorylated Erk, Ki67 and  $\beta$ -tubulin or actin. Assays were performed at least 3 times.

#### Cytokine Analysis of Fibroblast CM.

Serum free CM (50 $\mu$ l) was screened for a panel of 12 cytokines (IL-1 $\alpha$ , IL-1 $\beta$ , IL-2, IL-4, IL-6, IL-8, IL-10, IL-12, IL-17A, TNF- $\alpha$ , INF- $\gamma$ , GM-CSF) using the Multi-analyte ELISArray™ kit (Qiagen) according to manufactures instructions. Analysis of conditioned medium was completed twice.

#### Statistical Analysis.

Statistical analysis was performed using the InStat statistical program. Data analyzed for significance using Student T test. P values < 0.05 were considered significant.

#### Results

##### Differential generation of the HU177 epitope in ovarian tumors.

Studies have correlated enhanced collagen synthesis and ECM degradation with tumor progression (31,32). In this regard, biopsies of human ovarian tumors and benign granulomas were examined for expression of the HU177 cryptic collagen epitope. Serial sections from frozen tissues were stained by H&E or with anti-HU177 antibody. As shown in Fig. 17A, the HU177 cryptic collagen epitope (green) could be detected in the extracellular matrix (ECM) of malignant ovarian tumors while minimal detection was observed in the ECM of the benign ovarian lesions (Fig. 17B). Quantification of the relative levels of the HU177 cryptic collagen epitope (Fig. 17C) indicated a significant ( $P < 0.05$ ) increase in HU177 collagen epitope in tumors as compared to the benign lesions. To confirm the generation of the HU177 epitope in an experimental mouse model, its

expression of the HU177 collagen epitope was examined in SKOV-3 tumors growing in mice. As shown in Fig. 17D, while HU177 epitope was detected within the SKOV-3 tumors, little was observed in normal tissues including ovaries, liver and lungs. These findings are consistent with the restricted generation of the collagen epitope.

The HU177 epitope regulates ovarian tumor growth.

Given the differential generation of the HU177 epitope observed in vivo, it was determined whether the HU177 epitope plays a functional role in ovarian tumor growth. To examine this possibility, SKOV-3 ovarian tumor cells were seeded topically on the chorioallantoic membrane (CAM) of chick embryos. Twenty-four hours later, the embryos were either not treated or treated with a single topical application with anti-HU177 antibody or non-specific control. Following 7 days of incubation, the resulting tumors were dissected from the CAMs for analysis. As shown in Fig. 182A, SKOV-3 tumors dissected from chick embryos treated with anti-HU177 antibody were smaller than controls. Quantification indicated that targeting the HU177 epitope significantly ( $P < 0.05$ ) inhibited SKOV-3 tumor growth by approximately 50% as compared to controls (Fig. 18B). To confirm these findings in a murine model, SKOV-3 cells were injected subcutaneously into the flanks of nude mice. Five days later following establishment of small tumor lesions, mice were either untreated or treated (100ug/mouse 3x per week) intraperitoneally (i.p) with anti-HU177 Mab or control non-specific antibody. As shown in Fig. 18C, treatment with anti-HU177 antibody significantly ( $P < 0.05$ ) reduced tumor size by approximately 70% by day 28. Dose dependent studies indicated inhibition of tumor growth at doses of anti-HU177 antibody as low as 10 $\mu$ g/mouse 3 times per week (data not shown).

The HU177 epitope regulates angiogenesis and stromal cell accumulation in ovarian tumors.

The behavior of multiple cell types within the tumor microenvironment including stromal cells can be controlled by interactions with collagen (2,6,33-37). Therefore, apoptosis was examined within control and anti-HU177 treated SKOV-3 tumors using TUNEL staining. An approximately 1.8 fold increase in apoptosis was detected within anti-HU177 treated tumors as compared to control, however, due to variation in staining,

this increase did not meet statistical significance. Next, cellular proliferation was examined by quantifying Ki67 antigen expression within these tumors growing in vivo. As shown in Fig. 19A, SKOV-3 tumors from anti-HU177 Mab treated mice exhibited significantly ( $P < 0.05$ ) reduced (25%-40%) Ki67 expression as compared to no treatment or control antibody, respectively. Given previous studies indicating that blocking the HU177 epitope selectively inhibited endothelial cell adhesion to denatured collagen type-IV but not native intact collagen type-IV (15) and inhibited angiogenesis in vivo (15,18), the reduction in cellular proliferation within these tumors could be due to multiple mechanisms including inhibition of angiogenesis given the known role of angiogenesis in regulating tumor growth.

To examine the distribution of the HU177 epitope in ovarian tumors, SKOV-3 tumors were co-stained with antibodies directed to the HU177 epitope and CD-31 a marker of blood vessels. While the HU177 epitope was detected in association with some CD-31 positive vessels (Fig. 19B, top) it was more extensively associated with  $\alpha$ SMA expressing fibroblast-like stromal cells (Fig. 19B bottom). Given the distribution of the HU177 epitope in the vicinity of blood vessels and  $\alpha$ SMA expressing stromal cells, the effects of anti-HU177 Mab treatment on SKOV-3 tumor angiogenesis and the accumulation of tumor-associated  $\alpha$ SMA expressing cells was further analyzed. As shown in Fig. 19C, a significant ( $P < 0.05$ ) 35% inhibition of SKOV-3 ovarian tumor angiogenesis was observed and remarkably, a 70% reduction in  $\alpha$ SMA expressing stromal cells was also detected following treatment with anti-HU177 antibody (Fig. 19D).

These findings are consistent with the notion that reduced angiogenesis and  $\alpha$ SMA expressing stromal cell accumulation may contribute to the anti-tumor activity observed following selective blockade of the HU177 collagen epitope.

SKOV-3 tumor cells and fibroblast exhibit enhanced adhesion and migration on denatured collagen.

Previous studies have documented that changes in the native structure of ECM proteins can alter the ability of cells to bind to these denatured proteins in part by disrupting conformational dependent epitopes required for cell binding in the context of its native configuration and/or exposing previously hidden cryptic binding epitopes including

cryptic RGD containing sequences (12-16). However, the ability of distinct cell types to interact with denatured collagen may vary widely and likely depends on multiple factors including the expression and activation of cell surface receptors with the capacity to recognize and bind to the multiple cryptic epitopes exposed following denaturation. To examine whether cellular interactions with denatured collagen alters cellular behavior, SKOV-3 and fibroblast adhesion and migration on native and denatured collagen was compared. As shown in Fig. 20A and 20B, a small but significant ( $P<0.05$ ) enhancement of SKOV-3 (38%) and fibroblast (29%) adhesion was detected on denatured collagen as compared to native collagen. In similar studies, the basal migratory capacity of SKOV-3 and fibroblasts on native and denatured collagen was compared. As shown in Fig. 20C and 20D, again a small but significant ( $P<0.05$ ) enhancement of SKOV-3 (34%) and fibroblast (19%) migration was detected on denatured collagen as compared to native collagen. While these studies do not specifically indicate that the enhanced adhesion and migration of the cells on denatured collagen depends specifically on the HU177 epitope, given that multiple cryptic epitopes are exposed following denaturation, these observations, however, do indicate that interactions with denatured collagen can alter the behavior of SKOV-3 cells and fibroblasts in vitro.

The HU177 epitope regulates SKOV-3 and fibroblast adhesion and migration on denatured collagen.

Tumor and fibroblast adhesive interactions with denatured collagen, which has been shown to be present within the microenvironment of malignant cancers, may regulate tumor progression. Given studies indicating that denaturation of collagen can alter the adhesive and migratory behavior of SKOV-3 cells and fibroblasts, the role of the HU177 collagen epitope on regulating adhesion and migration of these cells was examined. As shown in Fig. 21A, selectively blocking the HU177 epitope exposed within denatured collagen, significantly ( $P<0.05$ ) inhibited adhesion of SKOV-3 cells to denatured collagen by approximately 40%. In contrast, the anti-HU177 antibody failed to inhibit adhesion to intact collagen (Fig. 21B). These data are consistent with previous studies indicating a selective inhibition of cellular interactions with denatured collagen given that the anti-

HU177 antibody does not bind native intact collagen (15-18). In similar studies, the effects of targeting the HU177 epitope on fibroblast adhesion to denatured collagen was examined. Similar to what was observed with SKOV-3 tumor cells, blocking the HU177 epitope significantly ( $P < 0.05$ ) inhibited fibroblast adhesion to denatured collagen by approximately 50% as compared to controls while this antibody had no effect on fibroblast adhesion on native intact collagen (Fig. 21C and 21D). These data indicate the ability of the anti-HU177 antibody to inhibit adhesion is restricted to those circumstances in which the HU177 epitope is generated and thus the anti-HU177 antibody does not alter adhesion to intact collagen thereby allowing a highly selective strategy to inhibit adhesive cellular interactions with denatured collagen.

Next, the migratory capacity of these cells on native and denatured collagen was examined. As shown in Fig. 21E through 21F, blocking the HU177 epitope exposed within denatured collagen also significantly ( $P < 0.05$ ) inhibited basal migration of SKOV-3 and fibroblasts by 35% to 38%, while migration on intact collagen was not effected (Fig. 21E-21H). Interestingly, while blocking the HU177 epitope inhibited adhesion and migration, it exhibited little effects on the growth of SKOV-3 cells or fibroblasts on denatured collagen when examined in vitro. These studies are consistent with the anti-HU177 antibody having minimal if any direct anti-proliferative activity on fibroblasts or SKOV-3 cells on denatured collagen in vitro.

#### Inhibition of growth factor-induced fibroblast migration by targeting the HU177 epitope.

Accumulating evidence indicates that recruitment of activated and/or cancer-associated fibroblasts may facilitate tumor growth and survival, in part by providing an important source of pro-tumorigenic factors including IL-6 (2,5,6,38). While it is clear that most dermal fibroblast do not represent a fully accurate model of cancer associated stromal cells found in vivo, following in vitro culture, the fibroblasts exhibited phosphorylated Erk and expressed  $\alpha$ SMA and PDGF-R $\alpha$ , important markers of CAF-like stromal cells. Therefore, these fibroblasts were used as a model of  $\alpha$ SMA expressing stromal cells and it was examined whether blocking the HU177 epitope could alter growth factor-induced migration. As shown in Fig. 22A and 22B, concentrated SKOV-3 CM as well as recombinant FGF-2 stimulation enhanced migration on denatured collagen.

Importantly, addition of the anti-HU177 antibody to the migration wells significantly ( $P < 0.05$ ) inhibited this growth factor stimulated response suggesting that not only can the HU177 epitope play a role in the basal cell migration, but also help regulate growth factor mediated motility.

Previous studies have indicated that FGF-2 stimulation can initiate a complex signaling cascade leading to the phosphorylation of multiple effector molecules and transcription factors such as Erk1/2, which help coordinate the complex events required for cellular migration (39-44). Given the known role of FGF-2 in regulating Erk activation, the effects of blocking fibroblast interactions with the HU177 epitope on FGF-2 stimulated Erk phosphorylation were examined. As shown in Fig. 22C, FGF-2 stimulated a small increase in Erk phosphorylation in cells attached to denatured collagen, while blocking the HU177 epitope reduced this phosphorylation. A mean reduction in Erk phosphorylation from 4 independent experiments of approximately 40% was observed (Fig. 22D). To confirm a role for MAP/Erk signaling in FGF-2 stimulated fibroblast motility on denatured collagen, migration assays were carried out in the presence of a MEK inhibitor. As shown in Fig. 22E, addition of the MEK inhibitor (PD98059) significantly ( $P < 0.05$ ) blocked FGF-2 stimulated migration on denatured collagen suggesting a role for MAP/Erk signaling in regulating this migratory response.

#### Identification of receptors for the HU177 epitope.

The repetitive PGxPG containing sequence as a critical component of the HU177 epitope was previously identified (15). In addition, other studies have indicated that antibodies directed to the HU177 epitope can bind to a variety of distinct PGxPG containing sequences with different N-terminal and C-terminal flanking sequences found in collagen (19). Given that a number of variations of this motif are found throughout collagen, it is possible that multiple receptors may have the ability to bind to these cryptic sites. To this end, integrin receptors are an important class of molecules known to mediate cellular interactions with ECM components and coordinate signaling cascades that govern cell motility. To define potential cell surface receptors for HU177 collagen epitope, the ability of various recombinant integrins to bind denatured collagen was examined. Integrin  $\alpha 2\beta 1$  and  $\alpha \nu\beta 3$  dose dependently bound denatured collagen, while  $\alpha 1\beta 1$  showed

minimal interactions (Fig. 23A). Interestingly, integrin  $\alpha 10\beta 1$ , a collagen binding receptor thought to have a limited tissue distribution outside of cartilage (45-48) also dose dependently bound denatured collagen. To confirm  $\alpha 10\beta 1$  binding to denatured collagen we carried out a second binding assay by immobilizing  $\alpha 10\beta 1$  on microliter wells and examining soluble denatured collagen binding. Denatured collagen dose dependently bound  $\alpha 10\beta 1$ , but not  $\alpha 3\beta 1$  (Fig. 23B). To identify which integrins capable of binding denatured collagen have the ability to bind the HU177 epitope, the effects of blocking the HU177 epitope on integrin binding were examined. As shown in Fig. 23C, blocking the HU177 epitope inhibited  $\alpha 10\beta 1$  binding by nearly 60%, while  $\alpha 2\beta 1$  binding was reduced by approximately 30% (Fig. 23D). Binding of  $\alpha \nu\beta 3$  to denatured collagen was unaffected (Fig. 23E). To confirm the integrin binding specificity, direct binding to the synthetic PGxPG containing HU177 epitope (PGF peptide) was performed. As shown in Fig. 23F, while  $\alpha 2\beta 1$  bound the HU177 epitope,  $\alpha 10\beta 1$  exhibited 4-fold greater binding, while  $\alpha \nu\beta 3$  failed to bind. Moreover, the PGF-peptide also partially competed binding of  $\alpha 10\beta 1$  to denatured collagen by approximately 60% (Fig. 23G). Taken together, these findings suggest that the little understood integrin  $\alpha 10\beta 1$  can bind the HU177 collagen epitope.

Integrin  $\alpha 10\beta 1$  co-localizes with  $\alpha$ SMA expressing cells in ovarian tumors.

Given the studies indicating the ability of  $\alpha 10\beta 1$  to bind the HU177 epitope, the expression of  $\alpha 10\beta 1$  within ovarian tumors was examined. As shown in Fig. 24A,  $\alpha 10\beta 1$  was detected within human ovarian tumors (left) and SKOV-3 tumors (right). Expression of  $\alpha 10\beta 1$  was associated predominately with  $\alpha$ SMA positive cells as suggested by extensive co-localization (Fig. 24B).

While minimal levels of  $\alpha 10$  integrin protein (Fig. 24C) and mRNA were detected in SKOV-3 cells, greater than 5 fold higher levels were detected in  $\alpha$ SMA expressing fibroblasts. Next, the effects of blocking  $\alpha 10\beta 1$  on fibroblast migration were examined. As shown in Fig. 24D, anti-  $\alpha 10$  antibody inhibited FGF-2 stimulated migration on denatured collagen. To confirm a role for  $\alpha 10\beta 1$  integrin in fibroblast migration on denatured collagen, expression  $\alpha 10\beta 1$  was integrin knocked down in these fibroblasts using  $\alpha 10$  specific shRNA. As shown in Fig. 24E, the relative levels of  $\alpha 10$  protein were reduced by approximately 70% while little change in  $\alpha 1$  integrin chain or actin was

observed. Next, the ability of fibroblasts expressing altered levels of  $\alpha 10$  integrin to migrate on denatured collagen was examined. As shown in Fig. 24F, while little if any change was observed in control transfected (Con-Kd-HF) fibroblasts as compared wild type parental cells (WT-HF), knocking down  $\alpha 10$  integrin significantly ( $P < 0.05$ ) inhibited fibroblast migration on denatured collagen by approximately 60% as compared to controls.

Given these results, it's possible that the reduction of  $\alpha$ SMA positive stromal cells observed following anti-HU177 treatment leads to a reduction in an important source of pro-tumorigenic cytokines that facilitate tumor growth and angiogenesis. To this end, it was examined whether CM from  $\alpha$ SMA expressing fibroblasts might contain soluble factors that enhance SKOV-3 cell growth. As shown in Fig. 24G and 24H, fibroblast CM enhanced proliferation and Ki67 antigen expression in SKOV-3 cells. These results are consistent with the ability of soluble factors released into the conditioned medium of these  $\alpha 10\beta 1$ -expressing fibroblasts to enhance SKOV-3 tumor cell proliferation in vitro. To characterize potential pro-tumorigenic factors expressed by these  $\alpha$ SMA-positive fibroblasts, concentrated serum free CM was screened using a multianalyte cytokine array for expression of 12 different cytokines. Among the cytokines that were expressed at the highest levels was IL-6 (Table 2).

Table 2 shows the analysis of cytokine expression in fibroblasts conditioned medium. Serum free conditioned medium (CM) was collected following a 24-hour incubation of  $\alpha 10\beta 1$  expressing human fibroblasts. Conditioned medium was concentrated 10 fold. Serum free 10X concentrated conditioned medium was examined for the presence of 12 different cytokines using the Multi-analyte ELISArray™ detection kit. Data values represents optical density (O.D) readings at a wavelength of 450nm from the human fibroblast conditioned medium sample (HFB), negative control buffer (Neg Cont) or Positive control samples provided in the assay kit (Pos Cont) for the expression of each of the 12 cytokines.

Table 2.

Cytokine	HFB (CM)	Neg Cont	Pos Cont
IL-1 $\alpha$	0.471	0.058	1.857
IL-1 $\beta$	0.491	0.060	2.607
IL-2	0.759	0.066	0.707
IL-4	0.692	0.026	1.448
IL-6	1.554	0.052	0.606
IL-8	3.785	0.043	3.292
IL-10	0.678	0.043	1.440
IL-12	0.877	0.053	1.708
IL-17A	2.747	0.054	1.670
IFN $\gamma$	1.409	0.045	1.089
TNF- $\alpha$	0.435	0.040	0.564
GMCSF	2.194	0.043	2.966

Interestingly, IL-6 has been shown to enhance growth of ovarian carcinoma cells (49,50) and thus, it was examined whether this pro-tumorigenic cytokine played a functional role in mediating the ability of  $\alpha$ SMA expressing fibroblast CM to stimulate proliferation of SKOV-3 tumor cells. As shown in Fig. 24I, fibroblast CM significantly enhanced SKOV-3 tumor cell proliferation and a function-blocking antibody directed to IL-6 inhibited this response. These data are consistent with a role for IL-6 expression from fibroblasts in promoting SKOV-3 tumor cell growth. Taken together, these findings suggest the possibility that  $\alpha$ SMA-expressing fibroblasts may serve as an important source of protumorigenic factors that facilitate SKOV-3 tumor growth and that selectively

reducing accumulation of  $\alpha$ SMA expressing stromal cells by inhibiting the HU177 collagen epitope contributes to the potent anti-tumor activity observed in vivo.

### Discussion

The array of mechanisms by which stromal cells such as endothelial cells and activated  $\alpha$ SMA expressing fibroblasts govern the malignant phenotype are diverse and include providing proteolytic enzymes that alter the biomechanical properties of ECM, the release of protumorigenic factors that act on both tumor and other cell types to alter their growth, survival and migratory behavior, and the release of molecules that influence the host immune response (1-6,51,52). Thus, selectively blocking the accumulation of protumorigenic stromal cells in malignant lesions likely represents an important therapeutic strategy. While targeting stromal cells may provide a complementary strategy for tumor therapy, prior to the invention described herein, it was challenging to selectively target them without disrupting their activity in normal tissues. The ECM represents an active control point for multiple mechanisms critical for regulating stromal cell behaviors ranging from migration and proliferation to gene expression (14). Therefore, inhibiting stromal cell-ECM interaction that selectively limit the accumulation of pro-tumorigenic stromal cells in malignant lesions might represent a useful strategy to control tumor progression.

Here we show that the HU177 collagen epitope is abundantly generated within ovarian carcinomas as compared to benign ovarian lesions. Importantly, previous studies have indicated that proteolytic enzymes such as MMPs can contribute to generation of the HU177 epitope in vivo (16). As described herein, this cryptic collagen epitope played a role in SKOV-3 tumor growth and these findings are consistent with a clinical trial assessing tolerability and toxicity of Mab D93/TRC093 (20). Results from this study suggested no dose limiting toxicities and evidence of anti-tumor activity as a subject with an ovarian cancer showed a reduction in metastatic liver lesions (20). While all subjects eventually progressed, 26% exhibited disease stabilization and a subject with hemangiopericytoma, a tumor known to be highly infiltrated with stromal cells exhibited stable disease for nearly a year (20).

Consistent with previous findings (15,18), the anti-HU177 antibody inhibited tumor associated angiogenesis. These data are in agreement with previous studies indicating that targeting the HU177 epitope could selectively inhibit endothelial cell adhesion and migration on denatured collagen, inhibit proliferation, upregulate expression of P27KIP1 and inhibit angiogenesis in vivo (15). Surprisingly, the results presented herein indicate that targeting the HU177 epitope can also reduce the accumulation of  $\alpha$ SMA expressing stromal cells within SKOV-3 tumors. As described herein, targeting the HU177 epitope inhibited SKOV-3 and  $\alpha$ SMA-expressing fibroblast adhesion and migration on denatured but not intact collagen, thereby specifically limiting the impact of this therapeutic agent to those tissues expressing the HU177 epitope. FGF-2 induced fibroblast migration on denatured collagen was shown to be dependent in part on MAP/Erk signaling as inhibition of MAP/Erk signaling blocked this migratory response.

Cell migration is governed by a complex and integrated set of signaling events that are coordinated in part by the unique composition and integrity of the local extracellular matrix. However, prior to the invention described herein, the mechanisms by which cells sense the structural changes in the integrity of a given ECM environment during tumor growth to facilitate cellular motility induced by growth factors were not completely understood. In fact, inappropriate and/or enhanced migration may contribute to tumor cell invasion and metastasis as well as the accumulation of CAF-like stromal cells that contribute to tumor progression. Integrin mediated interactions with ECM proteins are known to initiate assembly of a multiple-protein signaling complexes that coordinately regulate multiple downstream signaling cascades including Shc/Grb2/Ras and Fak/Src/Rap1 pathways that can activate MAPK/Erk signaling (41). The results presented herein suggest FGF-2 can enhance the phosphorylation of Erk in  $\alpha$ 10 $\beta$ 1-expressing fibroblasts and a function blocking antibody directed to the HU177 cryptic collagen epitope inhibited Erk phosphorylation. Given that MAPK/Erk signaling plays a role in the ability of  $\alpha$ 10 $\beta$ 1-expressing fibroblasts to migrate on denatured collagen and the fact that denatured collagen has been shown to be selectively generated within the tumor microenvironment (12,13,15,18), it would be interesting to speculate that the selective generation of the HU177 epitope within the ovarian tumor microenvironment may help

facilitate enhanced activation of Erk which may promote stromal cell accumulation. While multiple protein kinases are thought to contribute to the phosphorylation of Erk, the precise molecular mechanism by which cellular interactions with the HU177 epitope regulates FGF-2 induced activation of Erk were not known prior to the invention described herein. Studies are currently underway to confirm which kinases and/or phosphatases might contribute to the FGF-2 mediated regulation of Erk following interactions with the HU177 collagen epitope.

Given the reduction in  $\alpha$ SMA expressing cells in tumors treated with anti-HU177 antagonists, selectively inhibiting migration of this population of stromal cells may limit a major cellular source of pro-tumorigenic factors that play multiple roles in facilitating tumor cell survival and proliferation in vivo. In this regard, fibroblasts are known to express many pro-tumorigenic factors including IL-6, which has been previously shown to enhance proliferation of ovarian carcinoma cells (38,49,50). Consistent with these findings, the results presented herein suggest that blocking IL-6 inhibited fibroblast CM-induced SKOV-3 cell growth. Given these findings and the high levels of IL-6 expressed by fibroblasts, this data is consistent with a mechanism by which targeting the HU177 epitope selectively limits accumulation of  $\alpha$ SMA fibroblasts thereby reducing an important source of pro-tumorigenic factors that enhance angiogenesis and tumor growth.

Described herein is new evidence that the little understood integrin  $\alpha$ 10 $\beta$ 1 functions as a receptor for the HU177 collagen epitope in fibroblasts. Given the variations within the HU177 PGxPG consensus site and the possibility of unique geometrical configurations and distinct flanking amino acid sequences displayed in vivo, it is possible that additional receptors may also recognize the HU177 epitope. Interestingly, little is known concerning the functions of  $\alpha$ 10 $\beta$ 1 outside of chondrocyte and growth plate development (45-48). However,  $\alpha$ 10 mRNA has been detected in murine heart, muscle tissues and endothelial cells (45-48). Studies suggest that FGF-2 stimulation of mesenchymal stem cells (MSC) leads to upregulation of  $\alpha$ 10 (53). Moreover, MSC have also been implicated as potential sources of  $\alpha$ SMA expressing CAF-like cells in tumors (54). In addition, studies now suggest enhanced expression of  $\alpha$ 10 $\beta$ 1 in melanoma cell

lines as compared to primary melanocytes and inhibiting  $\alpha 10\beta 1$  in these cells resulted in a reduced migration (55).

Given the ability of  $\alpha 10\beta 1$  to bind the HU177 epitope, the data presented herein are in agreement with a mechanism by which generation of the HU177 epitope provides a previously unrecognized ligand for  $\alpha 10\beta 1$ -expressing stromal cells that facilitates FGF-2 induced activation of Erk and subsequently the accumulation of  $\alpha$ SMA positive stromal cells in ovarian tumors. In turn, the selective reduction in accumulation of this cell population by anti-HU177 antibody, in conjunction with its previously described anti-angiogenic effects, likely contribute to its potent anti-tumor activity. Taken together these findings provide new cellular and molecular insight into the roles of the HU177 cryptic epitope in ovarian tumor growth and provide new mechanistic understanding of the therapeutic impact observed in human subjects treated with Mab D93 (20).

The following references were cited in Example 18.

### **References**

- 1). Mursap, N, Diamandis, EP: Revisiting the complexity of the ovarian cancer microenvironment-clinical implications for treatment strategies. *Mol Cancer Res* 2012, 10: 1254-1264
- 2). Schauer, IG, Sood, AK, Mok, A, Liu, J: Cancer associated fibroblasts and their putative role in potentiating the initiation and development of epithelial ovarian cancer. *Neoplasia* 2011, 13:393-405
- 3). Hanahan, D, Coussens, LM: Accessories to the crime: functions of cells recruited to the tumor microenvironment. *Cancer Cell* 2012, 21: 309-421
- 4). Qian, BZ, Pollard, JW: Macrophage diversity enhances tumor progression and metastasis. *Cell* 2010, 141: 39-51
- 5). Bansai, R, Tomar, T, Ostman, A, Poelstra, K, Prakash, J: Selective targeting of interferon  $\gamma$  to stromal fibroblasts and pericytes as a novel therapeutic approach to inhibit angiogenesis and tumor growth. *Mol Cancer Ther* 2012, 11: 2419-2428
- 6). Mitra, AK, Zillhardt, M, Hua, Y, Tiwari, P, Murmann, AE, Peter, ME, Lengyel, E: MicroRNAs reprogram normal fibroblasts into cancer-associated fibroblast in ovarian cancer. *Cancer Discov* 2012, 2: 1100-1108

- 7). Yao, Q, Qu, X, Yang, Q, Mingqian, W, Kong, B: CLIC4 mediates TGF- $\beta$ 1-induced fibroblast-to-myofibroblast trans differentiation in ovarian cancer. *Oncol Reports* 2019, 22: 541-548
- 8). Crawford, Y, Kasman, I, Yu, L, Zhong, C, Wu, X, Modrusan, Z, Kaminker J, Ferrara, N: PDGF-C mediates the angiogenic and tumorigenic properties of fibroblasts associated with tumors refractory to anti-VEGF treatment. *Cancer Cell* 2009, 15: 21-34
- 9). Ricciardelli, C, Rodgers, RJ: Extracellular matrix of ovarian tumors. *Semin Reprod Med* 2006, 24, 270-282
- 10). Capo-Chichi, CD, Smith, ER, Yang, DH, Roland, IH, Vanderveer, L, Hamilton, TC, Godwin, AK, Xu, XX: Dynamic alterations of the extracellular matrix environment of ovarian surface epithelial cells in premalignant transformation, tumorigenicity, and metastasis. *Cancer* 2002 95, 1802-1815
- 11). Akalu, A, Roth, JM, Caunt, M, Policarpio, D, Liebes, L, Brooks, PC: Inhibition of angiogenesis and tumor metastasis by targeting a matrix immobilized cryptic extracellular matrix epitope in laminin. *Cancer Res* 2007, 67: 4353-4363
- 12). Hangai, M, Kitaya, N, Xu, J, Chan, CK, Kim, JJ, Werb, Z, Ryan, SJ, Brooks, PC: Matrix metalloproteinase-9-dependent exposure of a cryptic migratory control site in collagen is required before retinal angiogenesis. *Am J Pathol* 2002, 161: 1429-1437
- 13). Xu, J, Rodriguez, D, Petitclerc, E, Kim, JJ, Hangai, M, Yuen, SM, Davis, GE, Brooks, PC: Proteolytic exposure of a cryptic site within collagen type-IV is required for angiogenesis and tumor growth in vivo. *J Cell Biol* 2001, 154: 1069-1079
- 14). Cretu, A, Brooks, PC: Impact of the non-cellular microenvironment on metastasis: potential therapeutic and imaging opportunities. *J Cell Physiol* 2007, 213: 391-402
- 15). Cretu, A, Roth, JM, Caunt, M, Policarpio, D, Formenti, S, Gange, P, Liebes, L, Brooks, PC: Disruption of endothelial cell interactions with the novel HU177 cryptic collagen epitope inhibits angiogenesis. *Clin Cancer Res* 2007, 13: 3068-3078
- 16). Gagne, PJ, Tihonov, N, Li, X, Glaser, J, Qiao, J, Silberstein, M, Yee, H, Gagne, E, Brooks, PC: Temporal exposure of cryptic collagen epitopes within ischemic muscle during hindlimb reperfusion. *Am J Pathol* 2005, 167: 1349-1359
- 17). Ames, JJ, Vary, C PH, Brooks, PC: Signaling pathways and molecular mediators in

metastasis. *Biomechanical ECM Switches and Tumor Metastasis*. Springer Press 2012, 3: 71-89

18). Pernasetti, F, Nickel, J, Clark, D, Baeurle, PA, Van Epps, D, Freimark, B: Novel antidenatured collagen humanized antibody D93 inhibits angiogenesis and tumor growth: an extracellular matrix-based therapeutic approach. *Int J Oncol* 2006, 29: 1371-1379

19). Freimark, B, Clark, D, Pernasetti, F, Kickel, J, Myszka, D, Baeuerle, PA, van Epps, D: Targeting of humanized antibody D93 to sites of angiogenesis and tumor growth by binding to multiple epitopes on denatured collagens. *Mol Immunol* 2007, 44: 3741-3750

20). Robert, F, Gordon, MS, Rosen, LS, Mendelson, DS, Mulay, M, Adams, BJ, Alvare, D, Theuer, CP, Leigh, BR: Final results from a phase I study of TRC093 (humanized anti-cleaved collagen antibody) in patients with solid cancer. Annual meeting proceedings, 2010, ASCO. Abstract No 3038

21). Romero, I, Bast, RC: Minireview: human ovarian cancer: biology, current management, and paths to personalized therapy. *Endocrinol* 2012, 154: 1593-1602

22). Vaughan, S, Coward, JI, Bast, RC, Berchuck, A, Berek, JS, Brenton, JD, Coukos, G, Crum, CC, Drapkin, R, Etemadmoghadam, D, Friedlander, M, Gabra, H, Kaye, SB, Lord, CJ, Lengyel, E, Levine, DA, McNeish, IA, Menon, U, Mills, GB, Nephew, K, P, Oza, AM, Sood, AK, Stronach, EA, Walczak, H, Bowtell, DD, Balkwill, FR: Rethinking ovarian cancer: recommendations for improving outcomes. *Nat Rev Cancer* 2011, 11: 719-25

23). Kuman, RJ, Shih, M: The origin and pathogenesis of epithelial ovarian cancer: a proposed unifying theory. *Am J Surg Pathol* 2010, 34: 433-443

24). Kim, J, Coffey, DM, Creighton, CJ, Yu, Z, Hawkins, SM: High-grade serous ovarian cancer arises from fallopian tube in a mouse model. *Proc Nat Acad Sci USA* 2012, 109: 3921-3926

25). Ozols, RF, Bookman, MA, Connolly, DC, Daly, MB, Godwin, AK, Schilder, RJ, Xu, X, Hamilton, TC: Focus on epithelial ovarian cancer. *Cancer Cell* 2004 5: 19-24

26). Granot, D, Addadi, Y, Kalchenko, V, Harmelin, A, Kunz-Schugart, LA, Neeman, M: In vivo imaging of systemic recruitment of fibroblasts to the angiogenic rim of ovarian carcinoma tumors. *Cancer Res* 2007, 67: 9180-9190

- 27). Cai, J, Tang, H, Xu, L, Wang, X, Yang, C, Ruan, S, Guo, J, Hu, S, Wang, Z: Fibroblasts in omentum activated by tumor cells promote ovarian cancer growth, adhesion and invasiveness. *Carcinogenesis* 2013, 33: 20-29
- 28). Ko, SY, Barengo, N, Ladanyi, A, Lee, JS, Marini, F, Lengyel, E, Naora, H: HoxA9 promotes ovarian cancer growth by stimulating cancer-associated fibroblasts. *J Clin Invest* 2012, 122: 3603-3617
- 29). Roth, JM, Zelmanovich, A, Policarpio, D, Ng, B, MacDonald, S, Formenti, S, Liebes, L, Brooks, PC: Recombinant alpha 2(IV) NC1 domain inhibits tumor cell-extracellular matrix interactions, induces cellular senescence, and inhibits tumor growth in vivo. *Am J Pathol* 2005, 166: 901-911
- 30). Brooks, PC, Montgomery, AM, Rosenfeld, M, Reisfeld, RA, Hu, T, Klier, G, Cheresh, DA: Integrin  $\alpha\beta 3$  antagonists promote tumor regression by inducing apoptosis of angiogenic blood vessels. *Cell* 1994, 79: 1157-1164
- 31). Zhu, GG, Melkko, J, Risteli, J, Kauppila, A, Risteli, L: Differential processing of collagen type-I and type III procollagens in the tumor cysts and peritoneal ascites fluid of patients with benign and malignant ovarian tumors. *Clin Chim Acta* 1994, 229: 87-97
- 32). Santala, M, Risteli, J, Risteli, L, Pulstola, U, Kacinski, BM, Stanley, ER, Kauppila, A: Synthesis and breakdown of fibrillar collagens: concomitant phenomena in ovarian cancer. *Br J Cancer* 1998, 77: 1825-1831
- 33). Kawamura, K, Komohara, Y, Takaishi, K, Katabuchi, H, Takeya, M: Detection of M2 macrophages and colony stimulating factor 1 expression in serous and mucinous ovarian epithelial tumors. *Pathol International* 59: 300-305
- 34). Cubillos-Ruiz, JR, Rutkowski, M, Conejo-Garcia, JR: Blocking ovarian cancer progression by targeting tumor microenvironmental leukocytes. *Cell Cycle* 2010, 9: 260-268
- 35). Petitclerc, E, Stromblad, S, von Schalscha, TL, Mitjans, F, Piulats, J, Montgomery, AM, Cheresh, DA, Brooks, PC: Integrin  $\alpha\beta 3$  promotes M21 melanoma growth in human skin by regulating tumor cell survival. *Cancer Res* 1999, 59: 2724-2730
- 36). Anderberg, C, Pietras, K: On the origin of cancer-associated fibroblasts. *Cell Cycle* 2009, 8:1461-1465

- 37). Erez, N, Truitt, M, Olsen, P, Hanahan, D: Cancer-associated fibroblasts are activated in incipient neoplasia to orchestrate tumor-promoting inflammation in an NF $\kappa$ B-dependent manner. *Cancer Cell* 2010, 17: 135-147
- 38). Erez, N, Glanz, S, Raz, Y, Avivi, C, Barshack, I: Cancer associated fibroblasts express proinflammatory factors in human breast and ovarian tumors. *Biochem Biophys Res Commun* 2013, 437: 397-402
- 39). Cunningham, DL, Sweet, SMM, Cooper, HJ, Heath, JK: Differential phosphoproteomics of fibroblast growth factor signaling: identification of Src family kinase-mediated phosphorylation events. *J Proteome Res* 2010, 9: 2317-2328
- 40). Kanda, S, Miyata, Y, Kanetake, H, Smithgall, T, E: Fibroblast growth factor-2 induces the activation of Src through Fes, which regulates focal adhesion disassembly. *Exp Cell Res* 2006, 312: 3015-3022
- 41). Barberis, L, Wary, KK, Fiucci, G, Liu, F, Hirsch, E, Brancaccio, M, Altruda, F, Tarone, G, Giancotti, FG: Distinct roles of the adaptor protein Shc and focal adhesion kinase in integrin signaling to Erk. *J Biol Chem* 2000, 275: 36532-36540
- 42). Cho, AY, Klemke, RL: Extracellular-regulated kinase activation and CAS/Crk coupling regulate cell migration and suppress apoptosis during invasion of the extracellular matrix. *J Cell Biol* 2000, 149: 223-236
- 43). Kottakis, F, Polytarchou, C, Foltopoulou, P, Sanidas, I, Kampranis, SC, Tsihchlis, PN: FGF-2 regulates cell proliferation, migration and angiogenesis through an NDY1/KDM2B-miR-101-EZH2 pathway. *Mol Cell* 2011, 12: 285-298
- 44). Boilly, B, Vercoutter-Edouart, AS, Hondermarck, H, Nurcombe, V, Bourhis, XL: FGF signals for cell proliferation and migration through different pathways. *Cytokine Growth Factor Rev* 2000, 11: 295-302
- 45). Lehnert, K, Ni, J, Leung, E, Gough, S, Morris, CM, Liu, D, Wang, SX, Langley, R, Krissansen, GW: The integrin  $\alpha$ 10 subunit: expression pattern, partial gene structure, and chromosomal localization. *Cytogenet Cell Genet* 1998, 87: 238-244
- 46). Bengtsson, T, Camper, L, Schneller, M, Lundgren-Akerlund, E: Characterization of the mouse integrin subunit  $\alpha$ 10 gene and comparison with its human homologue genomic

- structure, chromosomal localization and identification of splice variants. *Matrix Biol.* 2001, 20: 565-576
- 47). Bengtsson, T, Aszodi, A, Nicolae, C, Hunziker, EB, Lundgren-Akerlund, E, Fassler, R: Loss of  $\alpha 10\beta 1$  integrin expression leads to moderate dysfunction of growth plate chondrocytes. *J. Cell Sci.* 2004, 118: 929-936
- 48). Camper, L, Holmval, K, Wangnerd, C, Asodi, A, Lundgren-Akerlund, E: Distribution of the collagen-binding integrin  $\alpha 10\beta 1$  during mouse development. *Cell Tissue Res* 2001, 306: 107-116
- 49). Wang, Y, Li, L, Jin, X, Sun, W, Zhang, X, Xu, RC: Interleukin-6 signaling regulates anchorage-independent growth, proliferation, adhesion and invasion in human ovarian cancer cells. *Cytokine.* 2012, 59: 228-236
- 50). Wang, Y, Xu, RC, Zhang, XL, Niu, XL, Qu, Y, Li, LZ, Meng, XY: Interleukine-8 secretion by ovarian cancer cells increases anchorage-independent growth, proliferation, angiogenic potential, adhesion and invasion. *Cytokine.* 2012, 59: 145-155
- 51). Santos, AM, Jung, J, Aziz, N, Kissil, JL, Pure, E: Targeting fibroblast activation protein inhibits tumor stromagenesis and growth in mice. *J Clin Invest* 2009, 119: 3613-3625
- 52). Kraman, M, Bambrough, PJ, Arnold, JN, Roberts, EW, Magiera, L, Jones, JO, Gopinathan, A, Tuveson, DA, Fearon, DT: Suppression of anti-tumor immunity by stromal cells expressing fibroblast activation protein- $\alpha$ . *Science* 2001, 250: 827-830
- 53). Varas, L, Ohlsson, LB, Honeth, G, Olsson, A, Bengtsson, T, Wiberg, C, Bockermann, R, Järnum, S, Richter, J, Pennington, D, Johnstone, B, Lundgren-Akerlund, E, Kjellman, C:  $\alpha 10$  integrin expression is upregulated on fibroblast growth factor-2-treated mesenchymal stem cells with improved chondrogenic differential potential. *Stem Cell Develop* 2007, 16: 965-978
- 54). Mishra, PJ, Mishra PJ, Glod, JW, Banerijee, D: Mesenchymal stem cells: flip side of the coin. *Cancer Res* 2009, 69: 1255-1258.
- 55). Wenke, AK, Kjellman, C, Lundgren-Akerlund, E, Uhlmann, C, Haass, NK, Herlyn, M, Bosserhoff, AK: Expression of integrin  $\alpha 10$  is induced in malignant melanoma. *Cell Oncol* 2007, 29: 373-386

Example 19: The HU177 collagen epitope is recognized by integrin  $\alpha 10\beta 1$  which regulates expression of the immune suppressive cytokine IL-10.

Fig. 25A is a bar chart wherein a peptide (cPG) containing the HU177 collagen epitope CPGFPGFC (SEQ ID NO: 16) was immobilized on microtiter wells and the ability of recombinant integrin receptors to bind was analyzed by ELISA. Data bars represent mean integrin binding to the HU177 collagen epitope. Fig. 25B-Fig. 25D is a series of bar charts showing that the expression of  $\alpha 10$  integrin chain in human C8161 melanoma cells was reduced by transfection of shRNA directed to the  $\alpha 10$  integrin chain. Twenty-four hour serum free conditioned medium from each melanoma variant was concentrated 10X and analyzed for the relative levels of cytokines. Fig. 25B is a bar graph wherein data bars represent relative levels of IL-10 as determined by ELISA. Fig. 25C is a bar graph wherein data bars represent relative levels of IL-2 as determined by ELISA. Fig. 25D is a bar graph wherein data bars represent relative levels of IL-4 as determined by ELISA. Thus, these results demonstrate that knocking down expression of an integrin receptor (Integrin  $\alpha 10\beta 1$ ), which can function as a receptor for the HU177 epitope in melanoma cells reduced expression of a potent immune suppressive molecule IL-10.

Example 20: The injection of a peptide (cPG) containing the HU177 collagen epitope induces expression of the immune suppressive growth factor TGF- $\beta$  in mouse circulation.

C57BL/6 mice were injected subcutaneously with B16F10 melanoma cells ( $0.5 \times 10^6$ ) and tumors were allowed to form. Mice were next injected 3X per week with 10ug per mouse of cPG peptide. Serum was collaged after 14 days. Serum was diluted in assay buffer and the relative levels of cytokines were examined by ELISA. Fig. 26A is a bar graph wherein data bars represent relative levels of TGF- $\beta$  as determined by ELISA from control (DMSO) treated mouse and two different cPG peptide treated mice. Fig. 26B is a bar graph wherein data bars represent relative levels of IL-4 as determined by ELISA from control (DMSO) treated mouse and two different cPG peptide treated mice. Fig. 26C is a bar graph wherein data bars represent relative levels of IL-1 $\beta$  as determined by ELISA from control (DMSO) treated mouse and two different cPG peptide treated mice.

Thus, these results demonstrate that injection of mice with a peptide containing the HU177 epitope itself can induce the expression of a potent immune suppressive molecule TGF- $\beta$ .

Example 21: Mab HU177 enhances the anti-tumor activity of the immune checkpoint inhibitor anti-PDL-1 antibody.

Mice (C57BL/6) were injected with  $3.5 \times 10^5$  B16F10 melanoma cells. Mice were allowed establish pre-existing tumors for 5 days prior to treatment. Mice were treated (100ug/mouse) with either anti-PD-L1 antibody alone, Anti-HU177 antibody alone or a combination of both antibodies 3 times a week for 15 days. Fig. 27A is a bar graph wherein data represents mean tumor volume at day 7 + SE from 7 mice per condition. Fig. 27B is a bar graph wherein data represents mean tumor volume at day 15 + SE from 7 mice per condition. Thus, these results demonstrate that murine Mab HU177 directed to the HU177 cryptic collagen epitope can enhance the anti-tumor activity of the immune checkpoint inhibitor anti-PD-L1.

Example 22: Synthetic collagen peptides containing the amino acid sequence RGD support T cell adhesion.

In order to demonstrate that T-cells can directly interact and bind to the cryptic collagen epitopes recognized by Mab XL313 (i.e., P-2 and P-4), synthetic peptides containing amino acid sequences of collagen type -1 (P1 through P-5) along with a mutated control collagen peptide (P-C) were immobilized on non-tissue culture wells (250 ng/well). Human T-cells (Jurkat) were added and allowed to attach to the collagen peptides. The results are presented in Fig. 28. Data bars indicate mean cell adhesion  $\pm$  standard deviation from triplicate wells. P-1 (CKGDRGDAGPC; SEQ ID NO: 19); P-2 (CQGPRGDKGEC; SEQ ID NO: 6); P-3 (CAGSRGDGGPC; SEQ ID NO: 7); P-4 (CQGIRGDKGEC; SEQ ID NO: 20); P-5 (CRGPRGDQGPC; SEQ ID NO: 9); P-C (CQGPSGAPGEC; SEQ ID NO: 10).

Example 23: Monoclonal antibody (Mab XL313) inhibits interactions between human T-cells and the cryptic collagen epitope peptide P-2 (CQGPRGDKGEC; SEQ ID NO: 6).

In order to demonstrate that Mab XL313 can inhibit human T-cell interactions with the cryptic collagen epitope peptide P-2 (CQGPRGDKGEC; SEQ ID NO: 6), the P-2 peptide was immobilized (100  $\mu\text{g}/\text{well}$ ) on non-tissue culture wells and human T-cells (Jurkat) were added in the presence (50  $\mu\text{g}/\text{ml}$ ) or absence of Mab XL313 or control, antibodies normal mouse Ig (Ab Cont) and anti-integrin receptor ( $\alpha\text{v}\beta\text{3}$ ) and allowed to attach to the collagen peptides. The results are presented in Fig. 29. Data bars indicate mean cell adhesion  $\pm$  standard deviation from triplicate wells.

Example 24: The Integrin receptor  $\alpha\text{v}\beta\text{3}$  dose dependently binds the cryptic collagen epitope peptide P-2.

In order to demonstrate that the integrin receptor  $\alpha\text{v}\beta\text{3}$  can bind to the cryptic collagen epitope peptide P-2, which is recognized by Mab XL313, solid phase ELISA was carried out. The cryptic collagen peptide P-2 was immobilized (100  $\mu\text{g}/\text{ml}$ ) on microtiter wells and increasing concentrations of recombinant integrin  $\alpha\text{v}\beta\text{3}$  was added and integrin binding was quantified. The results are presented in Fig. 30. Data bars indicate mean integrin binding  $\pm$  standard deviation from triplicate wells.

Example 25: Mab XL313 inhibits recombinant integrin receptor  $\alpha\text{v}\beta\text{3}$  binding to the cryptic collagen epitope peptide P-2.

In order to demonstrate that Mab XL313 specifically inhibits integrin receptor  $\alpha\text{v}\beta\text{3}$  binding to the cryptic collagen epitope peptide P-2, solid phase ELISA was carried out. The cryptic collagen peptide P-2 was immobilized (100  $\mu\text{g}/\text{ml}$ ) on microtiter wells and recombinant integrin  $\alpha\text{v}\beta\text{3}$  was added and it was allowed to bind in the presence (50  $\mu\text{g}/\text{ml}$ ) or absence of Mab XL313 or control antibody (Mab XL166 directed to other collagen RGD peptides). The results are presented in Fig. 31. Data bars indicate mean integrin binding  $\pm$  standard deviation from triplicate wells.

Example 26: Reducing expression of  $\beta 3$  integrin leads to reduced expression of PD-L1 in human T-cells.

In order to confirm the functional role of integrin  $\alpha v\beta 3$  in regulating the levels of the immune suppressive molecule PD-L1,  $\beta 3$  integrin expression was knocked down by shRNA in human T-cells. Whole cell lysates from control transfected (Cont) and  $\beta 3$  integrin shRNA transfected T-cells ( $\beta 3$  KD) were analyzed for expression of  $\beta 3$  integrin ( $\beta 3$  Int), PD-L1 and beta actin ( $\beta$ -Actin). Western blot analysis indicates clear reduction in the levels of PD-L1 in  $\beta 3$  integrin knock down cells as compared to control. The results are presented in Fig. 32.

Example 27: Reducing expression of  $\beta 3$  integrin prevents stimulation of PD-L1 by the XL313 cryptic collagen peptide P2 in human T-cells.

In order to confirm the functional role of integrin  $\alpha v\beta 3$  receptor in regulating the levels of the immune suppressive molecule PD-L1 by the XL313 cryptic collagen peptide P2, the expression of PD-L1 was examined in  $\beta 3$  integrin knock down and control transfected T-cells. Whole cell lysates from control transfected (Cont T-cells) and  $\beta 3$  integrin shRNA transfected T-cells ( $\beta 3$ /KD) that were stimulated with control peptide (PC) or the XL313 cryptic collagen peptide (P2) were analyzed by western blot for expression of PD-L1. While P2 peptide enhanced expression of PD-L1 in control transfected T-cells, P2 showed little ability to enhance the expression of PD-L1 in  $\beta 3$  integrin knock down cells ( $\beta 3$  KD). The results are presented in Fig. 33.

Example 28: Anti- XL313 antibody reverses the inhibitory effects of the cryptic collagen peptide P2 on T-cell migration.

Membranes of transwell migration chambers were coated with denatured collagen type-IV to mimic the altered basement membrane in tumor vessels. The results are presented in Fig. 34. Left). T-cell (Jurkat) migration in the presence or absence of the cryptic collagen peptide P2 (1.0ug/ml) and/or Mab XL313 and non-specific control antibody (50  $\mu$ g/ml). Right). T-cell (Jurkat) migration in the presence or absence of Raw

macrophage concentrated conditioned medium (CM) and/or Mab XL313 and non-specific control antibody (50 µg/ml). Data bars represent mean cell migration  $\pm$  SE from triplicate wells.

Example 29: The cryptic collagen peptide P2 induces expression of the immunosuppressive molecule LAG3 in human T-cells.

In order to confirm the functional ability of the XL313 cryptic collagen peptide P2 to regulate expression of the immune suppressive checkpoint molecule LAG3,  $\alpha\beta3$  expressing human T-cell lines Jurkat and CCL120.1 were stimulated with the cryptic collagen peptide P2 or control collagen peptides P1 or PC. Whole cell lysates from were analyzed for expression of PD-L1 and beta actin ( $\beta$ -Actin). Western blot analysis indicates clear increase in the levels of PD-L1 in P2 stimulated T-cells as compared to controls. The results are presented in Fig. 35.

Example 30: Anti-XL313 Mab reduces the levels of the immune suppressive molecule LAG-3 in melanoma tumors in vivo.

C57BL/6 mice were injected with B16F10 melanoma cells ( $0.5 \times 10^6$ ). Mice were treated (i.p) with anti-XL313 or control antibody (50 µg 3x/wks.). B16F10 tumors (N=3 from each group) were stained for expression of LAG-3 (green). The results are presented in Fig. 36. (Left). Examples of LAG-3 expression from each condition. Photos were taken at 200X and 400X magnification. (Right). Quantification (Image J) of mean  $\pm$  S.E relative LAG-3 expression from 5 100X fields from each of 3 different tumors from each condition.

Example 31: Anti-XL313 Mab enhances the levels of CD8+ T-cells in melanoma tumors in vivo.

C57BL/6 mice were injected with B16F10 melanoma cells ( $0.5 \times 10^6$ ). Mice were treated (i.p) with anti-XL313 or control antibody (50 µg 3x/wks.). Single cell suspensions of whole tumors from each condition were prepared and the levels of CD8+ T-cells from each tumor (N=4 per group) were quantified by flow cytometry. Data bars represent the

mean level of tumor CD8+ T-cells  $\pm$ SE from single cell suspensions from 4 tumors per condition. The results are presented in Fig. 37.

Example 32: Anti-HU177 Mab reduces the levels of immune suppressive CD4+/CTLA-4 positive T-Reg cells in melanoma tumors in vivo.

C57BL/6 mice were injected with B16F10 melanoma cells ( $0.5 \times 10^6$ ). Mice were untreated or treated (i.p) with anti-HU177 or control antibody (50  $\mu$ g 3x/wks.). Single cell suspensions of whole tumor from each condition were prepared and the levels of CD4+/CTLA-4 positive T-Reg cells from each tumor (N=4 per group) were quantified by flow cytometry. The results are presented in Fig. 38. Data bars represent the mean level of T-Reg-cells  $\pm$ SE from single cell suspensions from 4 tumors per condition.

### **OTHER EMBODIMENTS**

While the invention has been described in conjunction with the detailed description thereof, the foregoing description is intended to illustrate and not limit the scope of the invention, which is defined by the scope of the appended claims. Other aspects, advantages, and modifications are within the scope of the following claims.

The patent and scientific literature referred to herein establishes the knowledge that is available to those with skill in the art. All United States patents and published or unpublished United States patent applications cited herein are incorporated by reference. All published foreign patents and patent applications cited herein are hereby incorporated by reference. Genbank and NCBI submissions indicated by accession number cited herein are hereby incorporated by reference. All other published references, documents, manuscripts and scientific literature cited herein are hereby incorporated by reference.

**CLAIMS****We claim:**

1. A method of treating cancer in a subject comprising,  
identifying a subject that has been diagnosed with cancer;  
administering an immune checkpoint inhibitor; and  
administering an antagonist of collagen or a fragment thereof,  
thereby treating cancer in said subject.
2. The method of claim 1, wherein the immune checkpoint inhibitor comprises an inhibitor of CTLA-4, PD-1, PDL-1, Lag3, LAIR1, or LAIR2
3. The method of claim 1, wherein said inhibitor of PDL-1 comprises a PDL-1 antibody.
4. The method of claim 1, wherein said antagonist of collagen or a fragment thereof enhances anti-tumor activity of the immune checkpoint inhibitor.
5. The method of claim 1, further comprising inhibiting an inflammatory condition, wherein said inflammatory condition comprises dermatitis, pneumonitis, or colitis.
6. The method of claim 1, wherein the collagen comprises collagen type-I, collagen type II, collagen type III, or collagen type-IV.
7. The method of claim 6, wherein the antagonist of collagen type-IV or a fragment thereof comprises an antagonist of the XL313 cryptic collagen epitope or an antagonist of the HU177 cryptic collagen epitope.
8. The method of claim 7, wherein the antagonist of the XL313 cryptic collagen epitope comprises an antibody that binds a cryptic RGDKGE (SEQ ID NO: 1)-containing collagen epitope or wherein the antagonist of the HU177 cryptic collagen epitope comprises an antibody that binds a cryptic CPGFPGFC (SEQ ID NO: 16)-containing collagen epitope.
9. The method of claim 8, wherein the antibody comprises a monoclonal antibody.

10. The method of claim 9, wherein said monoclonal antibody comprises an XL313 monoclonal antibody or an HU177 monoclonal antibody.
11. The method of claim 1, wherein the subject is a human.
12. The method of claim 1, further comprising administering a chemotherapy agent.
13. The method of claim 1, wherein the cancer is selected from the group comprising of melanoma, central nervous system (CNS) cancer, CNS germ cell tumor, lung cancer, leukemia, multiple myeloma, renal cancer, malignant glioma, medulloblastoma, breast cancer, ovarian cancer, prostate cancer, bladder cancer, fibrosarcoma, pancreatic cancer, gastric cancer, head and neck cancer, colorectal cancer. For example, a cancer cell is derived from a solid cancer or hematological cancer. The hematological cancer is, e.g., a leukemia or a lymphoma. A leukemia is acute lymphoblastic leukemia (ALL), acute myelogenous leukemia (AML), chronic lymphocytic leukemia (CLL), small lymphocytic lymphoma (SLL), chronic myelogenous leukemia (CML), or acute monocytic leukemia (AMoL). A lymphoma is follicular lymphoma, Hodgkin's lymphoma (e.g., Nodular sclerosing subtype, mixed-cellularity subtype, lymphocyte-rich subtype, or lymphocyte depleted subtype), or Non-Hodgkin's lymphoma. Exemplary solid cancers include but are not limited to melanoma (e.g., unresectable, metastatic melanoma), renal cancer (e.g., renal cell carcinoma), prostate cancer (e.g., metastatic castration resistant prostate cancer), ovarian cancer (e.g., epithelial ovarian cancer, such as metastatic epithelial ovarian cancer), breast cancer (e.g., triple negative breast cancer), and lung cancer (e.g., non-small cell lung cancer).
14. The method of claim 1, wherein said immune checkpoint inhibitor is administered at a dose of 0.01-10 mg/kg bodyweight, and wherein said antagonist of collagen is administered at a dose of 0.01-25mg/kg bodyweight.
15. The method of claim 1, wherein said composition is administered once per hour, or wherein said composition is administered once every two weeks for 4 to 6 weeks.
16. A method of treating a disease characterized by abnormal immune suppression in a subject comprising,

identifying a subject that has been diagnosed with a disease characterized by abnormal immune suppression;

administering an immune checkpoint inhibitor; and

administering an antagonist of an integrin,

thereby treating in said subject.

17. The method of claim 16, wherein the immune checkpoint inhibitor comprises an inhibitor of CTLA-4, PD-1, PDL-1, Lag3, LAIR1, or LAIR2.

18. The method of claim 16, wherein said immune checkpoint inhibitor comprises a CTLA-4 antibody, a PD-1 antibody, a PDL-1 antibody, a Lag3 antibody, a LAIR1 antibody or a LAIR2 antibody.

19. The method of claim 18, wherein the integrin comprises integrin  $\alpha\beta3$ .

20. The method of claim 19, wherein said antagonist of integrin  $\alpha\beta3$  comprises an antibody targeting  $\alpha\beta3$  binding RGDKGE (SEQ ID NO: 1)-containing collagen epitope.

21. The method of claim 18, wherein the integrin comprises integrin  $\alpha10\beta1$ .

22. The method of claim 21, wherein said antagonist of integrin  $\alpha10\beta1$  comprises an antibody targeting  $\alpha10\beta1$  binding CPGFPGFC (SEQ ID NO: 16)-containing collagen epitope.

23. The method of claim 16, wherein the subject is a human.

24. The method of claim 16, further comprising administering a chemotherapy agent.

25. The method of claim 16, wherein the disease characterized by abnormal immune suppression comprises Type I diabetes, lupus, psoriasis, scleroderma, hemolytic anemia, vasculitis, Graves' disease, rheumatoid arthritis, multiple sclerosis, Hashimoto's thyroiditis, Myasthenia gravis, and vasculitis

26. The method of claim 16, wherein said immune checkpoint inhibitor is administered at a dose of 0.01-10 mg/kg bodyweight, and wherein said antagonist of an integrin is administered at a dose of 0.01-25 mg/kg bodyweight.
27. The method of claim 16, wherein said composition is administered once per hour, or wherein said composition is administered once every two weeks for 4 to 6 weeks.
28. A method of treating a disease characterized by an overactive immune response in a subject comprising,  
    identifying a subject that has been diagnosed with an overactive immune response;  
    and  
    administering a peptide comprising collagen or a fragment thereof,  
    thereby treating an overactive immune response in said subject.
29. The method of claim 28, wherein said overactive immune response comprises an autoimmune disease.
30. The method of claim 28, wherein the collagen comprises collagen type-I, collagen type II, collagen type III, or collagen type-IV.
31. The method of claim 28, wherein the peptide comprises RGDKGE (SEQ ID NO: 1) or CPGFPGFC (SEQ ID NO: 16).
32. The method of claim 28, wherein the subject is a human.
33. The method of claim 28, wherein said autoimmune disease comprises Graves' disease, Hashimoto's thyroiditis, Systemic lupus erythematosus (lupus), Type 1 diabetes, multiple sclerosis or rheumatoid arthritis.
34. A method for healing a wound in a subject comprising,  
    identifying a subject with a wound; and  
    administering a peptide comprising collagen or a fragment thereof to said wound,  
    thereby healing said wound in said subject.

35. The method of claim 34, wherein the collagen comprises collagen type-I, collagen type II, collagen type III, or collagen type-IV.

36. The method of claim 34, wherein the peptide comprises RGDKGE (SEQ ID NO: 1) or CPGFPGFC (SEQ ID NO: 16).

37. The method of claim 34, wherein the subject is a human.

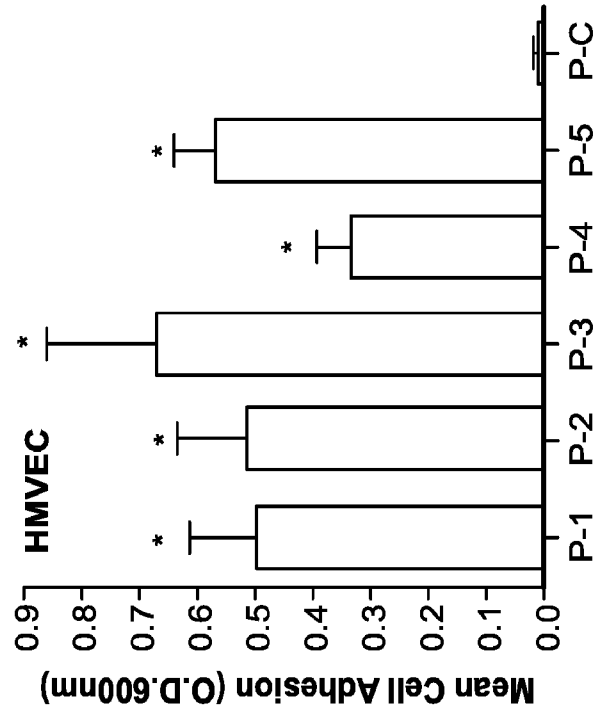


FIG. 1B

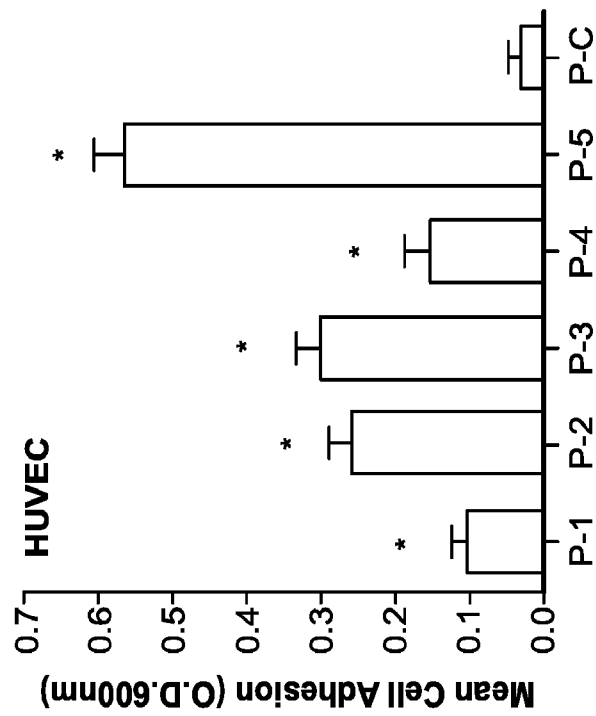


FIG. 1A

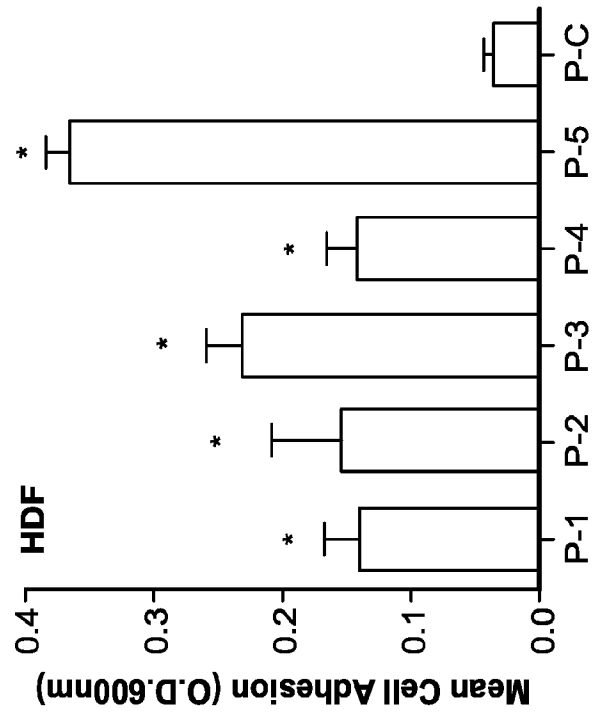


FIG. 1D

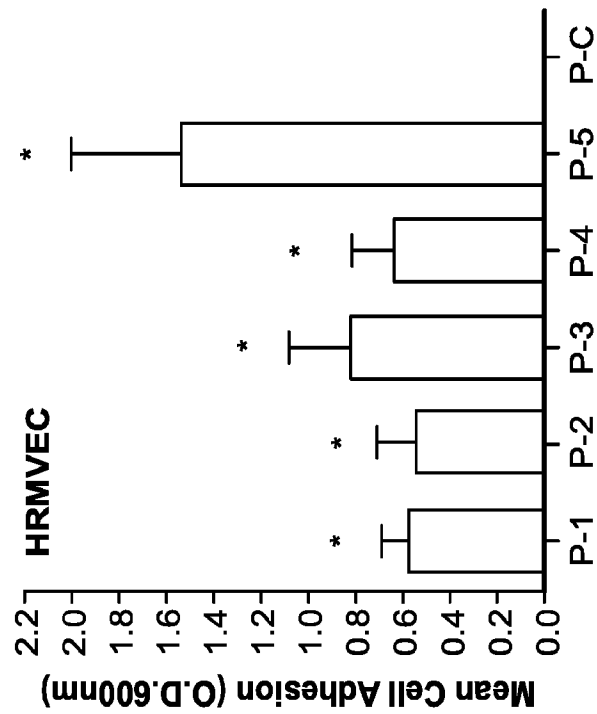


FIG. 1C

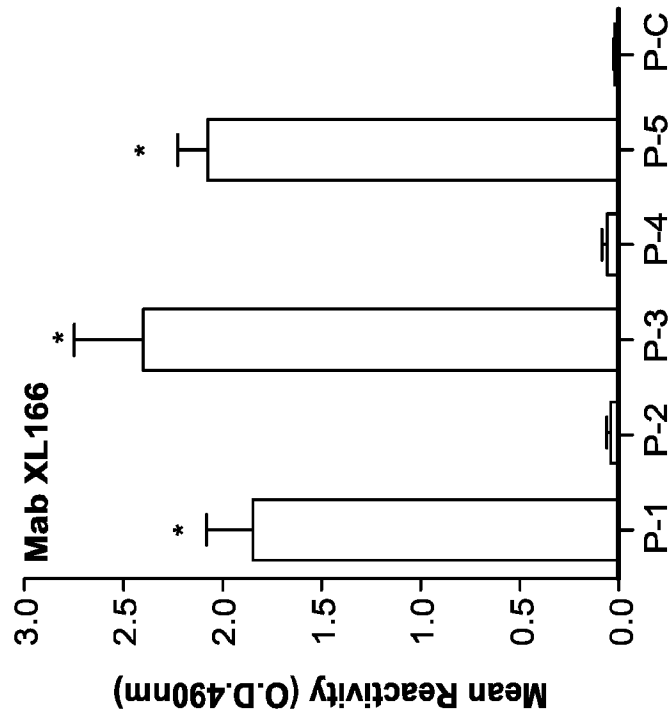


FIG. 1F

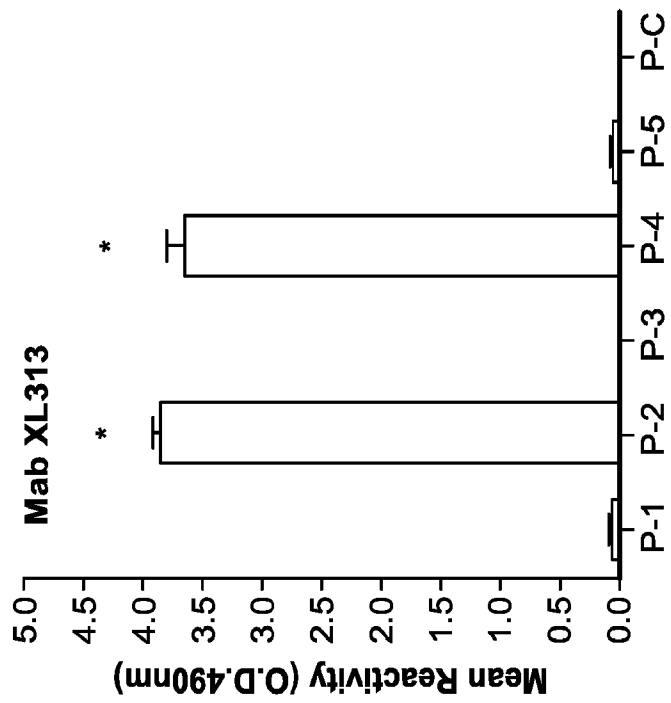


FIG. 1E

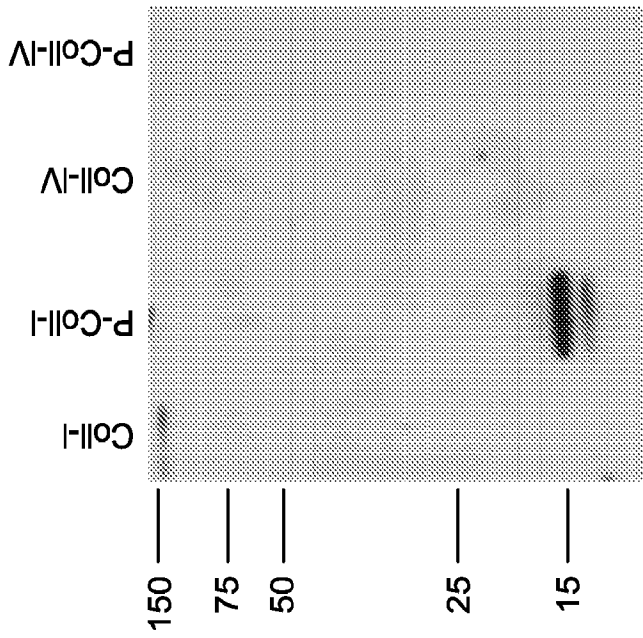


FIG. 2B

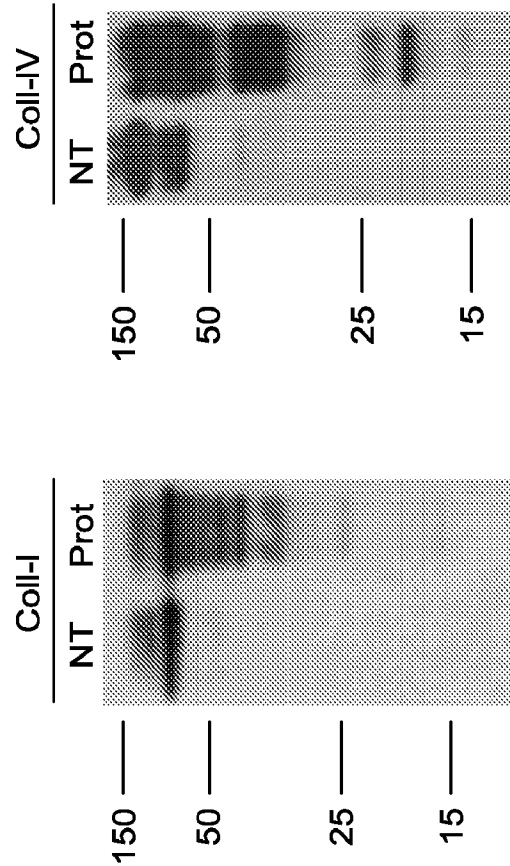


FIG. 2A

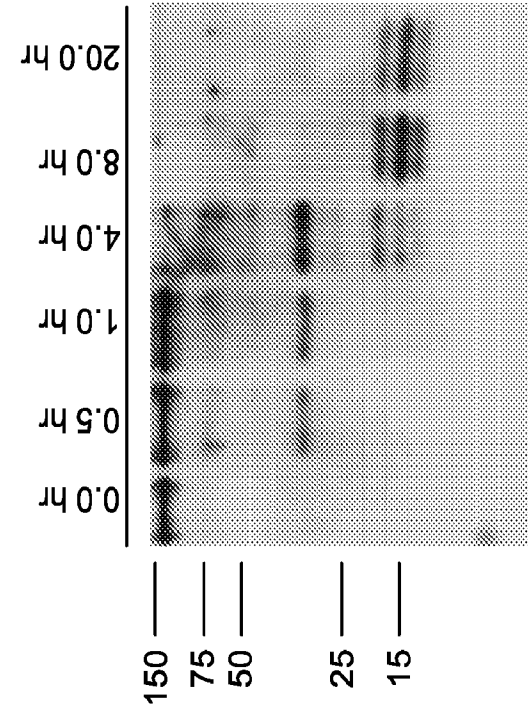


FIG. 2D

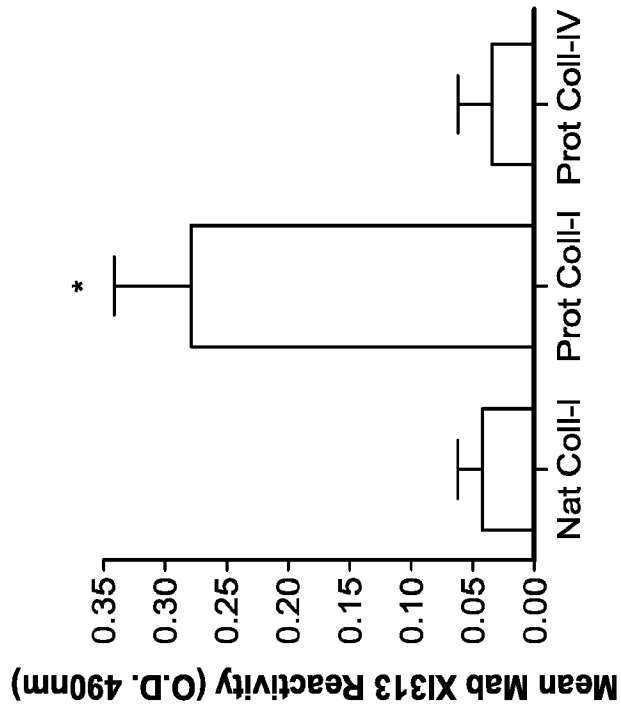


FIG. 2C

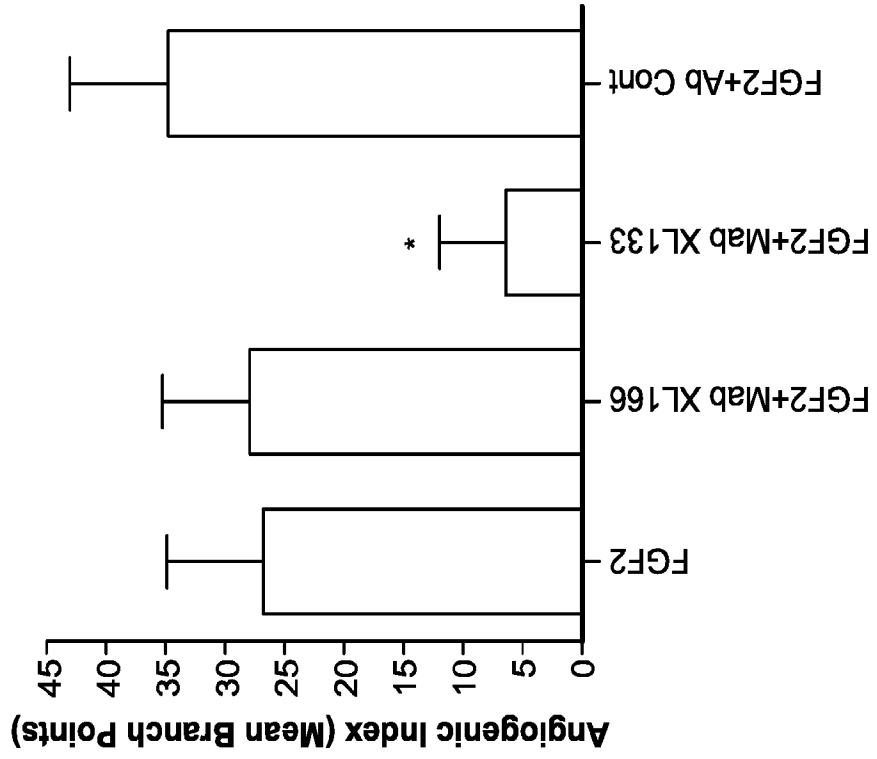


FIG. 3B

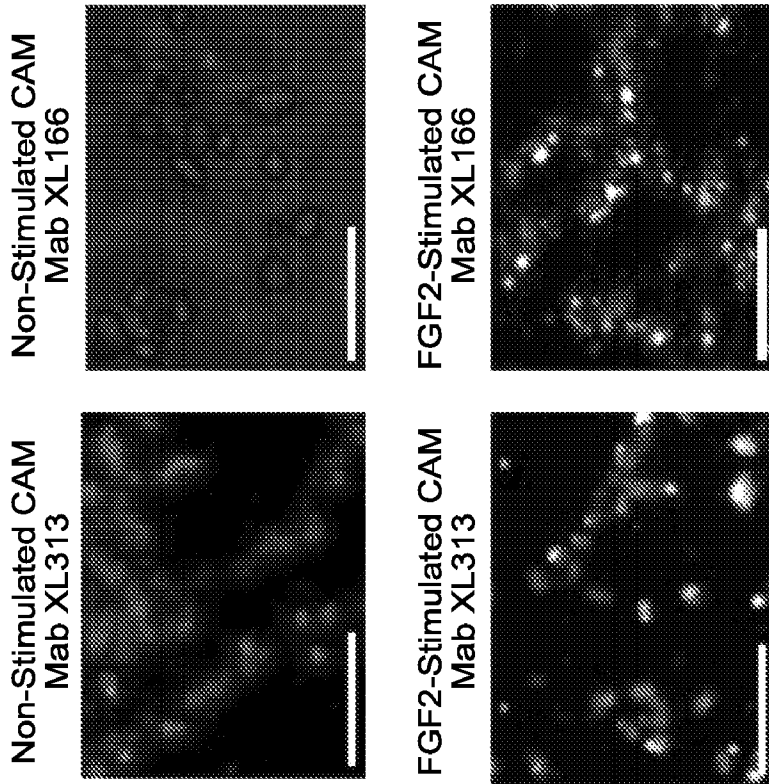


FIG. 3A

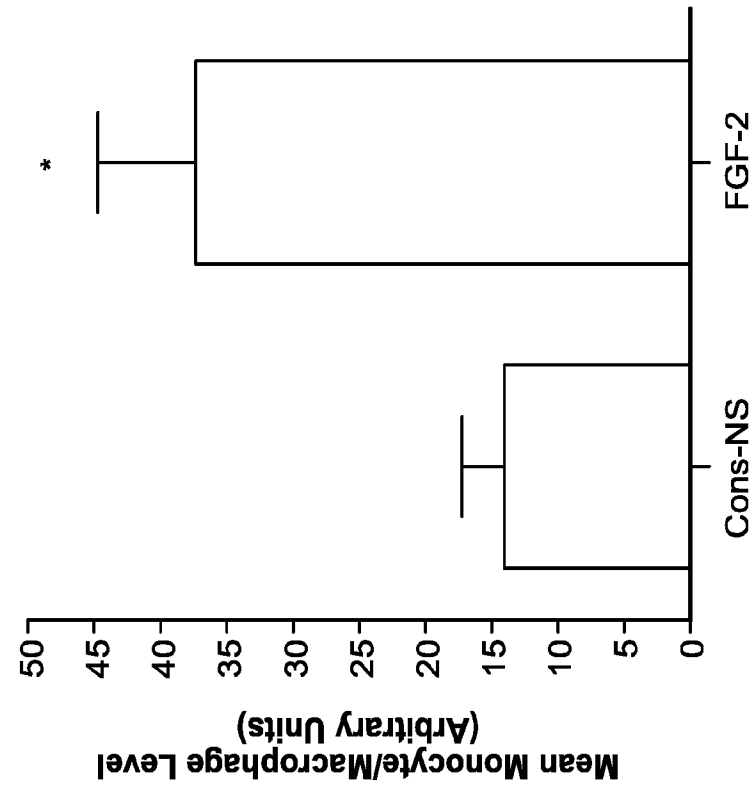


FIG. 3D

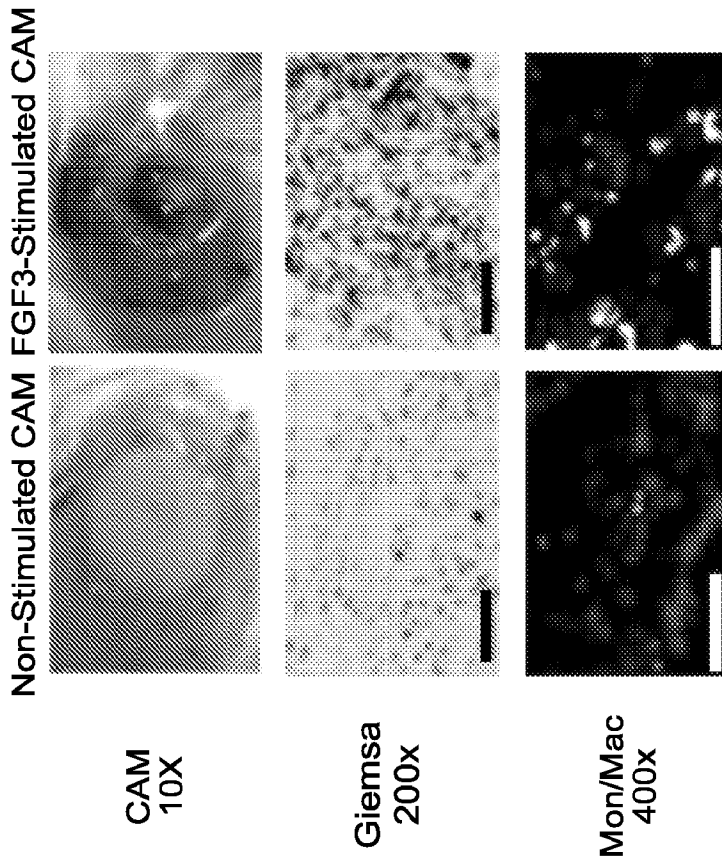


FIG. 3C

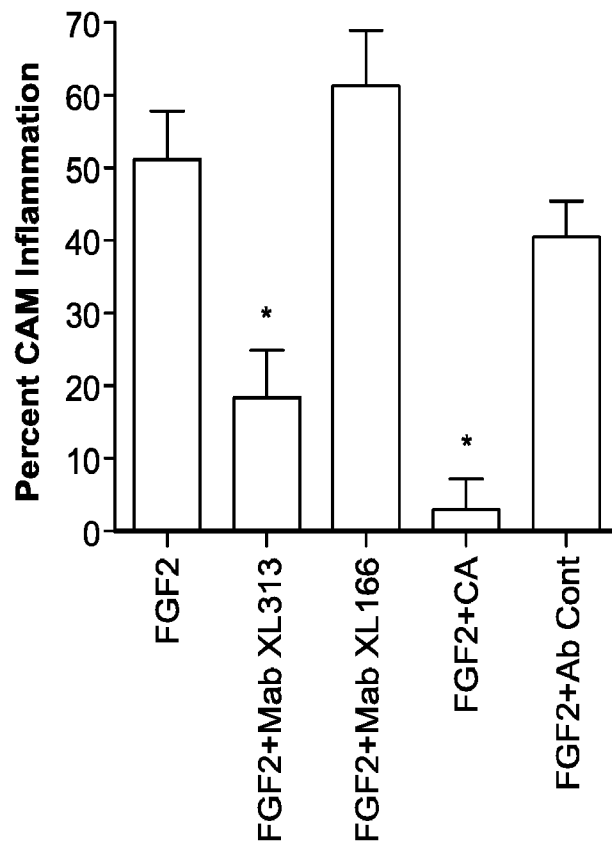


FIG. 3E

FIG. 4A

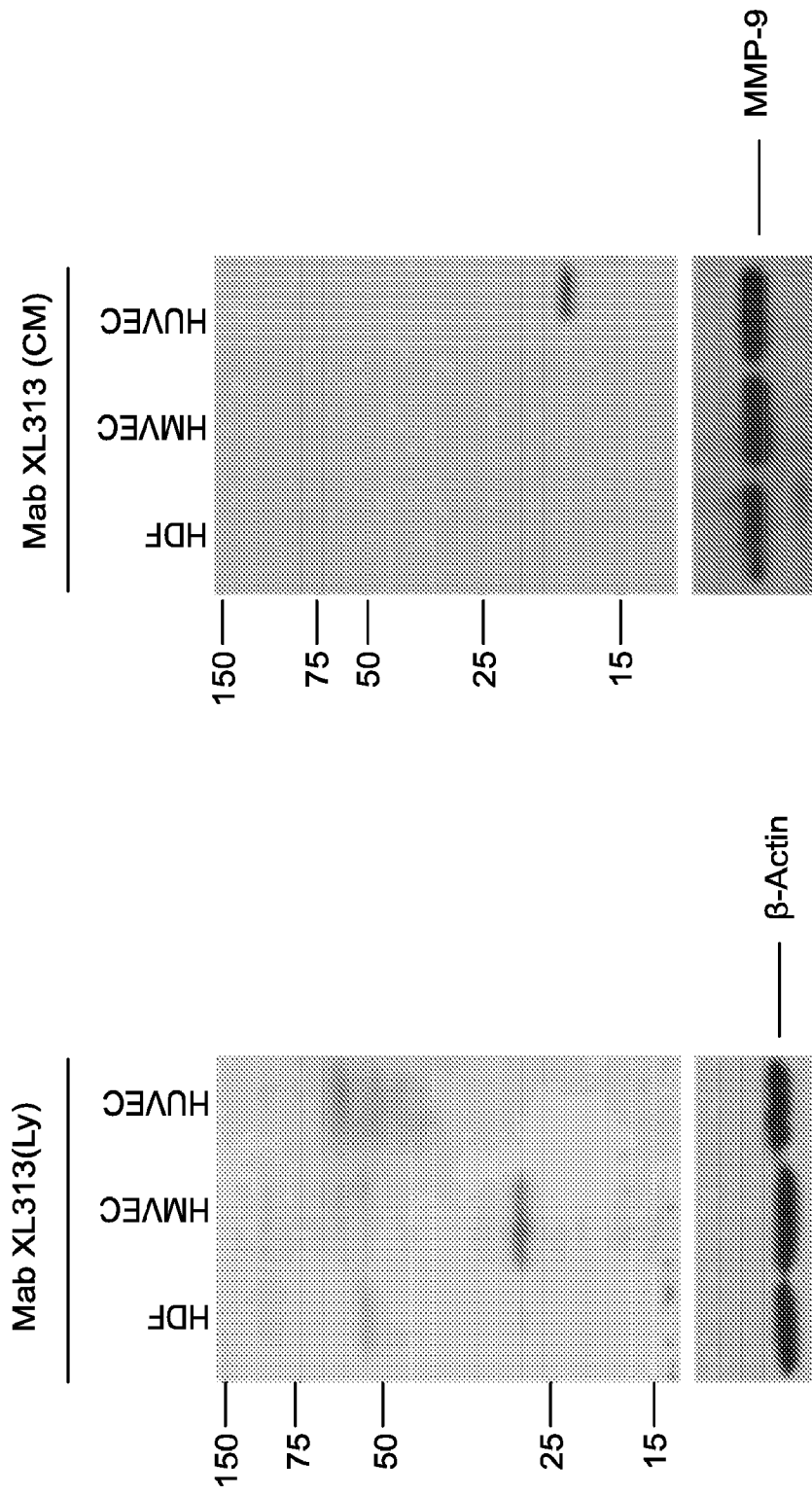


FIG. 4B

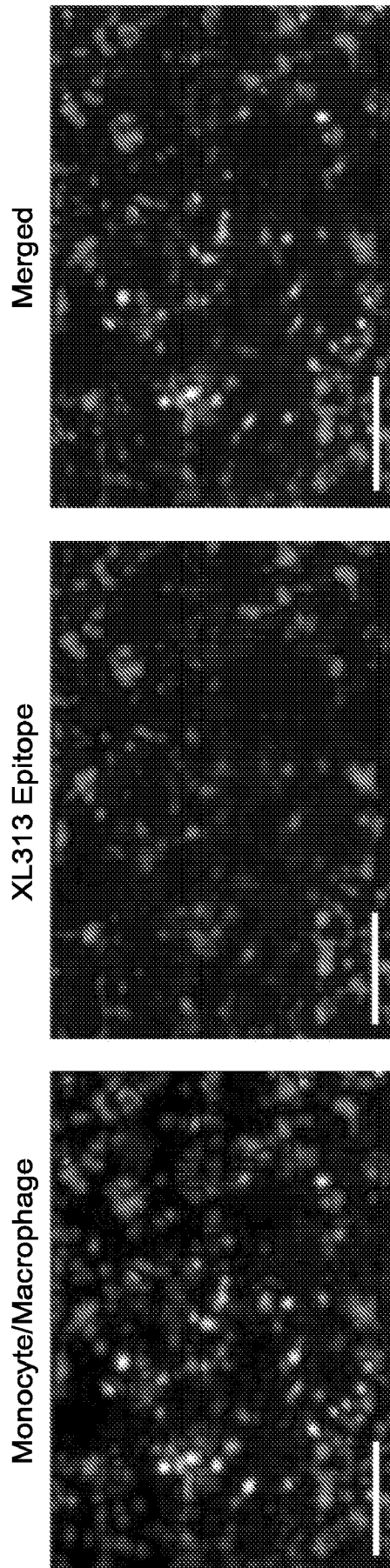


FIG. 4C

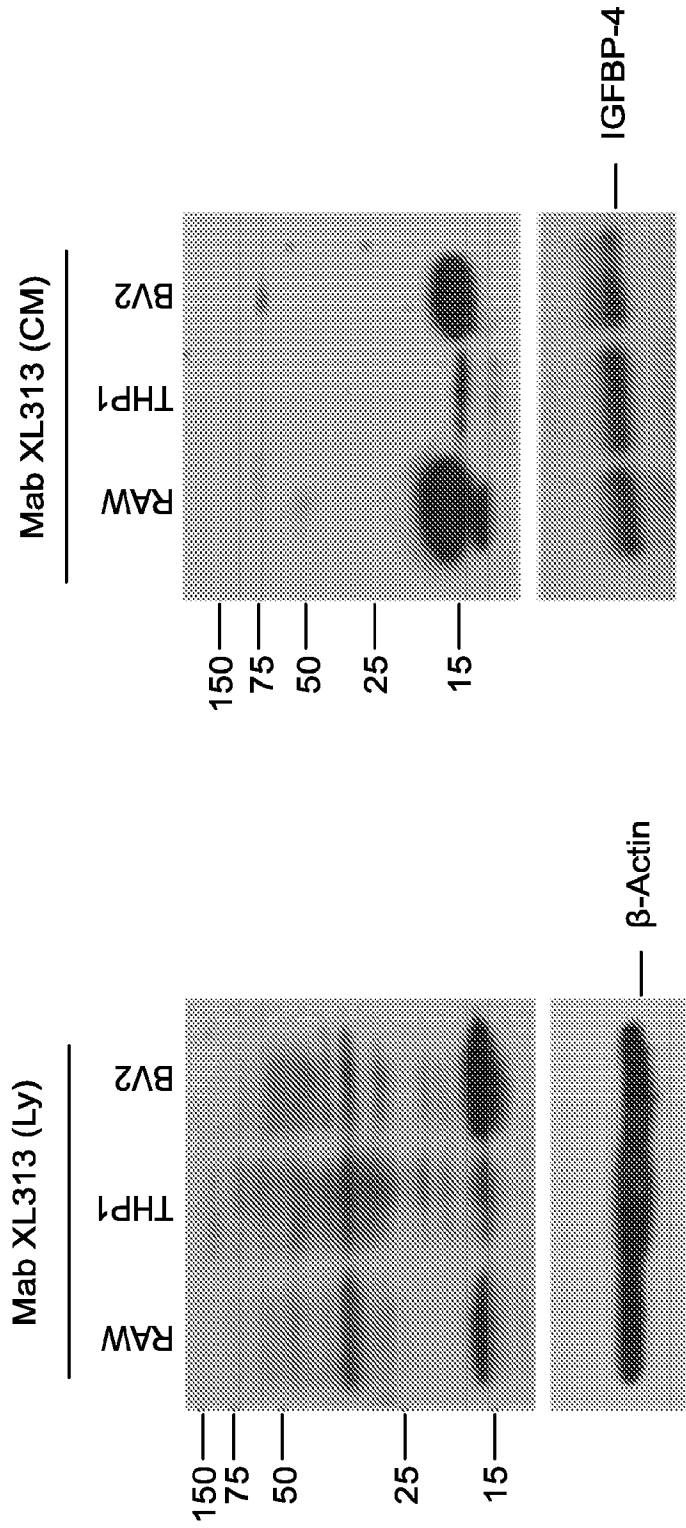


FIG. 4D

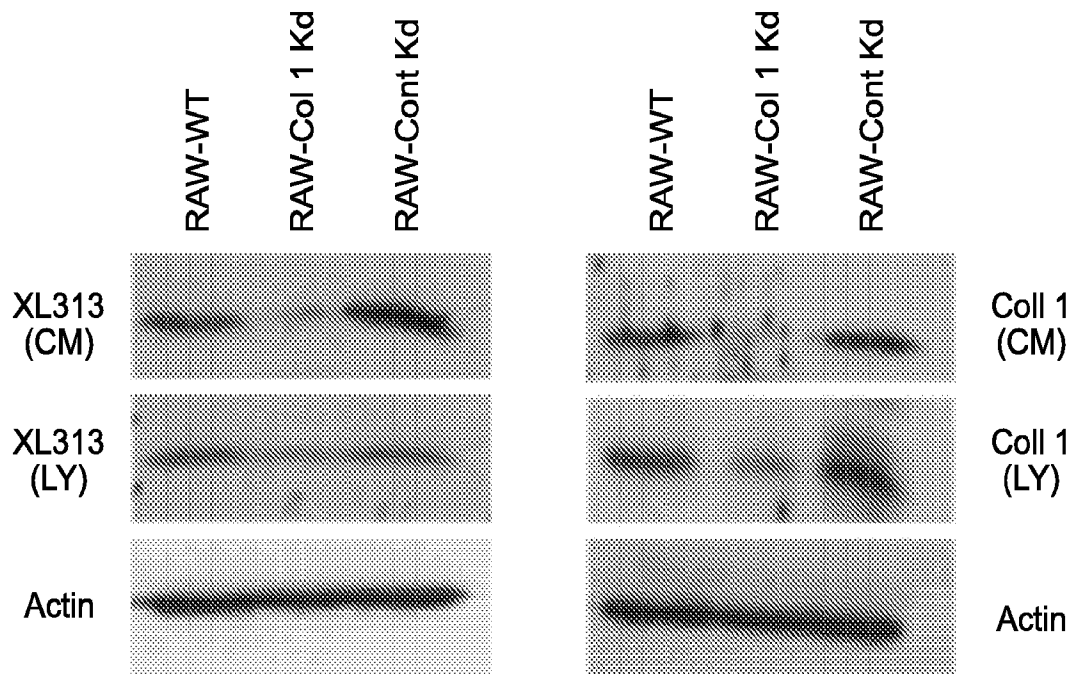


FIG. 5B

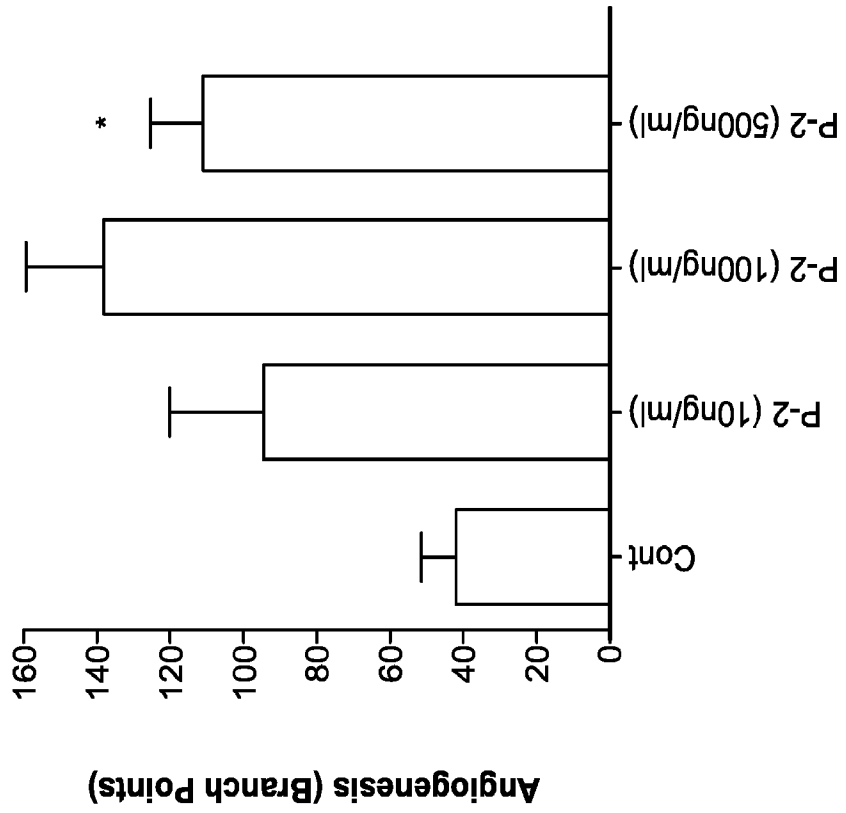


FIG. 5A

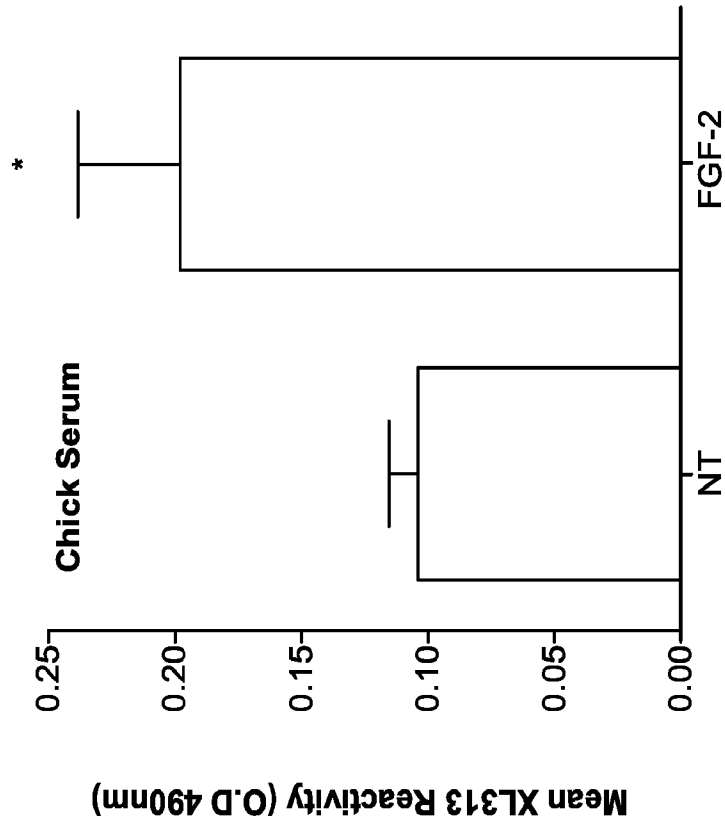


FIG. 5D

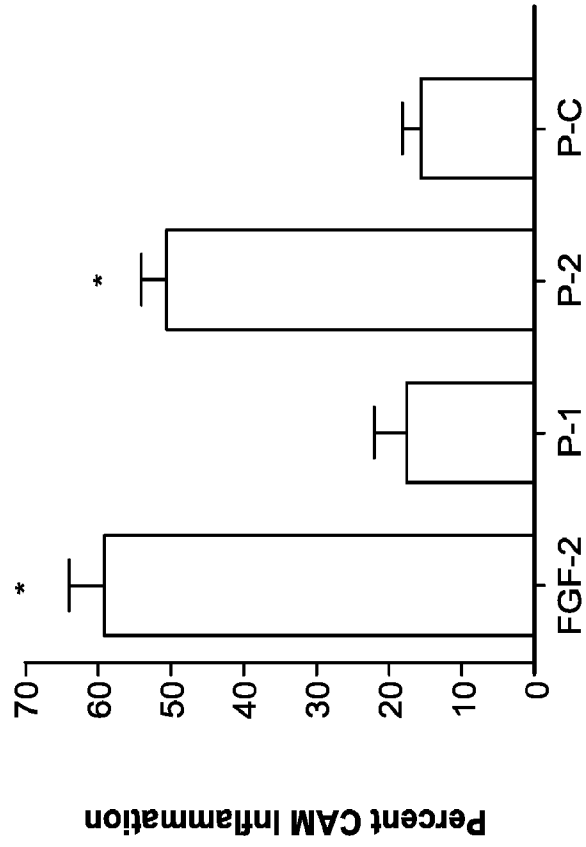
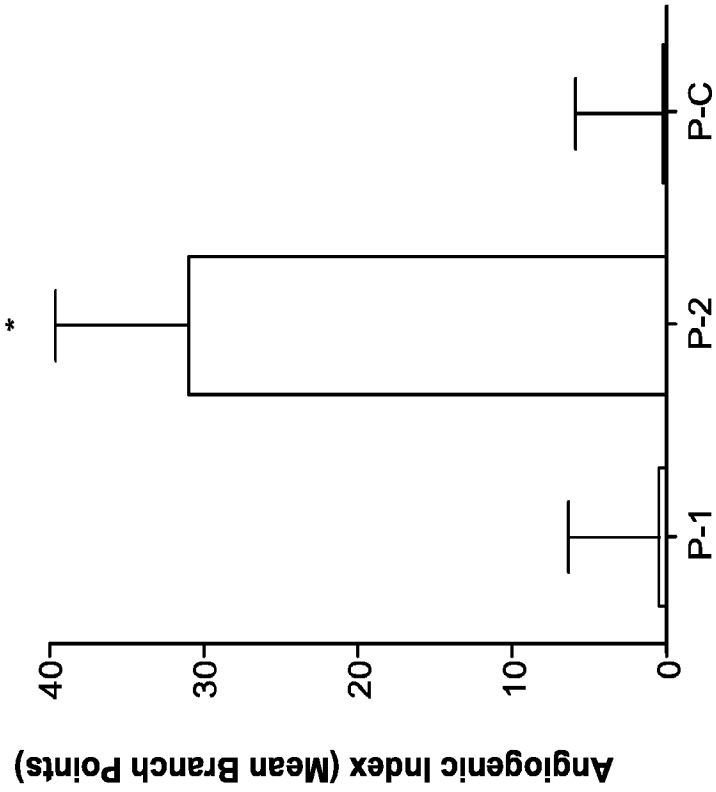


FIG. 5C



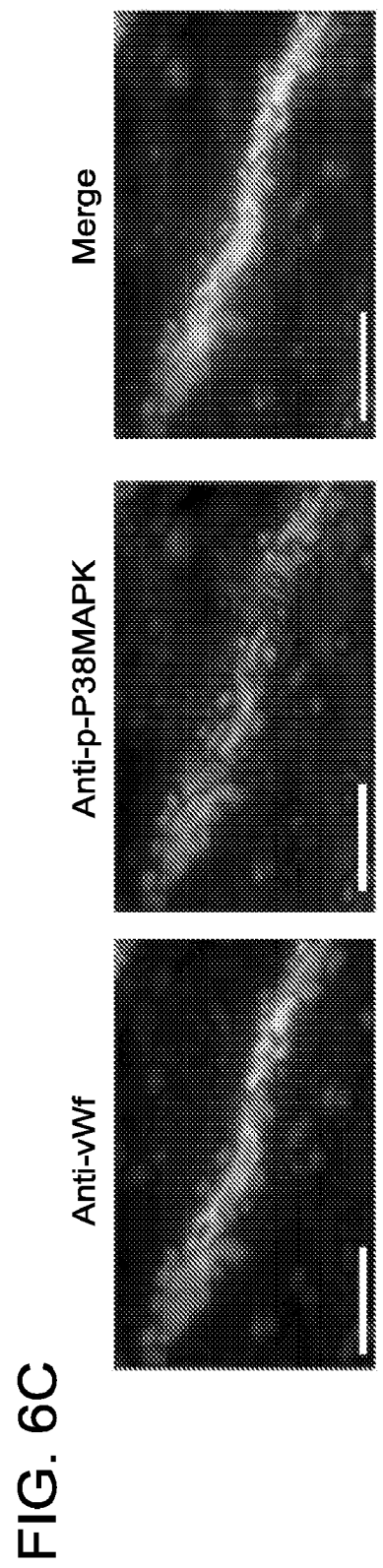
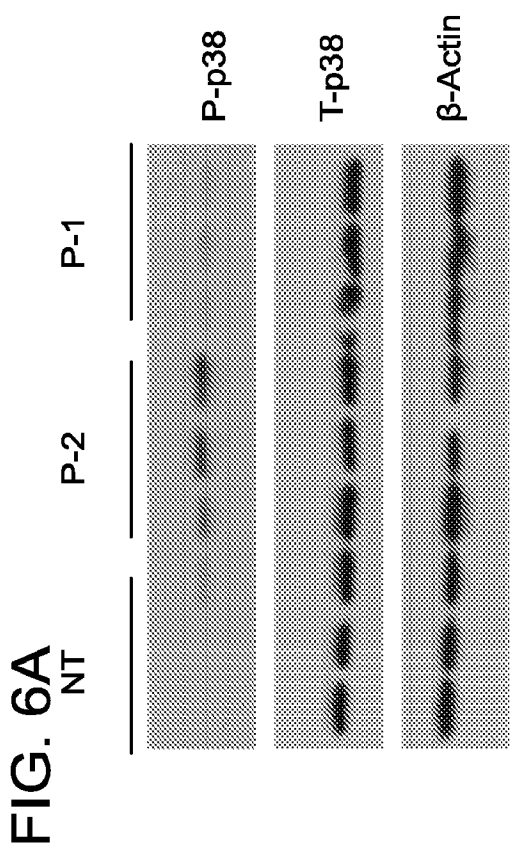
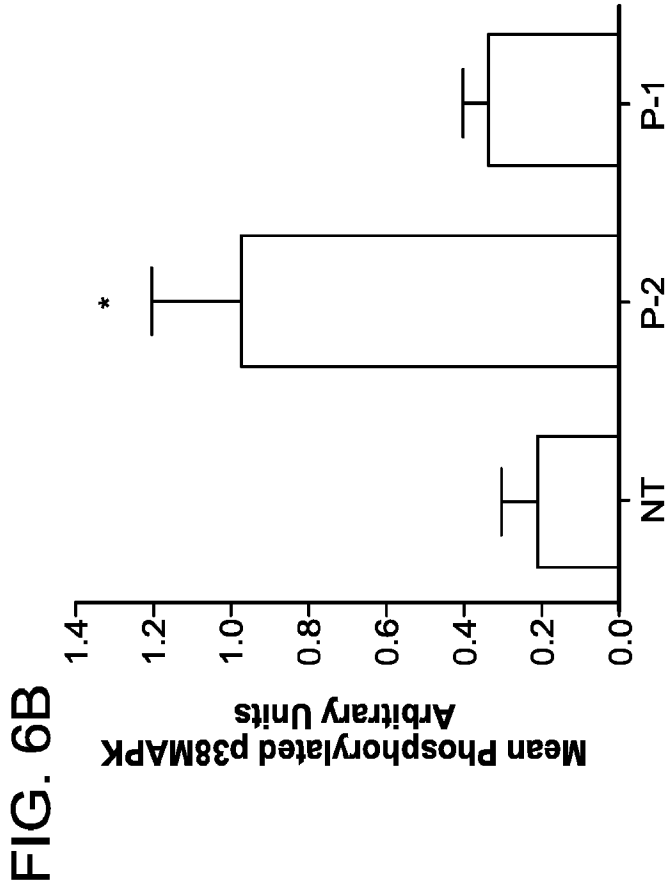


FIG. 6F

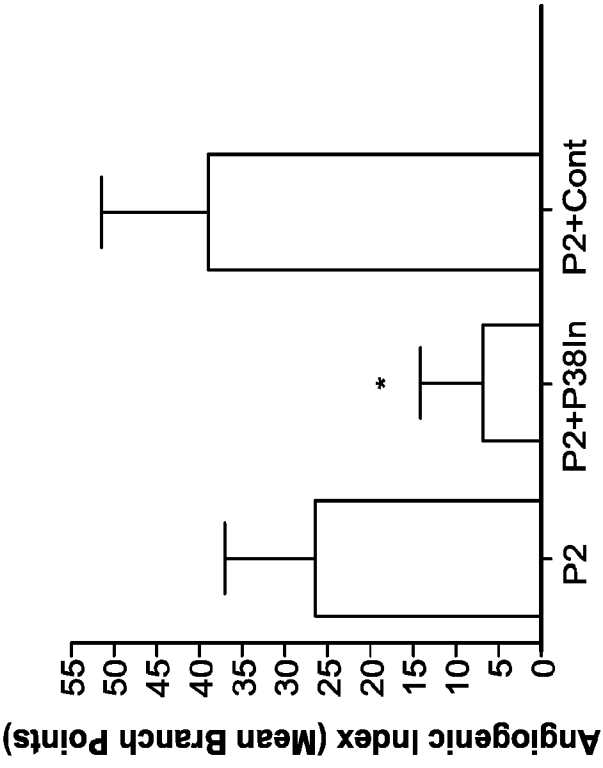


FIG. 6E

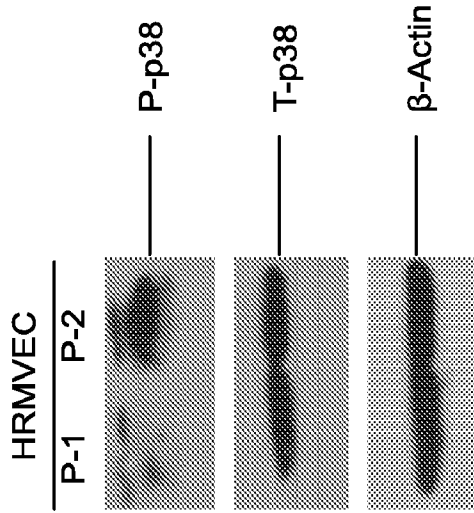
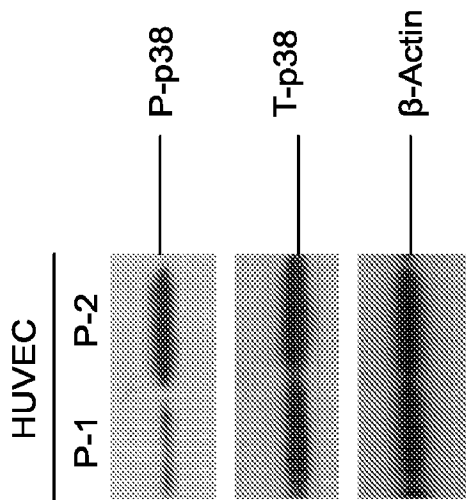


FIG. 6D



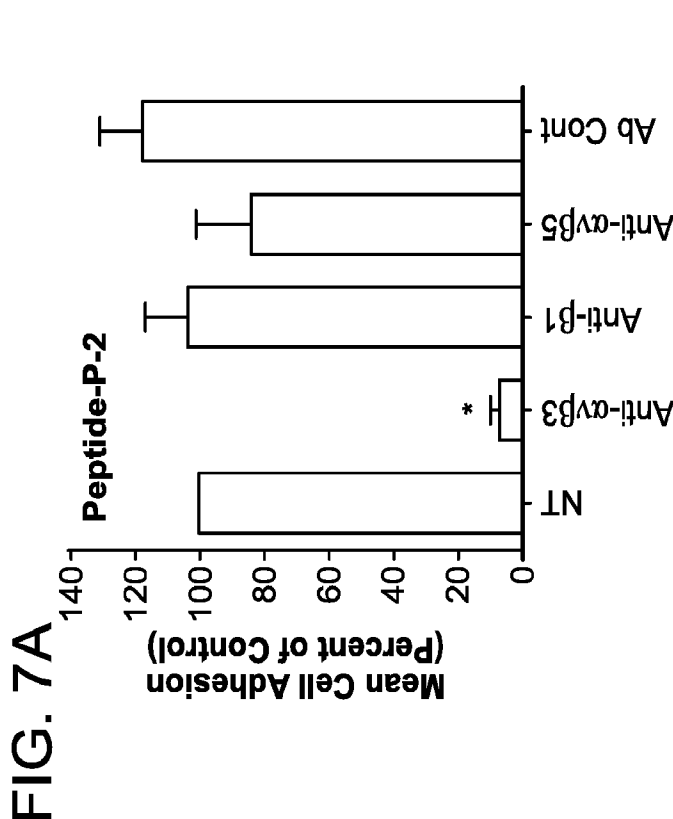
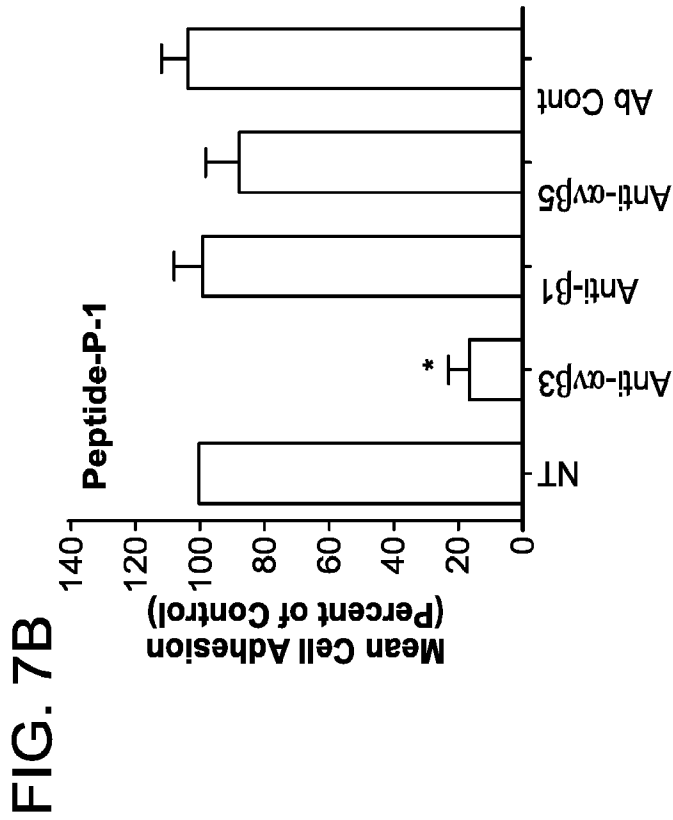


FIG. 7A

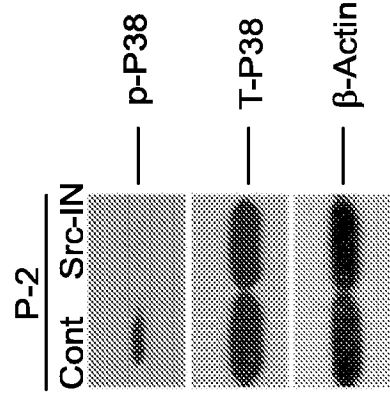
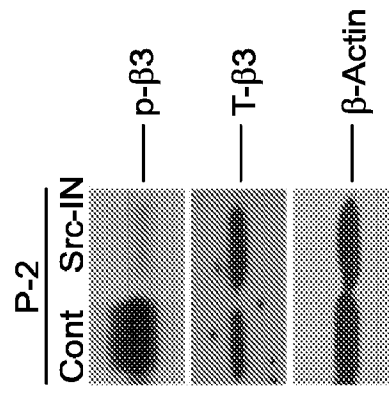
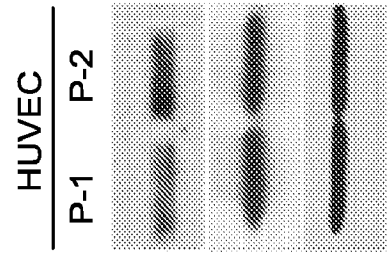
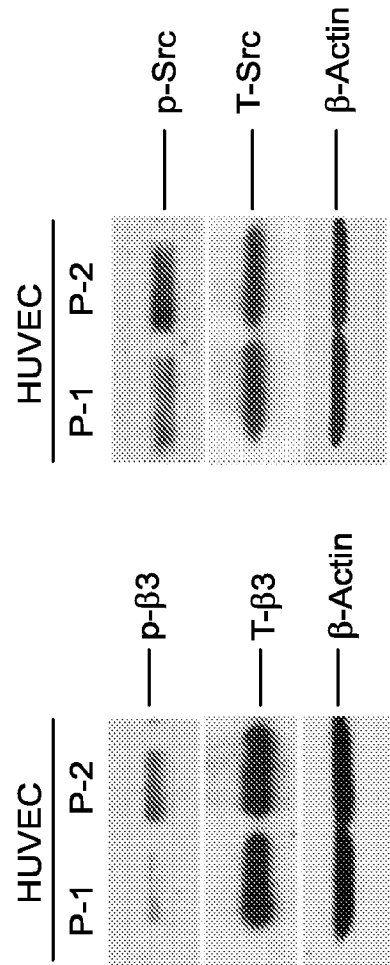
FIG. 7B

FIG. 7C

FIG. 7D

FIG. 7E

FIG. 7F



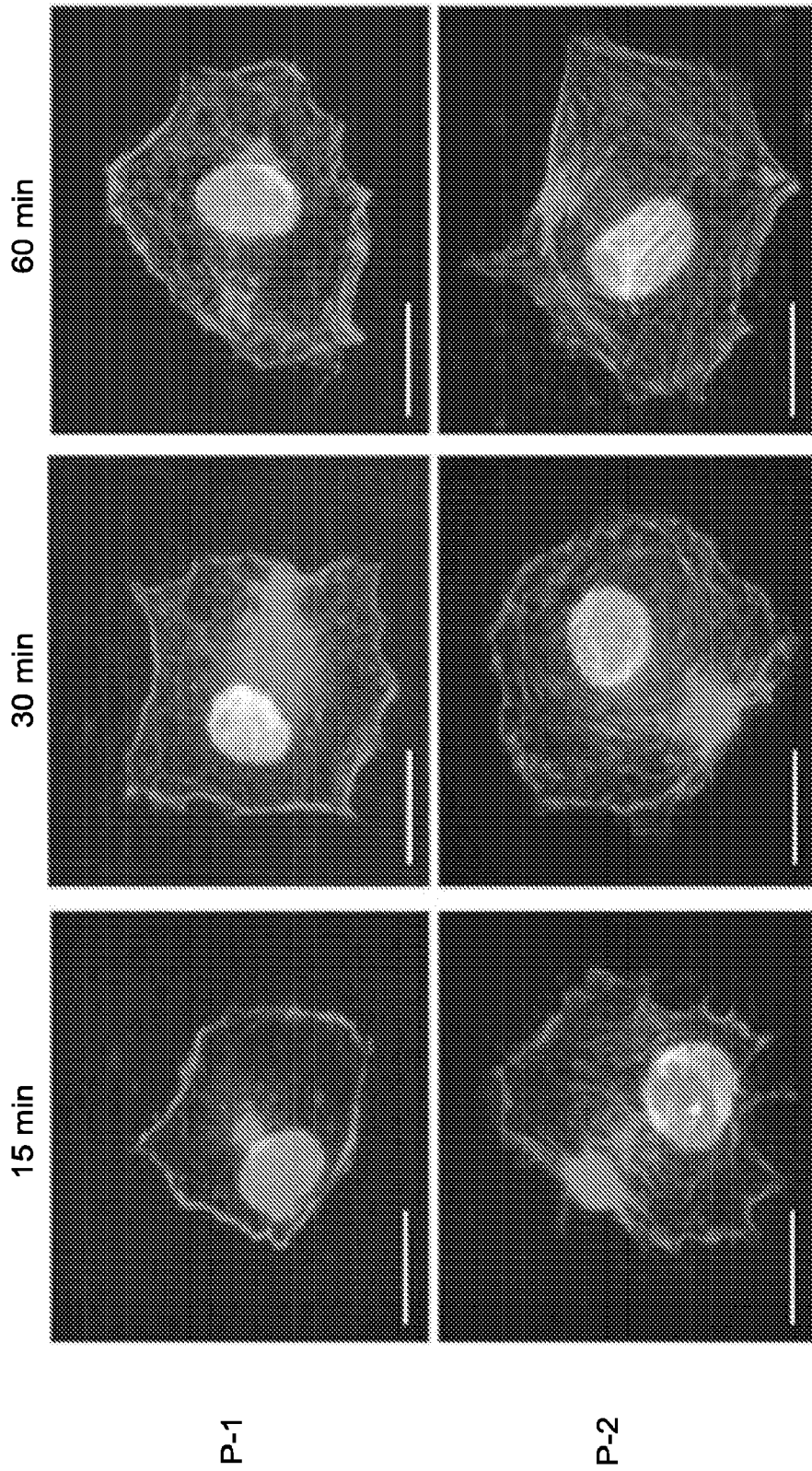


FIG. 7G

FIG. 8A

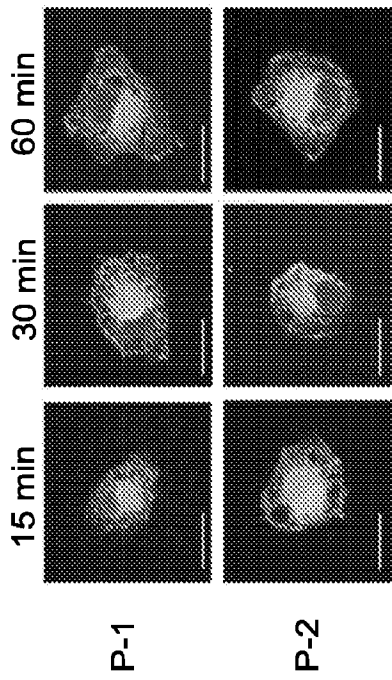


FIG. 8B

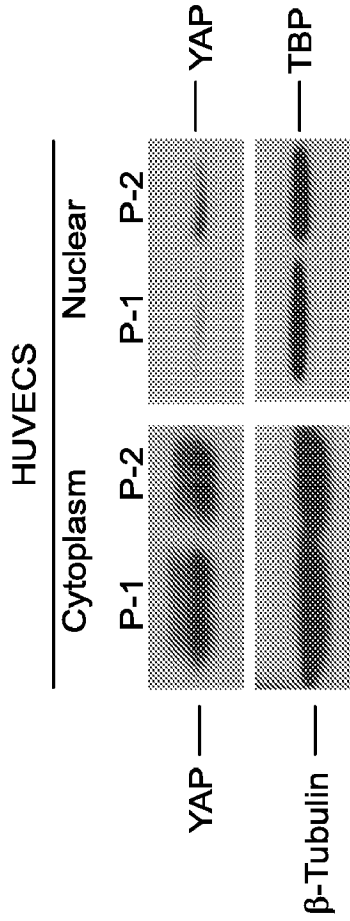


FIG. 8C

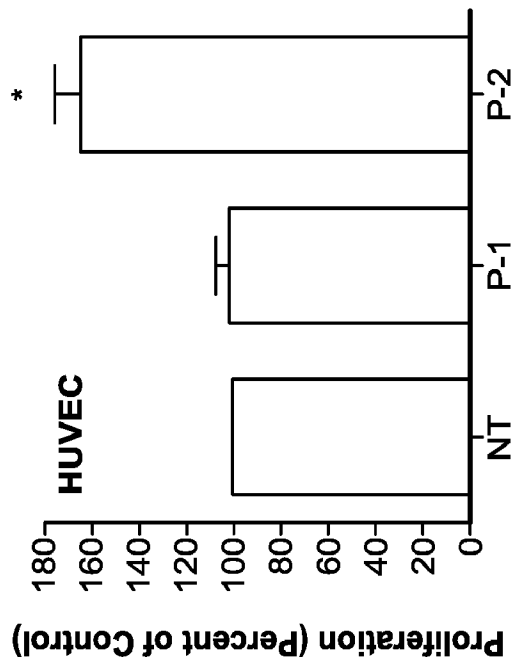
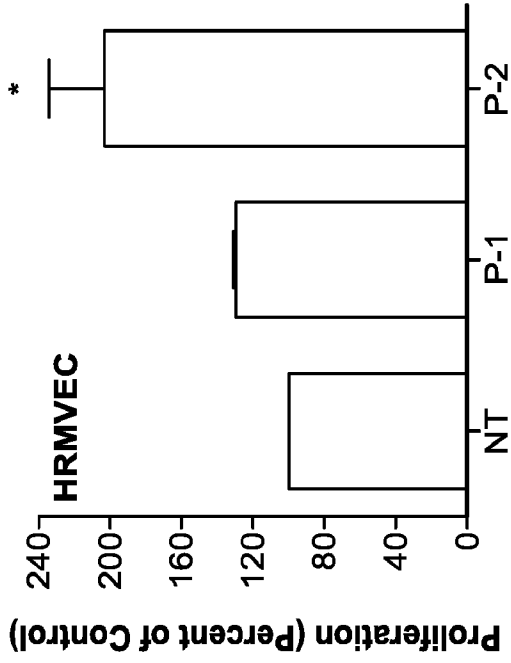


FIG. 8D



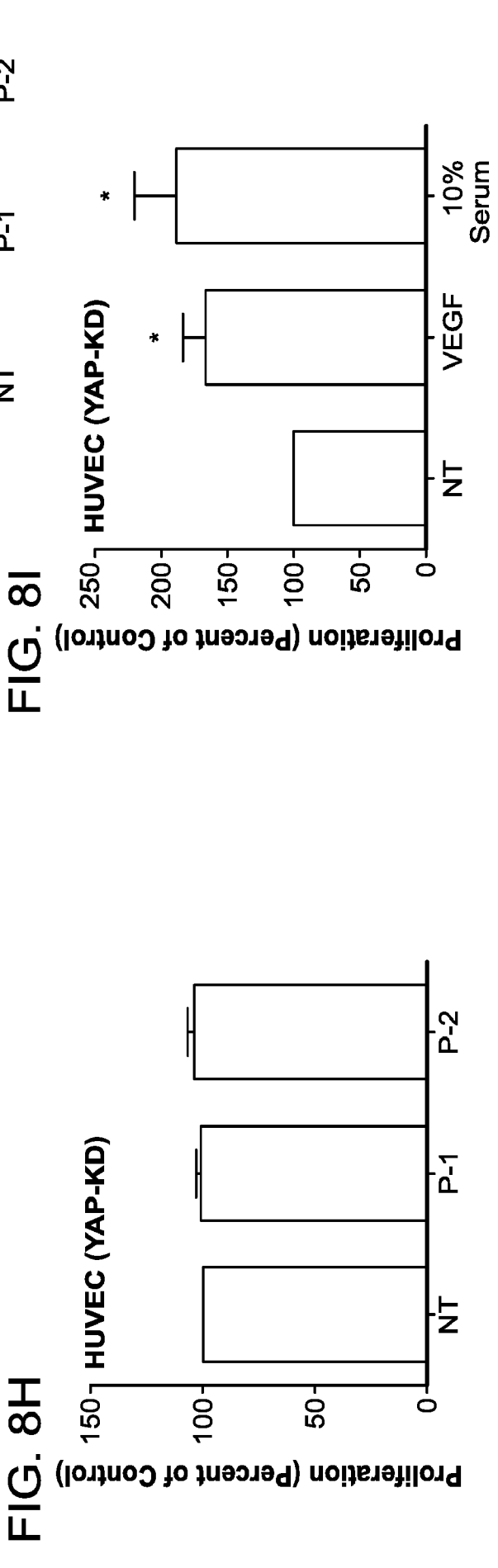
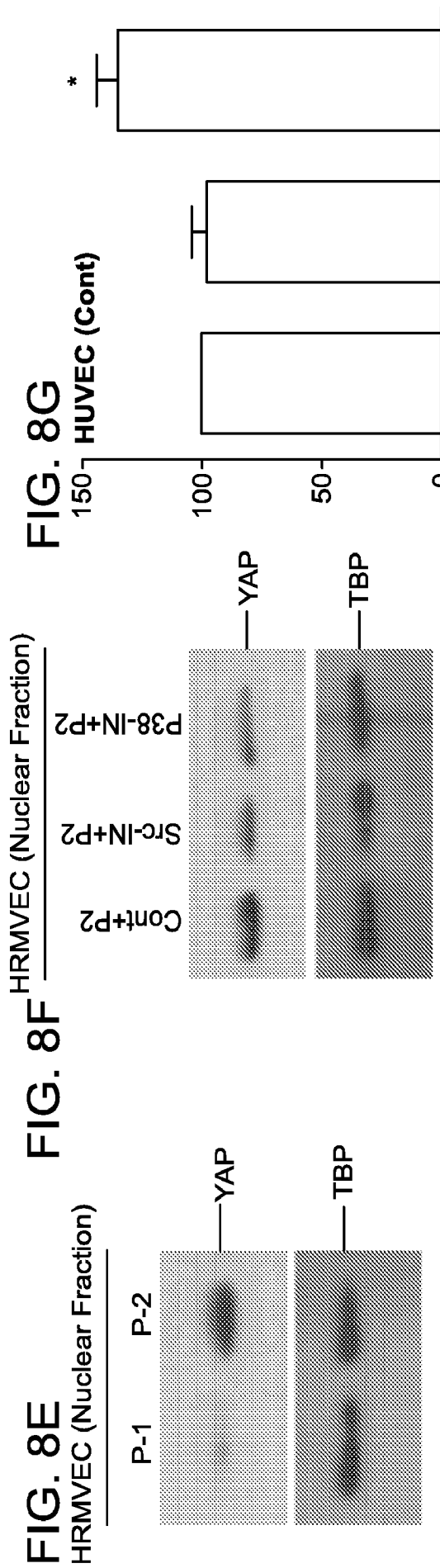
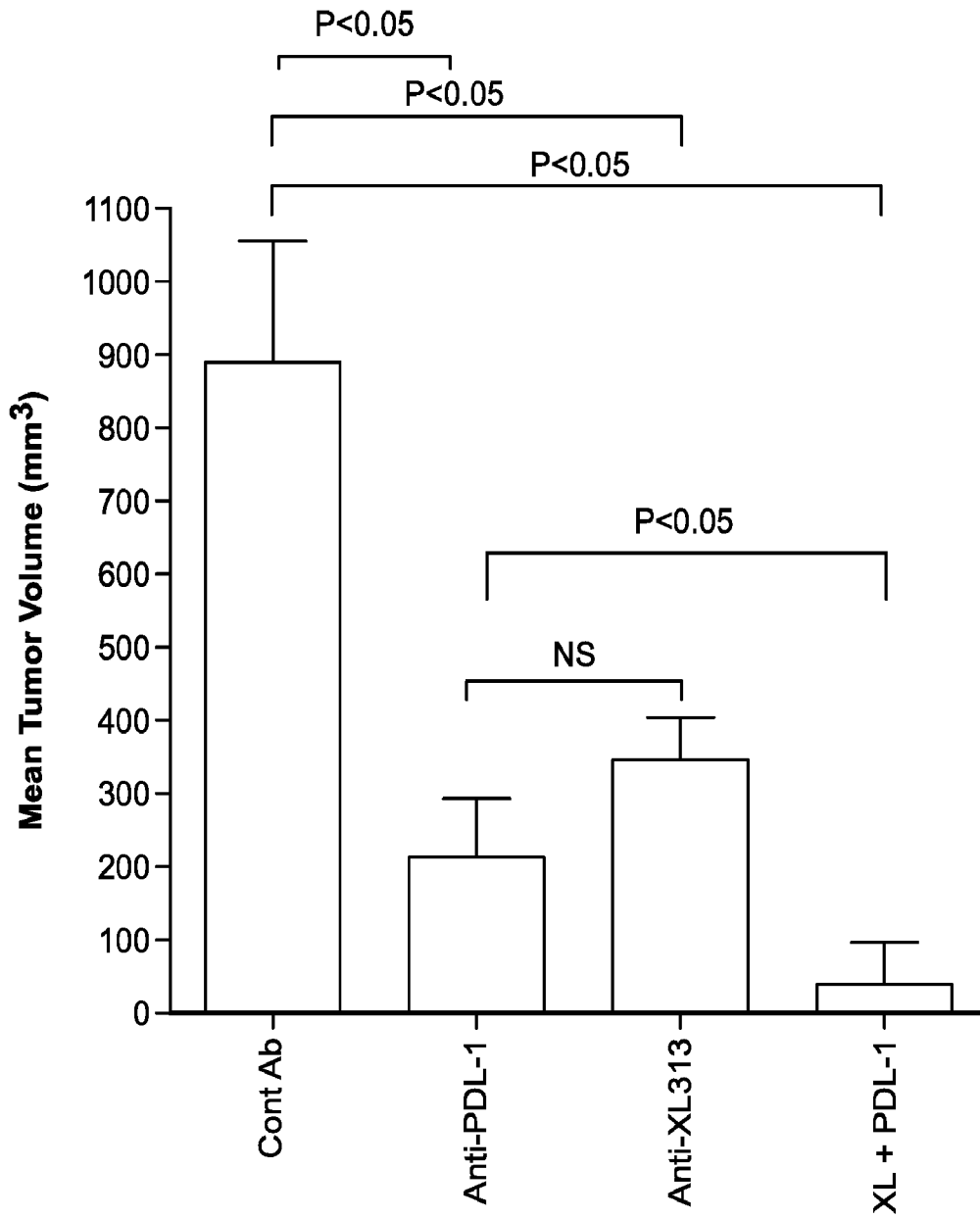


FIG. 9



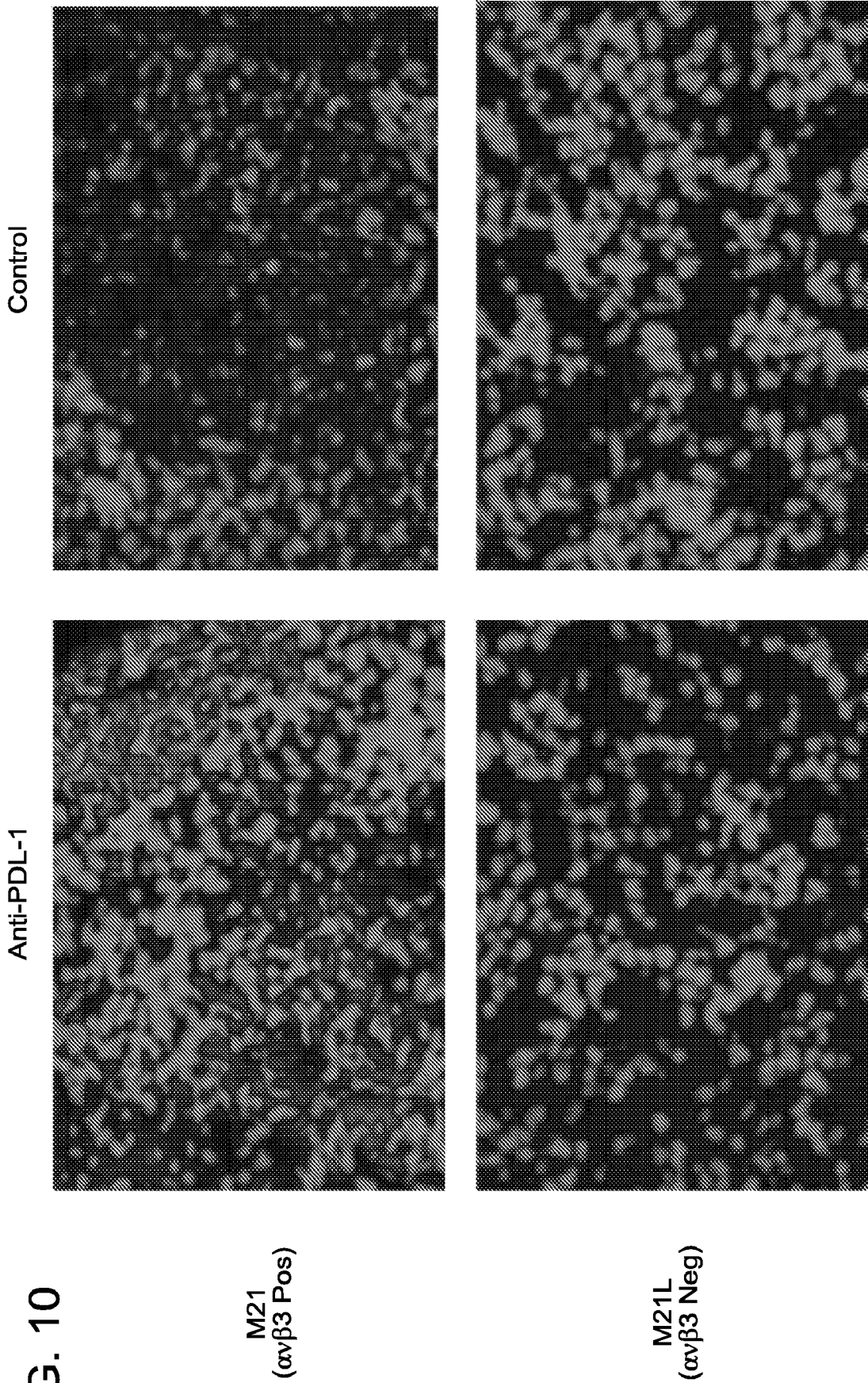


FIG. 10

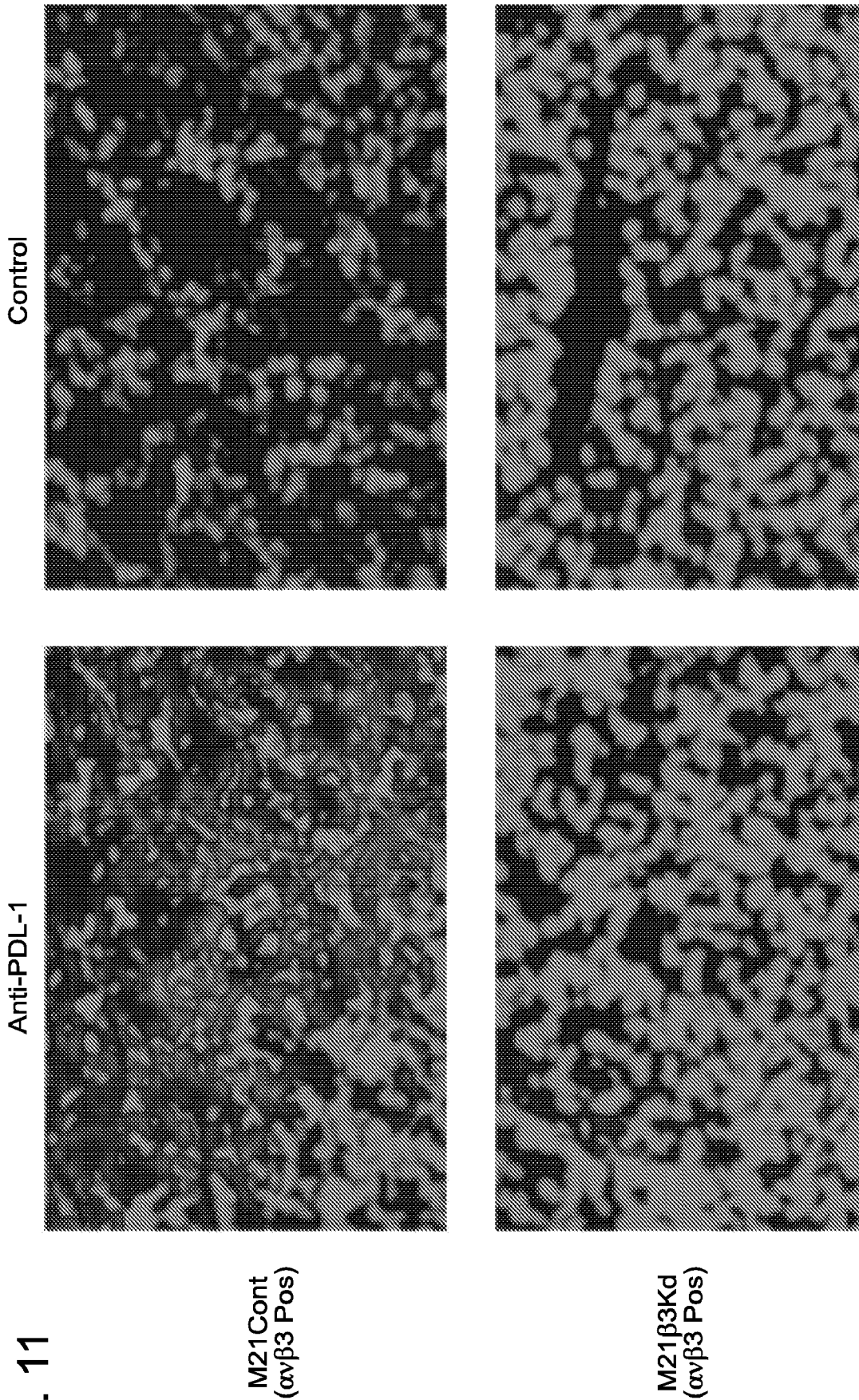


FIG. 11

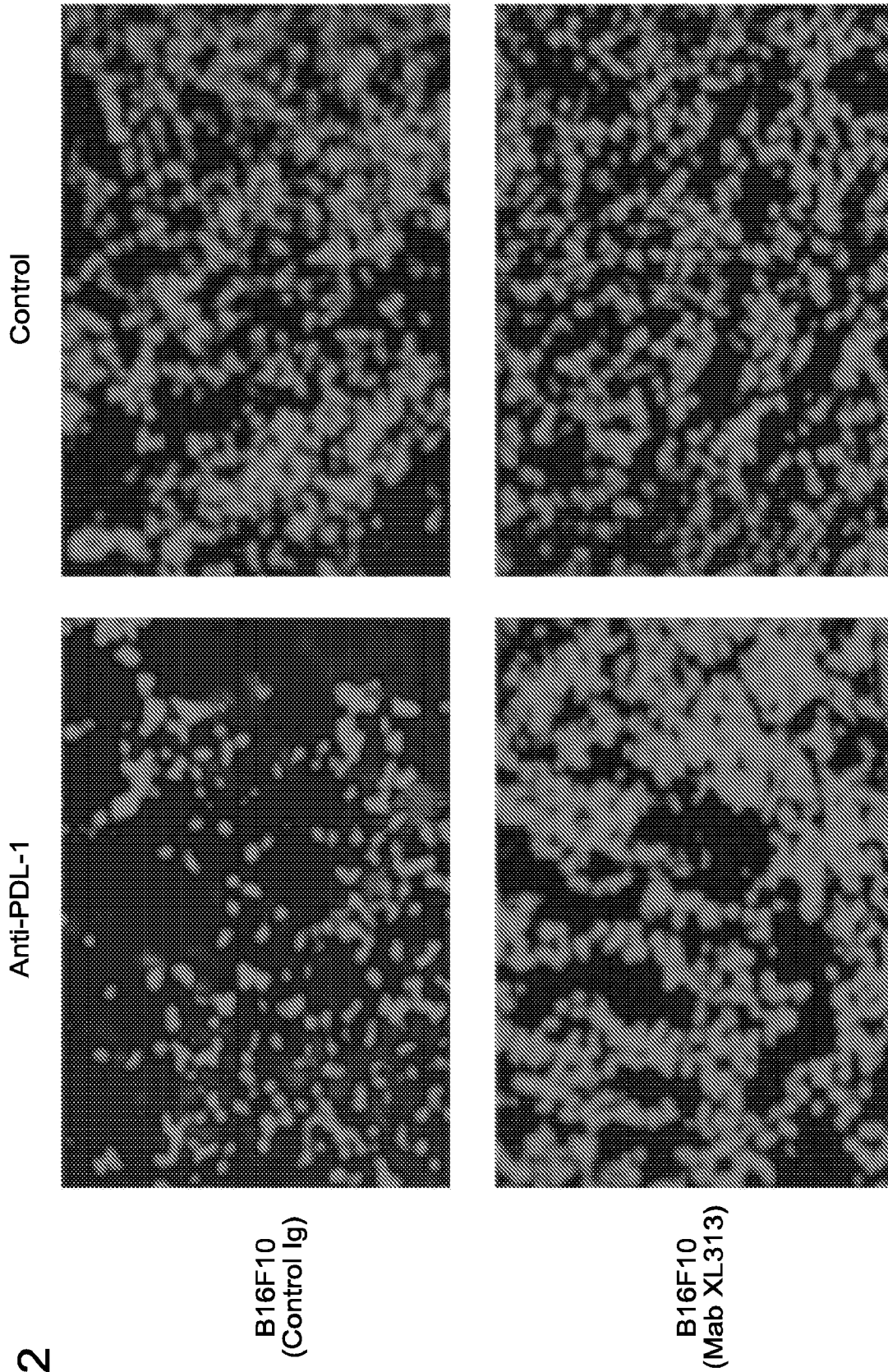


FIG. 12

FIG. 13

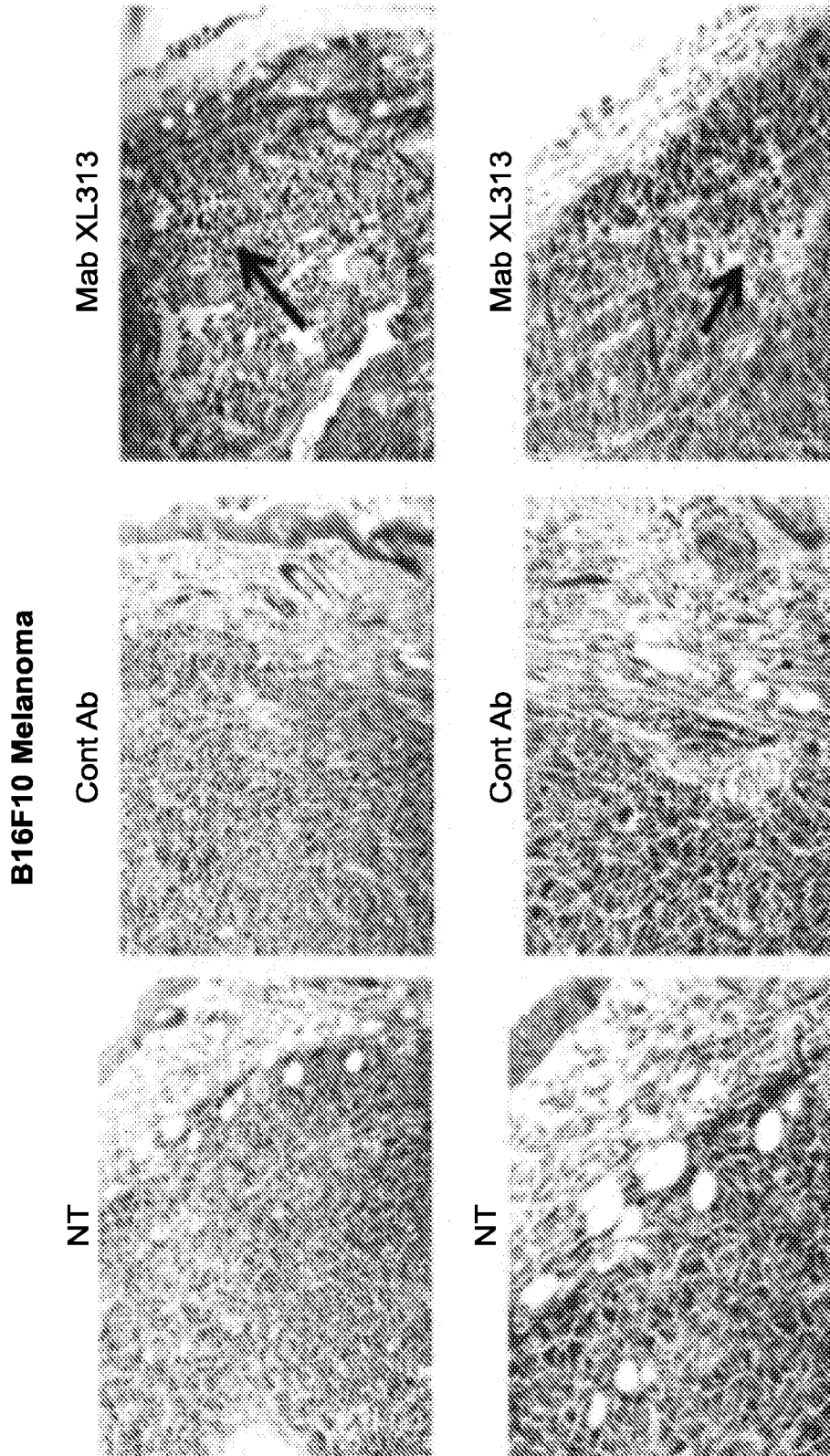


FIG. 14A

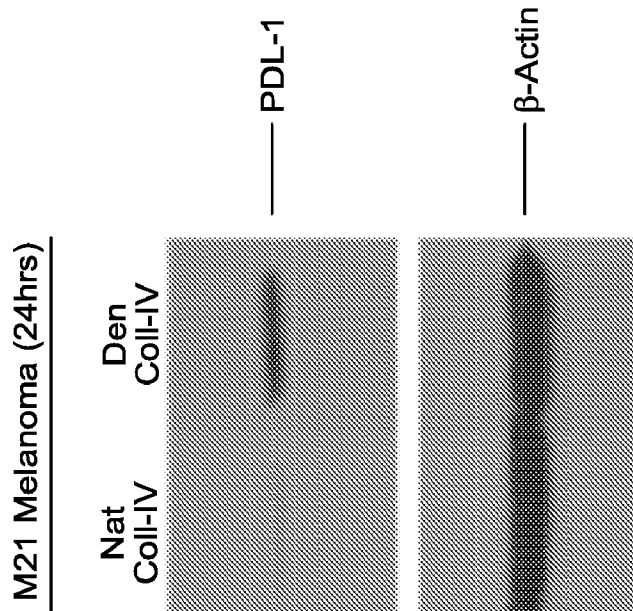


FIG. 14B

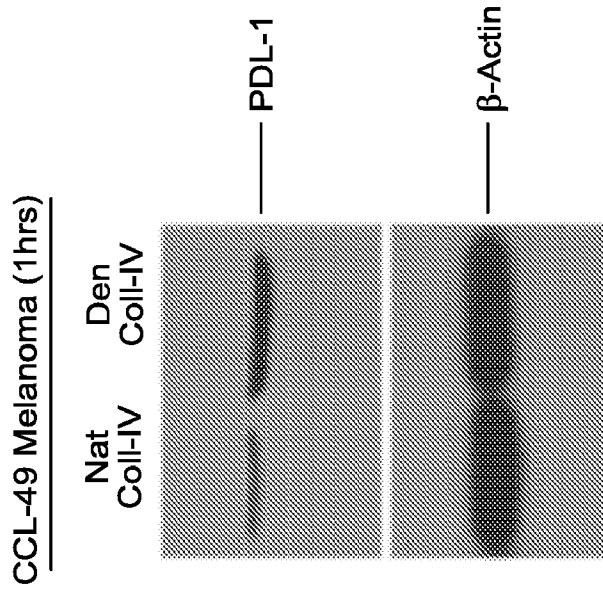


FIG. 14C

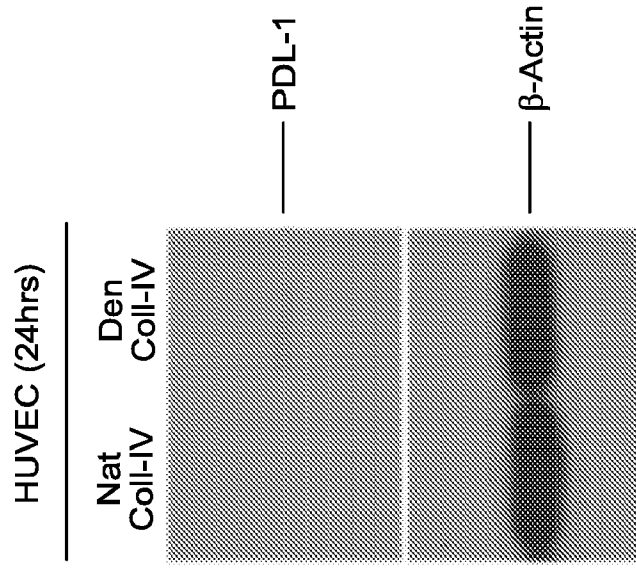


FIG. 15

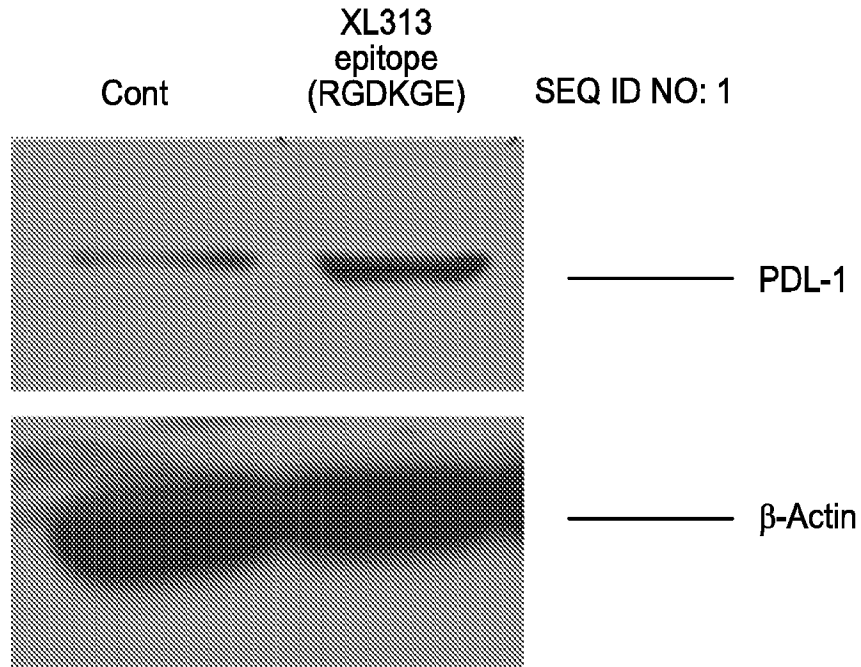


FIG. 16

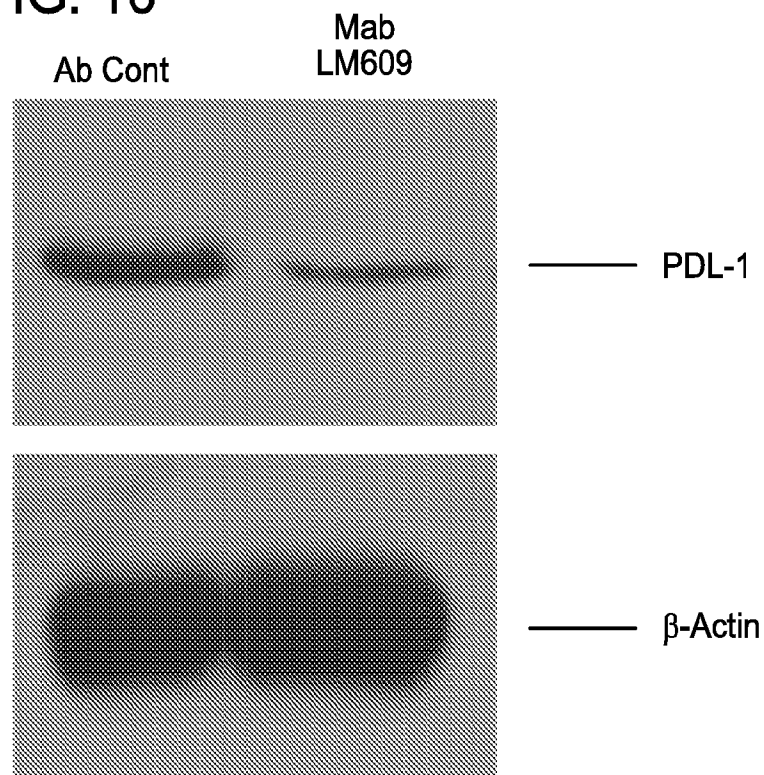
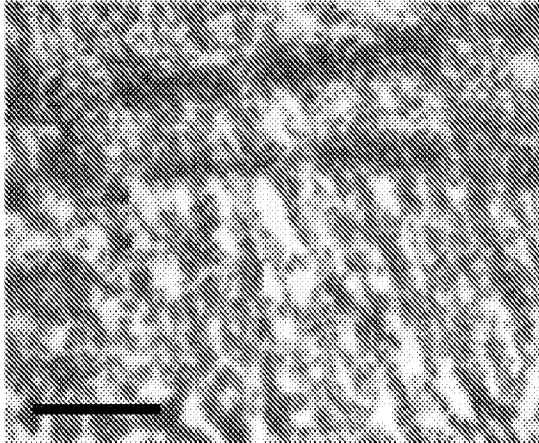


FIG. 17A

Malignant  
Ovarian Tumor (H&E)



Malignant  
Ovarian Tumor (HU177)

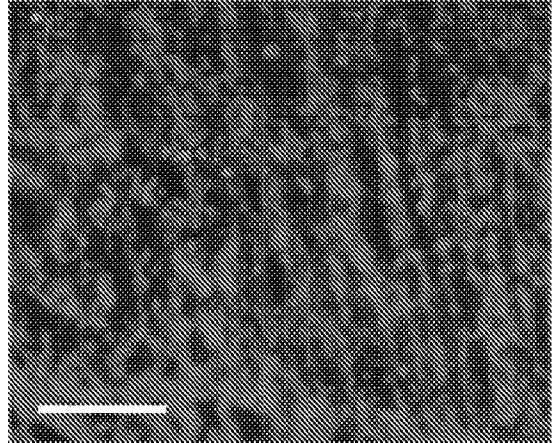
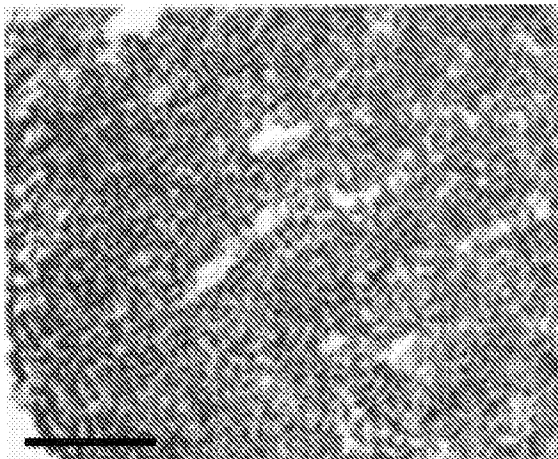


FIG. 17B

Benign  
Granuloma (H&E)



Benign  
Granuloma (HU177)

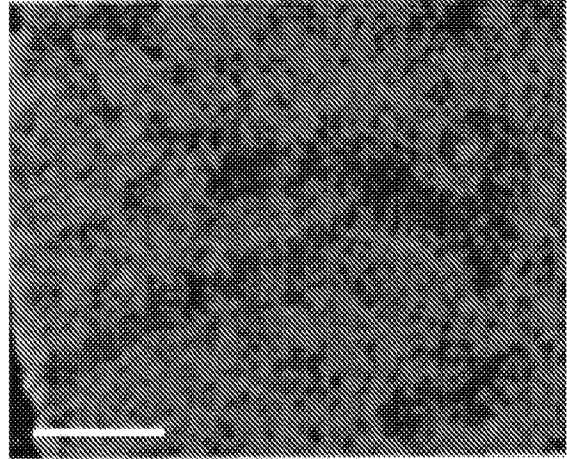


FIG. 17C

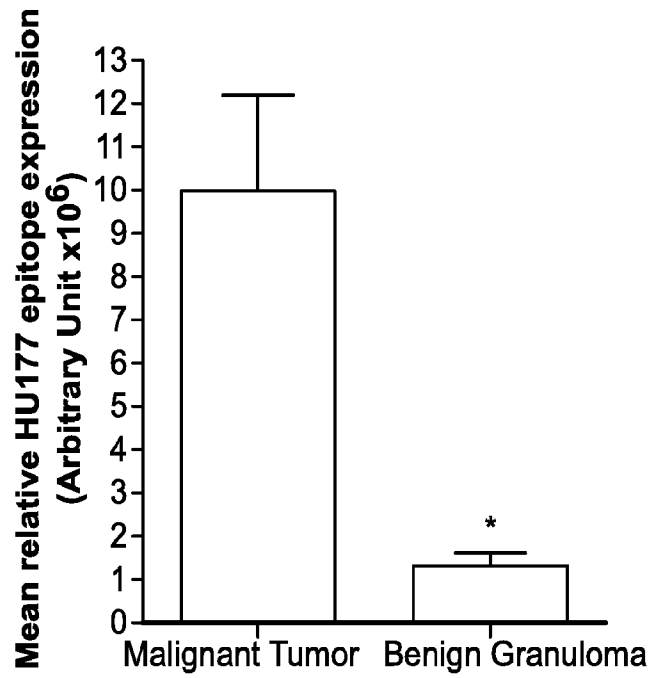


FIG. 17D

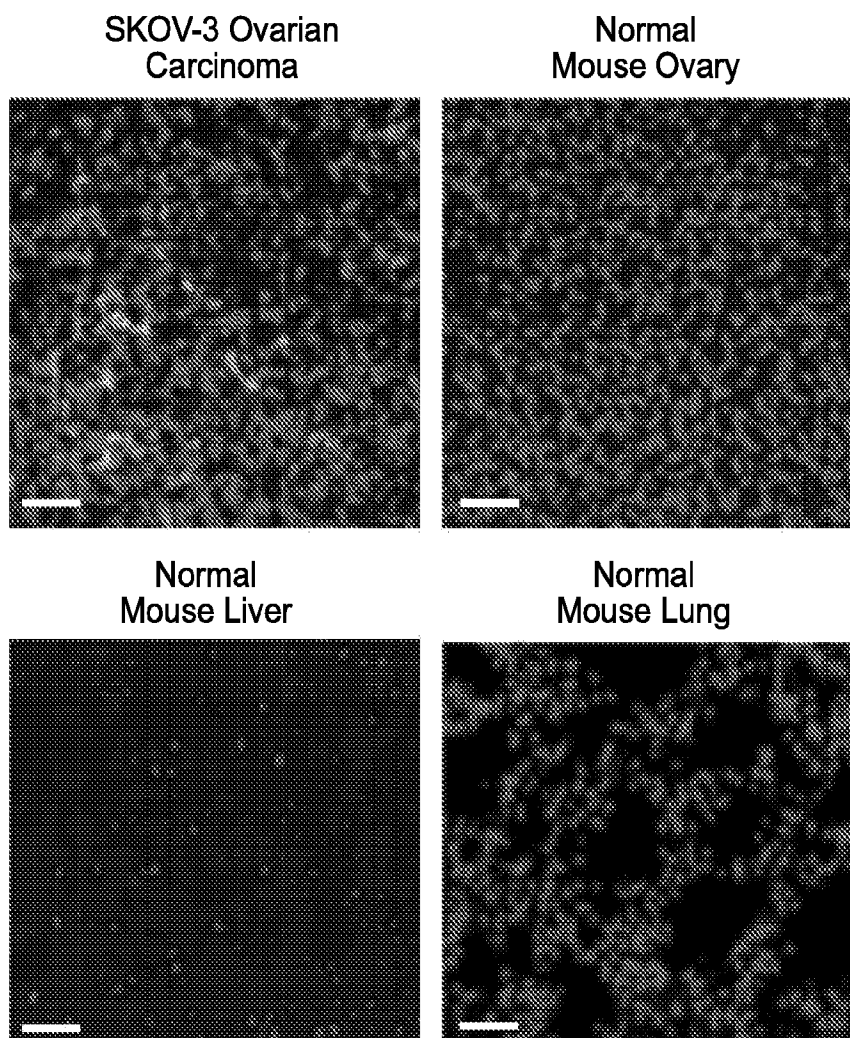


FIG. 18A

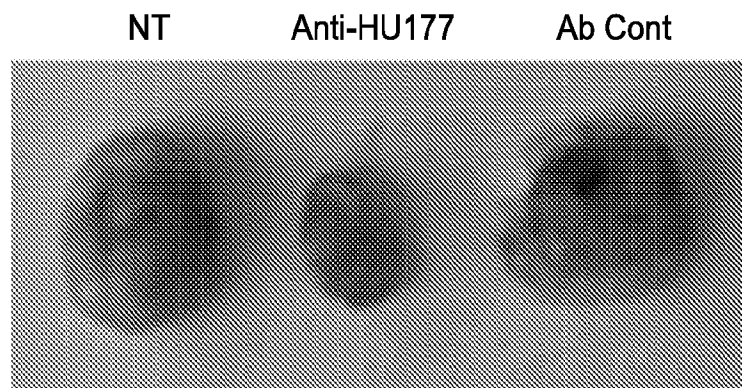


FIG. 18B

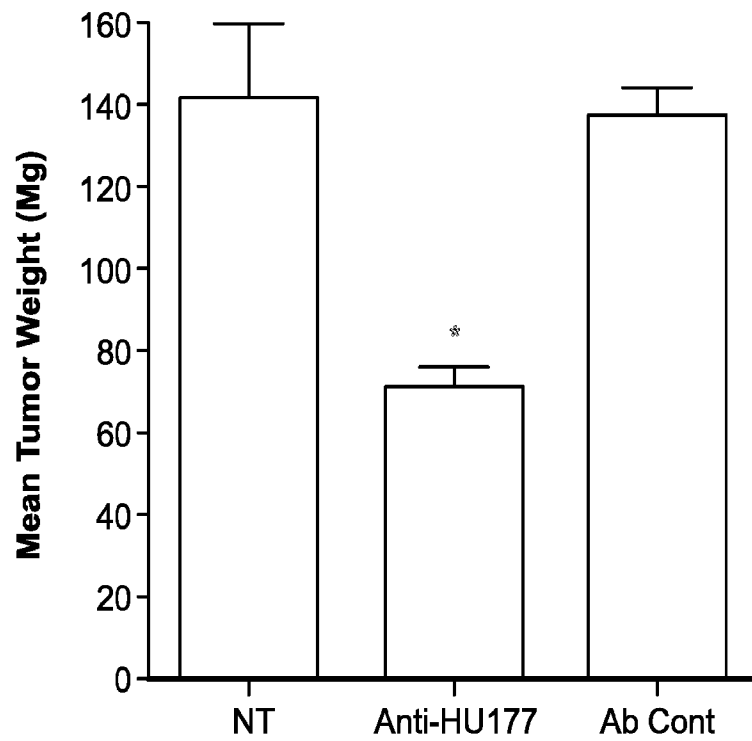


FIG. 18C

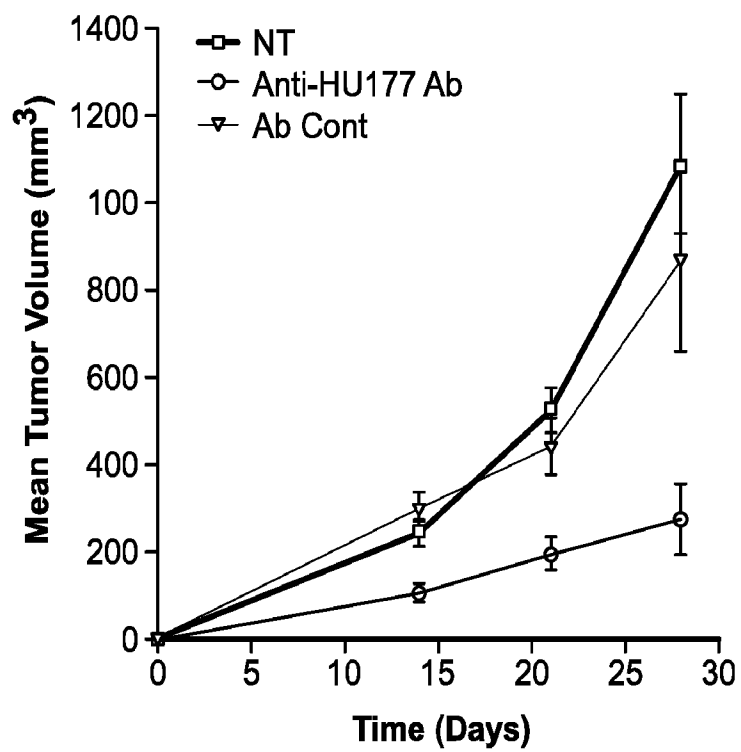


FIG. 19A

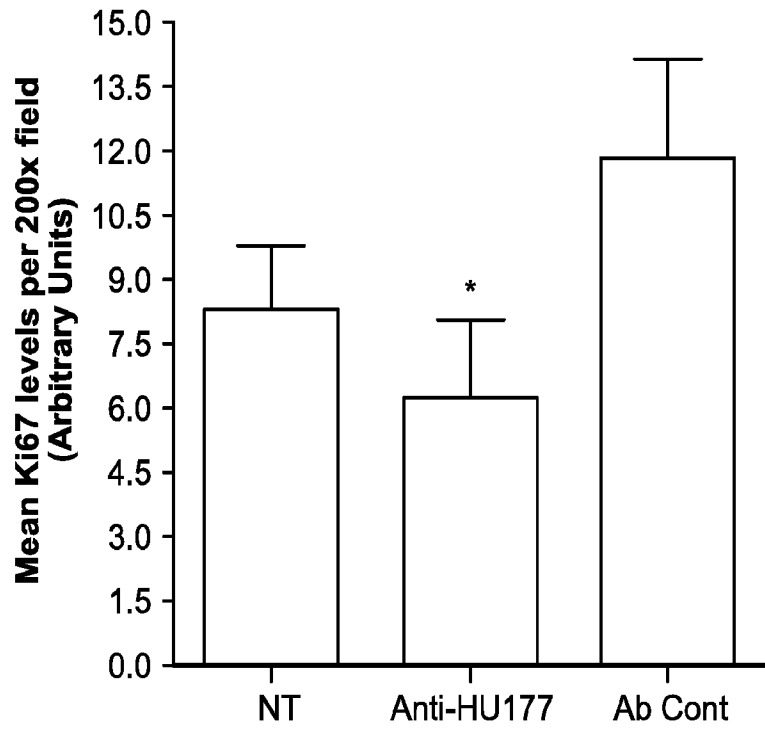


FIG. 19B

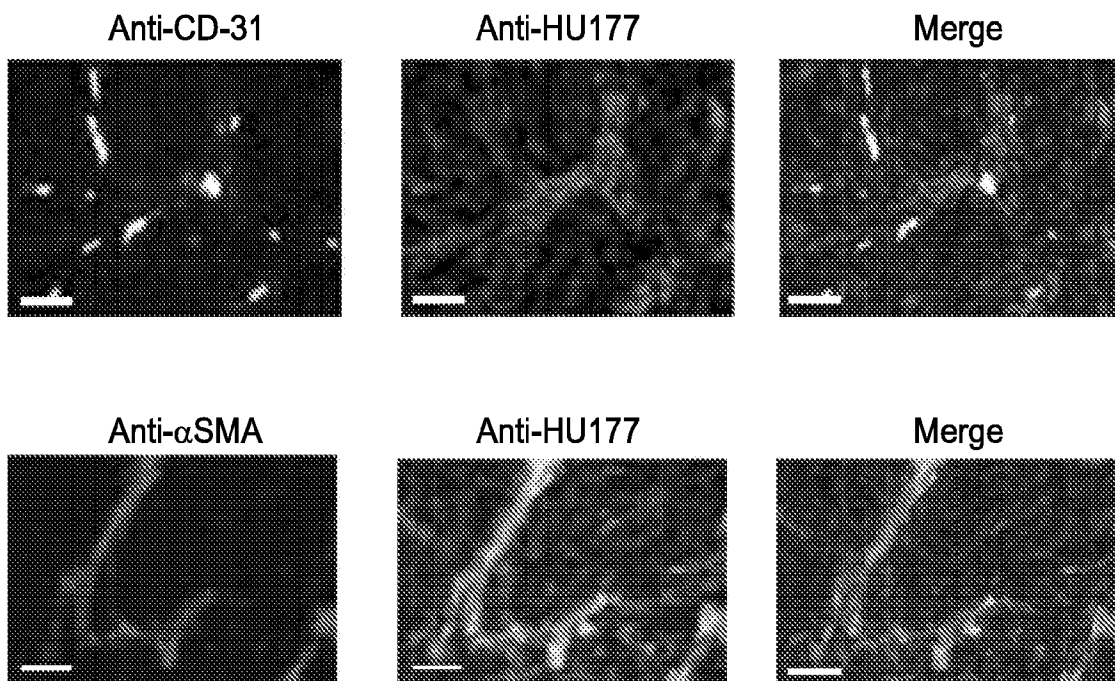


FIG. 19D

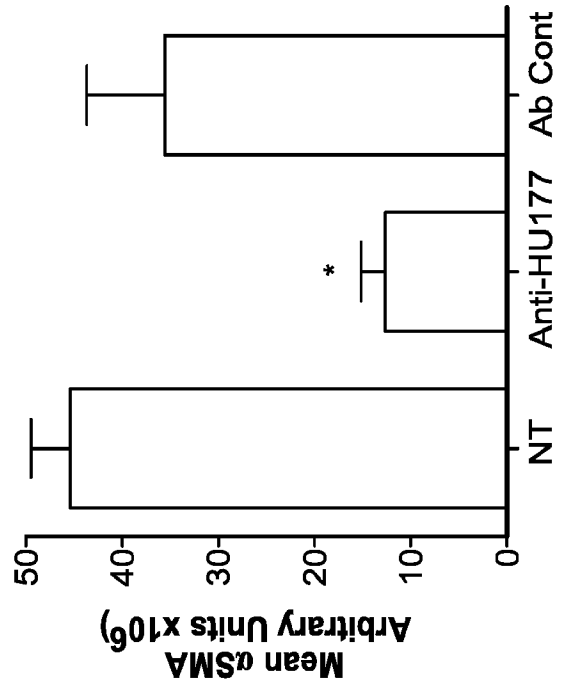
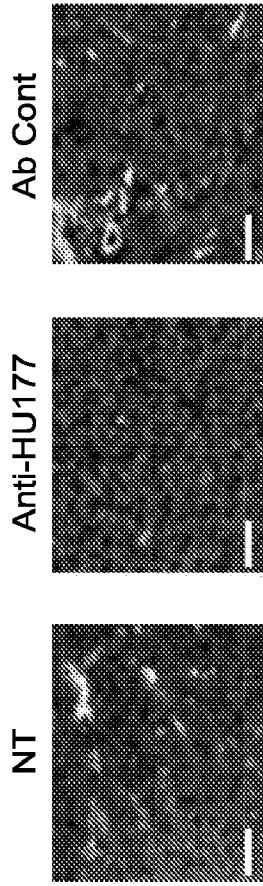


FIG. 19C

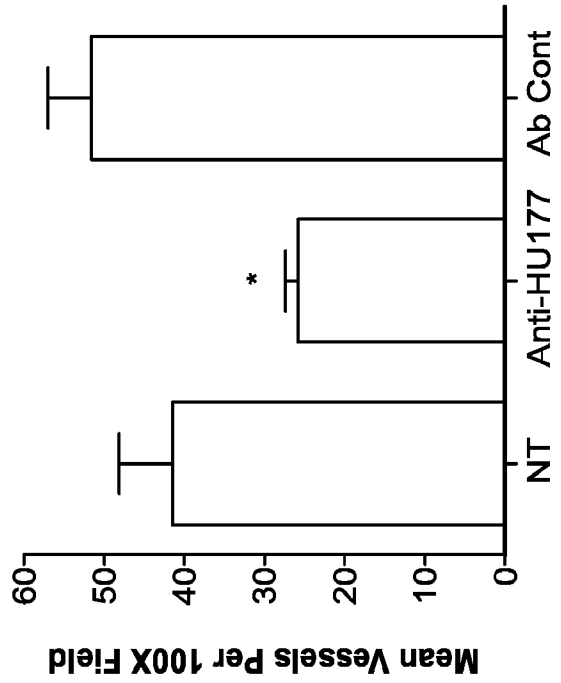
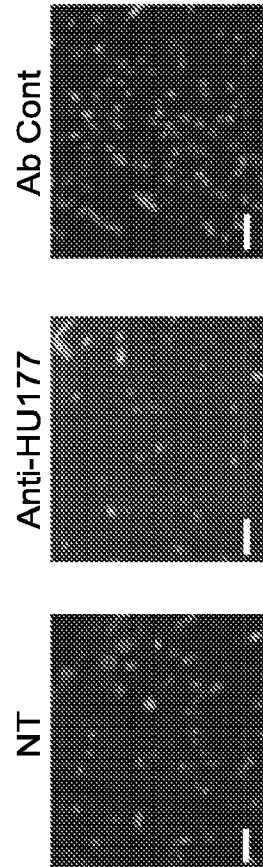


FIG. 20B

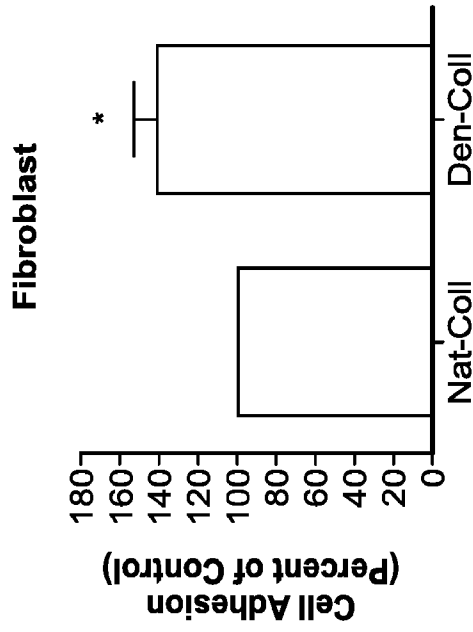


FIG. 20D

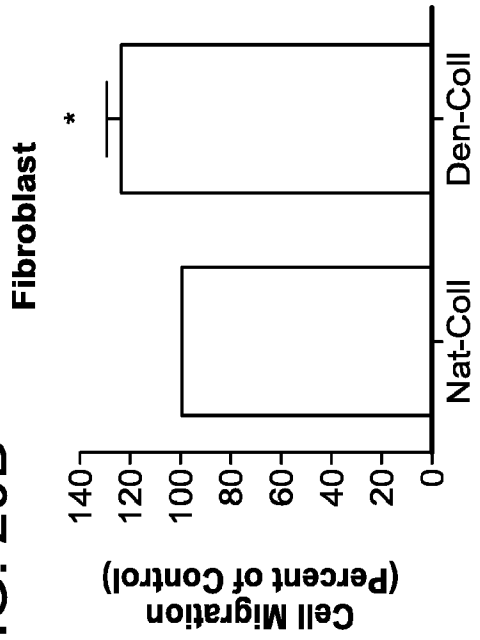


FIG. 20A

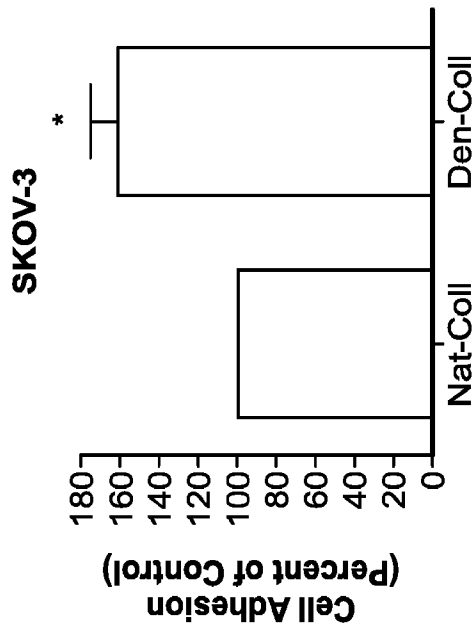


FIG. 20C

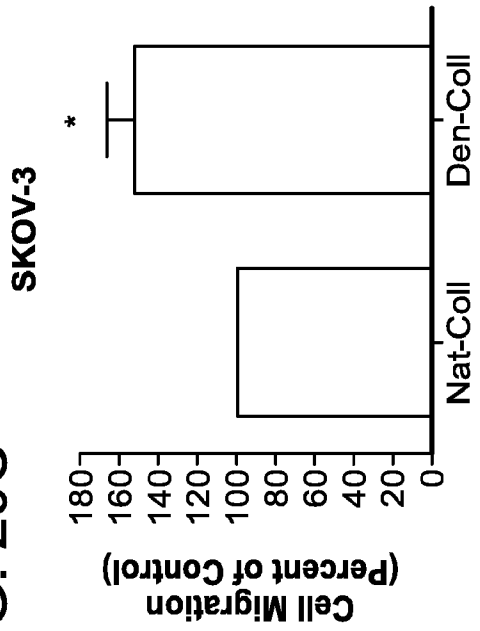


FIG. 21B

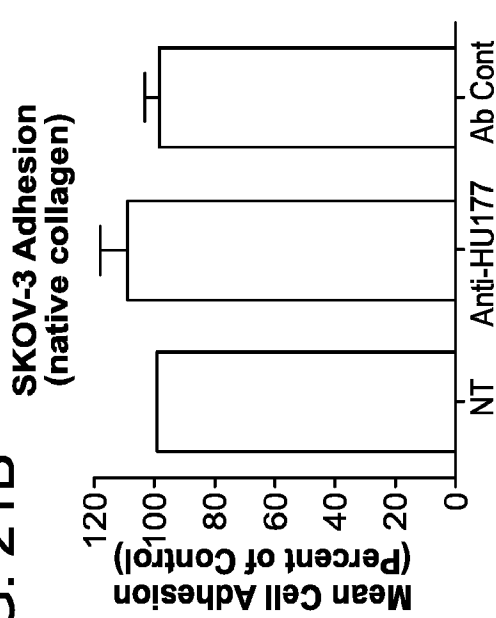


FIG. 21D

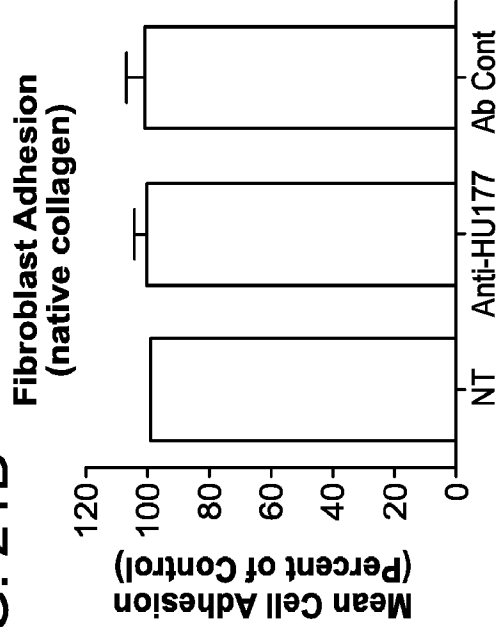


FIG. 21A

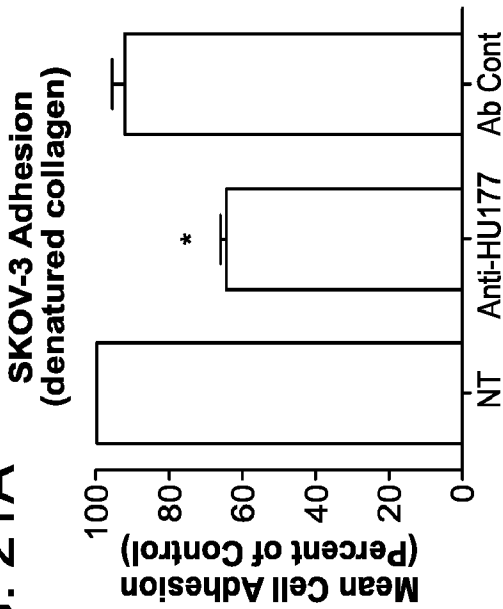


FIG. 21C

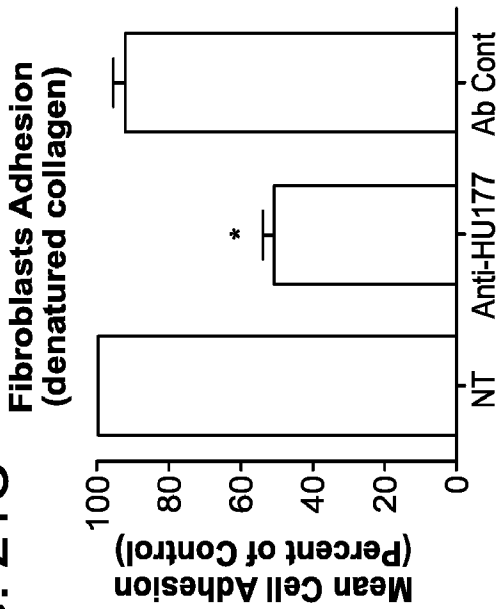


FIG. 21E

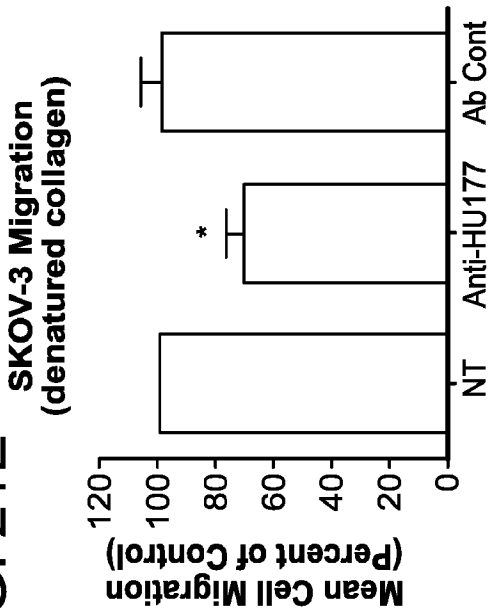


FIG. 21F

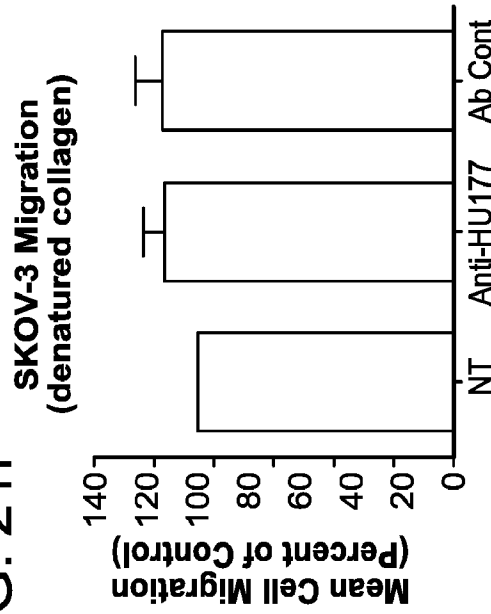


FIG. 21G

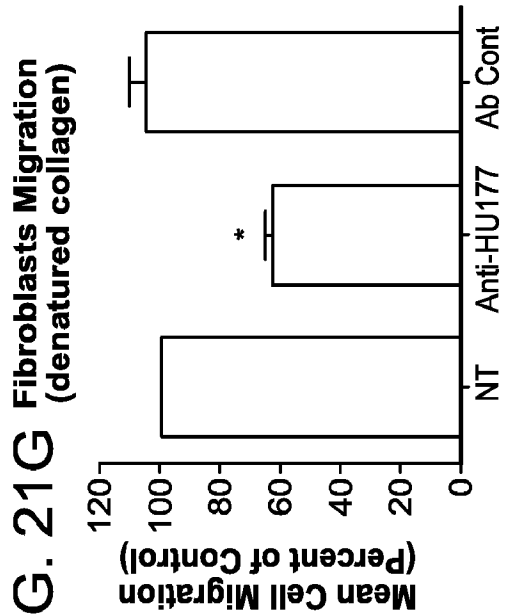


FIG. 21H

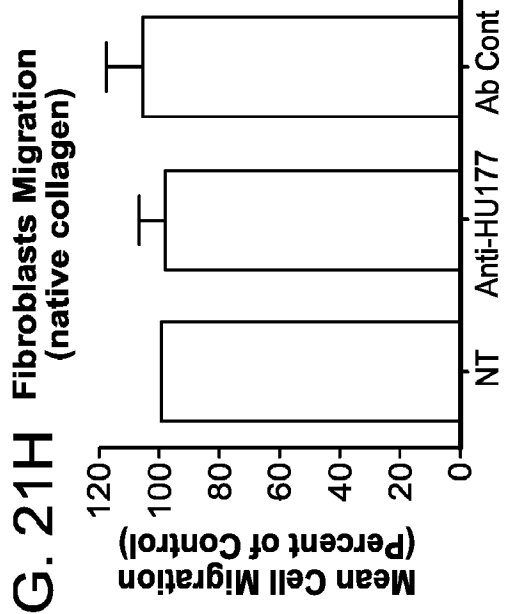


FIG. 22B

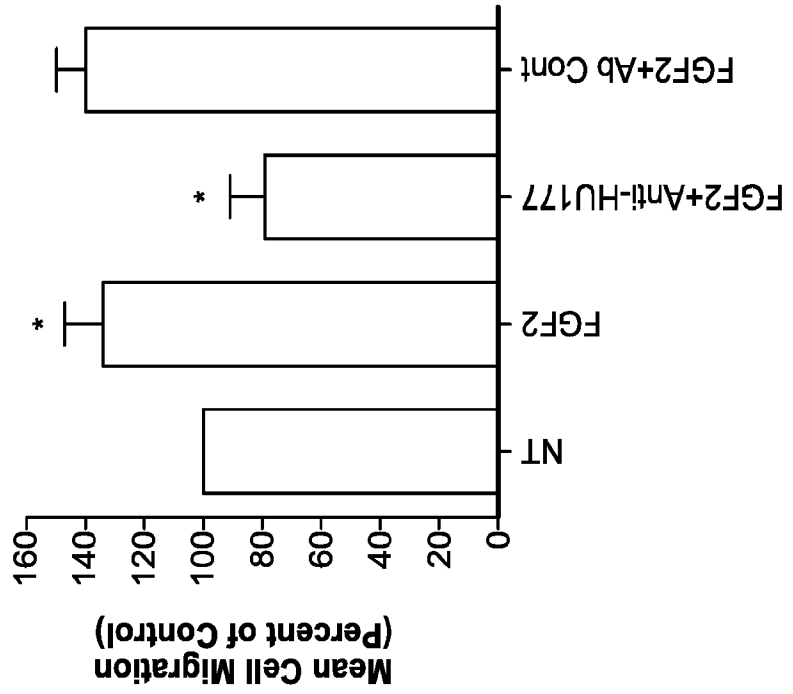


FIG. 22A

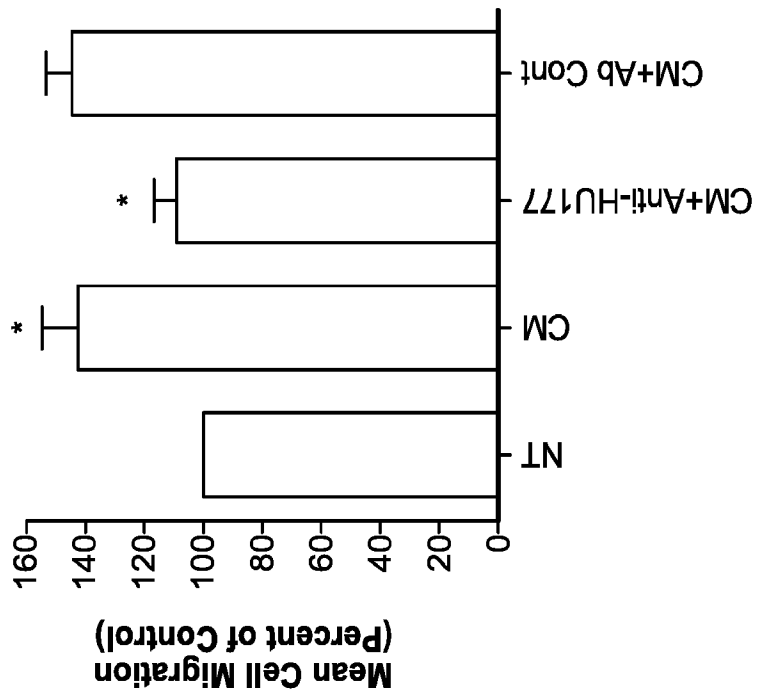


FIG. 22C

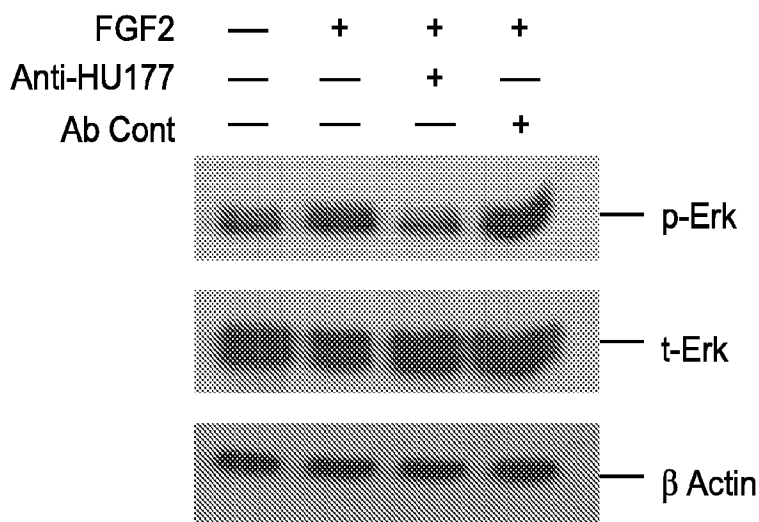


FIG. 22D

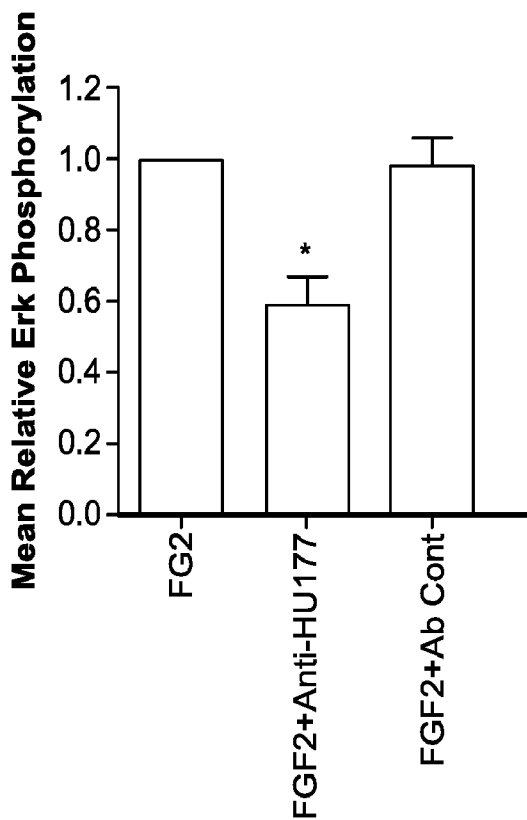


FIG. 22E

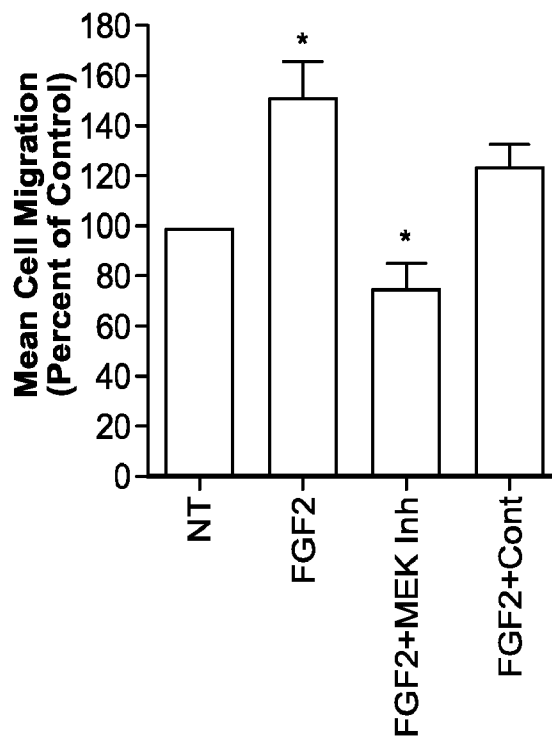


FIG. 23A

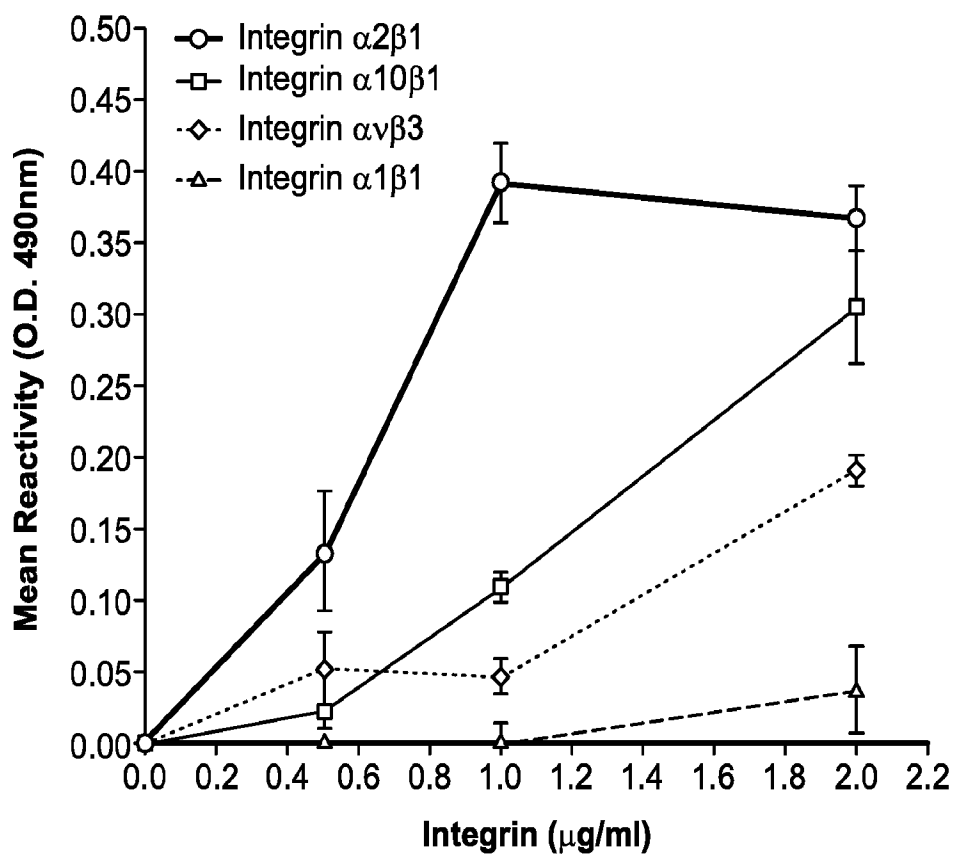


FIG. 23B

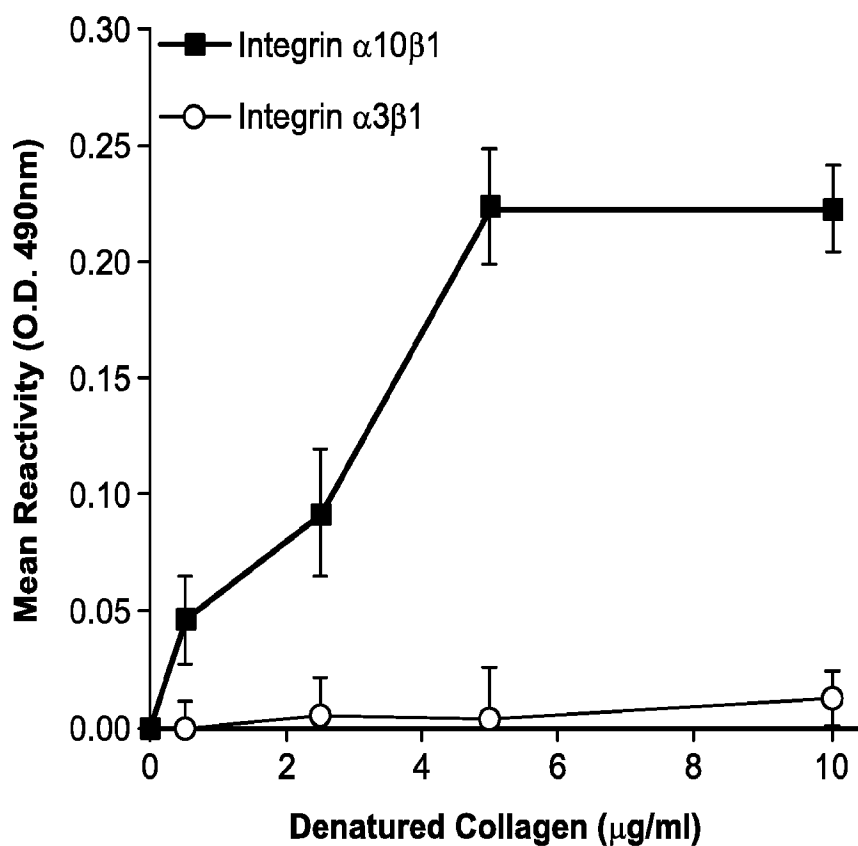


FIG. 23C

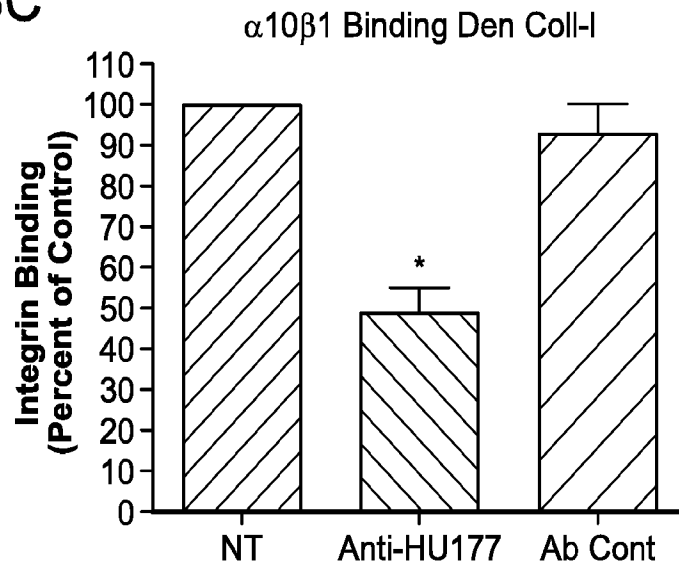


FIG. 23D

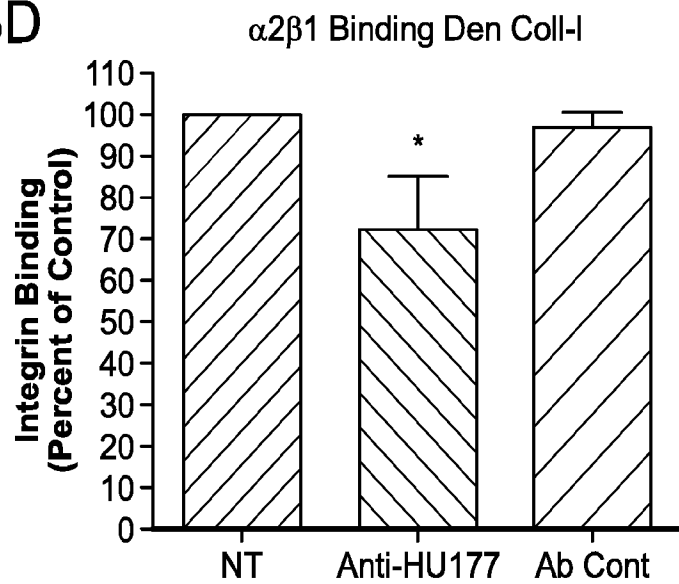


FIG. 23E

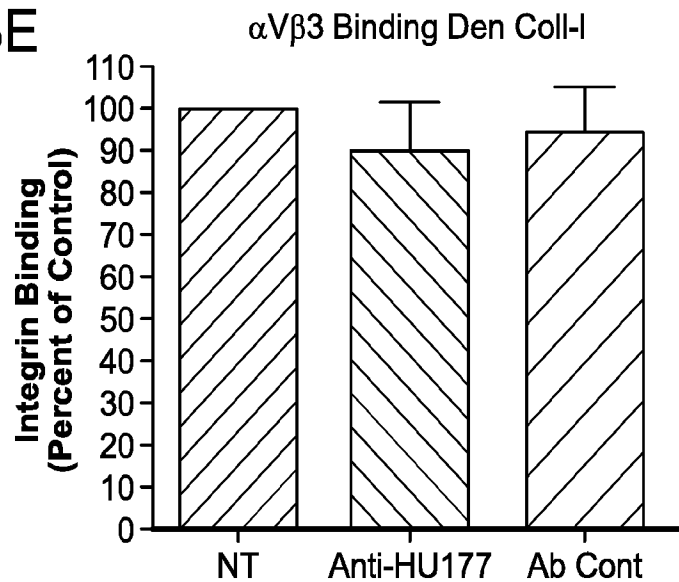


FIG. 23F

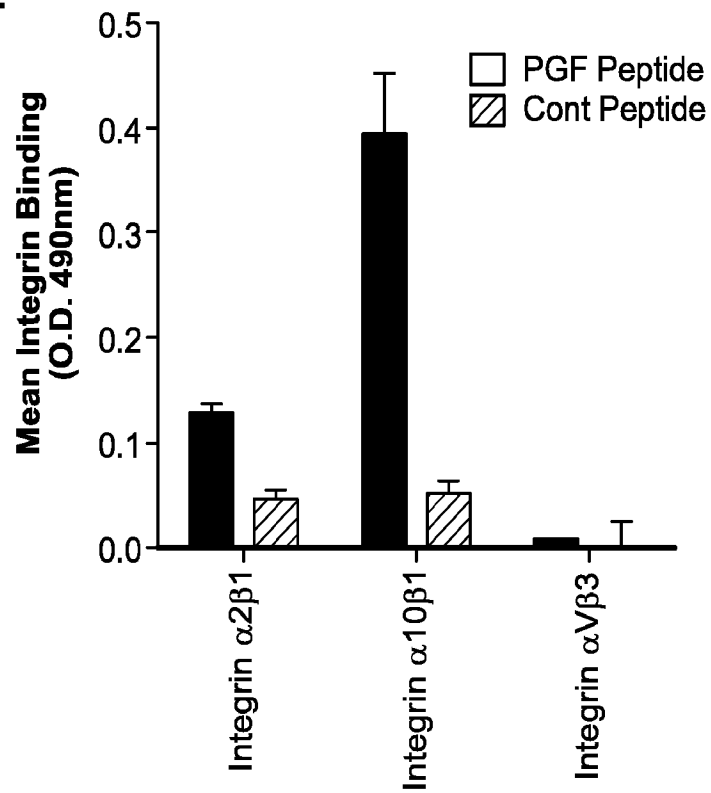


FIG. 23G

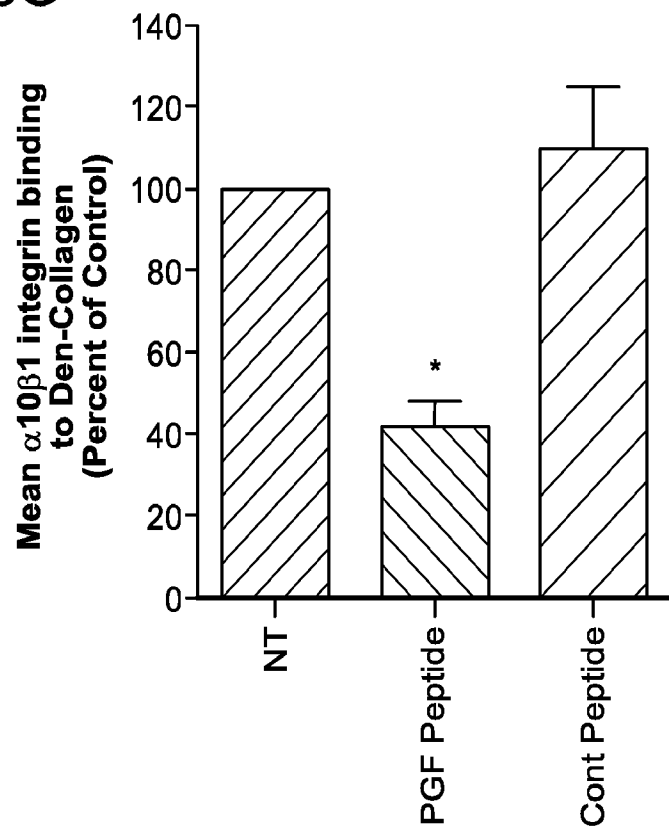


FIG. 24A

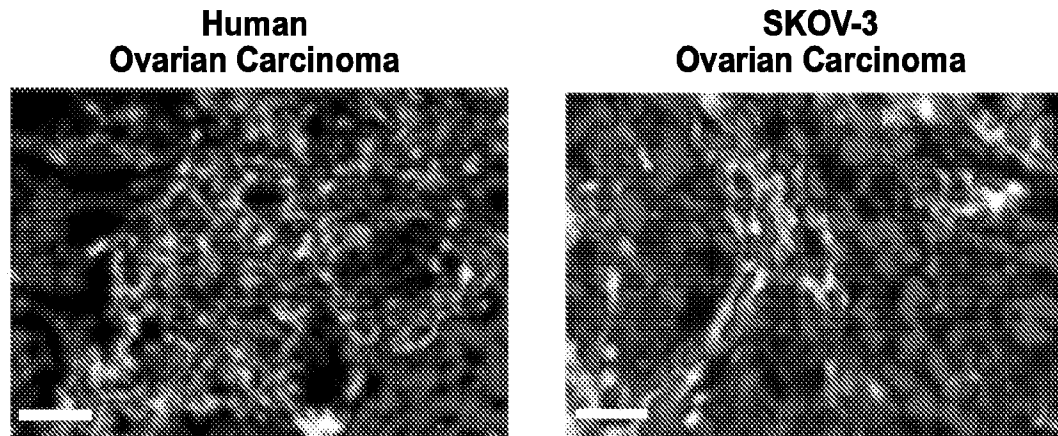


FIG. 24B

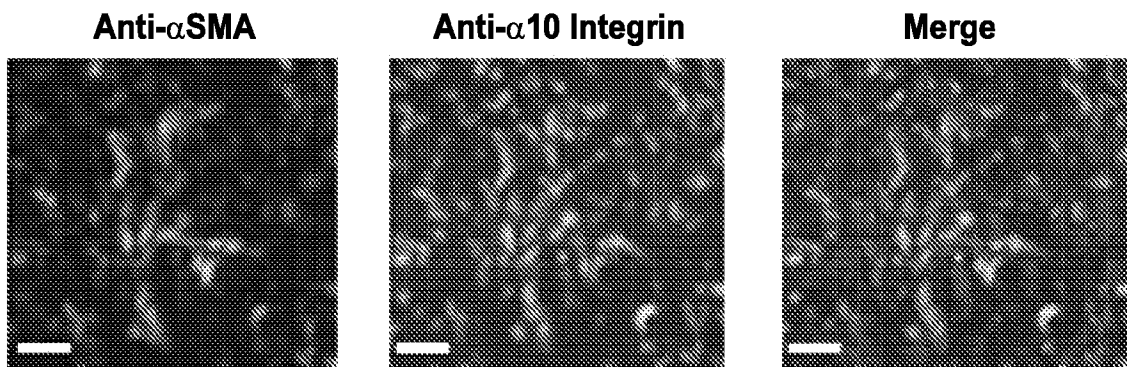


FIG. 24C

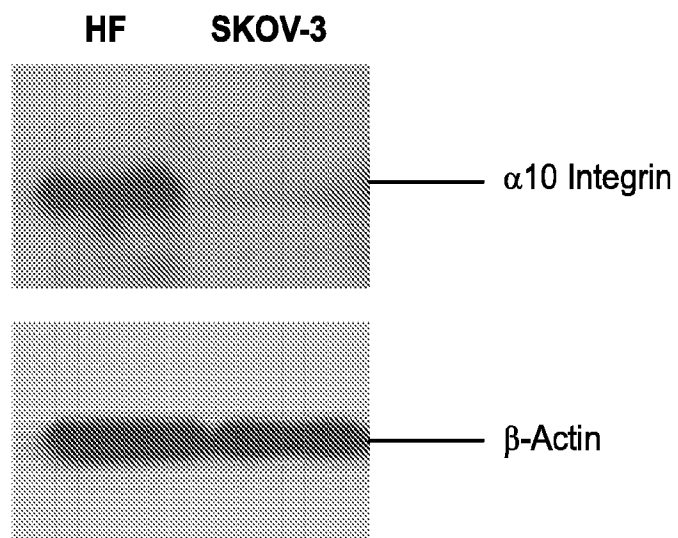


FIG. 24E

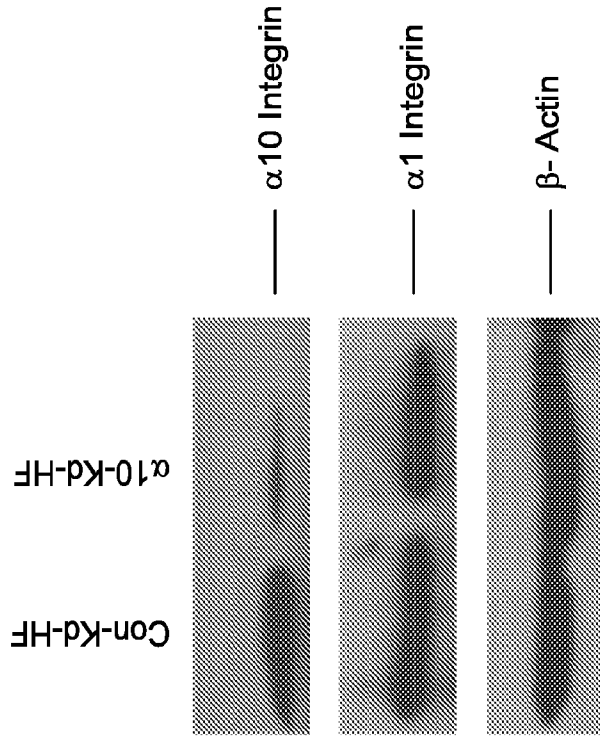


FIG. 24D

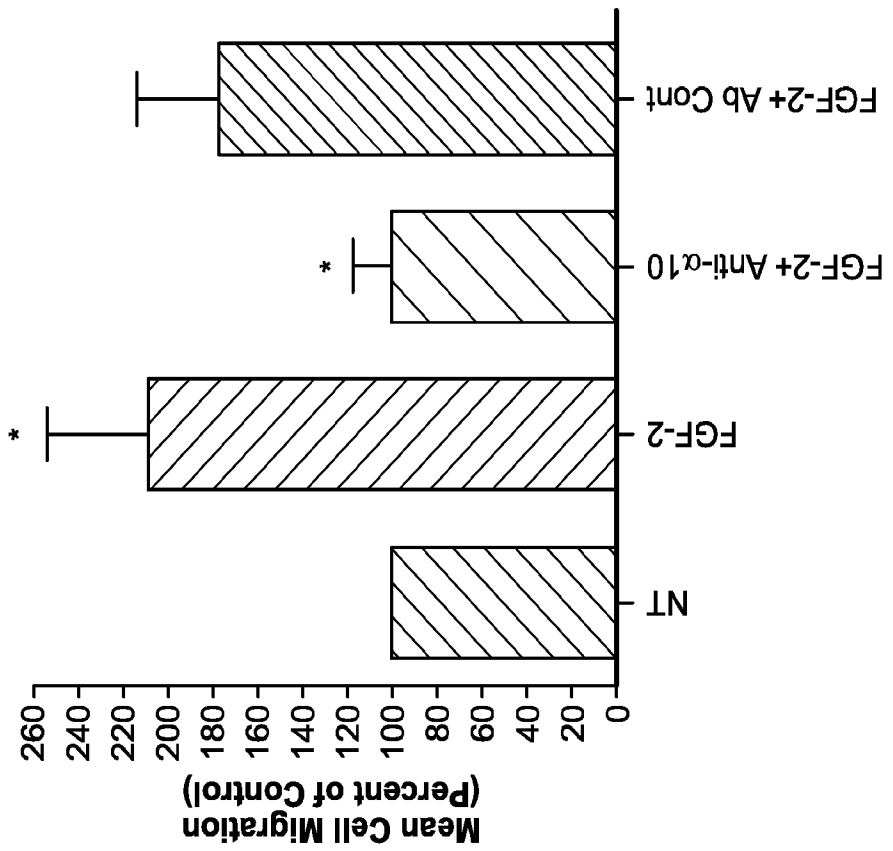


FIG. 24G

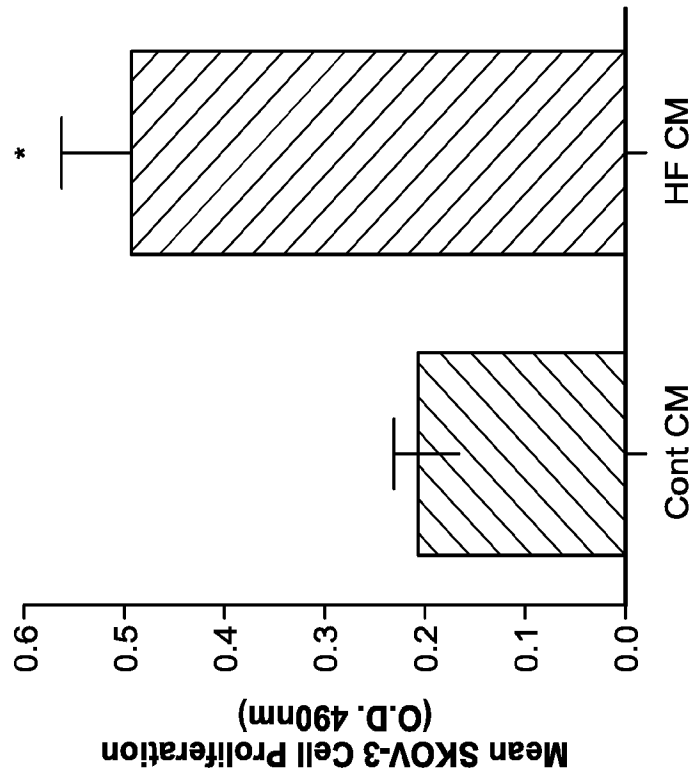


FIG. 24F

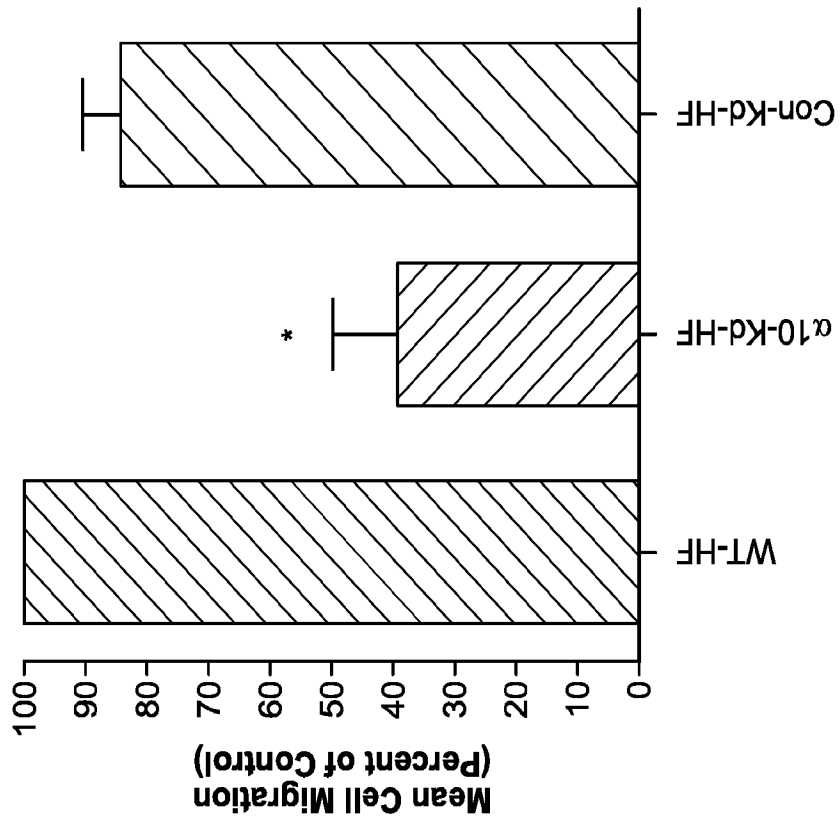


FIG. 24I

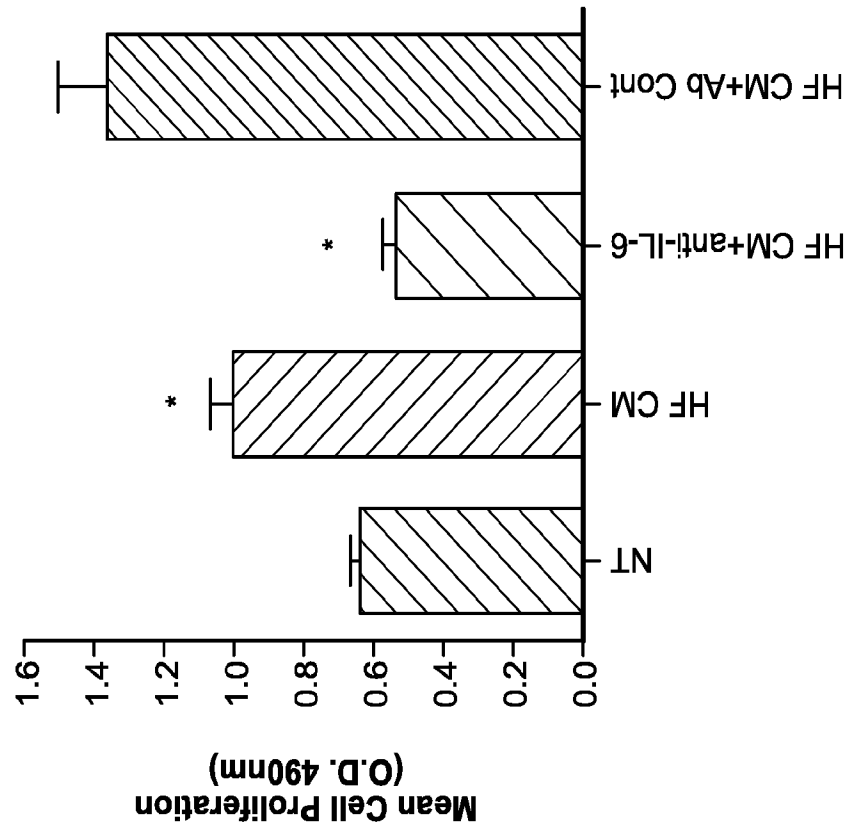


FIG. 24H

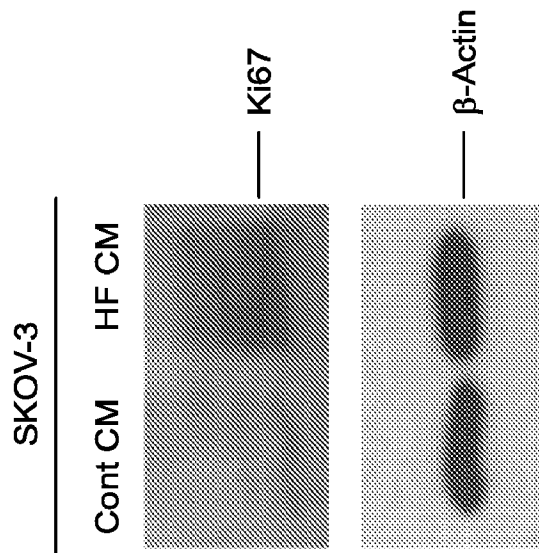


FIG. 25A

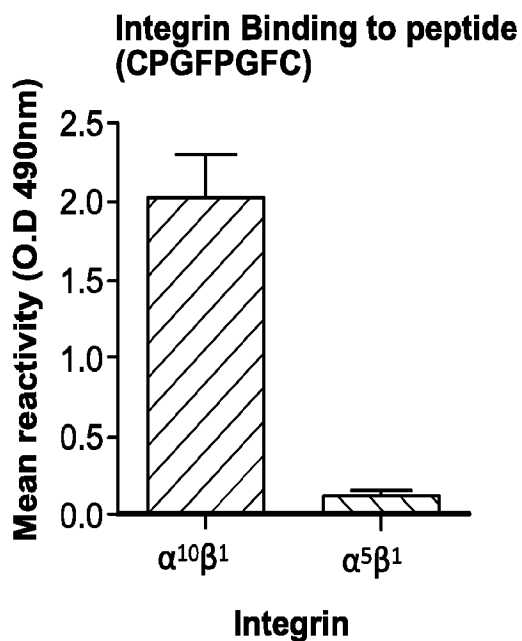


FIG. 25B

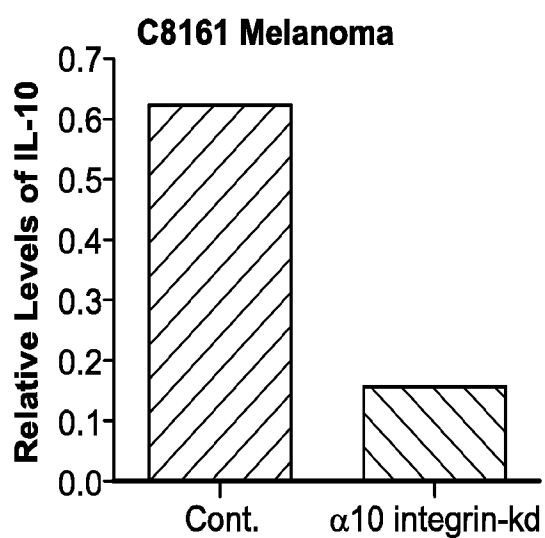


FIG. 25C

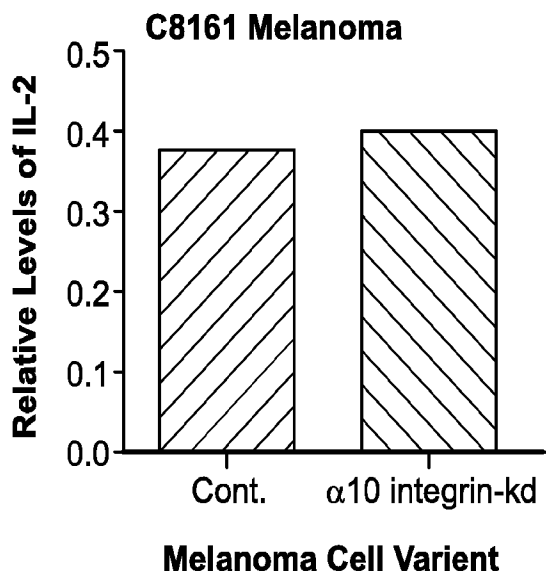


FIG. 25D

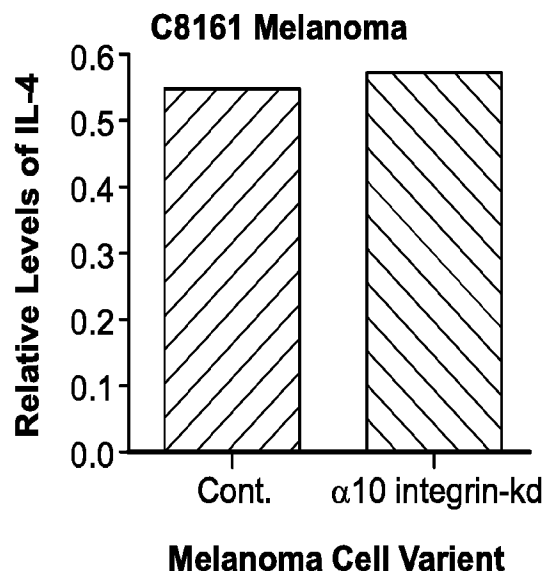


FIG. 26A

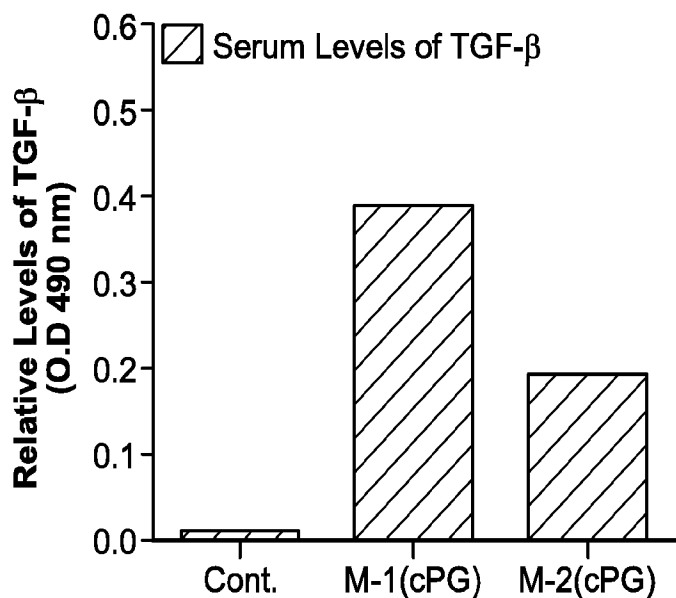


FIG. 26B

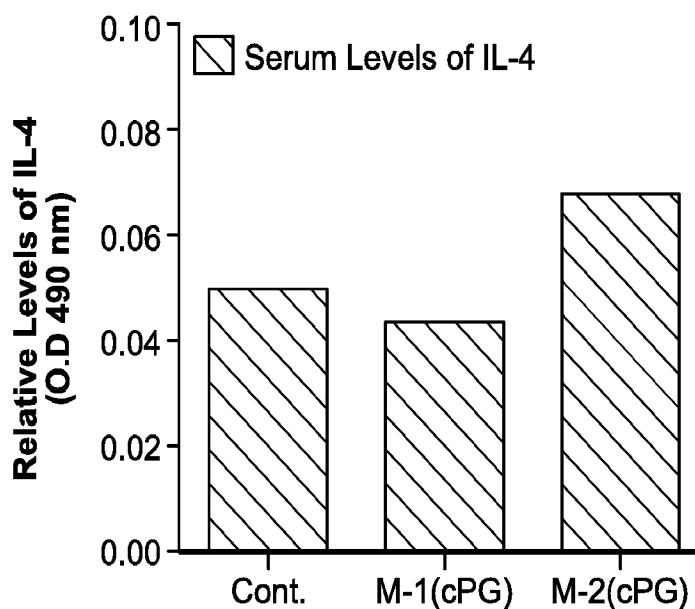


FIG. 26C

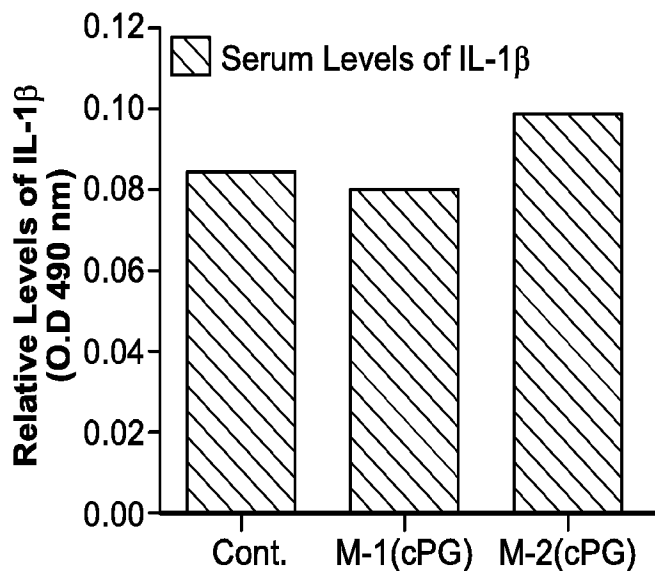


FIG. 27B

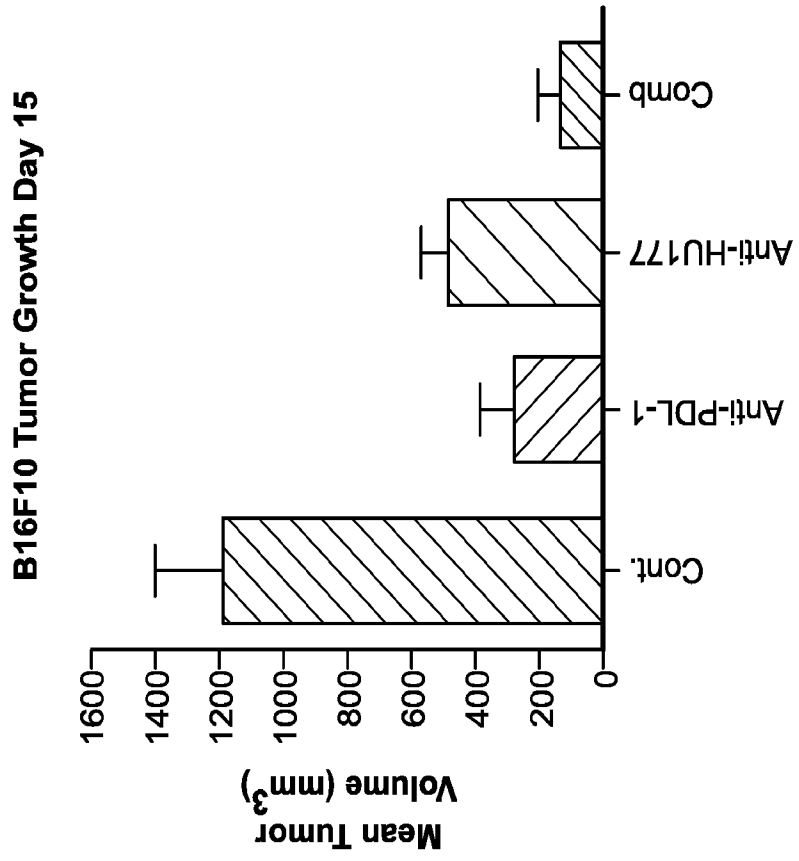


FIG. 27A

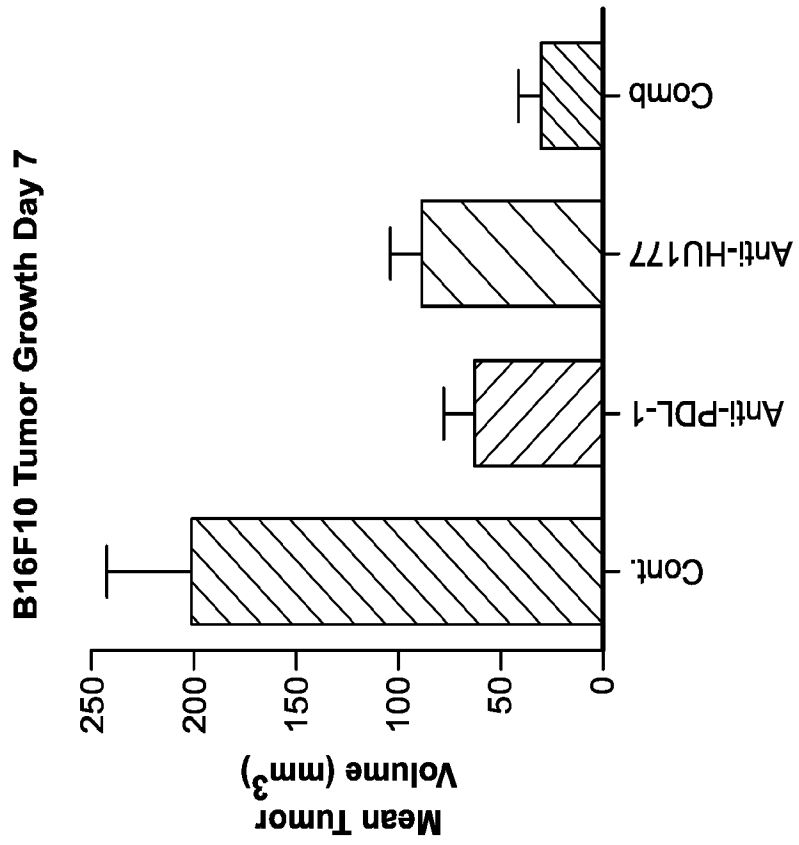


FIG. 29

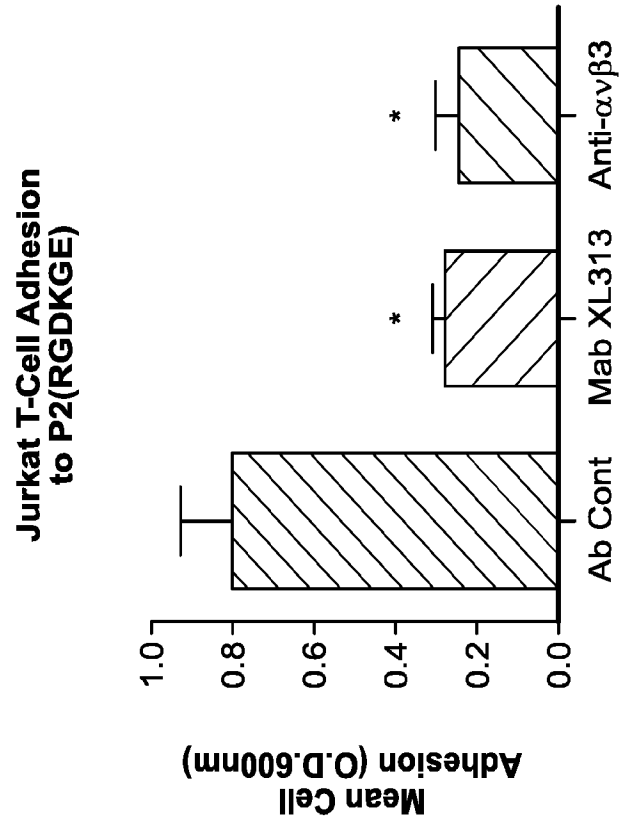


FIG. 28

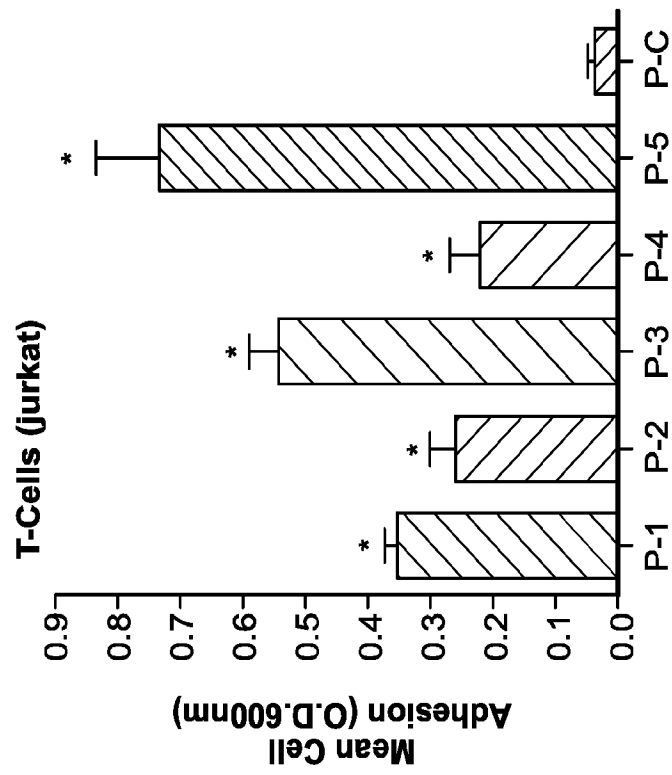


FIG. 31

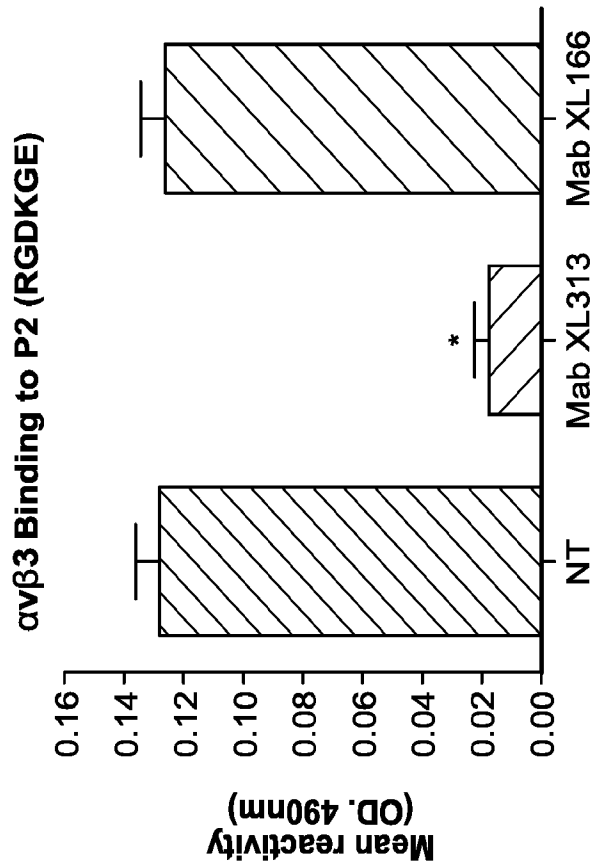


FIG. 30

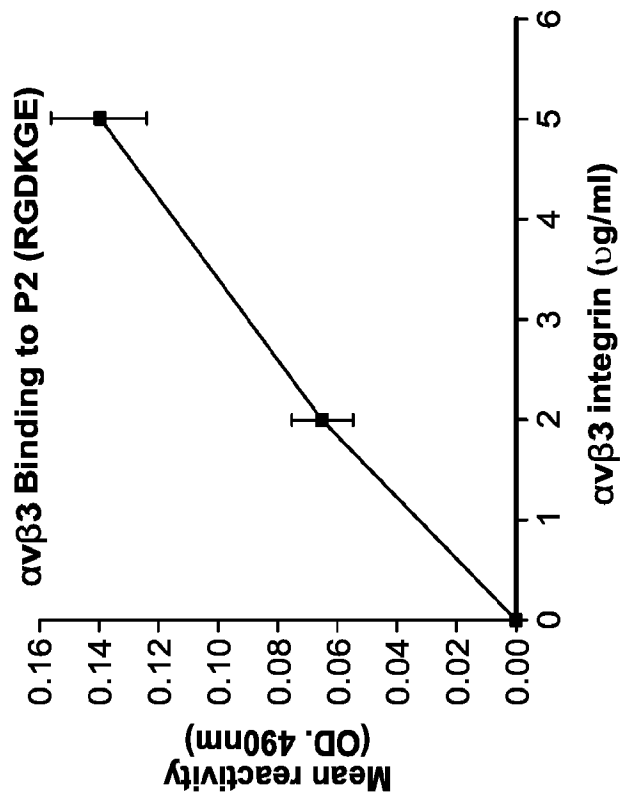


FIG. 32

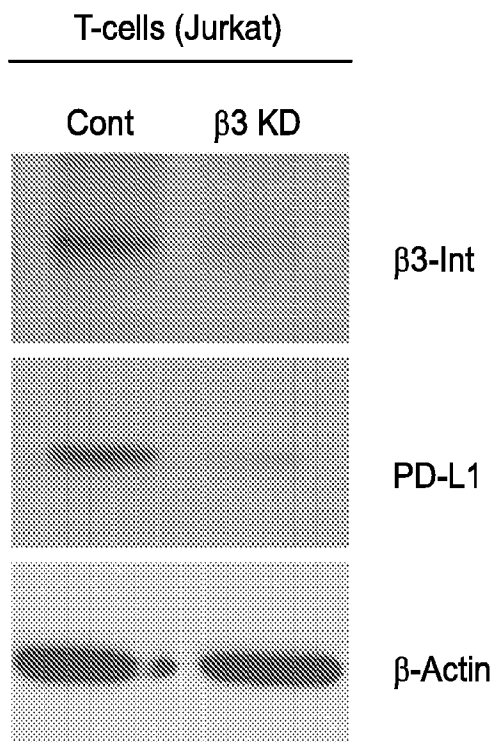


FIG. 33

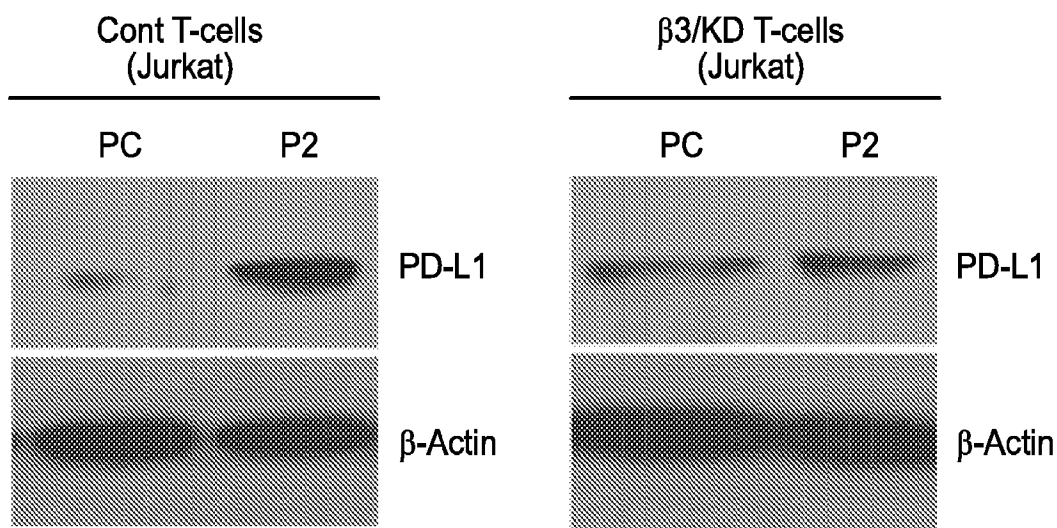


FIG. 34

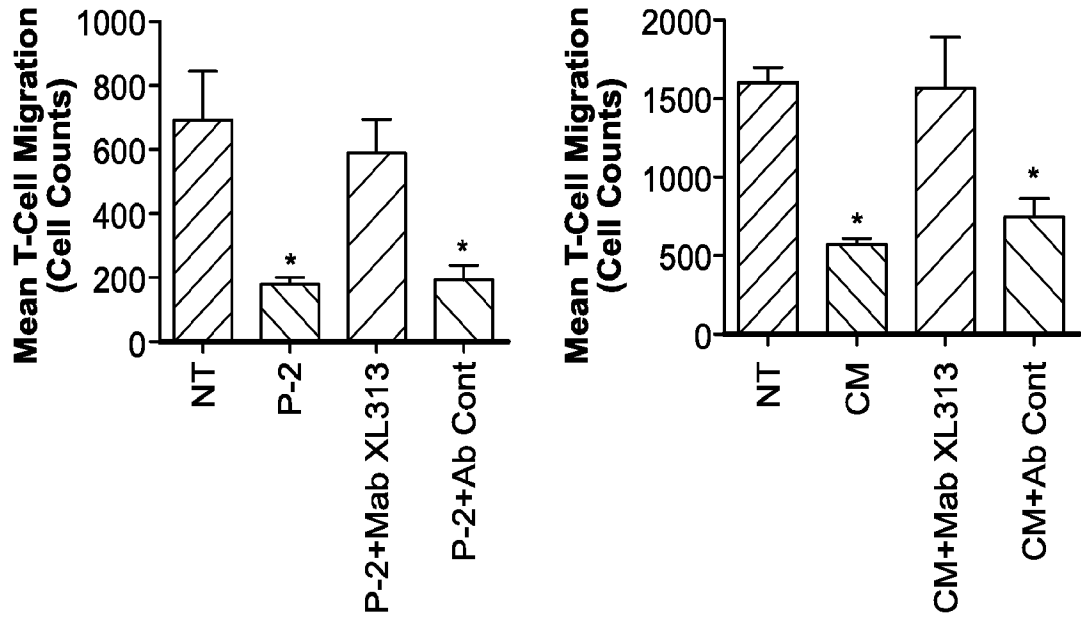


FIG. 35

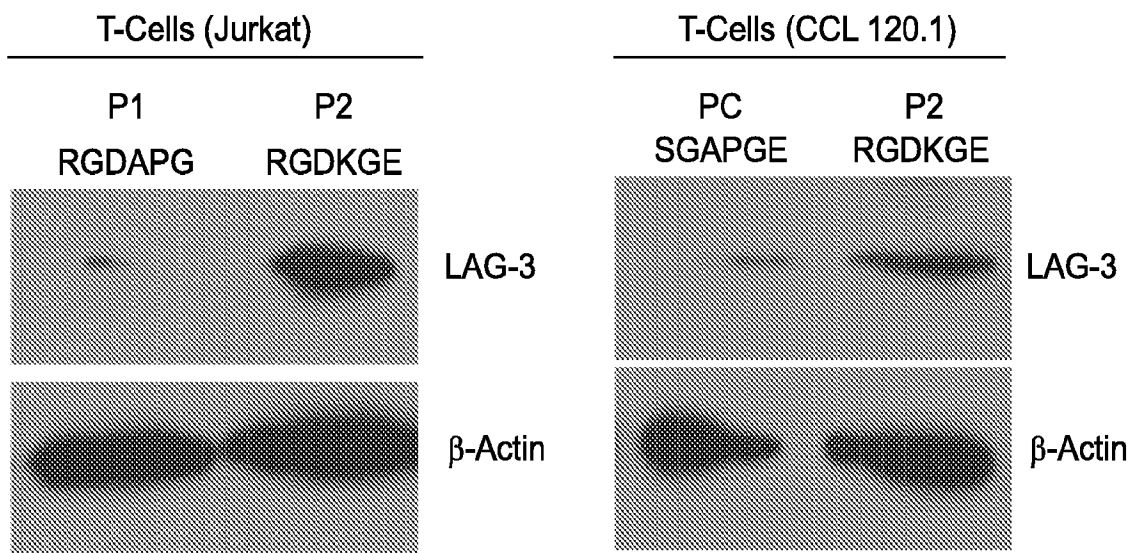


FIG. 36

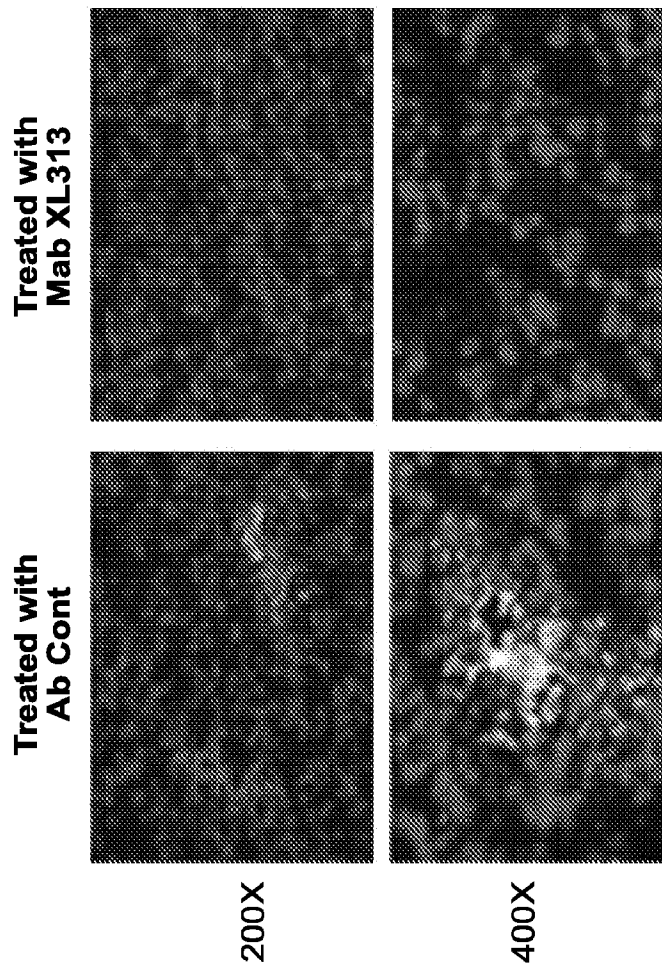
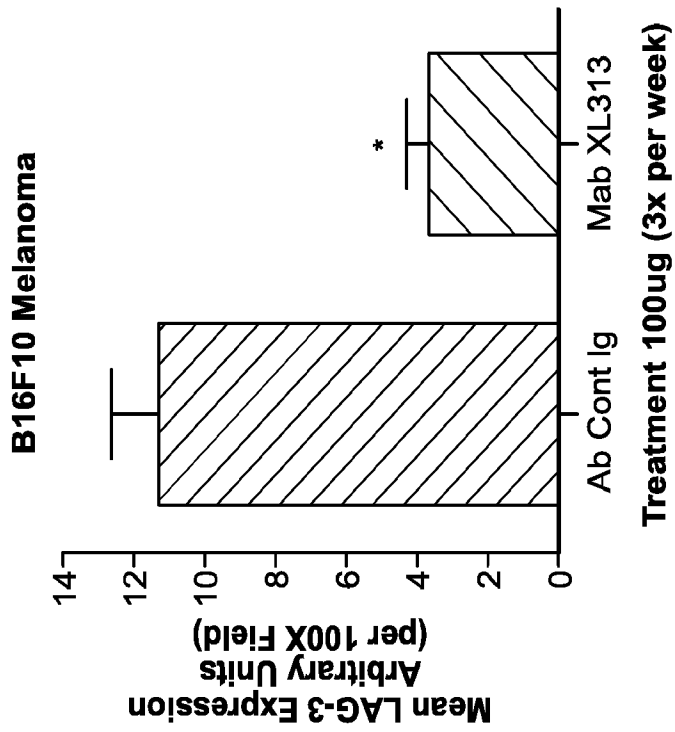


FIG. 37

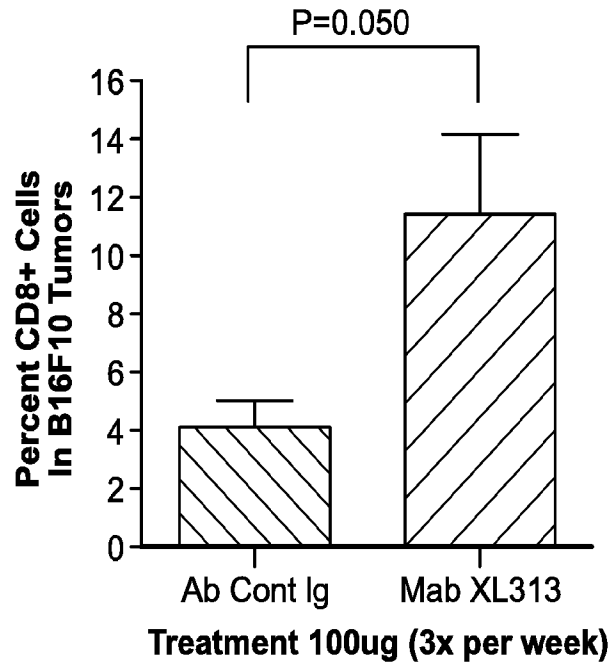


FIG. 38

